



Universiteit  
Leiden  
The Netherlands

## **Dissecting the immune microenvironment of breast cancer** Ciampricotti, M.

### **Citation**

Ciampricotti, M. (2023, September 14). *Dissecting the immune microenvironment of breast cancer*. Retrieved from <https://hdl.handle.net/1887/3640603>

Version: Publisher's Version

License: [Licence agreement concerning inclusion of doctoral thesis in the Institutional Repository of the University of Leiden](#)

Downloaded from: <https://hdl.handle.net/1887/3640603>

**Note:** To cite this publication please use the final published version (if applicable).

# **DISSECTING THE IMMUNE MICROENVIRONMENT OF BREAST CANCER**

**Metamia Ciampricotti**

**About the cover:**

Drawing from the findings presented in this thesis, the cover portrays the abstract dissection of the immune microenvironment of breast cancer. The colors derived from the tumor represent the diverse activated and inactivated adaptive immune cells and different polarized macrophages and neutrophils within this intricate system. This depiction is showcased through the lens of a microscope, capturing the essence of the research. The inclusion of mice on the back cover serves as a token of appreciation for their invaluable contribution.

Cover design: Metamia Ciampricotti & Nicole Solis

Lay-out: Murtaza Kapaasi

Printing: Gildeprint, Enschede

ISBN: 978-94-6419-899-7

The printing of the thesis was financially supported by the NKI-AVL.

© 2023 by Metamia Ciampricotti. All rights reserved. No part of this thesis may be reproduced, stored in a retrieval system, or transmitted in any form or by any means without prior permission of the author and the publisher holding the copyright of the articles.

The research described in this thesis was performed at the division of Immunology and at the division of Tumor Biology & Immunology of the Netherlands Cancer Institute – Antoni van Leeuwenhoek Hospital (NKI-AVL), Amsterdam, The Netherlands.

# **DISSECTING THE IMMUNE MICROENVIRONMENT OF BREAST CANCER**

Proefschrift

ter verkrijging van de graad van Doctor aan de  
Universiteit Leiden,  
op gezag van  
Rector Magnificus  
Prof.Dr.Ir. H. Bijl,  
volgens besluit van het College voor Promoties  
te verdedigen op donderdag  
14 september 2023 klokke 11:15 uur

Door  
Metamia Ciampricotti  
Geboren te Son en Breugel  
In 1984

**Promotores:**

Prof.dr. K.E. de Visser

Prof.dr. J Jonkers

**Promotiecommissie:**

Prof.dr. JG Borst

Prof.dr. P ten Dijke

Dr. FA Scheeren

Prof.dr. B.E. Snaar-Jagalska (LADCR, Leiden University)

Dr. Jan Van den Bossche (Amsterdam UMC, VUmc)

## TABLE OF CONTENTS

<b>Chapter 1</b>	Introduction	7
	<i>Toward understanding the role of the immune system in cancer progression and chemotherapy response</i>	7
	<i>Scope of Thesis</i>	25
<b>Chapter 2</b>	Development of metastatic HER2+ breast cancer is independent of the adaptive immune system	45
	<i>Journal of Pathology. 2011 May; 224(1):56-66</i>	
<b>Chapter 3</b>	Chemotherapy response of spontaneous mammary tumors is independent of the adaptive immune system	79
	<i>Nature Medicine.2012 Mar 6;18(3):344-6</i>	
<b>Chapter 4</b>	Therapeutic targeting of macrophages enhances chemotherapy efficacy by unleashing type I interferon response	95
	<i>Nat Cell Biol. 2019 Apr;21(4):511-521</i>	
<b>Chapter 5</b>	General discussion	155
<b>Chapter 6</b>	Addenda	185
	<i>English Summary</i>	186
	<i>Dutch Summary</i>	189
	<i>Acknowledgements</i>	193
	<i>Curriculum Vitae</i>	194
	<i>Publications</i>	195

# Chapter 1



# **Introduction**

**Toward understanding the role of the immune system in cancer progression and chemotherapy response**

**Scope of Thesis**

## **Abstract**

Over the last decades, it has become apparent that the immune system influences most of the hallmarks of cancer. Immune cells interact with cancer cells and other tumor-associated cells via direct cell-cell interactions and secretion of a variety of growth factors, cytokines, chemokines, and proteases. Historically it was thought that the immune system protects against tumor development. However, more recent clinical and experimental studies have reported pro-tumorigenic roles as well as anti-tumorigenic roles for various immune cell types during tumor progression and chemotherapy response. To date, it remains largely unclear why certain tumors elicit anti-tumor immune responses whereas other tumors elicit pro-tumor immune responses or are not regulated by the immune system at all. Here, we review current insights into how adaptive and innate immune cells participate in tumorigenesis and chemotherapy response. In addition, we highlight that understanding the inherent complexity of the immune system in cancer is paramount for the identification of novel prognostic and predictive biomarkers, and for the design of novel immunomodulatory treatment strategies to fight cancer.

### **1.1 Introducing the paradoxical role of the immune system in cancer**

Currently, it is known that the inter-tumoral and intra-tumoral heterogeneous nature of cancer is not only a consequence of aberrant mutations but also of the composition and activation state of the tumor microenvironment (TME)<sup>1</sup>. The TME contains fibroblasts, endothelial cells and immune cells of which their secreted inflammatory mediators such as metabolites, cytokines, chemokines, growth factors and proteases play a vital part in the cancer cell's ability to grow and to metastasize<sup>2</sup>. The immune system is an important player in tumorigenesis. Over the last century, compelling evidence has indicated that the immune system sometimes protects against cancer<sup>3-5</sup>. Already in 1909, Ehrlich, and later Thomas and Burnet, proposed that the immune system has the capacity to spontaneously recognize and kill cancer cells, and therefore protects against tumor development<sup>6,7</sup>. Immunotherapy, a cancer treatment that is based on boosting the ability of the adaptive immune system to destroy cancer cells, has evolved from a promising therapy to a clinical reality<sup>8</sup>. Clinical trials with immune checkpoint inhibitors, anti-cytotoxic T-lymphocyte antigen 4 (CTLA-4) and anti-programmed death ligand 1 (PD-L1), anti-PD-1 or a combination of these

agents have shown remarkable success in patients with advanced metastatic melanoma, renal cancer, non-small cell lung cancer, Hodgkin's lymphoma, bladder cancer and microsatellite instability (MSI) high colorectal tumors, and are now FDA approved for various cancer types<sup>9-11</sup>. Current efforts to enhance the therapeutic benefit of immunotherapy are focused on targeting evolving immunomodulatory pathways, for example T-cell metabolism<sup>12</sup>.

At the same time, however, an increasing body of evidence has shown that the immune system can also promote tumorigenesis<sup>1,13-16</sup>. The first link between cancer and inflammation was made by Virchow in 1863 when he hypothesized that cancer finds its origin at sites of chronic inflammation<sup>17</sup>. Indeed, as will be discussed below, epidemiological studies and molecular studies in genetically modified mouse models provide evidence for a causal link between chronic inflammation and cancer. Consequently, the tumor-promoting ability of inflammation was added to the hallmarks of cancer<sup>18</sup>.

To date, it is largely unclear why different tumors are differentially influenced by the immune system. Hence, for the development of novel immunomodulatory strategies, it is important to understand how cancer-promoting and cancer-inhibiting immune responses are regulated. Here we discuss the current understanding of the inherent complexity of the inflammatory TME, with a focus on lymphocytes and macrophages, during tumorigenesis and chemotherapy response. Moreover, we review recent therapeutic strategies that target pro-tumorigenic immune cells.

## 1.2 Clinical observations supporting a link between cancer and the immune system

Cells of both the innate and adaptive immune system infiltrate the majority of solid tumors, often resembling a chronic inflammatory state. Various clinical observations support the hypothesis that inflammation predisposes to cancer. For example, chronic inflammation caused by pathogens such as the bacterium *Helicobacter pylori* is associated with gastric cancer<sup>19</sup>. In addition, chronic hepatitis B or C increases the risk of hepatocellular carcinoma and parasitic infections with schistosomes and trematodes can cause cancers of the urinary bladder, the intrahepatic and extrahepatic biliary tract<sup>20,21</sup>. Besides infectious pathogens, exposure to environmental chemicals and irritants, such as tobacco smoke and asbestos or silica particles, can lead to chronic inflammation and is linked to lung cancer<sup>22-24</sup>.

Lastly, Crohn's disease, a type of inflammatory bowel disease (IBD), increases the risk of colorectal cancer <sup>25</sup>, and gallstones and chronic cholecystitis can increase the risk of gallbladder cancer <sup>26,27</sup>.

Cancer formation in the context of chronic inflammation is possibly the result of the incapacity of the host to resolve the persistence of initiating factors leading to a prolonged inflammatory response. The chronically activated innate immune cells produce high levels of reactive metabolites of oxygen, nitrogen, growth factors, pro-angiogenic and inflammatory mediators and proteases <sup>13,28</sup>, which can cause DNA damage and genomic instability, and lead to tumor development <sup>28</sup>. In addition, to sustain tumor growth and progression, tumors themselves can induce chronic inflammation <sup>13</sup>. Hence, chronically inflamed tumors are often described as "wounds that do not heal" <sup>29</sup>. Furthermore, chronic inflammation frequently leads to an immunosuppressive state, characterized by the exclusion or suppression of adaptive immune cells in the TME <sup>30</sup>. One of the most abundant immune cell types in tumors are tumor-associated macrophages <sup>31</sup>. Macrophage infiltration in many human cancers, such as breast cancer <sup>32</sup> and oesophageal cancer <sup>33</sup> is linked with poor prognosis. Also other immune cell types with immunosuppressive capacity, including neutrophils and regulatory T cells, are frequently observed in cancers and are linked with poor prognosis <sup>34,35</sup>. Importantly, long-term usage of non-steroidal anti-inflammatory drugs, such as aspirin, has shown to reduce cancer incidence and metastasis <sup>36,37</sup>, illustrating that it is possible to prevent cancer by suppressing chronic inflammation.

On the other hand, anti-tumor roles of the immune system were suggested by studies correlating increased intratumoral T cell numbers, activated CD8<sup>+</sup> T cells and CD4<sup>+</sup> Th1 cells with better survival across various cancer types, including colorectal cancer, melanoma, multiple myeloma and pancreatic cancer <sup>38-43</sup>. In addition, congenital and viral-induced acquired immunodeficiency's, such as AIDS, have been associated with increased incidence of certain types of malignancies such as leukemia and various viral-associated cancers, such as Kaposi sarcoma, skin cancer, cervical cancer and Merkel cell carcinoma <sup>27,44-48</sup>. However, the association between a suppressed immune system and cancer- outcome differs per tumor type <sup>49,50</sup>. For example, whereas breast cancer incidence is decreased in female immunosuppressed patients with organ transplants <sup>51</sup>, immunosuppressed organ transplantation patients are at increased risk for viral associated cancers such as lung, skin, non-Hodgkin lymphoma and endometrial

cancer<sup>52</sup>. This is because the adaptive immune system is rather capable of fighting viruses as there are viral-antigens that can be easily recognized. Another example is that memory CD4<sup>+</sup> T cells correlated with favorable outcome in lung adenocarcinoma patients but were associated with adverse outcome in bladder cancer patients<sup>53</sup>. These clinical observations suggest that distinct cancer types are differentially regulated by the immune system. Indeed, a body of accumulating clinical data indicates that different molecular subtypes of tumors are characterized by distinct immune landscapes<sup>54</sup>. Different patient-specific or tumor-specific characteristics may underlie the inter-patient heterogeneity in immune landscape. The activation of oncogenes or loss of tumor suppressor genes (TSGs) in cancer cells, epigenetics but also the patient characteristics such as microbiome, age, gender and therapy history dictate the immune composition, activation states and therefore different immune responses<sup>55</sup>.

Together these clinical observations illustrate a potential versatile impact of the immune system on tumorigenesis. The magnitude and phenotype of the immune response are shaped by various patient and tumor characteristics, including cancer location, cancer (sub)type and genetic make-up of the tumor. Identifying the exact mechanisms underlying the interactions between genetic aberrations in tumors and the immune landscape will be crucial for the design of personalized immunomodulatory treatment strategies. *In vivo* mechanistic studies will be key to understand the crosstalk between the immune system and cancer per cancer subtype. The various mouse models that can be used to dissect the immune composition and function in primary tumors as well as in metastatic lesions and therapy will be discussed in the next section.

### **1.3 Preclinical mouse models as tools to study the function of the immune system in tumorigenesis and cancer treatment**

Though clinical observations suggest an involvement of the immune system in tumorigenesis, these correlative data do not provide insights into mechanisms underlying the interplay between the immune system and cancer. Hence, different preclinical mouse cancer models have been used to mechanistically investigate the role of the immune system in cancer biology and therapy response, *i.e.*, human and mouse tumor cell line inoculation models, tumor transplantation models, including patient-derived xenograft (PDX) models, carcinogen-induced cancer models and genetically engineered mouse models (GEMMs)<sup>56</sup>. These different models have both

advantages and disadvantages for studying the interplay between cancer and the immune system.

Tumor allograft models, which rely on the ectopic or orthotopic injection of cancer cells grown in culture, are frequently used to study the role of immune cells in cancer. One major disadvantage of tumor cell line allograft models is that cancer cell lines are adapted to grow under *in vitro* culture conditions and have thereby acquired mutations over time <sup>57</sup>, which may not occur under *in vivo* conditions. Other disadvantages of cancer cell line allograft models include the diminished genetic heterogeneity, the derangement of the normal tumor architecture, the disparate tissue of origin location compared to spontaneous tumors and the fact that they are generally poor predictors of clinical response <sup>56</sup>. Furthermore, while human tumors develop via a multi-step process in which normal tissues progress through a pre-malignant phase into invasive cancers with co-evolving cancer cell-host interactions and an immunosuppressive microenvironment <sup>58</sup>, tumors formed after inoculation of cancer cells skip the premalignant phase. As such, spontaneous experimental tumors have different chemotherapy response profiles compared to inoculated tumor cells isolated from these spontaneous tumors <sup>59</sup>. In addition, immunotherapy efficacy exhibited enhanced sensitivity in mice with subcutaneously implanted tumors compared to mice bearing orthotopic tumors <sup>60</sup>, indicating that the endogenous T cell responses are niche-dependent or that the injection of a large number of cancer cells already primes the immune system or that immunosuppressive mechanisms differ per location. Since several studies have demonstrated that cancer cells can disseminate from very early neoplastic lesions <sup>61,62</sup>, this process will not be recapitulated in cancer cell line inoculation models. Consequently, the impact of the immune system on early neoplastic events and early metastasis formation cannot be investigated in tumor cell line inoculation models.

Many different types of patient-derived xenograft (PDX) models have been developed in which human tumor pieces or patient-derived circulating tumor cells (CTCs) are (orthotopically) transplanted into immunocompromised mice. The transplantation of small tumor fragments or CTCs into mice has some advantages over human cell lines because the resulting tumors frequently recapitulate the morphology, heterogeneity, vasculature, and molecular and genetic alterations of the original donor tumor <sup>56,63,64</sup>. However, given the necessity to use immunodeficient recipient mice, human tumor cell line inoculation models and PDX models, are not suited for

studies focusing on the interplay between the immune system and cancer cells <sup>63</sup>. This gap is currently being addressed by the generation of humanized mouse xenograft models where components of the human immune system, such as human CD34+ hematopoietic stem cells or precursor cells, are engrafted into immunodeficient mice <sup>65</sup>. The newer generations of humanized mouse models show a promising progress in mimicking human tumor heterogeneity, the TME and crosstalk between the tumor and immune cells <sup>66</sup>.

In contrast to cancer cell inoculation and tumor transplantation models, chemical- or viral-induced tumor models and GEMMs develop *de novo* tumors in a natural immune-proficient microenvironment. Genomic and microenvironmental heterogeneity that defines human cancer is well represented in the spontaneous tumors arising in conventional, conditional or somatic GEMMs <sup>67-70</sup>. Chemical- or viral-induced tumor and GEMMs have proven to be tremendously important in the inflammation and cancer field as they allow in-depth mechanistic characterization of the complex interactions between cancer cells and components of the immune system at all the different steps of tumorigenesis, drug response, and resistance <sup>70</sup>. Most work underlying the differential crosstalk of cancer cells with the immune system has been done in mice by utilizing tissue-specific promoters that induce somatic inactivation of TSGs or activation of oncogenes <sup>70</sup>. Mouse model engineering has taken a new direction with the discovery of the clustered regularly interspaced short palindromic repeats (CRISPR)-based genome editing approach <sup>71</sup>. CRISPR/Cas9 has proven to be an efficient gene targeting strategy with the potential for multiplexed genome editing for a wide spectrum of mutations found in human cancers <sup>72-76</sup>. An important factor to keep in mind when investigating the immune system with this approach is to circumvent somatic Cas9-specific immune responses <sup>77-79</sup>. Experiments should be performed in mice that have immunological tolerance to Cas9 or methods should be used such as the CRISPR-Cas9 bone marrow delivery system CHimeric IMMune Editing (CHIME), which allows rapid evaluation of gene function in immune cells lineages *in vivo* while keeping normal immune development and function <sup>80</sup>. In the next paragraphs, insights are provided into the role of the immune system during carcinogenesis and chemotherapy response, that have been obtained with these different experimental mouse tumor models.

## 1.4 Immunosurveillance and Immunoediting

The adaptive immune system is capable of recognizing and killing cancer cells, and thereby has the ability to protect against tumor development<sup>81</sup>. This process, when functioning optimal, is referred to as cancer immunosurveillance<sup>82</sup>. The effective recognition and elimination of cancer cells by the immune system in a stepwise process is nowadays also referred to as the cancer-immunity cycle<sup>55</sup>. The cancer-immunity cycle begins with DCs that take up and present tumor (neo)antigens on major histocompatibility class I (MHC-I) and MHCII molecules to T cells. Neoantigens are expressed by tumor cells and are generally tumor-specific antigens generated as a consequence of DNA mutations in cancer cells<sup>83</sup>. Subsequent, CD8<sup>+</sup> T cells and NK(T) cells (effector T cells) are primed in secondary lymphoid organs such as lymph nodes (LN) and spleen and then activated to travel to the tumor. After recognizing and attaching to the tumor cell through their T cell receptor (TCR) and the analogous neoantigen on the tumors MHC-I molecule, the tumor cell will be destroyed. The release of additional antigens upon the elimination of cancer cells improves the T cell response. In addition, type I interferons (IFNs) induced by stimulator of interferon genes (STING) in cancer cells can further augment the cancer-immunity cell cycle. The discovery and characterization of the cGAS–STING pathway in 2013 has provided a new understanding of the immunostimulatory capacity of double-stranded DNA (dsDNA)<sup>84</sup>. Detection of tumor-derived DNA by cGAS in dendritic cells fuels the cGAMP-dependent activation of STING and subsequent secretion of type I IFNs<sup>85,86</sup>. In several tumor transplantation models these innate immune signals enhanced tumor antigen presentation and thereby augment the antigen-specific CD8<sup>+</sup> T cell response, which linked to tumor regression<sup>87-89</sup>.

The experimental basis for the cancer immunosurveillance hypothesis was established using mice that lack the recombinaase activating gene (RAG)-2<sup>90</sup>. *Rag2*-deficient mice<sup>91</sup> lack mature lymphocytes and developed MCA-induced sarcomas more rapidly and with greater frequency than wild-type controls<sup>90</sup>. Various experimental studies have subsequently addressed the mechanisms underlying immunosurveillance. For example, enhanced development of spontaneous tumors has been reported in mice lacking components of the immune system, such as perforin, granzyme, cytotoxic cytokines, lymphocytes, or in mice defective for IFN signaling<sup>81</sup>. Despite these reported mechanisms of immunosurveillance, cancer is a very prevalent disease. This raises the question why the adaptive immune

system frequently fails to protect us from cancer. In fact, in order to generate effective anti-tumor immunity, several bottlenecks need to be overcome, such as failure of T cell priming against tumor antigens which can occur due to the lack of immunogenic tumor antigens or defects and deficiencies in antigen presentation, for example loss of MHC expression or dysregulation of the antigen processing apparatus. Other bottlenecks are defective DC and T cell activation, impaired trafficking or infiltration of the anti-tumor T cells into the tumor, the activation of immunosuppressive myeloid cells and Tregs, and induction of immune checkpoint molecules that suppress the priming or activation of effector T cells <sup>92</sup>.

The immune-mediated tumor-sculpting process is also referred to as immunoediting <sup>93</sup>. Developing tumors influence the anti-tumor immune response, while the anti-tumor immune response shapes the immunogenicity -the capacity of provoking an adaptive immune response- of the tumor. The immune-editing process is demonstrated by studies revealing that carcinogen-induced sarcomas and *de novo* epithelial carcinomas were more immunogenic when induced in mice lacking lymphocytes as compared to being induced in immunocompetent mice <sup>90</sup>. Furthermore, the so-called tumor 'equilibrium' phase can result in tumor dormancy, which can last for years <sup>94</sup>. During the equilibrium phase, cancer cells can become resistant against immune attack, escape immune control, and develop into full-blown tumors. Established tumors may subsequently benefit from immune cells and their soluble mediators present in the TME, favoring tumor outgrowth. This co-evolution of a tumor and the immune system explains why many established tumors are characterized by low immunogenicity and a high immunosuppressive state, which in most cases resembles chronic inflammation <sup>95</sup>. The goal of immunotherapy and immunomodulation is to unleash immunosurveillance and to change the odds in favor of elimination or at least equilibrium. It is therefore important to understand in which tumors immune cells are tumor-promoting or tumor-preventing.

## 1.5 The adaptive immune system in promoting tumorigenesis

The impact of the adaptive immune system during the development and progression of pathogen- and chemical-unrelated solid cancers is less well defined. Studies using GEM tumor models have shown opposite functions of various adaptive immune cell populations during *de novo* epithelial tumorigenesis <sup>96-101</sup>. For example, in experimental pancreatic islet tumors,

tumorigenesis in *RIP1-Tag2*, *Rag1*<sup>-/-</sup> mice was similar to *RIP1-Tag2*, *Rag*<sup>+/+</sup> mice <sup>101</sup>. While in a transgenic mouse model for skin tumorigenesis, *i.e.*, *K14-HPV16* mice, it was demonstrated that B lymphocytes activate inflammatory responses through antibody-mediated activation of Fc receptors (FcRs) on macrophages and mast cells, which stimulated their proangiogenic abilities and led to cancer progression <sup>96,99</sup>. In addition, the development of hepatocellular carcinoma in a chronic hepatitis mouse model was dependent on both T and B-lymphocytes <sup>97</sup>. Importantly, T and B-lymphocytes do not only play distinct roles depending on tumor type, but tumor subtypes are also differentially influenced by the adaptive immune system. In several transgenic mouse models of breast cancer, different components of the adaptive immune system were reported to promote metastasis formation <sup>98,102-104</sup>. For instance, metastasis formation in a mouse model for spontaneous breast adenocarcinomas, *i.e.*, MMTV-PyMT mice, revealed to be dependent on interleukin 4 (IL-4)-expressing CD4<sup>+</sup> T cells which promoted EGF secretion from tumor-associated macrophages (TAMs) <sup>98</sup>. However, regulatory T cells promoted the metastatic spread of orthotopically transplanted mammary tumors derived from the MMTV-*ErbB2* transgenic mouse model in a RANKL dependent manner <sup>102</sup>. And in a genetically engineered mouse model for invasive lobular carcinoma (ILC), *i.e.* *K14cre*; *Cdh1*<sup>F/F</sup>; *Trp53*<sup>F/F</sup> mice, it was demonstrated that tumor-derived CCL2-mediated induction of IL1b in TAMs stimulated IL-17 expression from  $\gamma\delta$  T cells, which resulted in the systemic granulocyte colony-stimulating factor (G-CSF)-dependent expansion and polarization of neutrophils, which in their turn suppressed effector CD8<sup>+</sup> T cells that were limiting the development of metastasis <sup>103,105</sup>. This systemic pro-metastatic inflammatory pathway was triggered upon loss of P53 in breast cancer cells <sup>104</sup>, illustrating that the genetic makeup of breast tumors shapes the crosstalk with the immune system. Hence, because different breast cancer subtypes are characterized by distinct (epi)genetic features that trigger unique gene expression patterns, combined with patient specific features that impact the immune landscape, distinct breast cancers hijack the adaptive immune system in different ways to contribute to metastasis <sup>104,106,107</sup>. Thus, different tumor types as well as tumor subtypes employ different mechanisms to circumvent or exploit components of the adaptive immune system for their own benefit. Numerous studies have elucidated that adaptive immune cells interact with many different components of the innate immune system. As such, for the development of therapeutics, future studies should gain insights into the interplay between adaptive and innate immune cells per individual cancer (sub)type or per genetic driver mutation.

## 1.6 Tumor-associated macrophages

### *Macrophage plasticity*

Macrophages were originally identified based on their phagocytic nature by Metchnikoff in 1882<sup>108</sup>. He suggested that macrophages fight infection by phagocytosis and play an important role in injury repair<sup>108</sup>. After decades of study, we now know that macrophages do more than defending the host from external invaders. Many preclinical studies have established that macrophages contribute to various cancer hallmarks including cancer proliferation, suppression of anti-tumor immune responses, angiogenesis and migration<sup>109-111</sup>. The current concept is that macrophages arise from two different lineages. Most tissue-resident macrophages arise from yolk sac progenitors and fetal liver during embryogenesis and are maintained through local proliferation. On the other hand, macrophages that fight pathogens in damaged tissues originate from bone-marrow derived macrophages (BMDMs) which get into the circulation as monocyte and then differentiate into macrophages once they enter the tissue<sup>112-115</sup>. Both tissue-resident as well as bone marrow-derived macrophages have shown to be important in tumor development in several mouse models<sup>116-119</sup>. Whether TAMs derive from circulating monocytes<sup>120,121</sup> will be discussed in the next paragraph.

Originally, macrophages were classified as ‘classically activated’ M1 and ‘alternatively activated’ M2- macrophages, based on a limited set of produced cytokines and expressed surface markers<sup>122,123</sup>. It is now generally accepted that the standardization and nomenclature of macrophages originating from cell culture studies, even though practical, does not fit TAM complexity *in vivo*<sup>124-126</sup>. Macrophages are inherently plastic, and therefore they can adapt their phenotype and function to the evolving changes in the TME during tumor progression. Over the years many studies have found a wide spectrum of macrophages with different polarization states and with specific tumor regulatory features that can include both inflammatory and immunosuppressive characteristics<sup>127</sup>. For instance, in a study where immune cells were isolated from human breast tumors, single-cell RNA-sequence (scRNA-seq) demonstrated that both M1 and M2 signatures were present in the same macrophage<sup>128</sup>. Similar results were found in gliomas<sup>129</sup>. Macrophage polarization in tumors has shown to be dependent on several different factors including tumor and organ type, intratumoral location, tumor stage and origin. For example, by transplanting differentiated peritoneal macrophages into the alveolar cavity, a study found that fully differentiated macrophages switched to resemble the

transcriptomic profile of lung macrophages<sup>130</sup>, demonstrating that the tissue environment in which macrophages reside dictates macrophage polarization as well as regulation. In addition, a recent study discovered that TAM heterogeneity is driven by tissue territories in human and mouse breast cancer by combining scRNA-seq with spatial localization, indicating that tumor regions, rather than defined activation states, are the key drivers of TAM plasticity and heterogeneity<sup>131</sup>. Furthermore, by performing lineage tracing and scRNA-seq a recent study showed that distinct populations of macrophages were enriched in mouse and human non-small cell lung cancer (NSCLC); *i.e.* tissue-resident macrophages provided a pro-tumorigenic niche to early tumors while during tumor growth monocyte-derived macrophages became dominant and tissue-resident macrophages were redistributed at the periphery of the TME<sup>119</sup>. Given the spatiotemporal and environmental context, gene-expression profiles and transcriptional regulatory pathways are crucial for the understanding of human and mouse tissue- and tumor macrophage regulation and discovery of novel marker genes as well as biomarkers<sup>132-135</sup>. For example, a study showed that a specific TAM gene signature derived from *K14cre; Cdh1<sup>FF</sup>; Trp53<sup>FF</sup>* mouse tumors could be used to predict poor survival in two separate cohorts of ILC patients when compared to the transcriptome profile of bulk tumor samples, indicating that matched mouse TAM transcriptome signatures can be used for outcome prediction<sup>136</sup>.

#### *Targeting tumor-associated macrophages via the CSF-1/CSF-1R pathway*

Since TAMs represent orchestrators of various tumor-promoting processes, TAMs have become interesting putative targets for therapeutic intervention. Various approaches aimed at targeting survival, recruitment or polarization of TAMs have shown potential in preclinical studies<sup>137</sup>.

Macrophage recruitment to tissues in mice can be initiated by a chemotactic factor, identified as colony stimulating factor-1 (CSF-1)<sup>138</sup>. The receptor for CSF-1, CSF-1R, a class III transmembrane tyrosine kinase receptor encoded by the *cfms* proto-oncogene<sup>139</sup>, is largely restricted to and expressed on almost all macrophages<sup>138</sup>. Initial positive support for blocking TAM recruitment or function via targeting CSF-1/CSF-1R signaling was found in M-CSF-deficient (*Csf1<sup>op</sup>/Csf1<sup>op</sup>*) mice *i.e.*, histopathological progression and metastasis of mammary tumors in *Csf1<sup>op</sup>/Csf1<sup>op</sup>* PyMT mice was delayed<sup>140</sup>. Later, others have found reduced tumor outgrowth of gastric cancer in M-CSF-deficient mice<sup>141</sup> and reduced tumor outgrowths of neuroblastoma xenotransplants and human MCF-7 mammary carcinoma

cell xenografts using antisense oligonucleotides and small interfering RNAs directed against mouse CSF-1<sup>142,143</sup>. Pharmaceutical targeting of the CSF-1/CSF-1R pathway, including antibodies against the receptor (anti-CSF-1R), the ligand (anti-CSF-1), and inhibitors of the tyrosine kinase domain of CSF-1R (such as BLZ945), have predominantly demonstrated anti-tumor effects in several preclinical models<sup>144-156</sup>. Interestingly, in some studies, such as in a mouse model of glioma, treatment with inhibitors of CSF-1R did not deplete TAMs but instead altered macrophage polarization, which resulted in blocked glioma progression<sup>145</sup>. Different findings upon CSF-1/CSF-1R pathway targeting are likely caused by different cancer (sub)types and cancer mouse models with their different TME and the use of a different type of inhibitor, doses, and timing of treatment initiation.

These preclinical studies have laid the foundation for the development and clinical testing of CSF-1R signaling pathway inhibitors<sup>137,157-161</sup>. Ries *et al* were the first to demonstrate the clinical benefit of a macrophage-targeting agent: the humanized anti-CSF-1R IgG1 monoclonal antibody (RG7155) reduced macrophages in tumor tissues, which resulted in clinical objective responses in 83% of patients with diffuse-type giant cell tumor<sup>157</sup>. In light of recent clinical trials for CSF-1R blockade therapy in cancer treatment, there are still several questions that need to be addressed. For example, how do we predict sensitivity to CSF-1R inhibition? Immuno-phenotyping of TAMs in patients may be vital to find biomarkers that can predict sensitivity to CSF-1R blockade and facilitate personalized immunotherapeutic treatments. Furthermore, though immune cells are not under mutational pressure like cancer cells, bidirectional feedback between cancer cells and their microenvironment could induce resistance of the tumor microenvironment to immuno-modulation of CSF-1R targeting. In fact, a study showed that treatment with anti-CSF-1R or the CSF-1R kinase inhibitor GW2580 increased breast cancer lung metastasis in a breast cancer allograft model<sup>162</sup>. Neutrophil blockade using G-CSF-1R decreased anti-CSF1R-induced neutrophil influx in blood, tumor and metastasis-associated lung tissue and reduced metastasis in these mice<sup>162</sup>. Another study in a mouse model for glioma discovered resistance to CSF-1R inhibition in more than 50% of the mice that initially responded to CSF-1R inhibition<sup>163</sup>. The resistance was initiated through IGF-1R/PI3K signaling, driven by macrophage-derived IGF-1<sup>163</sup>. These findings warrant that resistance to CSF-1R targeting needs to be taken into consideration. Furthermore, several studies have shown that TAMs presence was essential during therapies to elicit an anti-tumor

response <sup>164-166</sup>. As such, it will be important to understand whether macrophage depletion or repolarization is favored.

While preclinical experiments suggest that targeting TAMs, either by inhibiting pro-tumor macrophage function via depletion or by repolarization of macrophages, is an attractive anti-cancer approach, CSF-1R blockade alone has shown only marginal therapeutic benefit <sup>137</sup>. Therefore, current clinical and experimental- efforts are focused on finding the right combination partners for TAM targeting <sup>137</sup>. These optimally matched partners may vary from immune checkpoint blockades inhibitors <sup>167</sup>, adoptive transfer <sup>168 169</sup>, radiotherapy <sup>170</sup> to chemotherapy. The latter will be discussed in more detail in the next section <sup>171</sup>.

## **1.7 The role of the immune system in chemotherapy response**

Chemotherapy is frequently used to treat cancer patients. Although most tumors initially respond to chemotherapeutic drugs, tumors develop mechanisms of resistance to the treatment. Thus, it is urgently needed to investigate effective strategies to increase chemo-responsiveness and/or to prevent or eliminate chemoresistance. Cancer cell-intrinsic factors like resistance to apoptosis or overexpression of drug transporter proteins have been identified as causes of therapy resistance <sup>172</sup>. However, also cancer cell-extrinsic processes underlying poor chemotherapy response have been recognized <sup>173-176</sup>. In fact, an increasing amount of data reveals that both the adaptive and innate immune system play an important role in modulating the anti-cancer efficacy of chemotherapy <sup>173,177</sup>. There are many different types of chemotherapeutic drugs with different mechanisms of action, such as alkylating agents (*i.e.* cisplatin), anti-microtubule agents (*i.e.* paclitaxel), topoisomerase inhibitors (*i.e.* topotecan), anthracyclines (*i.e.* doxorubicin) and deoxynucleoside (*i.e.* gemcitabine). Besides differentially influencing cancer cells, these distinct cytotoxic drugs differentially affect immune cells, as has been observed in *in vitro* studies <sup>95,178</sup>. The influence of the immune system on chemo-responsiveness and/or chemo-resistance depends on the type of chemotherapeutic drug and dosing <sup>179</sup>. As such, immune cell depletion typically occurs with high-dose chemotherapy, while low-dose chemotherapy (also called metronomic) has immunomodulatory and anti-angiogenic effects <sup>180</sup>. Importantly, the interplay between chemotherapy and immune cells is bidirectional; *i.e.* chemotherapy can affect immune cells and the other way around, immune cells can affect chemotherapy efficacy. Various studies have elucidated that macrophages <sup>181</sup> and neutrophils <sup>182-184</sup>

counteract chemotherapy efficacy in certain cancer models. Similarly, combining chemotherapy with targeting treatments against MDSC's, B cells, Tregs or Th17, could as well be effective in certain cancer types<sup>179</sup>. On the other hand, CD8<sup>+</sup> T cell and DC functionality are necessary for a good chemotherapy response in several tumor cell line and tumor transplantation models<sup>177</sup>. Overall, numerous studies have illustrated the complexity of immunomodulation by conventional chemotherapeutics, which is highly context dependent. Hence, insights into the exact role of specific immune cell subsets in affecting the efficacy of chemotherapeutic drugs may contribute to the rational design of combinatorial therapies.

### *Chemotherapy response of tumor transplantation models is dependent on the adaptive immune system*

The influx of high T cell numbers in multiple human cancers, including breast cancer, before chemotherapy treatment, has shown to correlate with improved chemotherapy response<sup>185-190</sup>. In line with these data, experimental studies in highly immunogenic tumor models, e.g., cancer cell line allograft models and chemically- induced sarcomas, have indicated that T cells can contribute to the anti-cancer efficacy of certain chemotherapeutics<sup>185-189</sup>. As such, cytotoxic drugs, such as doxorubicin, oxaliplatin, cyclophosphamide, epothilone B, mitoxantrone, and melphalan lose their therapeutic efficacy on tumor cell line outgrowths in mice with a defective adaptive immune cell function, including *Rag*<sup>-/-</sup> mice<sup>177,185-187</sup>. The success of these chemotherapy treatments is dependent on the stimulation of an anti-cancer immune response through the induction of immunogenic tumor cell death (ICD)<sup>191</sup>. Chemotherapy-induced ICD starts with endoplasmic reticulum stress in dying cancer cells. This leads to phosphorylation of the signaling axis extracellular-signal-regulated kinase (PERK)-eukaryotic initiation factor 2 $\alpha$  (eIF2 $\alpha$ ), which is required for the translocation of calreticulin to the plasma membranes of cancer cells that serves as 'eat-me' signals for DCs<sup>185</sup>. Next, nuclear protein high mobility group box 1 (HMGB1) from cancer cells in the extracellular space binds to TLR4 on DCs and triggers their functional maturation and facilitates antigen presentation<sup>185</sup>. Next, the active secretion of adenosine tri-phosphate (ATP) from dying neoplastic cells promotes the proteolytic maturation and release of pro-inflammatory cytokines such as IL-1 $\beta$  from DCs and stimulates the NLRP3 inflammasome<sup>187</sup>. In addition, anthracyclines also require the production of type I IFNs by malignant cells after activation of a TLR3-elicited signal transduction cascade<sup>192</sup>. At last, effective antigen cross-presentation by DCs results in the activation of CD8<sup>+</sup> T-dependent tumor-killing

responses<sup>185-187</sup>. Proof for the immunogenic cell death cascade is largely based on cancer cell line transplantation models and the immunogenic MCA fibrosarcoma model, in which tumor initiation on itself is already suppressed by host immunity<sup>177,193</sup>. As described previously, cancer cell line inoculation models do not accurately mimic *de novo* tumors<sup>56</sup>. *De novo* tumors are characterized by extensive local and systemic immunosuppression which may facilitate escape from immune control during chemotherapy. Indeed, a study in *PyMT* mice indicated that TAM-derived IL-10 indirectly prevented CD8<sup>+</sup> T cell-dependent tumor-killing responses to chemotherapy by suppressing IL12 expression in intra-tumoral DCs<sup>194</sup>. There is a need for more studies that use *de novo* tumor models to study the impact of components of the adaptive immune system on the therapeutic efficacy of different chemotherapeutic drugs. We hypothesize that poorly immunogenic tumors might benefit from chemotherapy in combination with immunosuppression inhibitors, for example macrophage-targeting therapies, to unleash cytotoxic T lymphocytes with anti-tumor reactivity.

#### *Macrophages counteract chemotherapy response*

Many preclinical studies have shown by direct targeting of macrophages that macrophages counteract the anti-cancer efficacy of chemotherapy<sup>181,195,196</sup>. Currently, clinical trials with CSF-1R signaling pathway inhibitors in combination with chemotherapies are ongoing in cancer patients<sup>137</sup>. To maximize the clinical success of such macrophage-targeting compounds various questions still need to be addressed. For instance, it is unclear whether the influence of macrophages on chemotherapy efficacy depends on the type of chemotherapeutic drug used. Understanding this will help to determine the optimally matched combination therapy. Also, resistance to CSF-1R targeting in a chemotherapy context needs to be considered. Furthermore, observations in human breast cancer patients indicate that intratumoral presence of high numbers of macrophages and low numbers of CD8<sup>+</sup> T cells is associated with poor neoadjuvant chemotherapy response<sup>151,197</sup>. Thus, to develop similar and more specific predictive markers for immune-modulation-based therapies, we need to know what the mechanisms are by which macrophages counteract chemotherapy.

It has been reported that macrophages counteract chemotherapy response through a variety of mechanisms, such as matrix deposition and/or remodeling, activation of angiogenesis or revascularization, reduction of chemotherapy delivery to tumors through modulating vessel leakiness, providing survival signals to tumor-initiating cells and perhaps most

importantly: suppression of cytotoxic T cell immunity <sup>147,151,194,198-209</sup>. Although the exact mechanisms of how macrophages counteract chemotherapy efficacy of certain tumor (sub)types remain to be evaluated, these mechanisms could reside in macrophage polarization. Evidence for this hypothesis comes from both *in vitro* and *in vivo* studies that have indicated that chemotherapy can modify macrophage polarization; either skewing macrophages to gain pro-tumor M2-like functions or anti-tumor M1-like functions. For example, treatment with cisplatin or carboplatin increased the potency of 10 different cervical and ovarian cancer cell lines to skew monocytes to M2-like macrophages *in vitro* <sup>210</sup> while docetaxel skewed macrophages to an M1-like phenotype in 4T1-Neu transplants <sup>211</sup>. Furthermore, in a recent *in vitro* study, it was found that reactive oxygen species (ROS) induced by paclitaxel upregulated PD-L1 expression in macrophages <sup>212</sup>. *In vivo* evidence comes from reports that have indicated that chemotherapy efficacy is linked with macrophage polarization <sup>200,208,213,214</sup>. For instance, a study in *K14-HPV16* mice showed that B cell-depletion changed the chemokine expression of macrophages, which resulted in an improved chemotherapy response due to activated CD8<sup>+</sup> T lymphocytes via CCR5-dependent mechanisms <sup>213</sup>. Furthermore, paclitaxel repolarized TAMs through TLR4 signaling toward an M1-like pro-inflammatory profile, which contributed to the antitumor effect of paclitaxel <sup>214</sup>. Thus, macrophage polarization might dictate chemotherapy efficacy and investigating the polarization status of TAMs during treatment with different chemotherapeutic drugs in different cancer (sub)types could contribute to the development of combinational therapies and the identification of predictive markers. What the mechanisms are by which TAMs integrate external signals and translate them into a transcriptional program following chemotherapy are unclear and should be under active investigation. In conclusion, TAMs are promising pharmacological targets, but we need to gain a better understanding of the interactions of anti-cancer therapies with the innate and adaptive immune system. TAM-targeting compounds could pave the way for a better precision medicine approach and innovative combinations of conventional therapies. However, it will be critical to consider individual tumor profiles (tumor type, mutation status and the immune profiles of the tumor) to match with the appropriate immunomodulatory intervention.



## Scope of Thesis

Breast cancer is the most common type of cancer in women, representing 28% of all cancer cases ([www.cijfersoverkanker.nl](http://www.cijfersoverkanker.nl)). 1 in 8 women is estimated to receive a breast cancer diagnosis during her lifetime (<https://seer.cancer.gov/data/>). Breast cancer is a heterogeneous disease, which consists of five molecular subtypes: luminal-A, luminal-B, basal, HER2 positive and normal breast-like. Chemotherapy is one of the main therapeutic modalities for breast cancer patients, however, response rates vary, and resistance occurs among patients. In the past few decades, it has become clear that the tumor microenvironment plays an important role in cancer development, progression and therapy response. To improve the success rate of current therapies and to develop novel (immune)therapies we need to have a better understanding of the mechanisms underlying the crosstalk between cancer and the immune system. The overall goal of the research described in this thesis is to investigate the role of the adaptive and the innate immune system in breast cancer progression, metastasis formation and chemotherapy response. To study this, we use two independent spontaneous mouse models of mammary tumorigenesis representing two different subtypes of breast cancer:

1. The MMTV-*NeuT* mouse model: Oncogenic signaling of the human epidermal growth factor receptor-2 (*HER2/neu* or *ErbB2*), a proto-oncogene that belongs to a family of transmembrane receptor tyrosine kinases, has been shown to play a major role in 15%–20% of breast cancer patients<sup>215,216</sup>. Overexpression of HER2, due to amplification of the *HER2* gene, is an adverse prognostic factor associated with poorly differentiated, high-grade tumors, metastasis formation, relative resistance to certain chemotherapy regimens and greater risk of recurrence<sup>106,215</sup>. Anti-HER2 therapies have dramatically improved survival<sup>217</sup>. MMTV-*NeuT* transgenic mice express a mutated form of the rat *c-erbB-2* (*neuT*) oncogene under control of the mouse mammary tumor virus (MMTV) promoter. These mice develop metastatic mammary carcinomas within 4 months of age, which resemble human HER2<sup>+</sup> breast cancer<sup>218</sup>.

2. The *K14cre; Cdh1<sup>F/F</sup>; Trp53<sup>F/F</sup>* mouse model: Invasive lobular carcinoma (ILC), a histotype within luminal A breast cancer, is the second most common histotype of breast cancer after invasive ductal carcinoma and accounts for 5%–15% of all breast cancer cases<sup>219-221</sup>. ILC is often difficult to diagnose and less responsive to conventional chemotherapy<sup>221-223</sup>. Conditional

*K14cre; Cdh1<sup>F/F</sup>; Trp53<sup>F/F</sup>* mice have combined stochastic loss of E-cadherin and p53 in mammary- and skin epithelial cells, resulting around 6-8 months of age in the development of skin tumors and metastatic, invasive mammary carcinomas which resemble human ILCs <sup>222</sup>.

**Chapter 1** summarizes the current understanding of the paradoxical roles of adaptive and innate immune cells, with a focus on macrophages, in tumorigenesis and chemotherapy response. Here the limitations of our knowledge of current strategies targeting macrophages are being discussed. In addition, we propose that a better mechanistic understanding of the interactions between cancer cells and the immune landscape per cancer subtype, and upon therapy response is needed. In particular, more knowledge is needed about how cancer cell-intrinsic features shape the crosstalk with the immune system. These insights will provide a basis for the design of personalized immune intervention strategies for patients with cancer.

The role of the adaptive immune system in mammary tumorigenesis is only beginning to be understood. Different cancer types and subtypes have been shown to be regulated differently by the adaptive immune system <sup>98,102-104</sup>. In **Chapter 2** we elucidate the functional significance of the adaptive immune system during (pre-) malignant progression and pulmonary metastasis formation in MMTV-*NeuT* transgenic mice. By genetically eliminating the adaptive immune system from the transgenic MMTV-*NeuT* mouse model via intercrossing with *Rag2<sup>-/-</sup>* mice, lacking B and T lymphocytes <sup>91</sup>, we demonstrate that spontaneous HER2-driven mammary tumorigenesis and metastasis formation are neither suppressed nor promoted by the adaptive immune system. As outlined in detail in **Chapter 2**, the outcome of the interplay between the adaptive immune system and tumors is not only dependent on the tissue context, but also on the genetic pathways underlying tumor initiation and tumor maintenance.

Based on studies using tumor cell line transplantation models it has been reported that the adaptive immune system contributes to the therapeutic efficacy of certain chemotherapeutics via a process referred to as immunogenic cell death <sup>177</sup>. A major limitation of tumor models based on inoculation of cancer cells is that they do not resemble *de novo* tumors with co-evolving tumor-host interactions and an immunosuppressive microenvironment <sup>56</sup>. In **Chapter 3** we explore whether the adaptive immune system influences chemotherapy response of established spontaneous

mammary tumors in MMTV-*NeuT* and *K14cre*; *Cdh1<sup>F/F</sup>*; *Trp53<sup>F/F</sup>* mice. We intercrossed both mouse tumor models with T and B cell-deficient *Rag<sup>-/-</sup>* mice and treated tumor-bearing mice with various conventional chemotherapeutic drugs. In both mammary tumor models, the lack of T and B cells did not affect chemotherapy response. These data highlight that the role of the endogenous adaptive immune system in chemotherapy response might not be as crucial as proposed previously when using tumor cell line transplantation models <sup>177</sup>.

Currently, clinical trials testing various compounds targeting macrophages are ongoing in cancer patients <sup>137</sup>. However, essential questions still need to be addressed to maximize the clinical success of compounds that inhibit macrophage function. For example, it is unclear whether the influence of macrophages on the anti-cancer efficacy of chemotherapy depends on the type of chemotherapeutic drug used and what the exact mechanisms are by which these agents can increase the sensitivity of breast cancer to chemotherapeutic drugs. In **Chapter 4** we demonstrate that macrophage targeting through CSF1R blockade acts synergistically with platinum-containing drugs, but not with docetaxel, by inducing an intratumoral type 1 interferon response. The elimination of neutrophils further enhanced the beneficial effect of cisplatin and CSF1R blockade due to the activation of anti-tumor immunity.

Finally, in **Chapter 5**, the findings of this thesis are summarized and put into context of the current literature. I also discuss how the field may move forward to use immunomodulatory compounds in the clinical setting.

## References

- 1 Quail, D. F. & Joyce, J. A. Microenvironmental regulation of tumor progression and metastasis. *Nat Med* **19**, 1423-1437, doi:10.1038/nm.3394 (2013).
- 2 Wang, M. *et al.* Role of tumor microenvironment in tumorigenesis. *J Cancer* **8**, 761-773, doi:10.7150/jca.17648 (2017).
- 3 Pardoll, D. M. Immunology beats cancer: a blueprint for successful translation. *Nature immunology* **13**, 1129-1132, doi:10.1038/ni.2392 (2012).
- 4 Davis, I. D. An overview of cancer immunotherapy. *Immunol Cell Biol* **78**, 179-195, doi:10.1046/j.1440-1711.2000.00906.x (2000).
- 5 Rosenberg, S. A. Decade in review-cancer immunotherapy: entering the mainstream of cancer treatment. *Nat Rev Clin Oncol* **11**, 630-632, doi:10.1038/nrclinonc.2014.174 (2014).
- 6 Burnet, M. Cancer: a biological approach. III. Viruses associated with neoplastic conditions. IV. Practical applications. *British medical journal* **1**, 841-847 (1957).
- 7 Thomas, L. [Reaction of the spleen & thymus of rats to acid & basic nutrition]. *Zeitschrift fur mikroskopisch-anatomische Forschung* **65**, 45-58 (1959).
- 8 Alderton, G. K. & Bordon, Y. Tumour immunotherapy--leukocytes take up the fight. *Nature reviews. Immunology* **12**, 237 (2012).
- 9 Larkin, J. *et al.* Five-Year Survival with Combined Nivolumab and Ipilimumab in Advanced Melanoma. *N Engl J Med* **381**, 1535-1546, doi:10.1056/NEJMoa1910836 (2019).
- 10 Zhao, B., Zhao, H. & Zhao, J. Efficacy of PD-1/PD-L1 blockade monotherapy in clinical trials. *Ther Adv Med Oncol* **12**, 1758835920937612, doi:10.1177/1758835920937612 (2020).
- 11 Vaddepally, R. K., Kharel, P., Pandey, R., Garje, R. & Chandra, A. B. Review of Indications of FDA-Approved Immune Checkpoint Inhibitors per NCCN Guidelines with the Level of Evidence. *Cancers (Basel)* **12**, doi:10.3390/cancers12030738 (2020).
- 12 Kraehenbuehl, L., Weng, C. H., Eghbali, S., Wolchok, J. D. & Merghoub, T. Enhancing immunotherapy in cancer by targeting emerging immunomodulatory pathways. *Nat Rev Clin Oncol*, doi:10.1038/s41571-021-00552-7 (2021).
- 13 de Visser, K. E., Eichten, A. & Coussens, L. M. Paradoxical roles of the immune system during cancer development. *Nat Rev Cancer* **6**, 24-37, doi:10.1038/nrc1782 (2006).
- 14 Hanahan, D. & Coussens, L. M. Accessories to the crime: functions of cells recruited to the tumor microenvironment. *Cancer Cell* **21**, 309-322, doi:10.1016/j.ccr.2012.02.022 (2012).
- 15 Vilgelm, A. E. & Richmond, A. Chemokines Modulate Immune Surveillance in Tumorigenesis, Metastasis, and Response to Immunotherapy. *Front Immunol* **10**, 333, doi:10.3389/fimmu.2019.00333 (2019).
- 16 Hiam-Galvez, K. J., Allen, B. M. & Spitzer, M. H. Systemic immunity in cancer. *Nat Rev Cancer* **21**, 345-359, doi:10.1038/s41568-021-00347-z (2021).

- 17 Schmidt, A. & Weber, O. F. In memoriam of Rudolf Virchow: a historical retrospective including aspects of inflammation, infection and neoplasia. *Contrib Microbiol* **13**, 1-15, doi:10.1159/000092961 (2006).
- 18 Hanahan, D. & Weinberg, R. A. Hallmarks of cancer: the next generation. *Cell* **144**, 646-674, doi:S0092-8674(11)00127-9 [pii]0.1016/j.cell.2011.02.013 (2011).
- 19 Wroblewski, L. E., Peek, R. M., Jr. & Wilson, K. T. Helicobacter pylori and gastric cancer: factors that modulate disease risk. *Clin Microbiol Rev* **23**, 713-739, doi:10.1128/CMR.00011-10 (2010).
- 20 Mantovani, A., Allavena, P., Sica, A. & Balkwill, F. Cancer-related inflammation. *Nature* **454**, 436-444 (2008).
- 21 Coussens, L. M. & Werb, Z. Inflammation and cancer. *Nature* **420**, 860-867 (2002).
- 22 Dostert, C. *et al.* Innate immune activation through Nalp3 inflammasome sensing of asbestos and silica. *Science* **320**, 674-677, doi:10.1126/science.1156995 (2008).
- 23 Punturieri, A., Szabo, E., Croxton, T. L., Shapiro, S. D. & Dubinett, S. M. Lung cancer and chronic obstructive pulmonary disease: needs and opportunities for integrated research. *Journal of the National Cancer Institute* **101**, 554-559, doi:10.1093/jnci/djp023 (2009).
- 24 Liu, G., Cheresch, P. & Kamp, D. W. Molecular basis of asbestos-induced lung disease. *Annu Rev Pathol* **8**, 161-187, doi:10.1146/annurev-pathol-020712-163942 (2013).
- 25 Waldner, M. J. & Neurath, M. F. Colitis-associated cancer: the role of T cells in tumor development. *Seminars in Immunopathology* **31**, 249-256, doi:10.1007/s00281-009-0161-8 (2009).
- 26 Shacter, E. & Weitzman, S. A. Chronic inflammation and cancer. *Oncology (Williston Park, N.Y.)* **16**, 217-226, 229; discussion 230 (2002).
- 27 Dalglish, A. G. & O'Byrne, K. J. in *Advances in Cancer Research* Vol. 84 231-276 (2002).
- 28 Barcellos-Hoff, M. H., Lyden, D. & Wang, T. C. The evolution of the cancer niche during multistage carcinogenesis. *Nat Rev Cancer* **13**, 511-518, doi:10.1038/nrc3536 (2013).
- 29 Dvorak, H. F. Tumors: wounds that do not heal. Similarities between tumor stroma generation and wound healing. *N Engl J Med* **315**, 1650-1659, doi:10.1056/NEJM198612253152606 (1986).
- 30 Germolec, D. R., Shipkowski, K. A., Frawley, R. P. & Evans, E. Markers of Inflammation. *Methods Mol Biol* **1803**, 57-79, doi:10.1007/978-1-4939-8549-4\_5 (2018).
- 31 Zhang, Q. W. *et al.* Prognostic significance of tumor-associated macrophages in solid tumor: a meta-analysis of the literature. *PLoS One* **7**, e50946, doi:10.1371/journal.pone.0050946 (2012).
- 32 Zhao, X. *et al.* Prognostic significance of tumor-associated macrophages in breast cancer: a meta-analysis of the literature. *Oncotarget* **8**, 30576-30586, doi:10.18632/oncotarget.15736 (2017).

- 33 Yagi, T. *et al.* Tumour-associated macrophages are associated with poor prognosis and programmed death ligand 1 expression in oesophageal cancer. *Eur J Cancer* **111**, 38-49, doi:10.1016/j.ejca.2019.01.018 (2019).
- 34 Shaul, M. E. & Fridlender, Z. G. Tumour-associated neutrophils in patients with cancer. *Nat Rev Clin Oncol* **16**, 601-620, doi:10.1038/s41571-019-0222-4 (2019).
- 35 Kos, K. & de Visser, K. E. The Multifaceted Role of Regulatory T Cells in Breast Cancer. *Annu Rev Cancer Biol* **5**, 291-310, doi:10.1146/annurev-cancerbio-042920-104912 (2021).
- 36 Algra, A. M. & Rothwell, P. M. Effects of regular aspirin on long-term cancer incidence and metastasis: a systematic comparison of evidence from observational studies versus randomised trials. *The lancet oncology* **13**, 518-527, doi:10.1016/S1470-2045(12)70112-2 (2012).
- 37 Rothwell, P. M. *et al.* Short-term effects of daily aspirin on cancer incidence, mortality, and non-vascular death: analysis of the time course of risks and benefits in 51 randomised controlled trials. *Lancet* **379**, 1602-1612, doi:10.1016/S0140-6736(11)61720-0 (2012).
- 38 Clark, W. H., Jr. *et al.* Model predicting survival in stage I melanoma based on tumor progression. *J Natl Cancer Inst* **81**, 1893-1904 (1989).
- 39 Galon, J. *et al.* Type, density, and location of immune cells within human colorectal tumors predict clinical outcome. *Science* **313**, 1960-1964 (2006).
- 40 Laghi, L. *et al.* CD3+ cells at the invasive margin of deeply invading (pT3-T4) colorectal cancer and risk of post-surgical metastasis: a longitudinal study. *The lancet oncology* **10**, 877-884, doi:10.1016/S1470-2045(09)70186-X (2009).
- 41 Clemente, C. G. *et al.* Prognostic value of tumor infiltrating lymphocytes in the vertical growth phase of primary cutaneous melanoma. *Cancer* **77**, 1303-1310, doi:10.1002/(SICI)1097-0142(19960401)77:7<1303::AID-CNCR12>3.0.CO;2-5 (1996).
- 42 Scanlan, M. J., Simpson, A. J. & Old, L. J. The cancer/testis genes: review, standardization, and commentary. *Cancer Immun* **4**, 1 (2004).
- 43 Chen, Z. *et al.* Intratumoral CD8(+) cytotoxic lymphocyte is a favorable prognostic marker in node-negative breast cancer. *PLoS One* **9**, e95475, doi:10.1371/journal.pone.0095475 (2014).
- 44 Engels, E. A. & Goedert, J. J. Human immunodeficiency virus/acquired immunodeficiency syndrome and cancer: past, present, and future. *J Natl Cancer Inst* **97**, 407-409, doi:10.1093/jnci/dji085 (2005).
- 45 Ippoliti, G., Rinaldi, M., Pellegrini, C. & Viganò, M. Incidence of cancer after immunosuppressive treatment for heart transplantation. *Critical Reviews in Oncology/Hematology* **56**, 101-113 (2005).
- 46 Garc a-a-Vallejo, F., Dom nguez, M. C. & Tamayo, O. Autoimmunity and molecular mimicry in tropical spastic paraparesis/human T-lymphotropic virus-associated myelopathy. *Brazilian Journal of Medical and Biological Research* **38**, 241-250 (2005).

- 47 Gallagher, B., Wang, Z., Schymura, M. J., Kahn, A. & Fordyce, E. J. Cancer incidence in New York State acquired immunodeficiency syndrome patients. *Am J Epidemiol* **154**, 544-556 (2001).
- 48 Chapman, J. R., Webster, A. C. & Wong, G. Cancer in the transplant recipient. *Cold Spring Harb Perspect Med* **3**, doi:10.1101/cshperspect.a015677 (2013).
- 49 Stanton, S. E., Adams, S. & Disis, M. L. Variation in the Incidence and Magnitude of Tumor-Infiltrating Lymphocytes in Breast Cancer Subtypes: A Systematic Review. *JAMA Oncol* **2**, 1354-1360, doi:10.1001/jamaoncol.2016.1061 (2016).
- 50 Savas, P. *et al.* Clinical relevance of host immunity in breast cancer: from TILs to the clinic. *Nature reviews. Clinical oncology* **13**, 228-241, doi:10.1038/nrclinonc.2015.215 (2016).
- 51 Stewart, T., Tsai, S. C., Grayson, H., Henderson, R. & Opelz, G. Incidence of de-novo breast cancer in women chronically immunosuppressed after organ transplantation. *Lancet* **346**, 796-798 (1995).
- 52 Engels, E. A. *et al.* Spectrum of cancer risk among US solid organ transplant recipients. *JAMA* **306**, 1891-1901, doi:10.1001/jama.2011.1592 (2011).
- 53 Gentles, A. J. *et al.* The prognostic landscape of genes and infiltrating immune cells across human cancers. *Nature medicine* **21**, 938-945, doi:10.1038/nm.3909 (2015).
- 54 Wellenstein, M. D. & de Visser, K. E. Cancer-Cell-Intrinsic Mechanisms Shaping the Tumor Immune Landscape. *Immunity* **48**, 399-416, doi:10.1016/j.immuni.2018.03.004 (2018).
- 55 Chen, D. S. & Mellman, I. Oncology meets immunology: the cancer-immunity cycle. *Immunity* **39**, 1-10, doi:10.1016/j.immuni.2013.07.012 (2013).
- 56 de Ruiter, J. R., Wessels, L. F. A. & Jonkers, J. Mouse models in the era of large human tumour sequencing studies. *Open Biol* **8**, doi:10.1098/rsob.180080 (2018).
- 57 Frese, K. K. & Tuveson, D. A. Maximizing mouse cancer models. *Nat Rev Cancer* **7**, 645-658, doi:10.1038/nrc2192 (2007).
- 58 Schreiber, K., Rowley, D. A., Riethmuller, G. & Schreiber, H. Cancer immunotherapy and preclinical studies: why we are not wasting our time with animal experiments. *Hematology/oncology clinics of North America* **20**, 567-584, doi:10.1016/j.hoc.2006.03.001 (2006).
- 59 Olive, K. P. *et al.* Inhibition of Hedgehog signaling enhances delivery of chemotherapy in a mouse model of pancreatic cancer. *Science* **324**, 1457-1461, doi:1171362 [pii] 10.1126/science.1171362 (2009).
- 60 Devaud, C. *et al.* Tissues in different anatomical sites can sculpt and vary the tumor microenvironment to affect responses to therapy. *Molecular therapy : the journal of the American Society of Gene Therapy* **22**, 18-27, doi:10.1038/mt.2013.219 (2014).
- 61 Husemann, Y. *et al.* Systemic spread is an early step in breast cancer. *Cancer Cell* **13**, 58-68, doi:10.1016/j.ccr.2007.12.003 (2008).
- 62 Engel, J. *et al.* The process of metastatisation for breast cancer. *Eur J Cancer* **39**, 1794-1806 (2003).

- 63 Siolas, D. & Hannon, G. J. Patient-derived tumor xenografts: transforming clinical samples into mouse models. *Cancer Res* **73**, 5315-5319, doi:10.1158/0008-5472.CAN-13-1069 (2013).
- 64 Gao, H. *et al.* High-throughput screening using patient-derived tumor xenografts to predict clinical trial drug response. *Nature medicine* **21**, 1318-1325, doi:10.1038/nm.3954 (2015).
- 65 Morton, J. J., Bird, G., Refaeli, Y. & Jimeno, A. Humanized Mouse Xenograft Models: Narrowing the Tumor-Microenvironment Gap. *Cancer Res* **76**, 6153-6158, doi:10.1158/0008-5472.CAN-16-1260 (2016).
- 66 Yin, L., Wang, X. J., Chen, D. X., Liu, X. N. & Wang, X. J. Humanized mouse model: a review on preclinical applications for cancer immunotherapy. *Am J Cancer Res* **10**, 4568-4584 (2020).
- 67 Singh, M. *et al.* Assessing therapeutic responses in Kras mutant cancers using genetically engineered mouse models. *Nat Biotechnol* **28**, 585-593, doi:nbt.1640 [pii] 10.1038/nbt.1640 (2010).
- 68 Singh, M. & Ferrara, N. Modeling and predicting clinical efficacy for drugs targeting the tumor milieu. *Nat Biotechnol* **30**, 648-657, doi:10.1038/nbt.2286 (2012).
- 69 De Palma, M. & Hanahan, D. The biology of personalized cancer medicine: facing individual complexities underlying hallmark capabilities. *Molecular oncology* **6**, 111-127, doi:10.1016/j.molonc.2012.01.011 (2012).
- 70 Kersten, K., de Visser, K. E., van Miltenburg, M. H. & Jonkers, J. Genetically engineered mouse models in oncology research and cancer medicine. *EMBO Mol Med* **9**, 137-153, doi:10.15252/emmm.201606857 (2017).
- 71 Cong, L. *et al.* Multiplex genome engineering using CRISPR/Cas systems. *Science* **339**, 819-823, doi:10.1126/science.1231143 (2013).
- 72 Sanchez-Rivera, F. J. & Jacks, T. Applications of the CRISPR-Cas9 system in cancer biology. *Nat Rev Cancer* **15**, 387-395, doi:10.1038/nrc3950 (2015).
- 73 Maresch, R. *et al.* Multiplexed pancreatic genome engineering and cancer induction by transfection-based CRISPR/Cas9 delivery in mice. *Nat Commun* **7**, 10770, doi:10.1038/ncomms10770 (2016).
- 74 Dominguez, A. A., Lim, W. A. & Qi, L. S. Beyond editing: repurposing CRISPR-Cas9 for precision genome regulation and interrogation. *Nat Rev Mol Cell Biol* **17**, 5-15, doi:10.1038/nrm.2015.2 (2016).
- 75 Lamprecht Tratar, U., Horvat, S. & Cemazar, M. Transgenic Mouse Models in Cancer Research. *Front Oncol* **8**, 268, doi:10.3389/fonc.2018.00268 (2018).
- 76 Ciampricotti, M. *et al.* Rlf-Mycl gene fusion drives tumorigenesis and metastasis in a mouse model of small cell lung cancer. *Cancer Discov*, doi:10.1158/2159-8290.CD-21-0441 (2021).
- 77 Wang, D. *et al.* Adenovirus-Mediated Somatic Genome Editing of Pten by CRISPR/Cas9 in Mouse Liver in Spite of Cas9-Specific Immune Responses. *Human gene therapy* **26**, 432-442, doi:10.1089/hum.2015.087 (2015).
- 78 Annunziato, S. *et al.* Modeling invasive lobular breast carcinoma by CRISPR/Cas9-mediated somatic genome editing of the mammary gland. *Genes & development* **30**, 1470-1480, doi:10.1101/gad.279190.116 (2016).

- 79 Ajina, R. *et al.* SpCas9-expression by tumor cells can cause T cell-dependent tumor rejection in immunocompetent mice. *Oncoimmunology* **8**, e1577127, doi:10.1080/2162402X.2019.1577127 (2019).
- 80 LaFleur, M. W. *et al.* A CRISPR-Cas9 delivery system for in vivo screening of genes in the immune system. *Nat Commun* **10**, 1668, doi:10.1038/s41467-019-09656-2 (2019).
- 81 Kim, R., Emi, M. & Tanabe, K. Cancer immunoediting from immune surveillance to immune escape. *Immunology* **121**, 1-14, doi:10.1111/j.1365-2567.2007.02587.x (2007).
- 82 Burnet, F. M. The concept of immunological surveillance. Progress in experimental tumor research. Fortschritte der experimentellen Tumorforschung. Progres de la recherche experimentale des tumeurs **13**, 1-27 (1970).
- 83 Zhang, Z. *et al.* Neoantigen: A New Breakthrough in Tumor Immunotherapy. *Front Immunol* **12**, 672356, doi:10.3389/fimmu.2021.672356 (2021).
- 84 Motwani, M., Pesiridis, S. & Fitzgerald, K. A. DNA sensing by the cGAS-STING pathway in health and disease. *Nat Rev Genet*, doi:10.1038/s41576-019-0151-1 (2019).
- 85 Fuertes, M. B., Woo, S. R., Burnett, B., Fu, Y. X. & Gajewski, T. F. Type I interferon response and innate immune sensing of cancer. *Trends Immunol* **34**, 67-73, doi:10.1016/j.it.2012.10.004 (2013).
- 86 Woo, S. R. *et al.* STING-dependent cytosolic DNA sensing mediates innate immune recognition of immunogenic tumors. *Immunity* **41**, 830-842, doi:10.1016/j.immuni.2014.10.017 (2014).
- 87 Deng, L. *et al.* STING-Dependent Cytosolic DNA Sensing Promotes Radiation-Induced Type I Interferon-Dependent Antitumor Immunity in Immunogenic Tumors. *Immunity* **41**, 843-852, doi:10.1016/j.immuni.2014.10.019 (2014).
- 88 Corrales, L. *et al.* Direct Activation of STING in the Tumor Microenvironment Leads to Potent and Systemic Tumor Regression and Immunity. *Cell Rep* **11**, 1018-1030, doi:10.1016/j.celrep.2015.04.031 (2015).
- 89 Kwon, J. & Bakhoun, S. F. The Cytosolic DNA-Sensing cGAS-STING Pathway in Cancer. *Cancer Discov* **10**, 26-39, doi:10.1158/2159-8290.CD-19-0761 (2020).
- 90 Shankaran, V. *et al.* IFN $\gamma$ , and lymphocytes prevent primary tumour development and shape tumour immunogenicity. *Nature* **410**, 1107-1111 (2001).
- 91 Mombaerts, P. *et al.* RAG-1-deficient mice have no mature B and T lymphocytes. *Cell* **68**, 869-877. (1992).
- 92 Egen, J. G., Ouyang, W. & Wu, L. C. Human Anti-tumor Immunity: Insights from Immunotherapy Clinical Trials. *Immunity* **52**, 36-54, doi:10.1016/j.immuni.2019.12.010 (2020).
- 93 Dunn, G. P., Old, L. J. & Schreiber, R. D. The immunobiology of cancer immunosurveillance and immunoediting. *Immunity* **21**, 137-148 (2004).
- 94 Koebel, C. M. *et al.* Adaptive immunity maintains occult cancer in an equilibrium state. *Nature* **450**, 903-907 (2007).

- 95 Shiao, S. L., Ganesan, A. P., Rugo, H. S. & Coussens, L. M. Immune microenvironments in solid tumors: new targets for therapy. *Genes & development* **25**, 2559-2572, doi:25/24/2559 [pii] 10.1101/gad.169029.111 (2011).
- 96 de Visser, K. E., Korets, L. V. & Coussens, L. M. De novo carcinogenesis promoted by chronic inflammation is B lymphocyte dependent. *Cancer Cell* **7**, 411-423 (2005).
- 97 Haybaeck, J. *et al.* A lymphotoxin-driven pathway to hepatocellular carcinoma. *Cancer Cell* **16**, 295-308, doi:S1535-6108(09)00294-3 [pii] 10.1016/j.ccr.2009.08.021 (2009).
- 98 DeNardo, D. G. *et al.* CD4(+) T cells regulate pulmonary metastasis of mammary carcinomas by enhancing protumor properties of macrophages. *Cancer Cell* **16**, 91-102, doi:S1535-6108(09)00216-5 [pii] 10.1016/j.ccr.2009.06.018 (2009).
- 99 Andreu, P. *et al.* FcRgamma activation regulates inflammation-associated squamous carcinogenesis. *Cancer Cell* **17**, 121-134, doi:S1535-6108(09)00431-0 [pii] 10.1016/j.ccr.2009.12.019 (2010).
- 100 Willimsky, G. & Blankenstein, T. Sporadic immunogenic tumours avoid destruction by inducing T-cell tolerance. *Nature* **437**, 141-146 (2005).
- 101 Casanovas, O., Hicklin, D. J., Bergers, G. & Hanahan, D. Drug resistance by evasion of antiangiogenic targeting of VEGF signaling in late-stage pancreatic islet tumors. *Cancer Cell* **8**, 299-309 (2005).
- 102 Tan, W. *et al.* Tumour-infiltrating regulatory T cells stimulate mammary cancer metastasis through RANKL-RANK signalling. *Nature* **470**, 548-553, doi:10.1038/nature09707 (2011).
- 103 Coffelt, S. B. *et al.* IL-17-producing gammadelta T cells and neutrophils conspire to promote breast cancer metastasis. *Nature* **522**, 345-348, doi:10.1038/nature14282 (2015).
- 104 Wellenstein, M. D. *et al.* Loss of p53 triggers WNT-dependent systemic inflammation to drive breast cancer metastasis. *Nature*, doi:10.1038/s41586-019-1450-6 (2019).
- 105 Kersten, K. *et al.* Mammary tumor-derived CCL2 enhances pro-metastatic systemic inflammation through upregulation of IL1beta in tumor-associated macrophages. *Oncoimmunology* **6**, e1334744, doi:10.1080/2162402X.2017.1334744 (2017).
- 106 Burstein, H. J. The distinctive nature of HER2-positive breast cancers. *N Engl J Med* **353**, 1652-1654 (2005).
- 107 Desmedt, C. *et al.* Biological processes associated with breast cancer clinical outcome depend on the molecular subtypes. *Clin Cancer Res* **14**, 5158-5165, doi:14/16/5158 [pii] 10.1158/1078-0432.CCR-07-4756 (2008).
- 108 Gordon, S. Elie Metchnikoff, the Man and the Myth. *J Innate Immun* **8**, 223-227, doi:10.1159/000443331 (2016).
- 109 Mantovani, A., Marchesi, F., Malesci, A., Laghi, L. & Allavena, P. Tumour-associated macrophages as treatment targets in oncology. *Nat Rev Clin Oncol* **14**, 399-416, doi:10.1038/nrclinonc.2016.217 (2017).

- 110 Guc, E. & Pollard, J. W. Redefining macrophage and neutrophil biology in the metastatic cascade. *Immunity* **54**, 885-902, doi:10.1016/j.immuni.2021.03.022 (2021).
- 111 Kersten, K. *et al.* Spatiotemporal co-dependency between macrophages and exhausted CD8(+) T cells in cancer. *Cancer Cell*, doi:10.1016/j.ccell.2022.05.004 (2022).
- 112 Schulz, R. *et al.* Inhibiting the HSP90 chaperone destabilizes macrophage migration inhibitory factor and thereby inhibits breast tumor progression. *The Journal of experimental medicine* **209**, 275-289, doi:10.1084/jem.20111117 (2012).
- 113 Wynn, T. A., Chawla, A. & Pollard, J. W. Macrophage biology in development, homeostasis and disease. *Nature* **496**, 445-455, doi:10.1038/nature12034 (2013).
- 114 Epelman, S., Lavine, K. J. & Randolph, G. J. Origin and functions of tissue macrophages. *Immunity* **41**, 21-35, doi:10.1016/j.immuni.2014.06.013 (2014).
- 115 Lavin, Y., Mortha, A., Rahman, A. & Merad, M. Regulation of macrophage development and function in peripheral tissues. *Nat Rev Immunol* **15**, 731-744, doi:10.1038/nri3920 (2015).
- 116 Chen, Z. *et al.* Cellular and Molecular Identity of Tumor-Associated Macrophages in Glioblastoma. *Cancer Res* **77**, 2266-2278, doi:10.1158/0008-5472.CAN-16-2310 (2017).
- 117 Zhu, Y. *et al.* Tissue-Resident Macrophages in Pancreatic Ductal Adenocarcinoma Originate from Embryonic Hematopoiesis and Promote Tumor Progression. *Immunity* **47**, 323-338 e326, doi:10.1016/j.immuni.2017.07.014 (2017).
- 118 Loyher, P. L. *et al.* Macrophages of distinct origins contribute to tumor development in the lung. *The Journal of experimental medicine* **215**, 2536-2553, doi:10.1084/jem.20180534 (2018).
- 119 Casanova-Acebes, M. *et al.* Tissue-resident macrophages provide a pro-tumorigenic niche to early NSCLC cells. *Nature* **595**, 578-584, doi:10.1038/s41586-021-03651-8 (2021).
- 120 Franklin, R. A. *et al.* The cellular and molecular origin of tumor-associated macrophages. *Science* **344**, 921-925, doi:10.1126/science.1252510 (2014).
- 121 Engblom, C., Pfirschke, C. & Pittet, M. J. The role of myeloid cells in cancer therapies. *Nat Rev Cancer* **16**, 447-462, doi:10.1038/nrc.2016.54 (2016).
- 122 Mills, C. D., Kincaid, K., Alt, J. M., Heilman, M. J. & Hill, A. M. M-1/M-2 macrophages and the Th1/Th2 paradigm. *J Immunol* **164**, 6166-6173 (2000).
- 123 Biswas, S. K. & Mantovani, A. Macrophage plasticity and interaction with lymphocyte subsets: cancer as a paradigm. *Nature immunology* **11**, 889-896, doi:ni.1937 [pii] 10.1038/ni.1937 (2010).
- 124 Murray, P. J. *et al.* Macrophage Activation and Polarization: Nomenclature and Experimental Guidelines. *Immunity* **41**, 14-20, doi:10.1016/j.immuni.2014.06.008 (2014).

- 125 Chimal-Ramirez, G. K., Espinoza-Sanchez, N. A., Chavez-Sanchez, L., Arriaga-Pizano, L. & Fuentes-Panana, E. M. Monocyte Differentiation towards Protumor Activity Does Not Correlate with M1 or M2 Phenotypes. *Journal of immunology research* **2016**, 6031486, doi:10.1155/2016/6031486 (2016).
- 126 Vallerand, D. *et al.* Characterization of Breast Cancer Preclinical Models Reveals a Specific Pattern of Macrophage Polarization. *PLoS One* **11**, e0157670, doi:10.1371/journal.pone.0157670 (2016).
- 127 Ginhoux, F., Schultze, J. L., Murray, P. J., Ochando, J. & Biswas, S. K. New insights into the multidimensional concept of macrophage ontogeny, activation and function. *Nature immunology* **17**, 34-40, doi:10.1038/ni.3324 (2016).
- 128 Azizi, E. *et al.* Single-Cell Map of Diverse Immune Phenotypes in the Breast Tumor Microenvironment. *Cell* **174**, 1293-1308 e1236, doi:10.1016/j.cell.2018.05.060 (2018).
- 129 Muller, S. *et al.* Single-cell profiling of human gliomas reveals macrophage ontogeny as a basis for regional differences in macrophage activation in the tumor microenvironment. *Genome Biol* **18**, 234, doi:10.1186/s13059-017-1362-4 (2017).
- 130 Lavin, Y. *et al.* Tissue-resident macrophage enhancer landscapes are shaped by the local microenvironment. *Cell* **159**, 1312-1326, doi:10.1016/j.cell.2014.11.018 (2014).
- 131 Laviron, M. *et al.* Tumor-associated macrophage heterogeneity is driven by tissue territories in breast cancer. *Cell Rep* **39**, 110865, doi:10.1016/j.celrep.2022.110865 (2022).
- 132 Zilionis, R. *et al.* Single-Cell Transcriptomics of Human and Mouse Lung Cancers Reveals Conserved Myeloid Populations across Individuals and Species. *Immunity* **50**, 1317-1334 e1310, doi:10.1016/j.immuni.2019.03.009 (2019).
- 133 Bischoff, P. *et al.* Single-cell RNA sequencing reveals distinct tumor microenvironmental patterns in lung adenocarcinoma. *Oncogene*, doi:10.1038/s41388-021-02054-3 (2021).
- 134 Xing, X. *et al.* Decoding the multicellular ecosystem of lung adenocarcinoma manifested as pulmonary subsolid nodules by single-cell RNA sequencing. *Sci Adv* **7**, doi:10.1126/sciadv.abd9738 (2021).
- 135 Liao, S. Y. *et al.* Single-cell RNA sequencing identifies macrophage transcriptional heterogeneities in granulomatous diseases. *Eur Respir J* **57**, doi:10.1183/13993003.03794-2020 (2021).
- 136 Tuit, S. *et al.* Transcriptional Signature Derived from Murine Tumor-Associated Macrophages Correlates with Poor Outcome in Breast Cancer Patients. *Cell Rep* **29**, 1221-1235 e1225, doi:10.1016/j.celrep.2019.09.067 (2019).
- 137 Kowal, J., Kornete, M. & Joyce, J. A. Re-education of macrophages as a therapeutic strategy in cancer. *Immunotherapy* **11**, 677-689, doi:10.2217/imt-2018-0156 (2019).

- 138 Pixley, F. J. & Stanley, E. R. CSF-1 regulation of the wandering macrophage: complexity in action. *Trends Cell Biol* **14**, 628-638, doi:10.1016/j.tcb.2004.09.016 (2004).
- 139 Stanley, E. R., Guilbert, L. J., Tushinski, R. J. & Bartelmez, S. H. CSF-1--a mononuclear phagocyte lineage-specific hemopoietic growth factor. *J Cell Biochem* **21**, 151-159, doi:10.1002/jcb.240210206 (1983).
- 140 Lin, E. Y., Nguyen, A. V., Russell, R. G. & Pollard, J. W. Colony-stimulating factor 1 promotes progression of mammary tumors to malignancy. *J Exp Med* **193**, 727-740 (2001).
- 141 Oguma, K. *et al.* Activated macrophages promote Wnt signalling through tumour necrosis factor- $\alpha$  in gastric tumour cells. *EMBO J* **27**, 1671-1681, doi:emboj2008105 [pii] 10.1038/emboj.2008.105 (2008).
- 142 Aharinejad, S. *et al.* Colony-stimulating factor-1 blockade by antisense oligonucleotides and small interfering RNAs suppresses growth of human mammary tumor xenografts in mice. *Cancer Res* **64**, 5378-5384, doi:10.1158/0008-5472.CAN-04-0961 (2004).
- 143 Abraham, D. *et al.* Stromal cell-derived CSF-1 blockade prolongs xenograft survival of CSF-1-negative neuroblastoma. *Int J Cancer* **126**, 1339-1352, doi:10.1002/ijc.24859 (2010).
- 144 Ryder, M. *et al.* Genetic and pharmacological targeting of CSF-1/CSF-1R inhibits tumor-associated macrophages and impairs BRAF-induced thyroid cancer progression. *PLoS One* **8**, e54302, doi:10.1371/journal.pone.0054302 PONE-D-12-29549 [pii] (2013).
- 145 Pyonteck, S. M. *et al.* CSF-1R inhibition alters macrophage polarization and blocks glioma progression. *Nature medicine* **19**, 1264-1272, doi:10.1038/nm.3337 (2013).
- 146 Strachan, D. C. *et al.* CSF1R inhibition delays cervical and mammary tumor growth in murine models by attenuating the turnover of tumor-associated macrophages and enhancing infiltration by CD8 T cells. *Oncimmunology* **2**, e26968, doi:10.4161/onci.26968 2013ONCOIMM0278R [pii] (2013).
- 147 Mitchem, J. B. *et al.* Targeting tumor-infiltrating macrophages decreases tumor-initiating cells, relieves immunosuppression, and improves chemotherapeutic responses. *Cancer Res* **73**, 1128-1141, doi:0008-5472.CAN-12-2731 [pii] 10.1158/0008-5472.CAN-12-2731 (2013).
- 148 Holmgaard, R. B., Zamarin, D., Lesokhin, A., Merghoub, T. & Wolchok, J. D. Targeting myeloid-derived suppressor cells with colony stimulating factor-1 receptor blockade can reverse immune resistance to immunotherapy in indoleamine 2,3-dioxygenase-expressing tumors. *EBioMedicine* **6**, 50-58, doi:10.1016/j.ebiom.2016.02.024 (2016).
- 149 Lin, E. Y. *et al.* Macrophages regulate the angiogenic switch in a mouse model of breast cancer. *Cancer Res* **66**, 11238-11246, doi:10.1158/0008-5472.CAN-06-1278 (2006).
- 150 Casbon, A. J., Lohela, M. & Werb, Z. Delineating CSF-1-dependent regulation of myeloid cell diversity in tumors. *Oncimmunology* **4**, e1008871, doi:10.1080/2162402X.2015.1008871 (2015).

- 151 DeNardo, D. G. *et al.* Leukocyte complexity predicts breast cancer survival and functionally regulates response to chemotherapy. *Cancer Discov* **1**, 54-67, doi:10.1158/2159-8274.Cd-10-0028 (2011).
- 152 Candido, J. B. *et al.* CSF1R(+) Macrophages Sustain Pancreatic Tumor Growth through T Cell Suppression and Maintenance of Key Gene Programs that Define the Squamous Subtype. *Cell Rep* **23**, 1448-1460, doi:10.1016/j.celrep.2018.03.131 (2018).
- 153 Lohela, M. *et al.* Intravital imaging reveals distinct responses of depleting dynamic tumor-associated macrophage and dendritic cell subpopulations. *Proc Natl Acad Sci U S A* **111**, E5086-5095, doi:10.1073/pnas.1419899111 (2014).
- 154 Prada, C. E. *et al.* Neurofibroma-associated macrophages play roles in tumor growth and response to pharmacological inhibition. *Acta Neuropathol* **125**, 159-168, doi:10.1007/s00401-012-1056-7 (2013).
- 155 Swierczak, A. *et al.* The promotion of breast cancer metastasis caused by inhibition of CSF-1R/CSF-1 signaling is blocked by targeting the G-CSF receptor. *Cancer Immunol Res* **2**, 765-776, doi:10.1158/2326-6066.CIR-13-0190 (2014).
- 156 Pfirschke, C. *et al.* Macrophage-Targeted Therapy Unlocks Antitumoral Cross-talk between IFN $\gamma$ -Secreting Lymphocytes and IL12-Producing Dendritic Cells. *Cancer Immunol Res* **10**, 40-55, doi:10.1158/2326-6066.CIR-21-0326 (2022).
- 157 Ries, C. H. *et al.* Targeting tumor-associated macrophages with anti-CSF-1R antibody reveals a strategy for cancer therapy. *Cancer Cell* **25**, 846-859, doi:10.1016/j.ccr.2014.05.016 (2014).
- 158 Ries, C. H., Hoves, S., Cannarile, M. A. & Ruttinger, D. CSF-1/CSF-1R targeting agents in clinical development for cancer therapy. *Curr Opin Pharmacol* **23**, 45-51, doi:10.1016/j.coph.2015.05.008 (2015).
- 159 Cassier, P. A. *et al.* CSF1R inhibition with emactuzumab in locally advanced diffuse-type tenosynovial giant cell tumours of the soft tissue: a dose-escalation and dose-expansion phase 1 study. *The Lancet. Oncology* **16**, 949-956, doi:10.1016/S1470-2045(15)00132-1 (2015).
- 160 von Tresckow, B. *et al.* An Open-Label, Multicenter, Phase I/II Study of JNJ-40346527, a CSF-1R Inhibitor, in Patients with Relapsed or Refractory Hodgkin Lymphoma. *Clin Cancer Res* **21**, 1843-1850, doi:10.1158/1078-0432.CCR-14-1845 (2015).
- 161 Cannarile, M. A. *et al.* Colony-stimulating factor 1 receptor (CSF1R) inhibitors in cancer therapy. *J Immunother Cancer* **5**, 53, doi:10.1186/s40425-017-0257-y (2017).
- 162 Swierczak, A. *et al.* The Promotion of Breast Cancer Metastasis Caused by Inhibition of CSF-1R/CSF-1 Signaling Is Blocked by Targeting the G-CSF Receptor. *Cancer Immunol Res*, doi:10.1158/2326-6066.CIR-13-0190 (2014).
- 163 Quail, D. F. *et al.* The tumor microenvironment underlies acquired resistance to CSF-1R inhibition in gliomas. *Science* **352**, aad3018, doi:10.1126/science.aad3018 (2016).

- 164 van der Sluis, T. C. *et al.* Therapeutic Peptide Vaccine-Induced CD8 T Cells Strongly Modulate Intratumoral Macrophages Required for Tumor Regression. *Cancer Immunol Res* **3**, 1042-1051, doi:10.1158/2326-6066.CIR-15-0052 (2015).
- 165 Baer, C. *et al.* Suppression of microRNA activity amplifies IFN-gamma-induced macrophage activation and promotes anti-tumour immunity. *Nat Cell Biol* **18**, 790-802, doi:10.1038/ncb3371 (2016).
- 166 Guerriero, J. L. *et al.* Class IIa HDAC inhibition reduces breast tumours and metastases through anti-tumour macrophages. *Nature* **543**, 428-432, doi:10.1038/nature21409 (2017).
- 167 Gomez-Roca, C. *et al.* Anti-CSF-1R emactuzumab in combination with anti-PD-L1 atezolizumab in advanced solid tumor patients naive or experienced for immune checkpoint blockade. *J Immunother Cancer* **10**, doi:10.1136/jitc-2021-004076 (2022).
- 168 Sloas, C., Gill, S. & Klichinsky, M. Engineered CAR-Macrophages as Adoptive Immunotherapies for Solid Tumors. *Front Immunol* **12**, 783305, doi:10.3389/fimmu.2021.783305 (2021).
- 169 Cao, X., Lai, S. W. T., Chen, S., Wang, S. & Feng, M. Targeting tumor-associated macrophages for cancer immunotherapy. *Int Rev Cell Mol Biol* **368**, 61-108, doi:10.1016/bs.ircmb.2022.02.002 (2022).
- 170 Akkari, L. *et al.* Dynamic changes in glioma macrophage populations after radiotherapy reveal CSF-1R inhibition as a strategy to overcome resistance. *Sci Transl Med* **12**, doi:10.1126/scitranslmed.aaw7843 (2020).
- 171 Duan, Z. & Luo, Y. Targeting macrophages in cancer immunotherapy. *Signal Transduct Target Ther* **6**, 127, doi:10.1038/s41392-021-00506-6 (2021).
- 172 Vasan, N., Baselga, J. & Hyman, D. M. A view on drug resistance in cancer. *Nature* **575**, 299-309, doi:10.1038/s41586-019-1730-1 (2019).
- 173 Coffelt, S. B. & de Visser, K. E. Immune-mediated mechanisms influencing the efficacy of anticancer therapies. *Trends Immunol* **36**, 198-216, doi:10.1016/j.it.2015.02.006 (2015).
- 174 Shi, Y. *et al.* Next-Generation Immunotherapies to Improve Anticancer Immunity. *Front Pharmacol* **11**, 566401, doi:10.3389/fphar.2020.566401 (2020).
- 175 Galluzzi, L., Humeau, J., Buque, A., Zitvogel, L. & Kroemer, G. Immunostimulation with chemotherapy in the era of immune checkpoint inhibitors. *Nat Rev Clin Oncol* **17**, 725-741, doi:10.1038/s41571-020-0413-z (2020).
- 176 Kumar, A., Swain, C. A. & Shevde, L. A. Informing the new developments and future of cancer immunotherapy : Future of cancer immunotherapy. *Cancer Metastasis Rev* **40**, 549-562, doi:10.1007/s10555-021-09967-1 (2021).
- 177 Bezu, L. *et al.* Combinatorial strategies for the induction of immunogenic cell death. *Front Immunol* **6**, 187, doi:10.3389/fimmu.2015.00187 (2015).
- 178 Shree, T. *et al.* Macrophages and cathepsin proteases blunt chemotherapeutic response in breast cancer. *Genes & development* **25**, 2465-2479, doi:25/23/2465 [pii] 10.1101/gad.180331.111 (2011).

- 179 Kersten, K., Salvagno, C. & de Visser, K. E. Exploiting the Immunomodulatory Properties of Chemotherapeutic Drugs to Improve the Success of Cancer Immunotherapy. *Front Immunol* **6**, 516, doi:10.3389/fimmu.2015.00516 (2015).
- 180 Nars, M. S. & Kaneno, R. Immunomodulatory effects of low dose chemotherapy and perspectives of its combination with immunotherapy. *International journal of cancer. Journal internationale du cancer* **132**, 2471-2478, doi:10.1002/ijc.27801 (2013).
- 181 Larionova, I. *et al.* Interaction of tumor-associated macrophages and cancer chemotherapy. *Oncoimmunology* **8**, 1596004, doi:10.1080/2162402X.2019.1596004 (2019).
- 182 Acharyya, S. *et al.* A CXCL1 paracrine network links cancer chemoresistance and metastasis. *Cell* **150**, 165-178, doi:10.1016/j.cell.2012.04.042 (2012).
- 183 Di Mitri, D. *et al.* Tumour-infiltrating Gr-1+ myeloid cells antagonize senescence in cancer. *Nature* **515**, 134-137, doi:10.1038/nature13638 (2014).
- 184 Nywening, T. M. *et al.* Targeting both tumour-associated CXCR2(+) neutrophils and CCR2(+) macrophages disrupts myeloid recruitment and improves chemotherapeutic responses in pancreatic ductal adenocarcinoma. *Gut* **67**, 1112-1123, doi:10.1136/gutjnl-2017-313738 (2018).
- 185 Apetoh, L. *et al.* Toll-like receptor 4-dependent contribution of the immune system to anticancer chemotherapy and radiotherapy. *Nature medicine* **13**, 1050-1059, doi:10.1038/nm1622 (2007).
- 186 Obeid, M. *et al.* Calreticulin exposure dictates the immunogenicity of cancer cell death. *Nature medicine* **13**, 54-61, doi:nm1523 [pii] 10.1038/nm1523 (2007).
- 187 Ghiringhelli, F. *et al.* Activation of the NLRP3 inflammasome in dendritic cells induces IL-1beta-dependent adaptive immunity against tumors. *Nature medicine* **15**, 1170-1178, doi:nm.2028 [pii] 10.1038/nm.2028 (2009).
- 188 Vacchelli, E., Prada, N., Kepp, O. & Galluzzi, L. Current trends of anticancer immunochemotherapy. *Oncoimmunology* **2**, e25396, doi:10.4161/onci.25396 (2013).
- 189 Ma, Y. *et al.* Anticancer chemotherapy-induced intratumoral recruitment and differentiation of antigen-presenting cells. *Immunity* **38**, 729-741, doi:10.1016/j.immuni.2013.03.003 (2013).
- 190 Galluzzi, L. *et al.* Consensus guidelines for the definition, detection and interpretation of immunogenic cell death. *Journal for ImmunoTherapy of Cancer* **8**, e000337, doi:10.1136/jitc-2019-000337 (2020).
- 191 Kroemer, G., Galluzzi, L., Kepp, O. & Zitvogel, L. Immunogenic cell death in cancer therapy. *Annu Rev Immunol* **31**, 51-72, doi:10.1146/annurev-immunol-032712-100008 (2013).
- 192 Sistigu, A. *et al.* Cancer cell-autonomous contribution of type I interferon signaling to the efficacy of chemotherapy. *Nat Med* **20**, 1301-1309, doi:10.1038/nm.3708 (2014).

- 193 Mattarollo, S. R. *et al.* Pivotal role of innate and adaptive immunity in anthracycline chemotherapy of established tumors. *Cancer Res* **71**, 4809-4820, doi:0008-5472.CAN-11-0753 [pii] 10.1158/0008-5472.CAN-11-0753 (2011).
- 194 Ruffell, B. *et al.* Macrophage IL-10 blocks CD8+ T cell-dependent responses to chemotherapy by suppressing IL-12 expression in intratumoral dendritic cells. *Cancer Cell* **26**, 623-637, doi:10.1016/j.ccell.2014.09.006 (2014).
- 195 Cassetta, L. & Pollard, J. W. Targeting macrophages: therapeutic approaches in cancer. *Nat Rev Drug Discov* **17**, 887-904, doi:10.1038/nrd.2018.169 (2018).
- 196 Malfitano, A. M. *et al.* Tumor-Associated Macrophage Status in Cancer Treatment. *Cancers (Basel)* **12**, doi:10.3390/cancers12071987 (2020).
- 197 Campbell, M. J. *et al.* The prognostic implications of macrophages expressing proliferating cell nuclear antigen in breast cancer depend on immune context. *PLoS One* **8**, e79114, doi:10.1371/journal.pone.0079114 (2013).
- 198 Webb, M. W. *et al.* Colony stimulating factor 1 receptor blockade improves the efficacy of chemotherapy against human neuroblastoma in the absence of T lymphocytes. *Int J Cancer* **143**, 1483-1493, doi:10.1002/ijc.31532 (2018).
- 199 Nakasone, E. S. *et al.* Imaging tumor-stroma interactions during chemotherapy reveals contributions of the microenvironment to resistance. *Cancer Cell* **21**, 488-503, doi:S1535-6108(12)00079-7 [pii] 10.1016/j.ccr.2012.02.017 (2012).
- 200 Rolny, C. *et al.* HRG inhibits tumor growth and metastasis by inducing macrophage polarization and vessel normalization through downregulation of PlGF. *Cancer Cell* **19**, 31-44, doi:S1535-6108(10)00474-5 [pii] 10.1016/j.ccr.2010.11.009 (2011).
- 201 Stockmann, C. *et al.* Deletion of vascular endothelial growth factor in myeloid cells accelerates tumorigenesis. *Nature* **456**, 814-818, doi:nature07445 [pii] 10.1038/nature07445 (2008).
- 202 Bruchard, M. *et al.* Chemotherapy-triggered cathepsin B release in myeloid-derived suppressor cells activates the Nlrp3 inflammasome and promotes tumor growth. *Nature medicine* **19**, 57-64, doi:10.1038/nm.2999 (2013).
- 203 Germano, G. *et al.* Role of macrophage targeting in the antitumor activity of trabectedin. *Cancer Cell* **23**, 249-262, doi:10.1016/j.ccr.2013.01.008 (2013).
- 204 Jinushi, M. *et al.* Tumor-associated macrophages regulate tumorigenicity and anticancer drug responses of cancer stem/initiating cells. *Proceedings of the National Academy of Sciences of the United States of America* **108**, 12425-12430, doi:10.1073/pnas.1106645108 (2011).
- 205 Weizman, N. *et al.* Macrophages mediate gemcitabine resistance of pancreatic adenocarcinoma by upregulating cytidine deaminase. *Oncogene*, doi:onc2013357 [pii] 10.1038/onc.2013.357 (2013).
- 206 Hughes, R. *et al.* Perivascular M2 Macrophages Stimulate Tumor Relapse after Chemotherapy. *Cancer Res* **75**, 3479-3491, doi:10.1158/0008-5472.CAN-14-3587 (2015).

- 207 Baghdadi, M. *et al.* Chemotherapy-induced IL-34 enhances immunosuppression by tumor-associated macrophages and mediates survival of chemoresistant lung cancer cells. *Cancer Res*, doi:10.1158/0008-5472.CAN-16-1170 (2016).
- 208 Long, K. B. *et al.* IFN $\gamma$  and CCL2 Cooperate to Redirect Tumor-Infiltrating Monocytes to Degrade Fibrosis and Enhance Chemotherapy Efficacy in Pancreatic Carcinoma. *Cancer Discov* **6**, 400-413, doi:10.1158/2159-8290.CD-15-1032 (2016).
- 209 Karagiannis, G. S. *et al.* Neoadjuvant chemotherapy induces breast cancer metastasis through a TMEM-mediated mechanism. *Sci Transl Med* **9**, doi:10.1126/scitranslmed.aan0026 (2017).
- 210 Dijkgraaf, E. M. *et al.* Chemotherapy alters monocyte differentiation to favor generation of cancer-supporting M2 macrophages in the tumor microenvironment. *Cancer Res* **73**, 2480-2492, doi:10.1158/0008-5472.CAN-12-3542 (2013).
- 211 Kodumudi, K. N. *et al.* A novel chemoimmunomodulating property of docetaxel: suppression of myeloid-derived suppressor cells in tumor bearers. *Clin Cancer Res* **16**, 4583-4594, doi:1078-0432.CCR-10-0733 [pii] 10.1158/1078-0432.CCR-10-0733 (2010).
- 212 Roux, C. *et al.* Reactive oxygen species modulate macrophage immunosuppressive phenotype through the up-regulation of PD-L1. *Proceedings of the National Academy of Sciences of the United States of America* **116**, 4326-4335, doi:10.1073/pnas.1819473116 (2019).
- 213 Affara, N. I. *et al.* B cells regulate macrophage phenotype and response to chemotherapy in squamous carcinomas. *Cancer Cell* **25**, 809-821, doi:10.1016/j.ccr.2014.04.026 (2014).
- 214 Wanderley, C. W. *et al.* Paclitaxel Reduces Tumor Growth by Reprogramming Tumor-Associated Macrophages to an M1 Profile in a TLR4-Dependent Manner. *Cancer Res* **78**, 5891-5900, doi:10.1158/0008-5472.CAN-17-3480 (2018).
- 215 Slamon, D. J. *et al.* Studies of the HER-2/neu proto-oncogene in human breast and ovarian cancer. *Science* **244**, 707-712. (1989).
- 216 Gschwind, A., Fischer, O. M. & Ullrich, A. The discovery of receptor tyrosine kinases: targets for cancer therapy. *Nature reviews. Cancer* **4**, 361-370, doi:10.1038/nrc1360 (2004).
- 217 Gampenrieder, S. P., Castagnaviz, V., Rinnerthaler, G. & Greil, R. Treatment Landscape for Patients with HER2-Positive Metastatic Breast Cancer: A Review on Emerging Treatment Options. *Cancer Manag Res* **12**, 10615-10629, doi:10.2147/CMAR.S235121 (2020).
- 218 Boggio, K. *et al.* Interleukin 12-mediated prevention of spontaneous mammary adenocarcinomas in two lines of Her-2/neu transgenic mice. *J Exp Med* **188**, 589-596 (1998).
- 219 Henson, D. & Tarone, R. A study of lobular carcinoma of the breast based on the Third National Cancer Survey in The United States of America. *Tumori* **65**, 133-142 (1979).
- 220 Rosen, P. P. Pathological assessment of nonpalpable breast lesions. *Seminars in surgical oncology* **7**, 257-260 (1991).

- 221 Koufopoulos, N., Antoniadou, F., Kokkali, S., Pigadioti, E. & Khaldi, L. Invasive Lobular Carcinoma with Extracellular Mucin Production: Description of a Case and Review of the Literature. *Cureus* **11**, e5550, doi:10.7759/cureus.5550 (2019).
- 222 Derksen, P. W. *et al.* Somatic inactivation of E-cadherin and p53 in mice leads to metastatic lobular mammary carcinoma through induction of anoikis resistance and angiogenesis. *Cancer Cell* **10**, 437-449 (2006).
- 223 Lips, E. H. *et al.* Lobular histology and response to neoadjuvant chemotherapy in invasive breast cancer. *Breast Cancer Res Treat* **136**, 35-43, doi:10.1007/s10549-012-2233-z (2012).

## Chapter 2



# Development of metastatic HER2+ breast cancer is independent of the adaptive immune system

Metamia Ciampricotti<sup>1</sup>, Kim Vrijland<sup>1</sup>, Cheei-Sing Hau<sup>1</sup>, Tea Pemovska<sup>1</sup>, Chris W. Doornebal<sup>1</sup>, Ewoud N. Speksnijder<sup>2</sup>, Katharina Wartha<sup>3</sup>, Jos Jonkers<sup>1</sup>, Karin E. de Visser<sup>1,4</sup>

<sup>1</sup> Division of Molecular Biology, the Netherlands Cancer Institute, Plesmanlaan 121, 1066 CX Amsterdam, The Netherlands

<sup>2</sup> Current address: Department of Toxicogenetics, Leiden University Medical Center, Einthovenweg 20, 2333 ZC Leiden, The Netherlands

<sup>3</sup> Pharma Research and Early Development, Roche Diagnostics GmbH, Nonnenwald 2, 82377 Penzberg, Germany

<sup>4</sup>Address for correspondence:

Karin E. de Visser

Department of Molecular Biology

The Netherlands Cancer Institute

Plesmanlaan 121

1066 CX Amsterdam

The Netherlands

+31-20-5127979

k.d.visser@nki.nl

*Journal of Pathology. 2011 May; 224(1):56-66*

## **Abstract**

The tumour-modulating effects of the endogenous adaptive immune system are rather paradoxical. Whereas some clinical and experimental observations offer compelling evidence for the existence of immunosurveillance, other studies have revealed promoting effects of the adaptive immune system on primary cancer development and metastatic disease. We examined the functional significance of the adaptive immune system as a regulator of spontaneous HER2+ breast tumourigenesis and pulmonary metastasis formation using the MMTV-NeuT mouse model in which mammary carcinogenesis is induced by transgenic expression of the activated HER2/neu oncogene. Although T and B lymphocytes infiltrate human and experimental HER2+ breast tumours, genetic elimination of the adaptive immune system does not affect development of premalignant hyperplasias or primary breast cancers. In addition, we demonstrate that pulmonary metastasis formation in MMTV-NeuT mice is not dependent on the adaptive immune system. Thus, our findings reveal that spontaneous HER2 driven mammary tumourigenesis and metastasis formation are neither suppressed or altered by immunosurveillance mechanisms, nor promoted by the adaptive immune system.

## **Keywords**

Breast cancer, Metastasis, Her2/neu, Adaptive immune system, Innate immune system, Immunosurveillance

## Introduction

It has become generally accepted that chronic activation of innate immune cells contributes to cancer development and/or progression, however, the role of adaptive immune cells is still a matter of debate [1-3]. For decades, it was believed that the adaptive immune system protects organisms from tumour development, a process referred to as immunosurveillance [1,4]. This hypothesis is supported by epidemiological studies showing increased incidence of pathogen-associated cancers in immunocompromised patients [3]. In addition, the concept of tumour suppression and tumour editing by the adaptive immune system has been supported by studies in a chemically induced mouse sarcoma model [5-6]. However, the role of the adaptive immune system during development of pathogen and chemical unrelated solid cancers are less clear. In fact, recent studies using genetically engineered mouse (GEM) tumour models do reveal a more controversial function of the adaptive immune system during tumourigenesis. Whereas some studies using GEM models for spontaneous tumourigenesis did not reveal any modulating role for the adaptive immune system in tumour formation or progression [2,7], other experimental studies revealed an unexpected tumour-promoting role for certain components of the adaptive immune system [8-11]. For example, genetic elimination of the adaptive immune system in a transgenic mouse model for multistage skin carcinogenesis protected against spontaneous tumour formation [8,11]. Likewise, lymphocytes were shown to promote induction of chronic hepatitis and subsequent hepatocellular carcinoma development in lymphotoxin transgenic mice [9]. Thus, in addition to the concept of immunoediting in which the adaptive immune system “sculpts” developing tumours, these studies indicate existence of alternative pathways, in which a spontaneously developing tumour avoids or even harnesses components of the adaptive immune system to its own advantage. However, the degree to which these pathways are tissue-, organ-, cell type-, or oncogene-specific remains to be evaluated.

Breast cancer is a heterogeneous disease. The recent availability of advanced molecular technologies has led to the characterization of different molecular portraits of breast cancer, which can roughly be divided into five distinct breast cancer subtypes: “luminal-A”, “luminal-B”, “basal”, “HER2 positive” and “normal breast-like” [12-13]. These distinct subtypes of breast cancer are dependent on different oncogenic pathways, are characterized by unique gene expression patterns, have different prognostic

characteristics, and display differential sensitivity to anti-cancer drugs [14-15], and are thus also likely to be differentially regulated by the adaptive immune system. It has recently been shown that mammary tumour metastasis formation in the MMTV-PyMT breast cancer mouse model is dependent on CD4<sup>+</sup> T cells [10]; however, it is unknown whether this mechanism accounts for other breast cancer types.

Between 15 and 20 percent of invasive breast cancers are HER2<sup>+</sup> [16]. Overexpression of HER2 is an adverse prognostic factor associated with poorly differentiated, high-grade tumours, metastasis formation, relative resistance to certain chemotherapy regimens and greater risk of recurrence [14,16]. Prominent lymphocytic infiltrates and high expression of lymphocyte-associated genes in human HER2<sup>+</sup> breast cancers have been reported to correlate with lower recurrence rates [17]. Likewise, a recent clinical study demonstrated that a T cell metagene could be used as an independent predictor of favourable prognosis in patients with HER2<sup>+</sup> breast cancer [18]. These studies indicate that the intra-tumoural presence of lymphocytes is beneficial for breast cancer patients. However, from these clinical observations it is unclear whether the presence of lymphocytes *causes* a favourable prognosis, or whether the lymphocytes are present as *a consequence* of a distinct natural history of the good prognosis subtype of HER2<sup>+</sup> breast cancers, and thus represent a biological marker instead of a biological anti-cancer weapon. Importantly, immunocompromised patients are not at increased risk of developing breast cancer [3,19-20], suggesting that human breast cancer formation might not be suppressed by immunosurveillance mechanisms.

The aim of this study was to dissect the functional role of the adaptive immune system during *de novo* HER2<sup>+</sup> breast cancer development and pulmonary metastasis formation, using the MMTV-NeuT mouse model in which mammary tumourigenesis is induced by transgenic expression of the activated HER2/neu oncogene driven by the MMTV promotor [21-22].

## Materials and Methods

### Mice

MMTV-NeuT mice (Balb/c F>12) [22] were purchased from Charles River, and maintained by mating MMTV-NeuT males with Balb/c females. MMTV-NeuT mice were intercrossed with RAG-2<sup>-/-</sup> mice [23] on the Balb/c background (F>10) [24] to generate breeding colonies of NeuT/RAG-2<sup>+/-</sup> and NeuT/RAG-2<sup>-/-</sup> mice and wild type littermate control RAG-2<sup>+/-</sup> and RAG-2<sup>-/-</sup> mice. Genotyping was performed by PCR analysis on tail tip DNA as described previously [22-23]. Transgene positive female animals were monitored weekly by palpation for mammary tumour development. Once palpable tumours were present, tumour size was measured twice a week using a caliper. Ninety minutes before sacrifice, mice were injected i.p. with 50 mg/kg bodyweight bromodeoxyuridine (BrdU) (Sigma, Zwijndrecht, the Netherlands). All mice were kept in individually ventilated cages at the animal care facility of the Netherlands Cancer Institute and food and water were given *ad libitum*. All animal experiments were performed in accordance with institutional guidelines and national ethical regulations.

### Histology and Immunohistochemistry

Tissue samples were processed, sectioned and stained as described [25]. Details regarding antibodies, antigen retrieval methods and type of tissue sections can be found in Supplemental table 1a. All immunohistochemical experiments included negative controls for determination of background staining, which was negligible. Slides were digitally processed using the Aperio ScanScope (Aperio, Vista, CA) using ImageScope software version 10.0 (Aperio). Data shown are representative of results obtained following examination of tissues removed from a minimum of 5 patients or mice per group.

## Flow cytometry

Both 4<sup>th</sup> (inguinal) mammary glands were isolated from age-matched negative littermate mice and tumours (15x15 mm) were isolated from transgenic mice. After removal of lymph nodes, glands and tumours were mechanically chopped using the McIlwain Tissue Chopper (The Mickle Laboratory Engineering Co. Ltd., Guildford, UK) and digested for 1 hr at 37°C in a digestion mix of 3 mg/ml Collagenase Type A (Roche, Mannheim, Germany) and 1.5 mg/ml porcine pancreatic trypsin (Invitrogen, Breda, the Netherlands) in serum-free L15 medium (Invitrogen). Cells and organoids were centrifuged at 1200 rpm for 5 min, resuspended in L15 medium, 10% FCS, 100 IU/ml Penicillin and 100 µg/ml Streptomycin (Invitrogen) and dispersed through a 70 µm cell strainer (BD Falcon). Blood was collected in heparin-containing eppendorf tubes and treated with NH<sub>4</sub>Cl lysing buffer. Spleens were homogenized over a 70 µm filter (BD Falcon) and cells were treated with NH<sub>4</sub>Cl lysing buffer. Cells from tissues, blood and spleen were centrifuged for 5 min at 1200 rpm and resuspended in PBS supplemented with 1% BSA (Sigma) (PBS/BSA). Samples of 0.5x10<sup>6</sup> cells were incubated for 20 min at 4 °C in the dark with antibodies (Supplemental table 1b) Cells were washed with PBS/BSA, 7-AAD (eBioscience) was added (1:10) to exclude dead cells, and data acquisition was performed on a FACSCalibur using CellQuestPro software (BD Biosciences). Data analysis was performed using FlowJo software version 7.1.3 (Tree Star Inc., Ashland, OR).

## Orthotopic tumour transplantations

Mammary tumours (15x15 mm) were isolated from two NeuT/RAG-2<sup>+/-</sup> and two NeuT/RAG-2<sup>-/-</sup> mice. Small tumour pieces (1x1 mm, mechanically minced in ice-cold PBS) were grafted into the mammary fatpad of female Balb/c mice (8–12 weeks of age). Mice were anesthetized with hypnorm/dormicum/H<sub>2</sub>O (1:1:2, 7ml/kg) and a small abdominal skin incision was made. Using watchmaker forceps, a small pocket was generated in the 4<sup>th</sup> (inguinal) mammary gland fat pad into which a tumour piece was placed. The skin was stitched and temgesic was given for postoperative pain relief. After postoperative surveillance, tumour growth was monitored twice a week starting 1 week after transplantation.

## Luminex cytokine assays

Both 4<sup>th</sup> mammary glands were isolated from age-matched negative littermate mice and tumours (15x15 mm) were isolated from transgenic mice. After removal of lymph nodes, tissue was snap frozen and stored at -80°C. Frozen tissue was pulverized in liquid nitrogen using a mortar. The pulverized tissue was dispersed in Bio-Plex Cell Lysis Buffer (Bio-Rad, Munich, Germany), centrifuged for 15 min at 14.000 rpm at 4 °C, supernatant was collected, and protein concentration was determined using the Pierce BCA Protein Assay Kit (Thermo Fischer Scientific, Bonn, Germany) according to manufacturers' recommendations. Samples were stored at -80°C. Cytokine concentrations in protein lysates were determined with Bio-Plex Pro Cytokine Kits (Bio-Rad, Munich Germany) on a Luminex system. The assay was performed according to the manufacturers' recommendations. Data acquisition and analysis was performed on a Bio-Plex 200 reader, using Bio-Plex Manager 6.0 software (Bio-Rad, Munich Germany).

## Statistical analyses

Statistical analyses were performed using GraphPad Prism 5.01 (GraphPad Software Inc., La Jolla, CA). Specific tests used were the Mann-Whitney test (unpaired, two-tailed), Log-Rank test and Fisher's exact test. P values < 0.05 were considered statistically significant.

## Results

### **Human and mouse HER2+ breast tumours are characterized by influx of adaptive immune cells**

Given the paradoxical role of the adaptive immune system during *de novo* tumourigenesis [1-3], and considering the reported association between lymphocytic infiltrates and high expression of lymphocyte-associated genes with favourable prognosis in patients with HER2+ breast cancer [17] [18], we set out to investigate whether the adaptive immune system does modulate spontaneous HER2+ breast cancer formation. We utilized a mouse model for multi-stage HER2+ breast tumourigenesis, e.g. MMTV-NeuT mice. Female MMTV-NeuT mice develop hyperplastic lesions within 2 months of age, and invasive mammary tumours and pulmonary metastases around 4 months of age, resembling human HER2+ breast tumourigenesis [21-22]. Like human HER2+ breast tumours, tumours in MMTV-NeuT mice are characterized by infiltrating CD45<sup>+</sup> immune cells (Fig. S1). We investigated the nature of the inflammatory infiltrate in human and mouse HER2+ breast tumours by immunohistochemistry, and observed a prominent influx of macrophages (Fig. S1), as well as an influx of adaptive immune cells, i.e. B cells, and CD4<sup>+</sup> and CD8<sup>+</sup> T cells (Fig. 1). In human and mouse HER2+ tumours, the infiltrating leukocytes were mainly localized in stromal areas surrounding nests of cancer cells. Thus, both human and murine HER2+ breast cancers are characterized by infiltrating innate and adaptive immune cells.

Development of metastatic HER2+ breast cancer is independent of the adaptive immune system

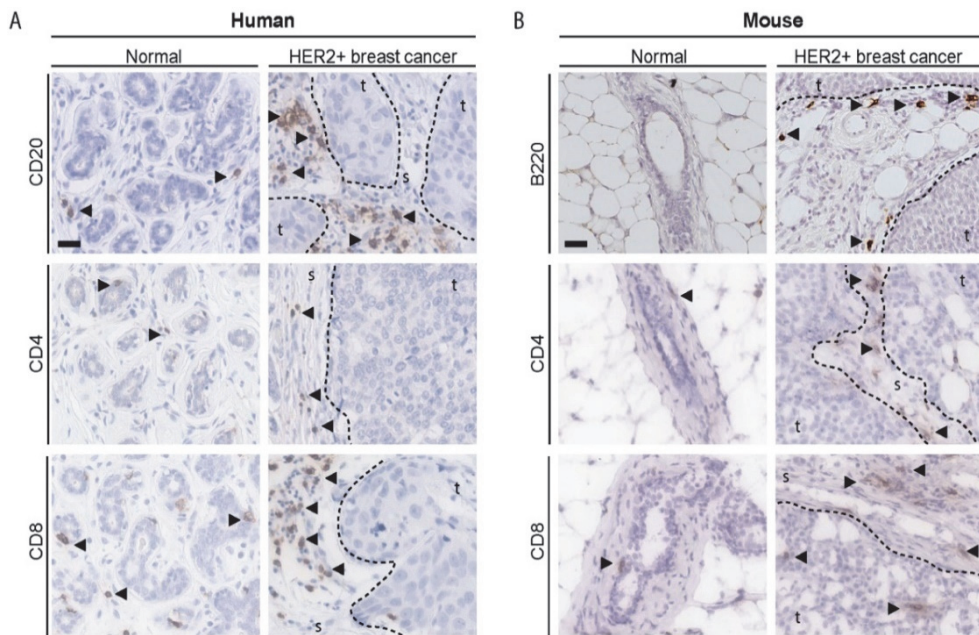


**Figure 1. Increased infiltrates of adaptive immune cells in human and mouse HER2+ breast cancer.** (A) Presence and location of CD20+, CD4+, and CD8+ cells (brown staining; arrowheads) in human normal mammary glands and human invasive HER2+ breast tumours. Representative images are shown (n=5/group). Scale Bar, 25  $\mu$ m. Dashed line, stromal-tumour interface; tumour, t; stroma, s. (B) Presence and location of B220+, CD4+ and CD8+ cells (brown staining; arrowheads) in normal mammary glands of adult wild-type mice and in HER2+ breast tumours from MMTV-NeuT mice (n=5/group). Representative images are shown. Scale Bar, 25  $\mu$ m. Dashed line, stromal-tumour interface; tumour, t; stroma, s.

2

## **Genetic elimination of the adaptive immune system does not alter latency, multiplicity, outgrowth and phenotype of mammary tumours**

To functionally address the modulating role of the adaptive immune system during HER2+ mammary tumourigenesis, we intercrossed MMTV-NeuT mice with Recombination-Activating Gene-2 homozygous null (Rag-2<sup>-/-</sup>) mice deficient for mature T and B lymphocytes, and generated cohorts of immuno-proficient NeuT/Rag-2<sup>+/-</sup> and immuno-deficient NeuT/Rag-2<sup>-/-</sup> mice (Fig. S2). We first examined whether absence of the adaptive immune system altered mammary tumour development. Strikingly, complete lymphocyte deficiency did not alter tumour latency (Fig. 2A) or tumour multiplicity (Fig. 2B). In addition, no differences in speed of tumour outgrowth between NeuT/Rag-2<sup>+/-</sup> and NeuT/Rag-2<sup>-/-</sup> mice (Fig. 2C) were observed. These data were further confirmed by comparable *in vivo* BrdU incorporation into breast cancer cells of both cohorts (Fig. S3). In order to address whether absence of the adaptive immune system resulted in mammary tumours with increased immunogenicity, 1x1 mm pieces of mammary tumours isolated from two independent NeuT/Rag-2<sup>+/-</sup> and two independent NeuT/Rag-2<sup>-/-</sup> mice were orthotopically transplanted in mammary glands of syngeneic Balb/c mice. Tumour take and latency were independent of the immunological status of the donor mice (Fig. 2D), suggesting that the adaptive immune system does not shape the immunogenicity of mammary tumours in MMTV-NeuT mice. We next evaluated morphological features of mammary glands of wild type RAG-2<sup>+/-</sup> and RAG-2<sup>-/-</sup> mice, as well as neoplastic mammary glands (2-months of age) and tumours of NeuT/Rag-2<sup>+/-</sup> and NeuT/Rag-2<sup>-/-</sup> mice. Absence of lymphocytes did not alter the phenotype of normal mammary glands, nor the progression towards early hyperplastic mammary lesions or their phenotype (Fig. 3). In addition, the histological phenotype of primary mammary tumours was comparable between T and B cell proficient and deficient MMTV-NeuT mice (Fig. 3). Taken together, these data indicate that the adaptive immune system has neither a protective nor a promoting role during mammary tumourigenesis in MMTV-NeuT mice.

Development of metastatic HER2+ breast cancer is independent of the adaptive immune system

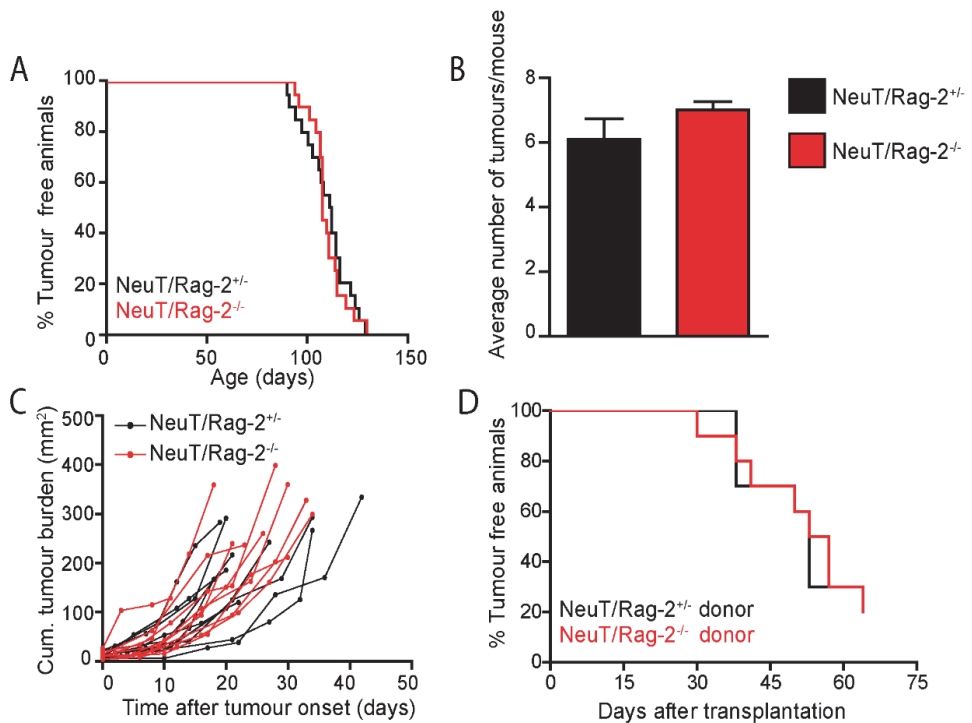


**Figure 2. The adaptive immune system does not regulate primary breast cancer development in MMTV-NeuT mice.** (A) Kaplan-Meier tumour-free survival curve of NeuT/Rag-2<sup>+/-</sup> mice and NeuT/Rag-2<sup>-/-</sup> mice (n=20/group). Mice were considered tumour free until a palpable tumour mass of 2x2 mm was detected. No statistically significant difference was observed as evaluated by Log-Rank test (p=0.84). (B) Average number of primary breast tumours per NeuT/Rag-2<sup>+/-</sup> mouse and NeuT/Rag-2<sup>-/-</sup> mouse (n=20/group) evaluated at the day the largest tumour reached 15x15 mm. No statistically significant differences were observed between both cohorts as evaluated by Mann-Whitney test (p=0.83). (C) Cumulative tumour burden (mm<sup>2</sup>) followed over time in individual NeuT/Rag-2<sup>+/-</sup> mice and NeuT/Rag-2<sup>-/-</sup> mice (n=10/group). (D) Kaplan-Meier tumour-free survival curve of Balb/c mice orthotopically transplanted with 1x1 mm tumour pieces isolated from NeuT/Rag-2<sup>+/-</sup> mice and NeuT/Rag-2<sup>-/-</sup> mice (n=10/group). Mice were considered tumour free until a palpable tumour mass of 3x2 mm was detected. No statistically significant difference was observed as evaluated by Log-Rank test (p=0.92).

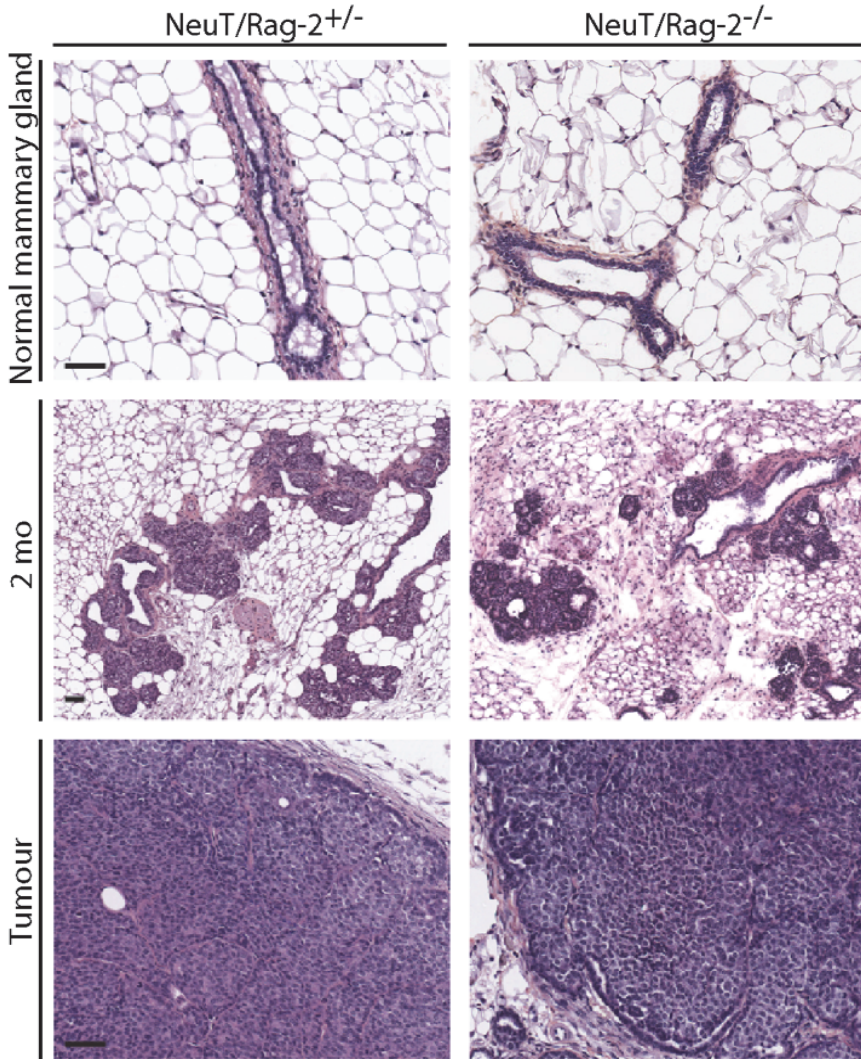


**Figure 3. Absence of the adaptive immune system does not alter tumour phenotype.** H&E stainings of normal mammary glands from age-matched wild type Rag-2<sup>+/-</sup> and Rag-2<sup>-/-</sup> mice, hyperplastic mammary lesions (2-mo of age) and mammary tumours of age-matched (4.5 mo of age) NeuT/Rag-2<sup>+/-</sup> mice and NeuT/Rag-2<sup>-/-</sup> mice. Representative images are shown (n=10/group). Scale Bar, 50  $\mu$ m.

## The adaptive immune system does not regulate the inflammatory tumour microenvironment in MMTV-NeuT mice

Adaptive immune cells have been shown to exert pro-tumour functions through activation of tumour promoting innate immune responses [8,10-11,26-27]. Mammary tumourigenesis in MMTV-NeuT mice is accompanied by increased influx of innate immune cells (Fig. 1B, Fig. S1B). We therefore examined whether presence of innate immune cells in HER2+ tumours was regulated by the adaptive immune system. Flow cytometric analysis of CD45<sup>+</sup> leukocytes in tumours from both NeuT/Rag-2<sup>+/-</sup> and NeuT/Rag-2<sup>-/-</sup> mice revealed a two-fold increase in CD45<sup>+</sup> cells as compared to normal mammary glands (Fig. 4A). However, no significant difference in CD45<sup>+</sup> leukocyte infiltrate in tumours of NeuT/Rag-2<sup>+/-</sup> and NeuT/Rag-2<sup>-/-</sup> mice was observed (Fig. 4A). Immunohistochemical analysis of hyperplasias and primary mammary tumours of NeuT/Rag-2<sup>-/-</sup> and NeuT/Rag-2<sup>+/-</sup> mice confirmed these results and showed no differences in the degree and location of infiltrating CD45<sup>+</sup> leukocytes (Figure 4B). To investigate whether the composition of the inflammatory infiltrates in tumours of the two cohorts was different, we profiled the two major leukocyte populations, *i.e.* F4/80<sup>+</sup>CD11b<sup>+</sup> macrophages and Gr1<sup>+</sup>CD11b<sup>+</sup> granulocytes. Both immune cell populations were increased in tumours of NeuT/Rag-2<sup>+/-</sup> and NeuT/Rag-2<sup>-/-</sup> mice as compared to normal mammary tissue (Fig. 4C, D and S4A). However, no significant changes were observed in the magnitude and location of both immune subsets between tumours of NeuT/Rag-2<sup>+/-</sup> and NeuT/Rag-2<sup>-/-</sup> mice (Fig. 4C, D, S4A). In addition, spleens of both tumour-bearing NeuT/Rag-2<sup>+/-</sup> and NeuT/Rag-2<sup>-/-</sup> mice were characterized by accumulation of Gr1<sup>+</sup>CD11b<sup>+</sup> leukocytes (Fig. S4B).

Cytokines, either secreted by cancer cells or by tumour-associated immune cells, are part of the tumour microenvironment and can influence cancer progression and prognosis [28-29]. We performed cytokine profiling on protein lysates generated from tumours of NeuT/Rag-2<sup>+/-</sup> and NeuT/Rag-2<sup>-/-</sup> mice to dissect whether the adaptive immune system regulates the local cytokine milieu in HER2+ tumours. None of the twenty-five cytokines and growth factors tested (Fig. 5 and data not shown for IL1a, IL1b, IL2, IL3, IL4, IL5, IL6, IL9, IL10, IL12p49, IL12p70, IL13, IL17, Eotaxin, G-CSF, GM-CSF, MIP1b, RANTES and CSF-1) displayed significantly altered levels in tumours samples from NeuT/Rag-2<sup>+/-</sup> and NeuT/Rag-2<sup>-/-</sup> mice. Together, these data indicate that the adaptive immune system does not sculpt the composition or cytokine profile of the inflammatory tumour microenvironment in HER2+ mammary tumours.

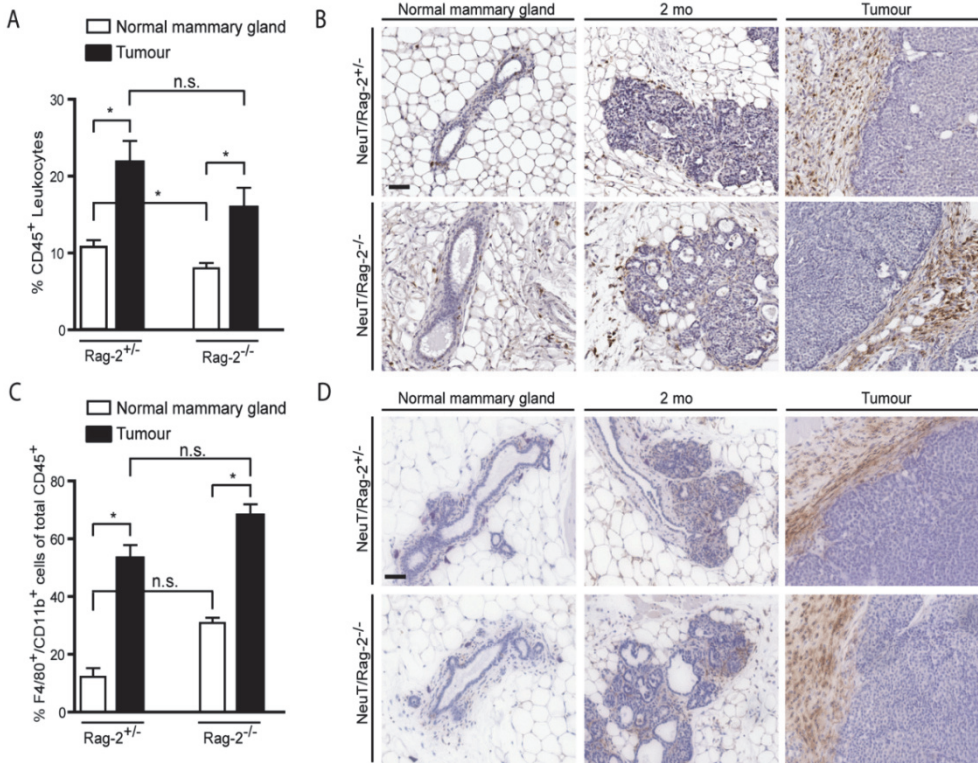


**Figure 4. The adaptive immune system does not regulate the inflammatory tumour microenvironment in MMTV-NeuT mice.** (A and C) Flow cytometric analysis of CD45<sup>+</sup> leukocytes (A) and F4/80<sup>+</sup>CD11b<sup>+</sup> macrophages (C) in normal mammary glands from age-matched wild type Rag-2<sup>+/-</sup> and Rag-2<sup>-/-</sup> mice and tumours of NeuT/Rag-2<sup>+/-</sup> and NeuT/Rag-2<sup>-/-</sup> mice. Data on CD45<sup>+</sup> leukocytes are depicted as the mean percentage gated on live cells ± SEM (A) and data on F4/80<sup>+</sup>CD11b<sup>+</sup> macrophages are depicted as mean percentage gated on live CD45<sup>+</sup> leukocytes ± SEM (C). (n=4/wild type cohort; n=8/tumour cohort). \*p<0.05 by Mann-Whitney test. n.s., not significant by Mann-Whitney test. (B and D) Immunodetection of CD45<sup>+</sup> leukocytes (B) and F4/80<sup>+</sup> macrophages (D) in normal mammary glands from age-matched wild type Rag-2<sup>+/-</sup> and Rag-2<sup>-/-</sup> mice, and in hyperplastic mammary lesions (2-mo of age) and mammary tumours of NeuT/Rag-2<sup>+/-</sup> mice and NeuT/Rag-2<sup>-/-</sup> mice. Representative images are shown. Scale Bar, 50 µm.

Development of metastatic HER2+ breast cancer is independent of the adaptive immune system

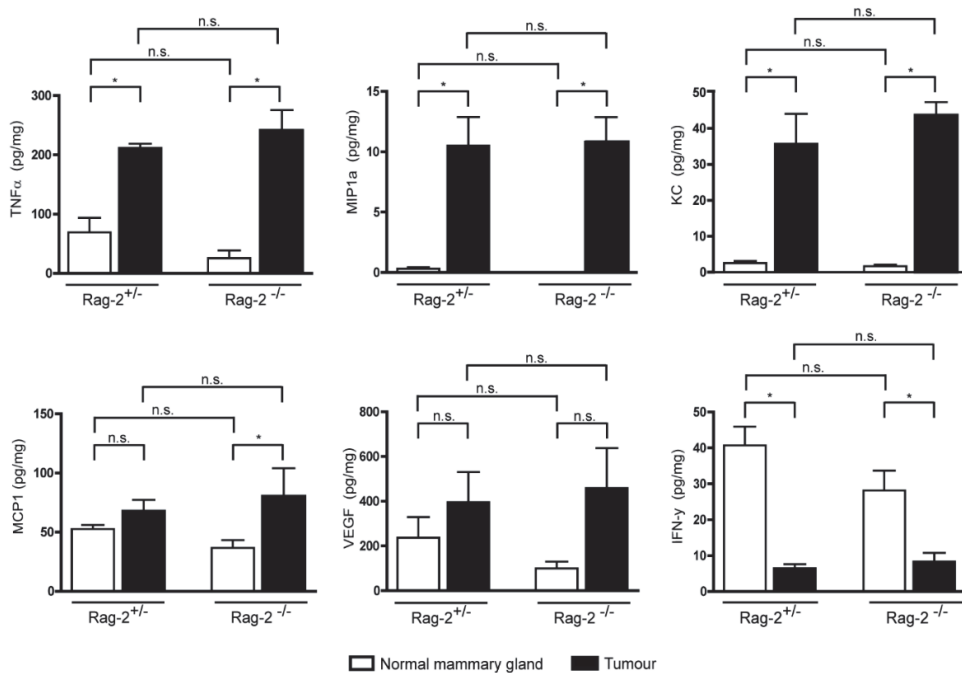


**Figure 5. The adaptive immune system does not sculpt the cytokine profile in breast tumours.** The cytokine profile in protein lysates of normal mammary glands from age-matched wild type Rag-2<sup>+/+</sup> and Rag-2<sup>-/-</sup> mice or mammary tumours (15x15 mm) of NeuT/Rag-2<sup>+/+</sup> mice and NeuT/Rag-2<sup>-/-</sup> mice was assessed using the Bio-Plex Pro Cytokine assay. Concentrations of TNF $\alpha$ , MIP1a, KC, MCP-1, VEGF and IFN- $\gamma$  are shown as pg/mg and are depicted as mean  $\pm$  SEM (n=5 mice/group). \* p < 0.05 by Mann-Whitney test. n.s., not significant.

## **Pulmonary metastasis formation in MMTV-NeuT mice is not regulated by the adaptive immune system**

Deficiency of the adaptive immune system did not alter any characteristics of primary HER2+ mammary cancer formation. Yet, it has been reported that lymphocytes can promote mammary cancer metastasis formation [10]. Therefore we set out to investigate spontaneous pulmonary metastasis formation in NeuT/Rag-2<sup>+/-</sup> and NeuT/Rag-2<sup>-/-</sup> mice. Serial sections of lungs isolated from NeuT/Rag-2<sup>+/-</sup> and NeuT/Rag-2<sup>-/-</sup> mice bearing end-stage mammary tumours were microscopically screened for the presence of metastases. This analysis did not reveal a significant change in metastasis incidence between both tumour cohorts (Fig. 6A). In addition, the size of metastases, the average number of metastases per mouse and the metastasis phenotype were unaffected in lymphocyte deficient MMTV-NeuT mice (Fig. 6B, C, D and S5). In conclusion, spontaneous pulmonary metastasis formation in MMTV-NeuT mice is not influenced by the endogenous adaptive immune system.

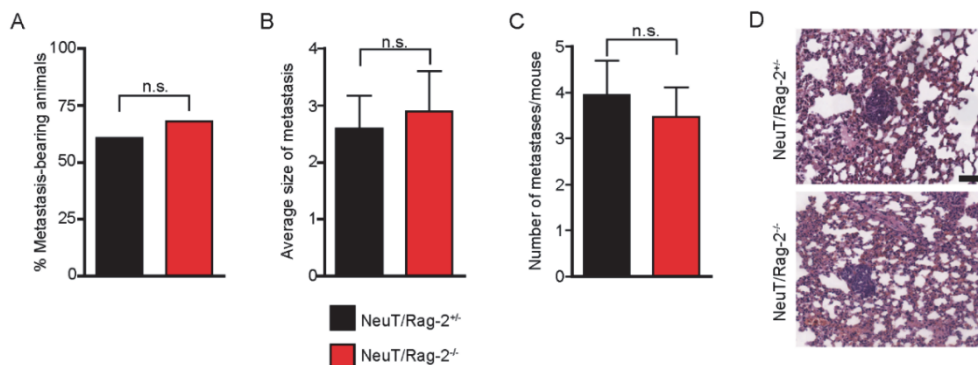


**Figure 6. Pulmonary metastasis formation in MMTV-NeuT mice is not regulated by the adaptive immune system.** Lungs of mice bearing end-stage mammary tumours were serially sectioned and ~11 sections 135 μm apart were H&E stained and microscopically screened for the presence of metastases (n=15 mice/cohort). (A) Percentage of tumour-bearing NeuT/Rag-2<sup>+/-</sup> and NeuT/Rag-2<sup>-/-</sup> mice with one or more pulmonary metastases. n.s., not significant by Fisher's exact test (p=0.77). (B) The average size of metastasis per mouse was determined by categorizing individual lung metastases based on their average diameter (Fig. S5). n.s., not significant by Mann-Whitney test (p=0.52). Error bars represent SEM. (C) The average number of metastases per metastasis-bearing mouse. n.s., not significant by Mann-Whitney test (p=0.83). Error bars represent SEM. (D) H&E stainings of lung tissue sections with a metastasis from NeuT/Rag-2<sup>+/-</sup> and NeuT/Rag-2<sup>-/-</sup> mice. Representative images are shown. Scale Bar, 50 μm.

## Discussion

Human HER2+ breast cancers are characterized by influx of adaptive immune cells (Fig. 1A)[17]. Presence of tumour infiltrating lymphocytes and expression of lymphocyte-associated genes in human HER2+ breast cancers have been reported to correlate with a good prognosis [17-18]. Whether this favourable prognosis is actually caused by the increased lymphocyte infiltration cannot be concluded from these clinical observations. In this study, we have investigated whether there is a causal relationship between the adaptive immune system and HER2 driven mammary tumourigenesis and metastasis formation. Using MMTV-NeuT mice, we found that absence of the adaptive immune system did not delay nor accelerate premalignant progression. Likewise, latency, growth, multiplicity, immunogenicity, histology and the inflammatory microenvironment of primary breast tumours arising in T and B cell deficient MMTV-NeuT mice were identical to those of immune proficient MMTV-NeuT mice. In addition, we demonstrate that pulmonary metastasis formation in MMTV-NeuT mice is not dependent on the adaptive immune system. Thus, our findings reveal that spontaneous HER2 driven mammary tumourigenesis and metastasis formation are not suppressed by immunosurveillance mechanisms, nor promoted by the adaptive immune system.

If we put these findings into context with previous studies, it becomes clear that the outcome of the dynamic interplay between adaptive immune system and nascent malignancies can be divided into three scenarios: protection, inertia and promotion [30]. Whereas spontaneous adaptive immune responses protect against chemical-induced sarcoma formation [5-6], viral oncogene driven skin tumourigenesis and lymphotoxin driven hepatocellular carcinoma development are promoted by the adaptive immune system [8-9,11] and large T antigen driven pancreatic cancer is not affected by the adaptive immune system [7]. Both a recent study by DeNardo et al. [10] and our study reveal in two independent transgenic mouse models for *de novo* breast cancer formation that primary mammary tumourigenesis is not influenced by the adaptive immune system. Thus, the tissue of origin likely plays an important role in determining the nature of the interplay between cancer cell and the adaptive immune system.

The absence of immunosurveillance in MMTV-NeuT mice might seem rather surprising, given the reported observation of adaptive immune responses directed against HER2/neu in the MMTV-NeuT mouse model during the pre-

malignant phase [31-32]. In addition, anti-HER2 CD4<sup>+</sup> and CD8<sup>+</sup> T cell responses have been described in patients with HER2+ breast cancer [33-34]. These observations suggest that the endogenous adaptive immune cell repertoire is not completely devoid of tumour-specific immune cells, and could thus -in theory- be involved in immunosurveillance mechanisms. Tumour transplantation studies have however shown that such spontaneous immune responses failed to reject transplanted Her2<sup>+</sup> tumour cells [32] and antibody-mediated depletion of T cells in MMTV-NeuT mice resulted only in a temporary marginal increase in tumour multiplicity [35]. Myeloid derived suppressor cells, regulatory T cells and regulatory dendritic cells have been reported to be involved in suppression of anti-tumour T cell responses in MMTV-NeuT mice [36-38]. Our study extends these observations by showing that -despite reported incomplete tolerance at early stages of tumourigenesis in MMTV-NeuT mice- spontaneous pre-malignant progression, tumour formation and development of metastases are not delayed or phenotypically altered by the unmanipulated adaptive immune system. That said, interventions aimed at increasing immunity towards HER2+ tumours, such as vaccination strategies or antibody therapies, have been reported to overcome the unresponsiveness of the adaptive immune system and result in successful tumour inhibition [39-41]. In addition, the therapeutic effect of anti-Her2 antibody therapy has been reported to depend on the adaptive immune system [42].

Strikingly, pulmonary metastasis formation in the MMTV-NeuT mouse model is not dependent on the adaptive immune system, whereas pulmonary metastasis formation in the MMTV-PyMT mouse model is promoted by the adaptive immune system [10]. These findings indicate that the outcome of the interplay between adaptive immune system and cancers is not solely dependent on the tissue context, but also on the genetic pathways underlying tumour initiation and tumour maintenance. This notion is underscored by recent publications reporting direct instruction of the inflammatory phenotype by particular oncogenes, such as Myc and Ras [43-45]. Thus, the genetic make-up of a particular tumour is critical for determining the nature of its crosstalk with the immune system. Given the heterogeneous nature of breast cancer, it is likely that also distinct subtypes of breast cancer are differently dependent on cancer cell extrinsic processes.

Similarly, functional differences between NeuT and PyMT might explain why the adaptive immune system affects pulmonary metastasis formation in the

MMTV-PyMT mouse model [10] but not in MMTV-NeuT mice. In the MMTV-PyMT mouse model, IL-4 producing CD4<sup>+</sup> T cells promoted pulmonary metastasis formation through enhancing epidermal growth factor (EGF) production by macrophages [10]. Macrophage-derived EGF subsequently stimulated epidermal growth factor receptor (EGFR)-dependent metastasis formation. In contrast, mammary tumourigenesis in the MMTV-NeuT mouse model is initiated by overexpression of an activated form of the EGFR family member HER2/ErbB2 [46], which does not require ligand for receptor activation. Hence, the metastatic capacity of NeuT-overexpressing tumours might be a cell-autonomous trait which is independent of EGFR activation by (macrophage-derived) EGF. However, the exact explanation for the observed differences awaits further investigation.

How could we translate these findings to the human situation? Lymphocyte infiltration and expression of a T cell gene expression signature have been shown to correlate with lower recurrence rates of HER2+ breast cancers [17-18]. In view of our data, it is plausible that the presence of lymphocytes in HER2+ breast cancers is not causal to improved metastasis-free survival rates, but rather a consequence of a distinct natural history of the good prognosis HER2+ tumours compared to the poor prognosis tumours. Importantly, the majority of patients analysed in these clinical studies were treated with radiotherapy [17] or chemotherapy [18]. The influx of lymphocytes in tumours of these patients might therefore be induced by cancer cells dying in response to anti-cancer therapy [47-48]. Thus, presence of lymphocytes or expression of a T cell metagene in treated HER2+ breast cancers might be a predictive rather than a prognostic indicator. Our data revealing absence of immunosurveillance in spontaneous HER2+ breast tumourigenesis are supported by epidemiological studies of cancer incidence in patients with a suppressed adaptive immune system. These patients suffer from increased incidence of viral-associated malignancies; however, the relative risk for breast cancer is not increased in these patients, and might actually be lower than in the general population [3,19-20].

Our data suggest that without a careful dissection of the dependence of different (breast) cancer subtypes on the adaptive immune system, therapies aimed at suppressing the adaptive immune system in unselected patient groups might actually have no effect, or even exacerbate disease. Mouse tumour models recapitulating many different subtypes of human (breast) cancer are available [49-51] and will be extremely useful for

predicting which patients would benefit from therapeutic targeting of the adaptive immune system. A deeper understanding of tumour- intrinsic and - extrinsic characteristics that influence the nature of the crosstalk with the immune system might open opportunities to suppress tumour-promoting immune responses and tip the balance over in favour of anti-tumour immune responses.

## Acknowledgments

We acknowledge technical assistance from the animal pathology department, animal facility and flow cytometry facility at the Netherlands Cancer Institute. We thank Sabine Linn, Marleen Kok and Ger Scholte for providing paraffin sections of human tissue. We thank Donne Majoor, Jane van Heteren, Ella van Huizen and Noura Makazaji for their technical support. We thank Hester van Zeeburg for critical comments and suggestions on the manuscript. We acknowledge financial support from the Dutch Cancer Society (KWF fellowship to KEdV; KWF grant 2006-3715 to KEdV and JJ) and the Netherlands Organization for Scientific Research, NWO (Vidi 917.96.307 to KEdV).

## Statement of author contributions

MC, JJ and KEdV conceived the study and participated in its design and coordination. MC, KV, C-SH, ENS, CWD and KEdV performed the intercrossings, established the tumour cohort, performed mouse colony maintenance and monitoring, performed weekly tumour palpations and sections. KV, TP, C-SH and ENS participated in handling of mouse tissues and performed immunohistochemical stainings. MC, CWD and KEdV performed microscopy. Flow cytometry and cytokine arrays were performed by MC, KV, KW and C-SH. MC, JJ and KEdV analysed data. MC, JJ and KEdV drafted the manuscript. All authors read and approved the final manuscript.

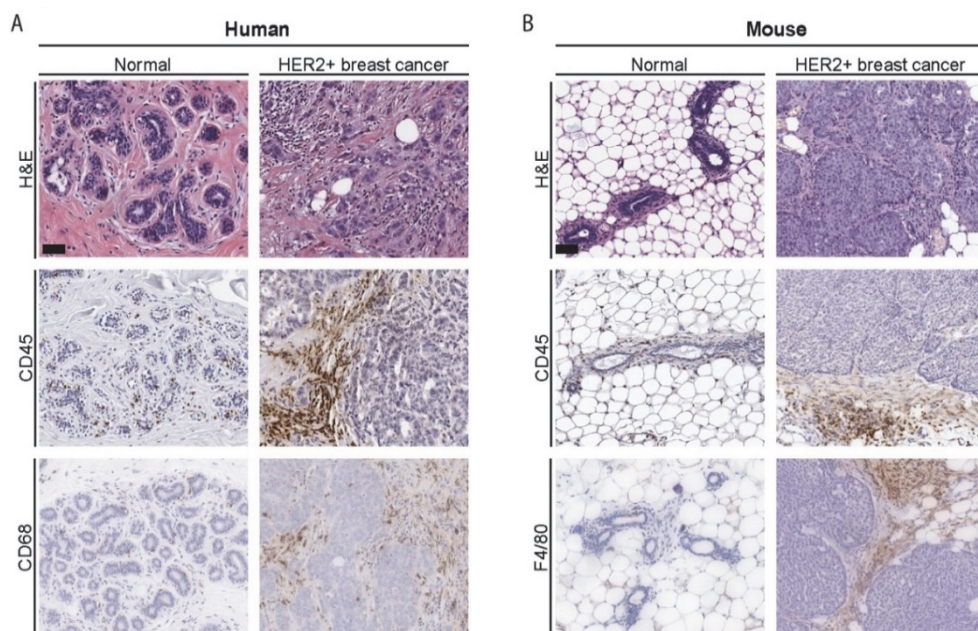
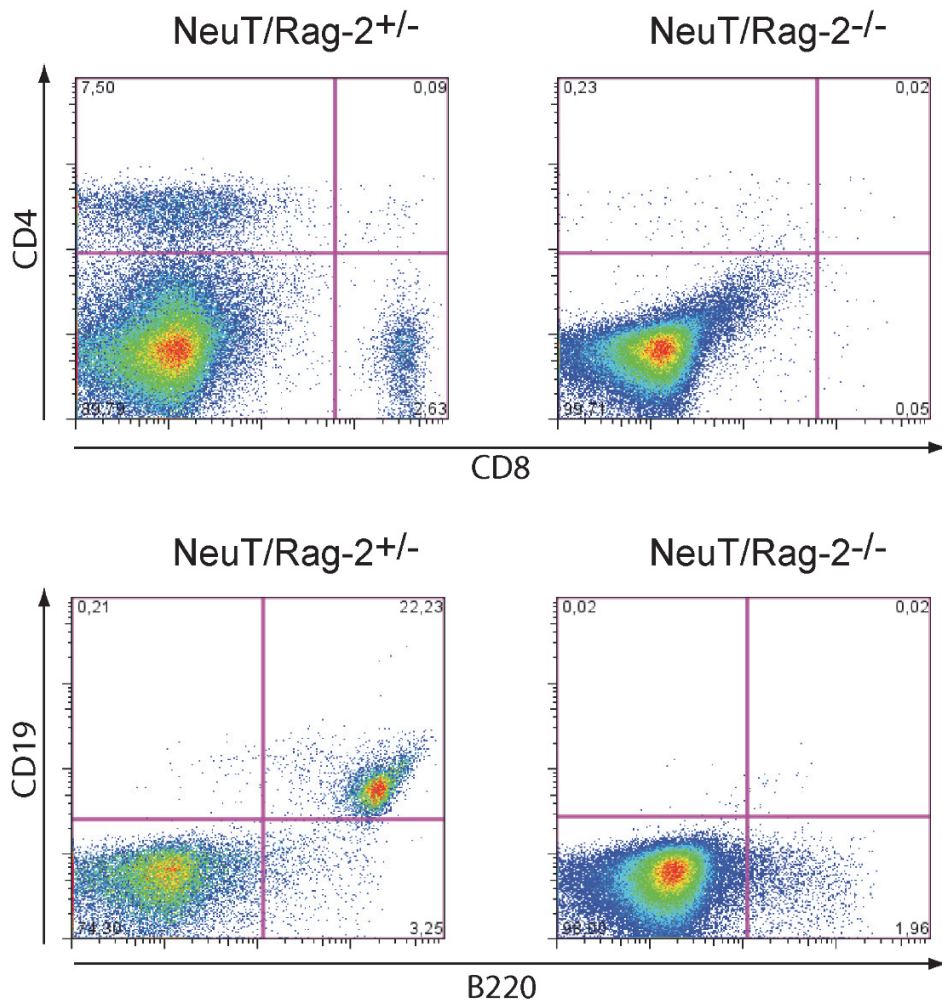


**Figure S1. Increased infiltration of immune cells in human and mouse HER2+ breast cancer.** Hematoxylin and eosin (H&E)-stained sections of human normal mammary glands, human invasive HER2+ breast tumors (A) and normal mammary glands of adult wild-type mice and HER2+ breast tumors of MMTV-NeuT mice (B). Immunodetection of CD45<sup>+</sup> leukocytes (brown staining) and macrophages (CD68<sup>+</sup> cells in human tissues and F4/80<sup>+</sup> cells in mouse tissues; brown staining). Representative images are shown. (n = 5 for human tissues, n = 8 for mouse tissues). Scale Bar, 50  $\mu$ m.

Development of metastatic HER2+ breast cancer is independent of the adaptive immune system



2

**Figure S2. Absence of CD4<sup>+</sup> and CD8<sup>+</sup> T cells and CD20<sup>+</sup>/CD19<sup>+</sup> B cells in NeuT/Rag-2<sup>-/-</sup> mice.** Flow cytometric analysis of CD4<sup>+</sup> and CD8<sup>+</sup> T cells and CD19<sup>+</sup>/B220<sup>+</sup> B cells in blood from NeuT/Rag-2<sup>+/-</sup> mice and NeuT/Rag-2<sup>-/-</sup> mice. Representative dot plots including percentages of CD4<sup>+</sup> and CD8<sup>+</sup> T cells (upper panel) and CD19<sup>+</sup>/B220<sup>+</sup> B cells (lower panel) gated on live CD45<sup>+</sup> leukocytes are shown.

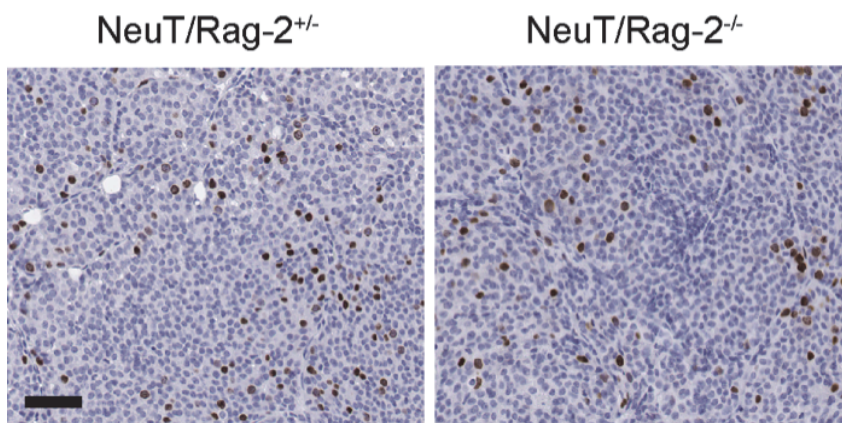


**Figure S3. The adaptive immune system does not modulate proliferation of breast cancer cells in MMTV-NeuT mice.** Immunodetection of proliferating cells positive for BrdU (brown staining). Ninety minutes before sacrifice, tumour-bearing mice were injected with BrdU (n= 7/group). BrdU incorporation was assessed by immunohistochemistry. Scale Bar, 50  $\mu$ m.

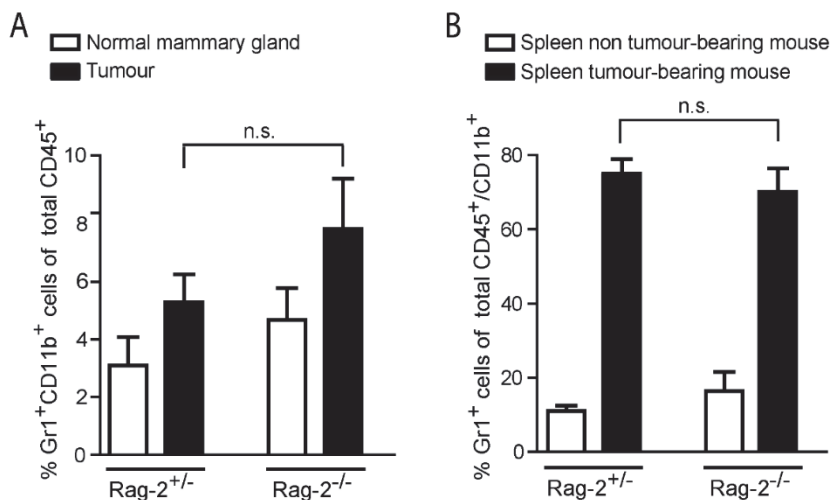


**Figure S4. Accumulation of Gr1+CD11b+ granulocytes in the tumormicroenvironment and spleen is not altered by the absence of the adaptive immune system.** (A) Flow cytometric analysis of Gr1<sup>+</sup>CD11b<sup>+</sup> granulocytes in normal mammary glands from age-matched wild type Rag-2<sup>+/-</sup> and Rag-2<sup>-/-</sup> mice and in tumors of NeuT/Rag-2<sup>+/-</sup> mice and NeuT/Rag-2<sup>-/-</sup> mice. Data on Gr1<sup>+</sup>CD11b<sup>+</sup> leukocytes are depicted as mean percentage gated on live CD45<sup>+</sup> leukocytes ± SEM (n = 4 per wild type cohort; n = 8 per tumor cohort). n.s., not significant by Mann-Whitney test. (B) Flow cytometric analysis of Gr1<sup>+</sup> leukocytes in spleens from age-matched wild type Rag-2<sup>+/-</sup> and Rag-2<sup>-/-</sup> mice (non tumour-bearing) and in spleens of tumour-bearing NeuT/Rag-2<sup>+/-</sup> mice and NeuT/Rag-2<sup>-/-</sup> mice. Data on Gr1<sup>+</sup> leukocytes are depicted as mean percentage gated on live CD45<sup>+</sup>/CD11b<sup>+</sup> leukocytes ± SEM (n = 4 per wild type cohort; n = 8 per tumor cohort). n.s., not significant by Mann-Whitney test.

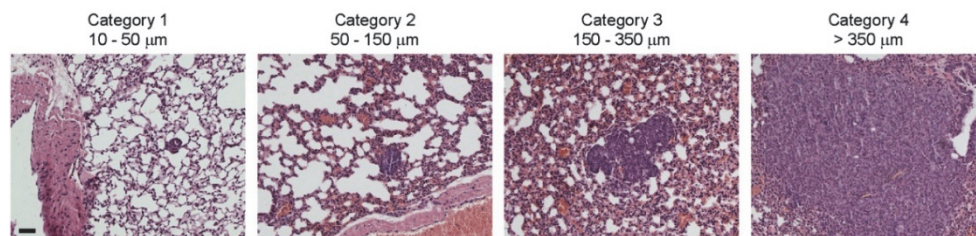


**Figure S5. Size-categories of pulmonary metastases.** H&E stainings of lung metastases from tumor-bearing NeuT/Rag-2<sup>+/-</sup> mice representing the different size categories. Size of individual metastases was determined by measurement of the average diameter (n = 15 mice/cohort). Category 1: 10 – 50  $\mu\text{m}$  diameter; Category 2: 50 – 150  $\mu\text{m}$  diameter; Category 3: 150 - 350  $\mu\text{m}$  diameter; Category 4: > 350  $\mu\text{m}$  diameter. Scale Bar, 50  $\mu\text{m}$ .

## Supplemental Table 1a

*Detailed information about antibodies used for immunohistochemistry*

Antibody specificity	Clone (company)	Dilution	Antigen retrieval	Tissue
Mouse anti-human CD45	HI30 (eBioscience <sup>1</sup> )	1:100	Citra buffer (Biogenex <sup>2</sup> )	Paraffin <sup>9</sup>
Mouse anti-human CD4	4B12 (Monosan <sup>3</sup> )	1:100	Citra buffer (Biogenex)	Paraffin
Mouse anti-human CD8	C8/144B (DAKO <sup>4</sup> )	1:200	Citra buffer (Biogenex)	Paraffin
Mouse anti-human CD20	L26 (DAKO)	1:1000	Citra buffer (Biogenex)	Paraffin
Mouse anti-human CD68	PG-M1 (DAKO)	1:150	3 min Proteinase K (DAKO)	Paraffin
Rat anti-mouse CD45	30-F11 (BD biosciences <sup>5</sup> )	1:200	Citra buffer (Biogenex)	Paraffin
Rat anti-mouse CD4	GK1.5 (hybridoma supernatant, NKI <sup>6</sup> )	1:1000	none	Cryo <sup>10</sup>
Rat anti-mouse CD8	2.43 (hybridoma supernatant, NKI)	1:1000	none	Cryo
Rat anti-mouse B220	RA3-6B2 (BD biosciences)	1:500	Citra buffer (Biogenex)	Paraffin
Rat anti-mouse F4/80	Cl:A3-1 (Serotec <sup>7</sup> )	1:300	none	Paraffin
Mouse anti-BrdU	Bu20a (DAKO)	1:100	Citra buffer (Biogenex)	Paraffin
Biotinylated goat anti-rat	(Southern Biotech <sup>8</sup> )	1:300	NA	
Biotinylated goat anti-mouse	(DAKO)	1:300	NA	

<sup>1</sup>San Diego, CA; <sup>2</sup>San Ramon, CA; <sup>3</sup>Uden, the Netherlands; <sup>4</sup>Denmark; <sup>5</sup>San Diego, CA; <sup>6</sup>purified hybridoma supernatant produced by protein core facility of NKI; <sup>7</sup>Dusseldorf, Germany; <sup>8</sup>Birmingham, AL

<sup>9</sup> Collected tissues and tumors were fixed for 24 hours in 10% neutral buffered formalin. Tissues were embedded in paraffin. For immunohistochemical analysis, 5µm thick paraffin sections were cut, deparaffinized, and stained.

<sup>10</sup> Tissue samples were frozen directly in glycerol-based freezing medium (OCT). 10-µm thick OCT-embedded tissue sections were cut using a Leica CM3050 S cryostat. Sections were air-dried, fixed in ice-cold acetone for 5-min, incubated for 10 min with avidin solution (DAKO), PBS washed, incubated for 10 min with biotin solution (DAKO), PBS washed and blocked for 30-min in blocking buffer (5% goat serum/2.5% bovine serum albumin/PBS). Antibodies were diluted in 0.5X blocking buffer and incubated with tissue sections for 1.5-hr at room temperature. Sections were washed with PBS and incubated with secondary antibody for 45-min at RT

**Supplemental Table 1b***Detailed information about antibodies used for flow cytometry*

<b>Antibody specificity</b>	<b>Clone (company)</b>	<b>Dilution</b>
FITC anti-mouseCD4	GK1.5 (eBioscience)	1:200
PE anti-mouse CD8	53-6.7 (eBioscience)	1:200
FITC anti-mouse CD19	MB19-1 (eBioscience)	1:200
PE anti-mouse B220	CD45R RAS3-6B2 (eBioscience)	1:200
APC anti-mouse CD45	30-F11 (eBioscience)	1:200
PE anti-mouse CD11b	M 1/70 (eBioscience)	1:200
FITC anti-mouse GR1	RB6-8C5 (eBioscience)	1:200
FITC anti-mouse F4/80	BM8 (eBioscience)	1:200

## References

1. Dunn GP, Old LJ, Schreiber RD. The immunobiology of cancer immunosurveillance and immunoediting. *Immunity* 2004; **21**: 137-148.
2. Willimsky G, Blankenstein T. Sporadic immunogenic tumours avoid destruction by inducing T-cell tolerance. *Nature* 2005; **437**: 141-146.
3. de Visser KE, Eichten A, Coussens LM. Paradoxical roles of the immune system during cancer development. *Nat Rev Cancer* 2006; **6**: 24-37.
4. Pardoll DM. Does the immune system see tumors as foreign or self? *Annu Rev Immunol* 2003; **21**: 807-839.
5. Shankaran V, Ikeda H, Bruce AT, *et al.* IFN $\gamma$  and lymphocytes prevent primary tumour development and shape tumour immunogenicity. *Nature* 2001; **410**: 1107-1111.
6. Dunn GP, Bruce AT, Ikeda H, *et al.* Cancer immunoediting: from immunosurveillance to tumor escape. *Nat Immunol* 2002; **3**: 991-998.
7. Casanovas O, Hicklin DJ, Bergers G, *et al.* Drug resistance by evasion of antiangiogenic targeting of VEGF signaling in late-stage pancreatic islet tumors. *Cancer Cell* 2005; **8**: 299-309.
8. de Visser KE, Korets LV, Coussens LM. De novo carcinogenesis promoted by chronic inflammation is B lymphocyte dependent. *Cancer Cell* 2005; **7**: 411-423.
9. Haybaeck J, Zeller N, Wolf MJ, *et al.* A lymphotoxin-driven pathway to hepatocellular carcinoma. *Cancer Cell* 2009; **16**: 295-308.
10. DeNardo DG, Barreto JB, Andreu P, *et al.* CD4(+) T cells regulate pulmonary metastasis of mammary carcinomas by enhancing protumor properties of macrophages. *Cancer Cell* 2009; **16**: 91-102.
11. Andreu P, Johansson M, Affara NI, *et al.* FcR $\gamma$  activation regulates inflammation-associated squamous carcinogenesis. *Cancer Cell* 2010; **17**: 121-134.
12. Perou CM, Sorlie T, Eisen MB, *et al.* Molecular portraits of human breast tumours. *Nature* 2000; **406**: 747-752.
13. Linn SC, Van 't Veer LJ. Clinical relevance of the triple-negative breast cancer concept: genetic basis and clinical utility of the concept. *Eur J Cancer* 2009; **45 Suppl 1**: 11-26.
14. Burstein HJ. The distinctive nature of HER2-positive breast cancers. *N Engl J Med* 2005; **353**: 1652-1654.
15. Desmedt C, Haibe-Kains B, Wirapati P, *et al.* Biological processes associated with breast cancer clinical outcome depend on the molecular subtypes. *Clin Cancer Res* 2008; **14**: 5158-5165.
16. Slamon DJ, Godolphin W, Jones LA, *et al.* Studies of the HER-2/neu proto-oncogene in human breast and ovarian cancer. *Science* 1989; **244**: 707-712.
17. Alexe G, Dalgin GS, Scandfeld D, *et al.* High expression of lymphocyte-associated genes in node-negative HER2+ breast cancers correlates with lower recurrence rates. *Cancer Res* 2007; **67**: 10669-10676.

18. Rody A, Holtrich U, Pusztai L, *et al.* T-cell metagene predicts a favorable prognosis in estrogen receptor-negative and HER2-positive breast cancers. *Breast Cancer Res* 2009; **11**: R15.
19. Stewart T, Tsai SC, Grayson H, *et al.* Incidence of de-novo breast cancer in women chronically immunosuppressed after organ transplantation. *Lancet* 1995; **346**: 796-798.
20. Engels EA, Goedert JJ. Human immunodeficiency virus/acquired immunodeficiency syndrome and cancer: past, present, and future. *J Natl Cancer Inst* 2005; **97**: 407-409.
21. Muller WJ, Sinn E, Pattengale PK, *et al.* Single-step induction of mammary adenocarcinoma in transgenic mice bearing the activated c-neu oncogene. *Cell* 1988; **54**: 105-115.
22. Boggio K, Nicoletti G, Di Carlo E, *et al.* Interleukin 12-mediated prevention of spontaneous mammary adenocarcinomas in two lines of Her-2/neu transgenic mice. *J Exp Med* 1998; **188**: 589-596.
23. Shinkai Y, Rathbun G, Lam KP, *et al.* RAG-2-deficient mice lack mature lymphocytes owing to inability to initiate V(D)J rearrangement. *Cell* 1992; **68**: 855-867.
24. Weijer K, Uittenbogaart CH, Voordouw A, *et al.* Intrathymic and extrathymic development of human plasmacytoid dendritic cell precursors in vivo. *Blood* 2002; **99**: 2752-2759.
25. Evers B, Speksnijder EN, Schut E, *et al.* A tissue reconstitution model to study cancer cell-intrinsic and -extrinsic factors in mammary tumourigenesis. *J Pathol* 2010; **220**: 34-44.
26. Hoebe K, Janssen E, Beutler B. The interface between innate and adaptive immunity. *Nat Immunol* 2004; **5**: 971-974.
27. Shanker A. Adaptive control of innate immunity. *Immunol Lett* 2010.
28. Seruga B, Zhang H, Bernstein LJ, *et al.* Cytokines and their relationship to the symptoms and outcome of cancer. *Nat Rev Cancer* 2008; **8**: 887-899.
29. Balkwill F. Tumour necrosis factor and cancer. *Nat Rev Cancer* 2009; **9**: 361-371.
30. de Visser KE. Spontaneous immune responses to sporadic tumors: tumor-promoting, tumor-protective or both? *Cancer Immunol Immunother* 2008; **57**: 1531-1539.
31. Takeuchi N, Hiraoka S, Zhou XY, *et al.* Anti-HER-2/neu immune responses are induced before the development of clinical tumors but declined following tumorigenesis in HER-2/neu transgenic mice. *Cancer Res* 2004; **64**: 7588-7595.
32. Kmiecik M, Morales JK, Morales J, *et al.* Danger signals and nonself entity of tumor antigen are both required for eliciting effective immune responses against HER-2/neu positive mammary carcinoma: implications for vaccine design. *Cancer Immunol Immunother* 2008; **57**: 1391-1398.
33. Disis ML, Calenoff E, McLaughlin G, *et al.* Existent T-cell and antibody immunity to HER-2/neu protein in patients with breast cancer. *Cancer Res* 1994; **54**: 16-20.

34. Peoples GE, Goedegebuure PS, Smith R, *et al.* Breast and ovarian cancer-specific cytotoxic T lymphocytes recognize the same HER2/neu-derived peptide. *Proc Natl Acad Sci U S A* 1995; **92**: 432-436.
35. Park JM, Terabe M, Donaldson DD, *et al.* Natural immunosurveillance against spontaneous, autochthonous breast cancers revealed and enhanced by blockade of IL-13-mediated negative regulation. *Cancer Immunol Immunother* 2008; **57**: 907-912.
36. Melani C, Chiodoni C, Forni G, *et al.* Myeloid cell expansion elicited by the progression of spontaneous mammary carcinomas in c-erbB-2 transgenic BALB/c mice suppresses immune reactivity. *Blood* 2003; **102**: 2138-2145.
37. Ambrosino E, Spadaro M, Iezzi M, *et al.* Immunosurveillance of ErbB2 carcinogenesis in transgenic mice is concealed by a dominant regulatory T-cell self-tolerance. *Cancer Res* 2006; **66**: 7734-7740.
38. Norian LA, Rodriguez PC, O'Mara LA, *et al.* Tumor-infiltrating regulatory dendritic cells inhibit CD8+ T cell function via L-arginine metabolism. *Cancer Res* 2009; **69**: 3086-3094.
39. Rovero S, Amici A, Carlo ED, *et al.* DNA vaccination against rat her-2/Neu p185 more effectively inhibits carcinogenesis than transplantable carcinomas in transgenic BALB/c mice. *J Immunol* 2000; **165**: 5133-5142.
40. Spadaro M, Lanzardo S, Curcio C, *et al.* Immunological inhibition of carcinogenesis. *Cancer Immunol Immunother* 2004; **53**: 204-216.
41. Rolla S, Ria F, Occhipinti S, *et al.* ErbB2 DNA vaccine combined with regulatory T cell deletion enhances antibody response and reveals latent low-avidity T cells: potential and limits of its therapeutic efficacy. *J Immunol* 2010; **184**: 6124-6132.
42. Park S, Jiang Z, Mortenson ED, *et al.* The therapeutic effect of anti-HER2/neu antibody depends on both innate and adaptive immunity. *Cancer Cell* 2010; **18**: 160-170.
43. Shchors K, Shchors E, Rostker F, *et al.* The Myc-dependent angiogenic switch in tumors is mediated by interleukin 1beta. *Genes Dev* 2006; **20**: 2527-2538.
44. Soucek L, Lawlor ER, Soto D, *et al.* Mast cells are required for angiogenesis and macroscopic expansion of Myc-induced pancreatic islet tumors. *Nat Med* 2007; **13**: 1211-1218.
45. Sparmann A, Bar-Sagi D. Ras-induced interleukin-8 expression plays a critical role in tumor growth and angiogenesis. *Cancer Cell* 2004; **6**: 447-458.
46. Yarden Y, Sliwkowski MX. Untangling the ErbB signalling network. *Nat Rev Mol Cell Biol* 2001; **2**: 127-137.
47. Casares N, Pequignot MO, Tesniere A, *et al.* Caspase-dependent immunogenicity of doxorubicin-induced tumor cell death. *J Exp Med* 2005; **202**: 1691-1701.
48. Apetoh L, Ghiringhelli F, Tesniere A, *et al.* Toll-like receptor 4-dependent contribution of the immune system to anticancer chemotherapy and radiotherapy. *Nat Med* 2007; **13**: 1050-1059.

## Chapter 2

49. Herschkowitz JI, Simin K, Weigman VJ, *et al.* Identification of conserved gene expression features between murine mammary carcinoma models and human breast tumors. *Genome Biol* 2007; **8**: R76.
50. Derksen PW, Liu X, Saridin F, *et al.* Somatic inactivation of E-cadherin and p53 in mice leads to metastatic lobular mammary carcinoma through induction of anoikis resistance and angiogenesis. *Cancer Cell* 2006; **10**: 437-449.
51. Frese KK, Tuveson DA. Maximizing mouse cancer models. *Nat Rev Cancer* 2007; **7**: 645-658.



## Chapter 3



# **Chemotherapy response of spontaneous mammary tumors is independent of the adaptive immune system**

Metamia Ciampricotti, Cheei-Sing Hau, Chris W. Doornebal, Jos Jonkers, Karin E. de Visser

Division of Molecular Biology, the Netherlands Cancer Institute, Plesmanlaan 121, 1066 CX Amsterdam, The Netherlands

3

Correspondence to Karin E. de Visser

e-mail: [k.d.visser@nki.nl](mailto:k.d.visser@nki.nl)

*Nature Medicine*.2012 Mar 6;18(3):344-6

## CORRESPONDENCE

### To the Editor:

On the basis of data published in *Nature Medicine*, the research groups of Zitvogel and Kroemer have launched the hypothesis that the adaptive immune system dictates therapeutic efficacy of certain chemotherapeutics<sup>1-3</sup>. Using *in vitro* systems and tumor transplantation models, they shown that cancer cells undergo immunogenic cell death in response to certain commonly used chemotherapeutics, specifically anthracyclins and oxaliplatin<sup>1-3</sup>, which leads to activation of effective antitumor T cell responses<sup>1-3</sup>. Consistent with these observations, the authors showed that anthracyclins and oxaliplatin lose their therapeutic efficacy on tumor cell line outgrowths in mice with defective adaptive immune cell function<sup>1-3</sup>. An important limitation of tumor cell line transplantation models is that they do not fully recapitulate *de novo* tumor formation with co-evolving tumor-host interactions and an immunosuppressive microenvironment<sup>4</sup>. We therefore set out to investigate the effects of the adaptive immune system on the chemoresponsiveness of spontaneous transforming rat Human Epidermal Growth Factor Receptor 2 (HER2)-positive mammary tumors in mouse mammary tumor virus (MMTV)-*NeuT* transgenic female mice (**Supplementary Methods**). Treatment of tumor-bearing MMTV-*NeuT* mice with cisplatin and oxaliplatin induced a threefold increase in intratumoral accumulation of CD3<sup>+</sup> T lymphocytes, whereas we observed no shift in the intratumoral ratio of CD4<sup>+</sup> to CD8<sup>+</sup> T cells or a change in influx of forkhead box P3 (FoxP3)<sup>+</sup> T cells (**Supplementary Fig. 1**). To test the functional role of the adaptive immune system in the chemotherapy response, we intercrossed MMTV-*NeuT* (BALB/c) mice with T cell- and B cell-deficient *Rag2*<sup>-/-</sup> (BALB/c) mice. Absence of the adaptive immune system did not affect mammary tumorigenesis in these mice (**Supplementary Methods**). Outgrowth of mammary tumors in MMTV-*NeuT*;*Rag2*<sup>+/-</sup> mice was effectively inhibited by treatment with cisplatin, oxaliplatin and doxorubicin (**Fig. 1**). These chemotherapeutics were equally effective in inhibiting the growth of mammary tumors in T cell- and B cell-deficient MMTV-*NeuT*;*Rag2*<sup>-/-</sup> mice (**Fig. 1**), indicating that the adaptive immune system does not contribute to response of spontaneous mammary tumors in MMTV-*NeuT* mice to cisplatin, oxaliplatin, or doxorubicin.

## Chemotherapy response of spontaneous mammary tumors is independent of the adaptive immune system

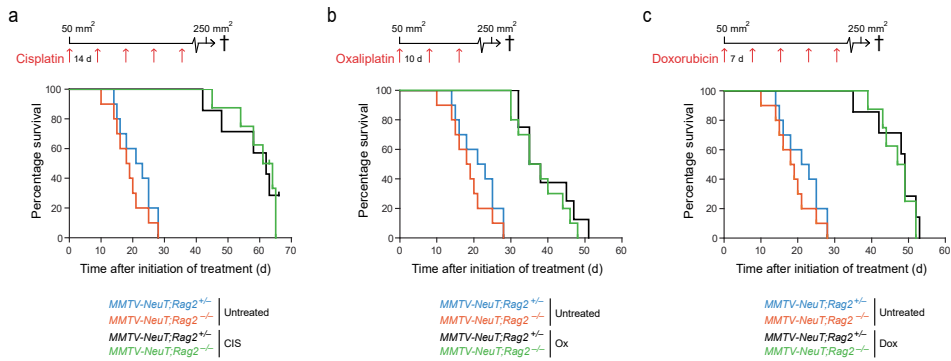


**Figure 1** Chemotherapy efficacy in tumor-bearing MMTV-*NeuT* mice is independent of the adaptive immune system

(a) Kaplan-Meier survival curves of untreated and cisplatin (CIS)-treated MMTV-*NeuT*; *Rag2*<sup>+/-</sup> and MMTV-*NeuT*; *Rag2*<sup>-/-</sup> mice (Supplementary Methods). Cisplatin-treated MMTV-*NeuT*; *Rag2*<sup>+/-</sup> ( $n = 7$ , with 2 censored) compared to cisplatin-treated MMTV-*NeuT*; *Rag2*<sup>-/-</sup> mice ( $n = 8$ , with 1 censored),  $P = 0.99$ ; untreated MMTV-*NeuT*; *Rag2*<sup>+/-</sup> mice ( $n = 10$ ) compared to untreated MMTV-*NeuT*; *Rag2*<sup>-/-</sup> mice ( $n = 10$ ),  $P = 0.30$ ; all cisplatin-treated mice compared to all untreated mice,  $P < 0.0002$  (log-rank test). The main cause of death of the censored mice was cisplatin-induced renal toxicity. (b) Kaplan-Meier tumor-specific survival curves of untreated and oxaliplatin (Ox)-treated MMTV-*NeuT*; *Rag2*<sup>+/-</sup> and MMTV-*NeuT*; *Rag2*<sup>-/-</sup> mice (Supplementary Methods). Oxaliplatin-treated MMTV-*NeuT*; *Rag2*<sup>+/-</sup> mice ( $n = 8$ ) compared to oxaliplatin-treated MMTV-*NeuT*; *Rag2*<sup>-/-</sup> mice ( $n = 10$ ),  $P = 0.5$ ; oxaliplatin-treated mice compared to untreated mice,  $P < 0.0001$  (log-rank test). (c) Kaplan-Meier tumor-specific survival curves of untreated and doxorubicin (Dox)-treated MMTV-*NeuT*; *Rag2*<sup>+/-</sup> and MMTV-*NeuT*; *Rag2*<sup>-/-</sup> mice (Supplementary Methods). Doxorubicin-treated MMTV-*NeuT*; *Rag2*<sup>+/-</sup> ( $n = 7$ ) compared to doxorubicin-treated MMTV-*NeuT*; *Rag2*<sup>-/-</sup> mice ( $n = 8$ ),  $P = 0.62$ ; doxorubicin-treated mice compared to untreated mice,  $P < 0.0002$  (log-rank test). All mice were killed when a cumulative tumor size of 250 mm<sup>2</sup> was reached. All experimental groups were run in parallel; the same control groups are shown in the three panels. The average age of mice at the start of treatment was 124 d.

These data stand in contrast to the previously reported dependency of the anticancer efficacy of oxaliplatin and doxorubicin on antitumor adaptive immune responses<sup>1-3</sup>. To exclude the possibility that unique properties of the MMTV-*NeuT* mouse model, such as overexpression of an activated oncogene or the presence of multiple mammary tumors, obscure any potential benefit of the adaptive immune system in chemoresponsiveness, we verified our findings in a second independent mouse model of spontaneous mammary tumorigenesis: conditional *K14cre*; *Cdh1*<sup>flox/flox</sup>; *Trp53*<sup>flox/flox</sup> mice which develop invasive mammary carcinomas at around 6 months of age (**Supplementary Methods**). We intercrossed *K14cre*; *Cdh1*<sup>flox/flox</sup>; *Trp53*<sup>flox/flox</sup> (FVB/N) mice T-cell- and B-cell-deficient *Rag1*<sup>-/-</sup> (FVB/N) mice. Absence of the adaptive immune system did not affect mammary tumorigenesis in these mice (**Fig. 2** and data not shown). Intratumoral influx of CD3<sup>+</sup> T cells and FoxP3<sup>+</sup> T cells and the intratumoral ratio of CD4<sup>+</sup> to CD8<sup>+</sup> T cells in *K14cre*; *Cdh1*<sup>flox/flox</sup>; *Trp53*<sup>flox/flox</sup>; *Rag1*<sup>+/-</sup> mice was not changed as a result of chemotherapy treatment (**Supplementary Fig. 2**). The growth of mammary tumors in *K14cre*; *Cdh1*<sup>flox/flox</sup>; *Trp53*<sup>flox/flox</sup>; *Rag1*<sup>+/-</sup> mice was inhibited by oxaliplatin and cisplatin (**Fig. 2**) but was unaffected by doxorubicin (data not shown). The response profiles of spontaneous tumors arising in *K14cre*; *Cdh1*<sup>flox/flox</sup>; *Trp53*<sup>flox/flox</sup>; *Rag1*<sup>-/-</sup> mice to cisplatin and oxaliplatin were not statistically significantly different from those in *K14cre*; *Cdh1*<sup>flox/flox</sup>; *Trp53*<sup>flox/flox</sup>; *Rag1*<sup>+/-</sup> mice (**Fig. 2**). Moreover, depletion of CD8<sup>+</sup> T cells did not influence the chemoresponsiveness of the tumors in *K14cre*; *Cdh1*<sup>flox/flox</sup>; *Trp53*<sup>flox/flox</sup>; *Rag1*<sup>+/-</sup> mice (**Supplementary Fig. 3**). These data indicate that absence of the adaptive immune system did not alter the efficacy of chemotherapy in tumor-bearing *K14cre*; *Cdh1*<sup>flox/flox</sup>; *Trp53*<sup>flox/flox</sup> mice.

## Chemotherapy response of spontaneous mammary tumors is independent of the adaptive immune system

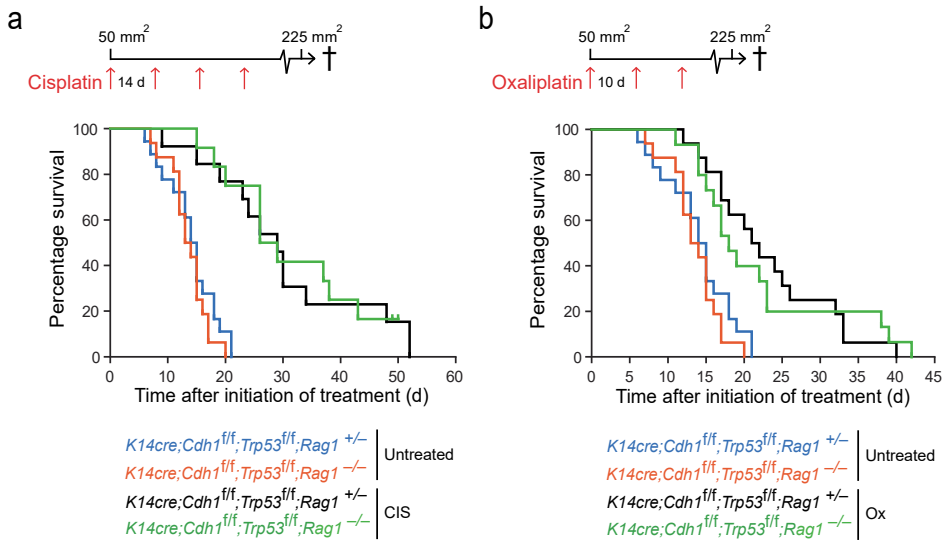


**Figure 2** Chemotherapy efficacy in tumor-bearing *K14cre; Cdh1<sup>flox/flox</sup>; Trp53<sup>flox/flox</sup>* mice is independent of the adaptive immune system.

**(a)** Kaplan-Meier survival curves of untreated and cisplatin-treated *K14cre; Cdh<sup>flox/flox</sup>; Trp53<sup>flox/flox</sup>; Rag-1<sup>+/-</sup>* and *K14cre; Cdh<sup>flox/flox</sup>; Trp53<sup>flox/flox</sup>; Rag-1<sup>-/-</sup>* mice (Supplementary Methods). Cisplatin-treated *K14cre; Cdh<sup>flox/flox</sup>; Trp53<sup>flox/flox</sup>; Rag-1<sup>+/-</sup>* (n=13, with 1 censored) compared to cisplatin-treated *K14cre; Cdh<sup>flox/flox</sup>; Trp53<sup>flox/flox</sup>; Rag-1<sup>-/-</sup>* mice (n=12 with 2 censored): P=0.81; cisplatin-treated mice compared to untreated mice, P<0.0001; untreated *K14cre; Cdh<sup>flox/flox</sup>; Trp53<sup>flox/flox</sup>; Rag-1<sup>+/-</sup>* (n=18) compared to untreated *K14cre; Cdh<sup>flox/flox</sup>; Trp53<sup>flox/flox</sup>; Rag-1<sup>-/-</sup>* mice (n=16), P=0.33 (log-rank test). Mice were killed when the tumor reached a size of 225 mm<sup>2</sup>. The main cause of death of the censored mice was cisplatin-induced renal toxicity. **(b)** Kaplan-Meier tumor-specific survival curve of untreated and oxaliplatin-treated *K14cre; Cdh<sup>flox/flox</sup>; Trp53<sup>flox/flox</sup>; Rag-1<sup>+/-</sup>* and *K14cre; Cdh<sup>flox/flox</sup>; Trp53<sup>flox/flox</sup>; Rag-1<sup>-/-</sup>* mice (Supplementary Methods). Oxaliplatin treated *K14cre; Cdh<sup>flox/flox</sup>; Trp53<sup>flox/flox</sup>; Rag-1<sup>+/-</sup>* (n=16) compared to oxaliplatin-treated *K14cre; Cdh<sup>flox/flox</sup>; Trp53<sup>flox/flox</sup>; Rag-1<sup>-/-</sup>* mice (n=15), P=0.88; oxaliplatin-treated mice compared to untreated mice, P<0.0003 (log-rank test). Mice were killed when the tumor reached a size of 225 mm<sup>2</sup>. All experimental groups were run in parallel; the same control groups are shown in both panels. Average age of mice at the start of treatment was 213 d.

Using two independent clinically relevant spontaneous mammary tumor models, we found that the adaptive immune system is dispensable for therapeutic efficacy of three independent chemotherapeutics. In contrast, the Zitvogel and Kroemer groups reported that two of these drugs, oxaliplatin and doxorubicin, induced immunogenic cell death<sup>1-3</sup>. It is most likely that this discrepancy is a result of the fact that we used spontaneous mammary tumor models, whereas Zitvogel and Kroemer used tumor cell line transplantation models or the immunogenic 3-methylcholanthrene fibrosarcoma model<sup>5</sup>. Tumors produced by inoculation of cancer cells do not resemble established spontaneous tumors. Transplanted tumor cells produce palpable outgrowths without going through a premalignant phase, and their stromal microenvironment does not reflect the microenvironment of sporadic tumors. The dissimilarity between these two types of mouse tumor models is further underscored by the observation that spontaneous tumors have different chemotherapy response profiles than inoculated tumor cells isolated from these spontaneous tumors<sup>6</sup>. Inoculation of cancer cells results in massive tumor-cell necrosis and release of tumor antigens, which could trigger acute adaptive immune responses, whereas spontaneously arising tumors frequently trigger chronic innate immune responses that preclude acute T cell priming<sup>4,7</sup>. In tumor transplantation models, chemotherapy-induced immunogenic cell death may be sufficiently strong to effectively activate the (already primed) endogenous adaptive immune cell repertoire, resulting in enhanced T cell-mediated tumor cell death. Likewise, chemotherapy-induced cell death may be effective in immunogenic tumor models expressing strong antigens and may explain why in the 3-methylcholanthrene fibrosarcoma model, where host immunity has been shown to suppress tumor initiation, CD8<sup>+</sup> T cells contribute to the modest response to localized doxorubicin exposure<sup>5</sup>. In established spontaneous tumors, however, chemotherapy either does not induce immunogenic cell death or, more likely, induces immunogenic cell death that is not powerful enough to overcome the immunosuppressive networks present in *de novo* tumors. This is underscored by a recent study in which blockade of chronic inflammatory conditions in spontaneous mammary tumors in combination with chemotherapy improved survival in a CD8<sup>+</sup> T cell-dependent manner<sup>8</sup>. Of note, our data do not exclude the possibility that chemotherapy-induced immunogenic cell death can increase the efficacy of immunotherapy in *de novo* tumors. Synergistic effects of chemotherapy and immunotherapy have indeed been observed in experimental and clinical settings<sup>9-10</sup>. In conclusion, our findings indicate that the role of the endogenous adaptive immune system in chemotherapy response may not be as crucial as proposed

Chemotherapy response of spontaneous mammary tumors is independent of the adaptive immune system

previously<sup>1-3</sup>. Our findings urge for a careful analysis of the involvement of adaptive immunity in chemo-responsiveness in a larger set of *de novo* tumor models representing different types of human cancer. Moreover, it will be crucial to extend these findings to the clinical situation. This is not an easy task, as the influx of lymphocytes into human cancers on itself is associated with improved prognosis independent of anti-cancer therapy<sup>8</sup>. The current results cannot not rule out that for certain human cancers, chemotherapy can induce or enhance tumor-specific T cell responses. However, our data indicate that *de novo* epithelial tumor models provide no support for this, and the proposed role of immunogenic tumor cell death in anticancer chemotherapy is therefore still hypothetical. Understanding why the adaptive immune system does not contribute to chemoresponsiveness may yield new strategies to enhance antitumor immunity and the benefit of chemotherapy.

## ACKNOWLEDGMENTS

We thank Ton N. Schumacher for helpful discussions. We thank the protein facility at the Netherlands Cancer Institute for providing anti-CD8. Research described in this Correspondence was supported by grants from the Dutch Cancer Society (KWF grants 2006-3715 and 2011-5004 to KEdV and JJ), the Netherlands organization for Scientific Research (NWO grant VIDI 917.96.307 to KEdV), and the Association for International Cancer Research (AICR grant 11-0677 to KEdV).

## AUTHOR CONTRIBUTIONS

J.J and K.E.d.V. designed the study. M.C., C-S.H. and C.W.D. performed the experiments. K.E.d.V. took the initiative for this *Correspondence* and wrote the manuscript. All co-authors provided comments that helped shape the final submission

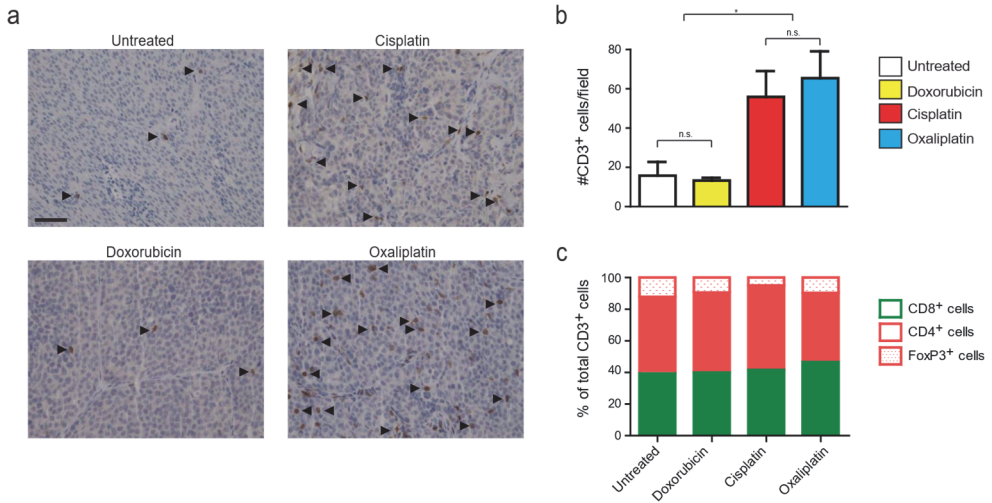
## COMPETING FINANCIAL INTERESTS

The authors declare no competing financial interests.

## References

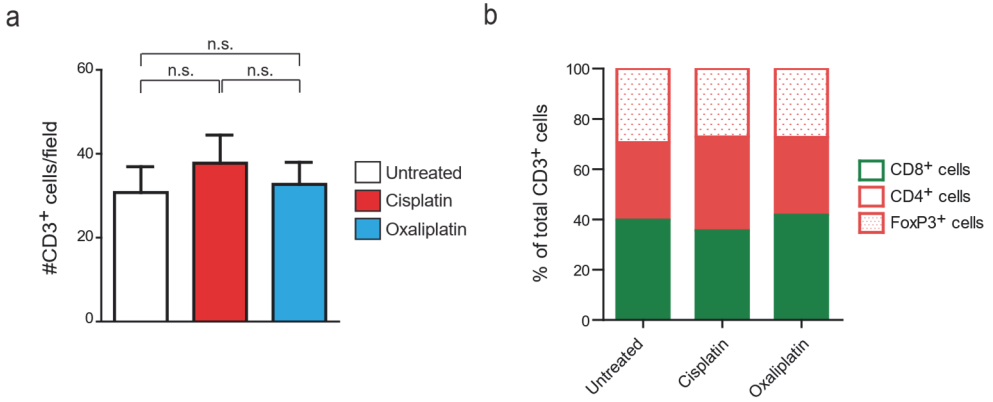
1. Apetoh, L., *et al. Nat Med* **13**, 1050-1059 (2007).
2. Obeid, M., *et al. Nat Med* **13**, 54-61 (2007).
3. Ghiringhelli, F., *et al. Nat Med* **15**, 1170-1178 (2009).
4. Schreiber, K., Rowley, D.A., Riethmuller, G. & Schreiber, H. *Hematol Oncol Clin North Am* **20**, 567-584 (2006).
5. Mattarollo, S.R., *et al. Cancer Res* **71**, 4809-4820 (2011).
6. Olive, K.P., *et al. Science* **324**, 1457-1461 (2009).
7. Willimsky, G., *et al. J Exp Med* **205**, 1687-1700 (2008).
8. DeNardo, D.G., *et al. Cancer Discov* **1**, 54-67 (2011).
9. Ramakrishnan, R., *et al. J Clin Invest* **120**, 1111-1124 (2010).
10. Robert, C., *et al. N Engl J Med* **364**, 2517-2526 (2011).

## Chemotherapy response of spontaneous mammary tumors is independent of the adaptive immune system



### Supplementary Figure 1 Intra-tumoral influx of CD3<sup>+</sup> T lymphocytes after chemotherapy treatment of mammary tumor-bearing *MMTV-NeuT* mice

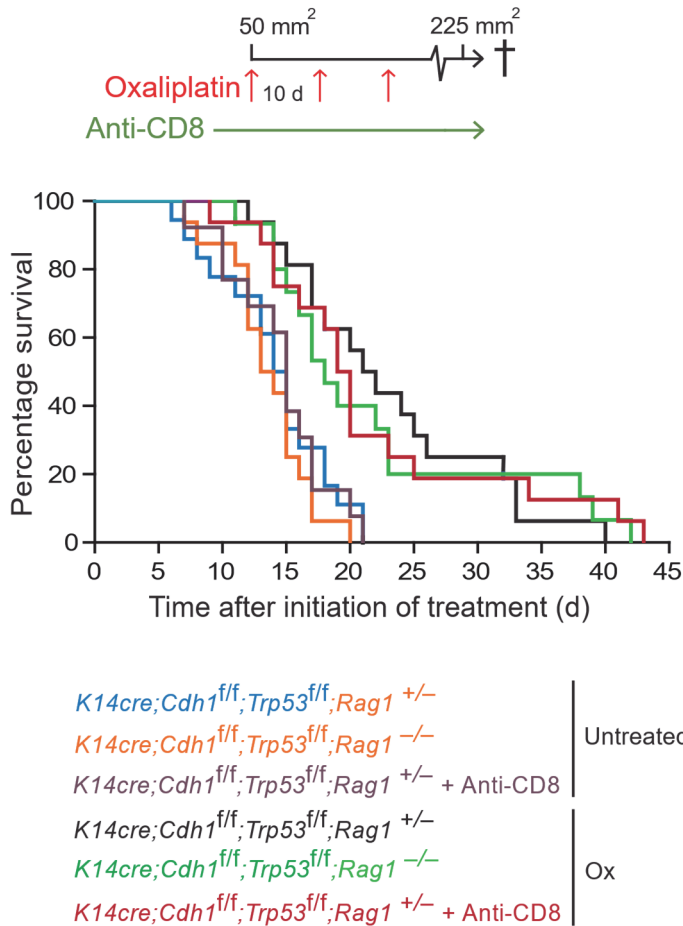
(a) Presence of CD3<sup>+</sup> T lymphocytes (brown staining; arrowheads) in end-stage mammary tumors of untreated and chemotherapy (cisplatin, doxorubicin, and oxaliplatin) treated *MMTV-NeuT* mice. Representative images are shown; Scale bar, 50  $\mu$ m. (b) Values represent average numbers of tumor-infiltrating CD3<sup>+</sup> lymphocytes from five high-power fields per mouse (untreated, n=7; cisplatin, n=7; doxorubicin, n=6; oxaliplatin, n=5). Error bars represent SEM. Untreated vs doxorubicin; P=0.37, Untreated vs cisplatin; P=0.018, Untreated vs oxaliplatin; P=0.018 and cisplatin vs oxaliplatin; P=0.53 (Mann Whitney test). (c) Proportion of CD4<sup>+</sup>, CD8<sup>+</sup> and FoxP3<sup>+</sup> T lymphocytes of total intra-tumoral influx of CD3<sup>+</sup> T lymphocytes. Influx of CD4<sup>+</sup>, CD8<sup>+</sup> and FoxP3<sup>+</sup> T lymphocytes was determined by immunohistochemistry; five high-power fields per tumor were counted (untreated, n=6; cisplatin, n=3; doxorubicin, n=5; oxaliplatin, n=6). P>0.05 (Mann Whitney test).



**Supplementary Figure 2** Intra-tumoral influx of CD3<sup>+</sup> T lymphocytes after chemotherapy treatment of mammary tumor-bearing *K14cre; Cdh1<sup>fllox/fllox</sup>; Trp53<sup>fllox/fllox</sup>* mice.

(a) Values represent average numbers of tumor-infiltrating CD3<sup>+</sup> lymphocytes from five high-power fields per mouse (untreated, n=9; cisplatin, n=9; oxaliplatin, n=10). Error bars represent SEM. Untreated vs cisplatin; P=0.44, Untreated vs oxaliplatin; P=0.62 and cisplatin vs oxaliplatin; P=0.50 (Mann Whitney test). (b) Proportion of CD4<sup>+</sup>, CD8<sup>+</sup> and FoxP3<sup>+</sup> T lymphocytes of total intra-tumoral influx of CD3<sup>+</sup> T lymphocytes. Influx of CD4<sup>+</sup>, CD8<sup>+</sup> and FoxP3<sup>+</sup> T lymphocytes was determined by immunohistochemistry; five high-power fields per tumor were counted (untreated, n=9; cisplatin, n=9; oxaliplatin, n=7). P>0.05 (Mann Whitney test).

Chemotherapy response of spontaneous mammary tumors is independent of the adaptive immune system



**Supplementary Figure 3** Kaplan-Meier survival curve of untreated and oxaliplatin treated *K14cre; Cdh<sup>flox/flox</sup>; Trp53<sup>flox/flox</sup>; Rag-1<sup>+/-</sup>* mice in combination with anti-CD8 (clone 2.43) treatment. Anti-CD8 treatment (i.p.; first injection 400 µg, followed by 150 µg. every 7 days) was initiated when the mammary tumor reached a size of 25 mm<sup>2</sup> till tumor outgrowth. Oxaliplatin treatment (3 cycles of 6 mg/kg i.v. with intervals of 10 days) was initiated when the mammary tumor reached a size of 50 mm<sup>2</sup>. Oxaliplatin and anti-CD8 treated *K14cre; Cdh<sup>flox/flox</sup>; Trp53<sup>flox/flox</sup>; Rag-1<sup>+/-</sup>* mice (n=16) versus anti-CD8 treated *K14cre; Cdh<sup>flox/flox</sup>; Trp53<sup>flox/flox</sup>; Rag-1<sup>+/-</sup>* (n=13): P=0.009. Untreated *K14cre; Cdh<sup>flox/flox</sup>; Trp53<sup>flox/flox</sup>; Rag-1<sup>+/-</sup>* mice (n=18) versus anti-CD8 treated *K14cre; Cdh<sup>flox/flox</sup>; Trp53<sup>flox/flox</sup>; Rag-1<sup>+/-</sup>* mice: P=0.94. Oxaliplatin treated *K14cre; Cdh<sup>flox/flox</sup>; Trp53<sup>flox/flox</sup>; Rag-1<sup>+/-</sup>* (n= 16) versus oxaliplatin and anti-CD8 treated = *K14cre; Cdh<sup>flox/flox</sup>; Trp53<sup>flox/flox</sup>; Rag-1<sup>+/-</sup>*: P=0.97. Oxaliplatin treated *K14cre; Cdh<sup>flox/flox</sup>; Trp53<sup>flox/flox</sup>; Rag-1<sup>+/-</sup>* (n=15) versus oxaliplatin and anti-CD8 treated *K14cre; Cdh<sup>flox/flox</sup>; Trp53<sup>flox/flox</sup>; Rag-1<sup>+/-</sup>*: P=0.74 (Log-Rank). Mice were sacrificed when the tumor reached a size of 225 mm<sup>2</sup>.

## Supplementary methods

### Transgenic mouse models

Female *MMTV-NeuT* mice (Balb/c), which express the transforming rat oncogene *ErbB2* (*Her-2*) under control of the *MMTV* promoter and develop multifocal carcinomas around 4 months of age<sup>1</sup>, were originally purchased from Charles River Italy, and maintained on the Balb/c background at the animal facility of the Netherlands Cancer Institute. *MMTV-NeuT* mice were intercrossed with *RAG2*<sup>-/-</sup> mice (Balb/c) to generate colonies of *MMTV-NeuT*;*RAG2*<sup>+/-</sup> and *MMTV-NeuT*;*RAG2*<sup>-/-</sup> mice. Genotyping was performed by PCR analysis on tail tip DNA as described previously<sup>2</sup>. Absence of the adaptive immune system did not affect latency, outgrowth, multiplicity and phenotype of primary mammary tumors<sup>2</sup>.

Female *K14cre*; *Cdh1*<sup>flf</sup>; *Trp53*<sup>flf</sup> mice (FVB/N), which have cre-recombinase mediated stochastic loss of both E-cadherin and p53 in mammary epithelial cells, develop invasive mammary carcinomas around 6 months of age<sup>3</sup> and were maintained on the FVB/N background at the animal facility of the Netherlands Cancer Institute. *K14cre*; *Cdh1*<sup>flf</sup>; *Trp53*<sup>flf</sup> mice were intercrossed with *RAG1*<sup>-/-</sup> mice (FVB/N) to generate colonies of *K14cre*; *Cdh1*<sup>flf</sup>; *Trp53*<sup>flf</sup>; *Rag1*<sup>+/-</sup> and *K14cre*; *Cdh1*<sup>flf</sup>; *Trp53*<sup>flf</sup>; *Rag1*<sup>-/-</sup> mice. Genotyping was performed by PCR analysis on tail tip DNA as described previously<sup>3-4</sup>. Absence of the adaptive immune system did not affect latency, outgrowth and phenotype of primary mammary tumors (**Fig. 2** and data not shown).

Female animals were monitored weekly for mammary tumor development by palpation. Once palpable tumors were present, tumor size was measured twice a week using a caliper. All mice were kept in individually ventilated cages at the animal care facility of the Netherlands Cancer Institute and food and water were given *ad libitum*. All animal experiments were performed in accordance with institutional guidelines and national ethical regulations.

### *In vivo* chemotherapy treatment

Cisplatin (RVG 101430, Pharmachemie BV, Haarlem, Netherlands) treatment of *MMTV-NeuT*;*Rag2*<sup>+/-</sup> and *MMTV-NeuT*;*Rag2*<sup>-/-</sup> mice was initiated when a cumulative tumor burden of 50 mm<sup>2</sup> was reached. Cisplatin

Chemotherapy response of spontaneous mammary tumors is independent of the adaptive immune system

was administered i.v. at 6 mg/kg per dose for 5 cycles with intervals of 14 days.

Oxaliplatin (RVG 34033, Pharmachemie BV, Haarlem, Netherlands) treatment of *MMTV-NeuT;Rag2<sup>+/-</sup>* and *MMTV-NeuT;Rag2<sup>-/-</sup>* mice was initiated when a cumulative tumor burden of 50 mm<sup>2</sup> was reached. Oxaliplatin was diluted 1:5 with NaCl before being administered i.v. at a dose of 6 mg/kg for 3 cycles with intervals of 10 days.

Doxorubicin (RVG 14735, Pharmachemie BV, Haarlem, Netherlands) treatment of *MMTV-NeuT;Rag2<sup>+/-</sup>* and *MMTV-NeuT;Rag2<sup>-/-</sup>* mice was initiated when a cumulative tumor burden of 50 mm<sup>2</sup> was reached. Doxorubicin was diluted 1:1 with NaCl before being administered i.v. at a dose of 5 mg/kg for 5 cycles with intervals of 7 days.

Cisplatin treatment of *K14cre; Cdh1<sup>fl/fl</sup>; Trp53<sup>fl/fl</sup>; Rag1<sup>+/-</sup>* and *K14cre; Cdh1<sup>fl/fl</sup>; Trp53<sup>fl/fl</sup>; Rag1<sup>-/-</sup>* mice was initiated when the mammary tumor reached a size of 50 mm<sup>2</sup>. Cisplatin was administered i.v. at 6 mg/kg per dose for 4 cycles with intervals of 14 days.

Oxaliplatin treatment of *K14cre; Cdh1<sup>fl/fl</sup>; Trp53<sup>fl/fl</sup>; Rag1<sup>+/-</sup>* and *K14cre; Cdh1<sup>fl/fl</sup>; Trp53<sup>fl/fl</sup>; Rag1<sup>-/-</sup>* mice was initiated when the mammary tumor reached a size of 50 mm<sup>2</sup>. Oxaliplatin was diluted 1:5 with NaCl before being administered i.v. at a dose of 6 mg/kg for 3 cycles with intervals of 10 days.

3

### **Cd8<sup>+</sup> T cell depletion**

Anti-CD8 (2.43, purified from hybridoma supernatant, NKI) treatment of *K14cre; Cdh1<sup>fl/fl</sup>; Trp53<sup>fl/fl</sup>; Rag1<sup>+/-</sup>* mice was initiated when the mammary tumor reached a size of 25 mm<sup>2</sup> till tumor outgrowth. Anti-CD8 was administered i.p. A dose of 400 µg was used for the first injection, followed by 150 µg every 7 days.

### **Immunohistochemistry**

For immunodetection of CD4<sup>+</sup> and CD8<sup>+</sup> T cells, 10-µm frozen tissue sections were cut using a Leica CM3050 S cryostat. Sections were air-dried, fixed in ice-cold acetone for 5 min, incubated for 10 min with avidin solution (DAKO), PBS washed, incubated for 10 min with biotin solution (DAKO), PBS washed and blocked for 30 min in blocking buffer (5% goat serum/2.5%

bovine serum albumin/PBS). Antibodies, rat anti-mouse CD4 (GK1.5, purified hybridoma supernatant, Netherlands Cancer Institute; 1:1000) and rat anti-mouse CD8 (2.43, purified hybridoma supernatant, Netherlands Cancer Institute, 1:1000), were diluted in 0.5X blocking buffer and incubated with tissue sections for 1.5-hr at room temperature. Sections were washed with PBS and incubated with secondary antibody (biotinylated goat anti-rat, Southern Biotech, Birmingham, AL, 1:300) for 45 min at RT. Sections were washed in PBS and ABC reagent (DAKO) was applied for 30 min. Antibodies were visualized by treatment with Fast 3,3'-diaminobenzidine (Sigma), dehydrated in graded alcohols (70%, 95%, 100% ethanol) and mounted in mounting medium (Klinipath).

For immunodetection of CD3<sup>+</sup> and FOXP3<sup>+</sup> cells, tumor samples were immersion-fixed in 10% neutral-buffered formalin followed by dehydration through graded alcohols, xylene and embedded in paraffin. 4- $\mu$ m-thick paraffin sections were cut, deparaffinised and boiled in antigen retrieval Citra buffer (Biogenex) according to the manufacturer's recommendations. Primary antibodies were diluted in blocking buffer (5% goat serum/2.5% bovine serum albumin/PBS) at 1:100 for rabbit anti-mouse CD3 (RM-9107-S, Neomarkers, Fremont, CA) and at 1:400 for rat anti-mouse Foxp3 (14-5773, eBioscience, San Diego, CA). Sections were incubated with primary antibody 2-4-hr at room temperature, followed by PBS washing, brief (5 min) incubation in blocking buffer and subsequent incubation with biotinylated secondary antibody anti-rabbit (DAKO, Denmark, 4858, 1:1000) and goat anti-rat (Santa Cruz biotechnology, CA, U.S. sc-2041, 1:100) 45-min at room temperature. After PBS washing, HRP-conjugated Streptavidin (DAKO, Denmark) was applied for 30 min. Sections were then washed in PBS and antibodies were visualized by treatment with Fast 3,3'-diaminobenzidine (Sigma), dehydrated in graded alcohols (70%, 95%, 100% ethanol) and mounted in Entellan mounting medium (Merck, Germany).

All immunohistochemical experiments included negative controls for determination of background staining, which was negligible. Slides were digitally processed using the Aperio ScanScope (Aperio, Vista, CA) using ImageScope software version 10.0 (Aperio). Data shown are representative of results obtained following examination of tissues removed from a minimum of 3 mice per group. Influx of CD4<sup>+</sup>, CD8<sup>+</sup> and FoxP3<sup>+</sup> T lymphocytes was determined by counting five high-power microscopic fields per tumor (20x fields for *MMTV-NeuT* mouse model and 40x fields for the *K14cre; Cdh1<sup>fl/fl</sup>; Trp53<sup>fl/fl</sup>* mouse model).

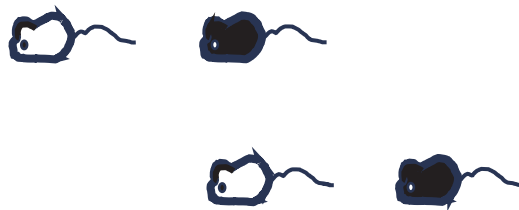
## Statistical analyses

Statistical analyses were performed using GraphPad Prism 5.01 (GraphPad Software Inc., La Jolla, CA). Specific tests used were the Mann-Whitney test (unpaired, two-tailed) and Log-Rank test. P values < 0.05 were considered statistically significant.

## References

1. Boggio, K., *et al. J Exp Med* **188**, 589-596 (1998).
2. Ciampricotti, M., *et al. J Pathol* (2011).
3. Derksen, P.W., *et al. Cancer Cell* **10**, 437-449 (2006).
4. Evers, B., *et al. J Pathol* **220**, 34-44 (2010).

## Chapter 4



# Therapeutic targeting of macrophages enhances chemotherapy efficacy by unleashing type I interferon response

Camilla Salvagno<sup>1</sup>, Metamia Ciampricotti<sup>1,9,12</sup>, Sander Tuit<sup>2,10,12</sup>, Cheei-Sing Hau<sup>1</sup>, Antoinette van Weverwijk<sup>1</sup>, Seth B. Coffelt<sup>1,11</sup>, Kelly Kersten<sup>1</sup>, Kim Vrijland<sup>1</sup>, Kevin Kos<sup>1</sup>, Thomas Ulas<sup>2</sup>, Ji-Ying Song<sup>3</sup>, Chia-Huey Ooi<sup>4</sup>, Dominik Rüttinger<sup>5</sup>, Philippe A. Cassier<sup>6</sup>, Jos Jonkers<sup>7</sup>, Joachim L. Schultze<sup>2,8</sup>, Carola H. Ries<sup>5</sup> and Karin E. de Visser<sup>1\*</sup>

<sup>1</sup>Division of Tumor Biology & Immunology, Oncode Institute, Netherlands Cancer Institute, Amsterdam, The Netherlands. <sup>2</sup>Genomics and Immunoregulation, LIMES-Institute, University of Bonn, Bonn, Germany. <sup>3</sup>Division of Experimental Animal Pathology, Netherlands Cancer Institute, Amsterdam, The Netherlands. <sup>4</sup>Roche Innovation Center Basel, Roche Pharma Research and Early Development, Basel, Switzerland. <sup>5</sup>Roche Innovation Center Munich, Roche Pharma Research and Early Development, Penzberg, Germany. <sup>6</sup>Department of Medicine, Centre Léon Bérard, Lyon, France. <sup>7</sup>Division of Molecular Pathology, Oncode Institute, Netherlands Cancer Institute, Amsterdam, The Netherlands. <sup>8</sup>Platform for Single Cell Genomics and Epigenomics (PRECISE) at the German Center for Neurodegenerative Diseases and the University of Bonn, Bonn, Germany. <sup>9</sup>Present address: Molecular Pharmacology Program and Department of Medicine, Memorial Sloan Kettering Cancer Center, New York, NY, USA. <sup>10</sup>Present address: Department of Anatomy and Embryology, Leiden University Medical Center, Leiden, The Netherlands. <sup>11</sup>Present address: Cancer Research UK Beatson Institute and Institute of Cancer Sciences, University of Glasgow, Glasgow, UK. <sup>12</sup>These authors contributed equally: Metamia Ciampricotti, Sander Tuit.

\*e-mail: k.d.visser@nki.nl

*Nat Cell Biol.* 2019 Apr;21(4):511-521

## Abstract

Recent studies have revealed a role for macrophages and neutrophils in limiting chemotherapy efficacy; however, the mechanisms underlying the therapeutic benefit of myeloid-targeting agents in combination with chemotherapy are incompletely understood. Here, we show that targeting tumour-associated macrophages by colony-stimulating factor-1 receptor (CSF-1R) blockade in the *K14cre; Cdh1<sup>F/F</sup>; Trp53<sup>F/F</sup>* transgenic mouse model for breast cancer stimulates intratumoural type I interferon (IFN) signalling, which enhances the anticancer efficacy of platinum-based chemotherapeutics. Notably, anti-CSF-1R treatment also increased intratumoural expression of type I IFN-stimulated genes in patients with cancer, confirming that CSF-1R blockade is a powerful strategy to trigger an intratumoural type I IFN response. By inducing an inflamed, type I IFN-enriched tumour microenvironment and by further targeting immunosuppressive neutrophils during cisplatin therapy, antitumour immunity was activated in this poorly immunogenic breast cancer mouse model. These data illustrate the importance of breaching multiple layers of immunosuppression during cytotoxic therapy to successfully engage antitumour immunity in breast cancer.

## Introduction

Poor chemotherapy response is a major obstacle to successful cancer treatment. There is a growing appreciation for the influential role of the immune system on the success of cytotoxic anticancer therapy<sup>1</sup>. Although the adaptive immune system contributes to the therapeutic benefit of certain chemotherapeutic drugs in immunogenic tumour models<sup>2</sup>, it frequently fails to be unleashed by these same agents in less immunogenic transgenic mouse tumour models<sup>3,4,5</sup>, suggesting the involvement of immunosuppressive mechanisms. Indeed, macrophages and neutrophils are frequently the most abundant immune cells in tumours, and clinical studies have reported a correlation between these myeloid cells and poor chemotherapy efficacy<sup>4,6,7,8,9,10</sup>. Experimental animal studies confirm a causal relationship between tumour-associated myeloid cells and poor chemotherapy response<sup>4,5,11,12,13,14,15,16,17,18,19,20</sup>. For example, inhibition of macrophages in mammary tumour-bearing MMTV-PyMT mice increases paclitaxel efficacy via activation of antitumour immunity<sup>4,5</sup>. Notably, macrophage-targeting and neutrophil-targeting agents are currently under clinical evaluation<sup>21,22,23</sup>. Although promising, the aforementioned preclinical studies only show a transient therapeutic effect of combined myeloid cell targeting and chemotherapy. A deeper understanding of the mechanisms of action is needed to facilitate the rational design of therapeutic combination strategies that convert 'cold' non-T cell-inflamed tumours into 'hot' inflamed tumours, thus engaging durable antitumour immunity in otherwise poorly immunogenic tumours.

By combining *in vivo* intervention experiments and mechanistic studies in the *K14cre; Cdh1<sup>F/F</sup>; Trp53<sup>F/F</sup>* (KEP) mouse model for spontaneous mammary tumorigenesis<sup>24</sup> with validation studies in tumour biopsies of patients treated with anti-colony-stimulating factor-1 receptor (anti-CSF-1R), here, we demonstrate that CSF-1R inhibition synergizes with platinum-based chemotherapy by unleashing an intratumoural type I interferon (IFN) response. Besides this anti-CSF-1R-mediated conversion of the tumour microenvironment (TME) into a type I IFN-enriched milieu, it takes breaching of an additional layer of immunosuppression to engage antitumour immunity during cytotoxic therapy.

## Results

### CSF-1R blockade does not affect mammary tumour growth or metastasis in KEP mice

We set out to assess the role of CSF-1–CSF-1R signalling, which is vital for macrophages<sup>25</sup>, in tumour progression in the KEP model, which spontaneously develops mammary tumours resembling human invasive lobular carcinomas (ILCs) at 6–8 months of age<sup>24</sup>. Similar to human ILCs, KEP tumours are strongly infiltrated by macrophages (Supplementary Fig. 1a,b). Whereas in the MMTV-PyMT breast cancer model it has been reported that two distinct macrophage populations reside within the TME: CD11b<sup>hi</sup>MHCII<sup>hi</sup>CD206<sup>hi</sup> mammary tissue macrophages and CD11b<sup>lo</sup>MHCII<sup>hi</sup>CD206<sup>lo</sup> tumour-associated macrophages (TAMs)<sup>26</sup>, in mammary tumours of KEP mice, all F4/80<sup>+</sup> macrophages express high levels of CD11b, low levels of CD206 and only a proportion of these cells expresses major histocompatibility complex class II (MHCII) (Supplementary Fig. 1c). These differences in intratumoural macrophage phenotypes between mouse tumour models underscore the complexity of macrophage plasticity in different tumour contexts. In line with the macrophage influx, CSF-1 protein levels are increased in KEP tumours versus healthy mammary glands of age-matched wild-type littermates (Fig. 1a). Both cancer cells and host cells in KEP tumours express *Csf1* mRNA, whereas *Csf1* mRNA is barely detectable in healthy mammary glands (Fig. 1b). CSF-1R is highly expressed on TAMs and to a lesser extent on infiltrating monocytes and neutrophils (Supplementary Fig. 1d), but not on other tumour-associated immune cells or CD45<sup>-</sup> cells (Supplementary Fig. 1d).

To determine whether intratumoural macrophage accumulation depends on CSF-1–CSF-1R signalling and whether macrophages influence tumour outgrowth and dissemination, we treated tumour-bearing KEP mice with a chimeric mouse IgG1 antagonistic antibody (2G2) that binds to mouse CSF-1R with high affinity (dissociation constant ( $K_d$ ) = 0.2 nM) or with a control antibody<sup>21</sup>. CSF-1R blockade strongly reduced the TAM population (Fig. 1c,d) and, as a result, also the total CD45<sup>+</sup> population (Supplementary Fig. 1e). Treatment with anti-CSF-1R alone did not influence tumour-specific survival (Fig. 1f) or spontaneous metastasis formation (Supplementary Fig. 1f). We also investigated the therapeutic activity of anti-CSF-1R in the KEP-based model of spontaneous breast cancer metastasis<sup>27</sup>. In this model,

after orthotopic transplantation of a KEP-derived tumour piece followed by surgical removal of the outgrown tumour, mice develop overt multi-organ metastatic disease. Anti-CSF-1R was started either after a palpable mammary tumour had developed (continuous setting) or after mastectomy (adjuvant setting) and continued until the development of metastatic disease (Supplementary Fig. 1g). Regardless of the treatment schedule, metastasis-specific survival and metastatic burden in the lungs were similar between control and anti-CSF-1R groups (Supplementary Fig. 1h,i). Thus, anti-CSF-1R monotherapy fails to affect outgrowth and dissemination of KEP mammary tumours.

# Chapter 4

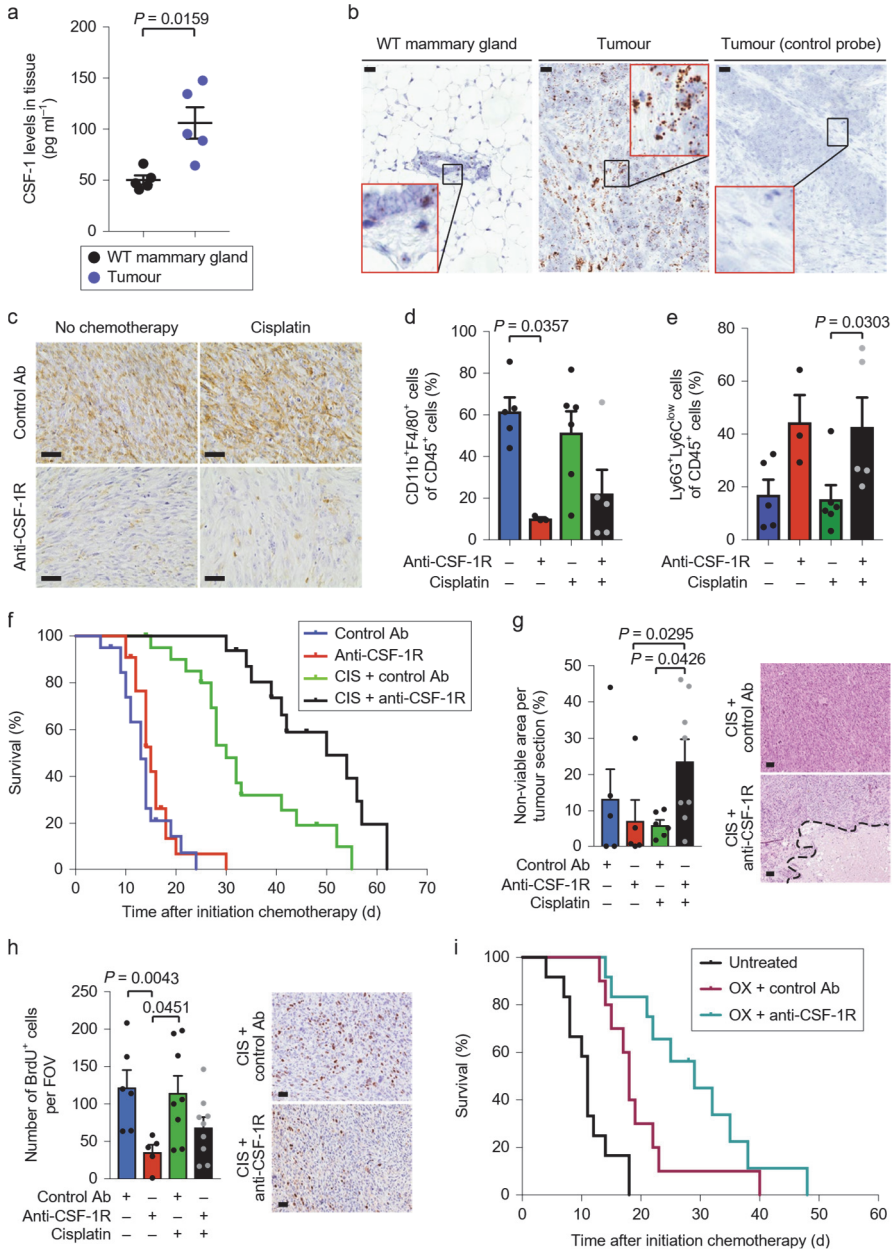


**Fig. 1 | CSF-1R blockade improves the anticancer efficacy of platinum-based chemotherapeutic drugs in the KEP mouse model for de novo mammary tumorigenesis.**

**a**, CSF-1 protein levels in end-stage mammary tumours of KEP mice and mammary glands of age-matched wild-type (WT) mice ( $n = 5$  animals per group) measured by Luminex cytokine array. **b**, Representative images of RNA in situ hybridization of *Csf1* (brown signal) in end-stage KEP tumours and normal mammary glands of age-matched WT mice. Data are representative of three animals per group. Scale bars, 25

## Therapeutic targeting of macrophages enhances chemotherapy efficacy by unleashing type I interferon response

$\mu\text{m}$ . **c**, Representative immunohistochemistry images of F4/80<sup>+</sup> macrophages in tumours of time-point-sacrificed KEP mice treated as indicated. Data are representative of five animals per group. Scale bars, 25  $\mu\text{m}$ . **d,e**, Proportion of CD11b<sup>+</sup>F4/80<sup>+</sup> macrophages (**d**) and Ly6G<sup>+</sup>Ly6C<sup>low</sup> neutrophils (**e**) gated on CD45<sup>+</sup> cells, as determined by flow cytometry in tumours of end-stage KEP mice treated as indicated (untreated:  $n = 5$  animals; anti-CSF-1R:  $n = 3$  animals; cisplatin:  $n = 6$  animals; cisplatin + anti-CSF-1R:  $n = 5$  animals). **f**, Kaplan–Meier tumour-specific survival curves of KEP mice treated with control antibody (Ab) ( $n = 20$  animals), anti-CSF-1R ( $n = 22$  animals), cisplatin (CIS) + control Ab ( $n = 21$  animals) or cisplatin + anti-CSF-1R ( $n = 16$  animals). Cisplatin + control Ab versus control Ab:  $P = 0.0001$ ; cisplatin + control Ab versus anti-CSF-1R:  $P = 0.0001$ ; cisplatin + anti-CSF-1R versus cisplatin + control Ab:  $P = 0.0011$  (two-tailed log-rank test). **g**, Percentage of non-viable area per tumour section of time-point-sacrificed KEP mice quantified by digital area analysis of H&E-stained sections (control Ab:  $n = 5$  animals; anti-CSF-1R:  $n = 5$  animals; cisplatin + control Ab:  $n = 6$  animals; cisplatin + anti-CSF-1R:  $n = 8$  animals). Representative H&E sections are shown, and the dashed line separates the viable from the non-viable area. Scale bars, 50  $\mu\text{m}$ . **h**, Quantification of BrdU<sup>+</sup> cells in viable areas of mammary tumours of time-point-sacrificed KEP mice (control Ab:  $n = 6$  animals, anti-CSF-1R:  $n = 5$  animals, cisplatin + control Ab:  $n = 8$  animals, cisplatin + anti-CSF-1R:  $n = 9$  animals). The values represent the average number of BrdU<sup>+</sup> cells per field of view (FOV) quantified by counting five high-power microscopic fields per tumour. Representative BrdU immunohistochemistry stainings are shown. Scale bars, 25  $\mu\text{m}$ . **i**, Kaplan–Meier tumour-specific survival curves of untreated KEP mice ( $n = 12$  animals) or mice treated with oxaliplatin (OX) + control Ab ( $n = 10$  animals) and oxaliplatin + anti-CSF-1R ( $n = 12$  animals). Oxaliplatin + control Ab versus no treatment:  $P = 0.0015$ ; oxaliplatin + control Ab versus oxaliplatin + anti-CSF-1R:  $P = 0.0507$  (two-tailed log-rank test). Data presented in **a**, **d**, **e**, **g** and **h** are mean  $\pm$  s.e.m., and statistical analysis was performed using the two-tailed Mann–Whitney test.

4

### CSF-1R blockade in tumour-bearing KEP mice enhances the anticancer efficacy of platinum-based chemotherapy

We next tested the anticancer efficacy of anti-CSF-1R in combination with two conventional chemotherapeutics with a different mode of action: cisplatin, a platinum-based anticancer drug that crosslinks DNA and induces apoptosis, and docetaxel, an antimetabolic agent that interferes with cell division through stabilization of microtubules. Successful blockade of the CSF-1R pathway during treatment of tumour-bearing KEP mice with chemotherapy and anti-CSF-1R was confirmed by the reduction in the number of TAMs (Fig. 1c,d and Supplementary Fig. 2a,b). Interestingly, anti-CSF-1R synergized with cisplatin, resulting in prolonged survival compared to cisplatin + control antibody-treated mice (Fig. 1f). By contrast, no therapeutic synergy was observed in docetaxel + anti-CSF-1R-treated mice (Supplementary Fig. 2c). The therapeutic synergy observed upon cisplatin + anti-CSF-1R was associated with more necrosis in KEP tumours (Fig. 1g)

but not with more cleaved caspase 3<sup>+</sup> apoptotic cells (Supplementary Fig. 2d). Perhaps other mechanisms of cell death are involved or the timing of our analysis was suboptimal for this parameter. Furthermore, anti-CSF-1R monotherapy—and to a lesser extent, the combination with cisplatin—decreased the number of BrdU<sup>+</sup>-proliferating cells (Fig. 1h). No significant changes in the number and pericyte coverage of CD31<sup>+</sup> microvessels, the amount of intratumoural DNA double-strand breaks and intratumoural cisplatin-adduct formation were observed at the time-point analysed (Supplementary Fig. 2e–h). As expected, none of these parameters was changed in the docetaxel setting (Supplementary Fig. 2i–m).

To assess whether the anti-CSF-1R-mediated therapeutic synergy was unique to cisplatin or could be extended to drugs with a similar mechanism of action, we tested another platinum-containing drug, oxaliplatin, and also found that the survival benefit of oxaliplatin was improved by combined CSF-1R blockade (Fig. 1i and Supplementary Fig. 2n). These data demonstrate that anti-CSF-1R acts synergistically with platinum-based chemotherapeutic drugs to extend the survival of mammary tumour-bearing KEP mice.

### **CSF-1R inhibition alters the innate immune landscape of KEP tumours**

Macrophages are key orchestrators of the inflammatory TME<sup>28</sup>. Thus, we set out to assess the effect of anti-CSF-1R on the innate immune landscape of KEP tumours. Despite the strong reduction of CD11b<sup>+</sup>F4/80<sup>+</sup> TAMs on anti-CSF-1R, up to 20% of the intratumoural CD45<sup>+</sup> immune cells still expresses the macrophage marker F4/80 (Fig. 1d). Detailed analysis of this surviving CD11b<sup>+</sup>F4/80<sup>+</sup> population revealed that an increased proportion of these cells expresses the inflammatory monocyte marker Ly6C compared to CD11b<sup>+</sup>F4/80<sup>+</sup> cells in control antibody-treated tumours (Fig. 2a and Supplementary Fig. 3a). Moreover, the surviving CD11b<sup>+</sup>F4/80<sup>+</sup> cells in cisplatin + anti-CSF-1R-treated tumours express elevated levels of the co-stimulatory molecules CD80 and CD86, slightly elevated MHCII levels, decreased levels of the chemokine receptors C-C chemokine receptor type 2 (CCR2) and CX3C chemokine receptor 1 (CX3CR1), and increased levels of programmed cell death 1 ligand 1 (PD-L1) compared to intratumoural CD11b<sup>+</sup>F4/80<sup>+</sup> cells in cisplatin + control antibody-treated mice (Fig. 2b–g). Furthermore, in the independent orthotopically transplanted *K14cre; Trp53<sup>F/F</sup>* (KP) mammary tumour model, intratumoural

CD11b<sup>+</sup>F4/80<sup>+</sup> myeloid cells remaining after CSF-1R inhibition display an altered phenotype corresponding to that in anti-CSF-1R-treated KEP tumours (Fig. 2h–m). Thus, anti-CSF-1R depletes the majority of CD11b<sup>+</sup>F4/80<sup>+</sup> TAMs, whereas a small population of CD11b<sup>+</sup>F4/80<sup>+</sup> cells with a distinct phenotype survives. To explore whether these surviving cells could derive from circulating monocytes, we transferred tdTomato<sup>+</sup> monocytes into control antibody or anti-CSF-1R-treated tumour-bearing KEP mice. After 4 d, the transferred monocytes that infiltrated tumours of anti-CSF-1R-treated, and not control antibody-treated, animals partially acquired the phenotype of the surviving intratumoural CD11b<sup>+</sup>F4/80<sup>+</sup> cell population (that is, loss of CX3CR1 and elevated PD-L1 expression) (Supplementary Fig. 3b–d). These findings suggest that the surviving CD11b<sup>+</sup>F4/80<sup>+</sup> cells in anti-CSF-1R-treated tumours may derive from newly recruited circulating monocytes, although other mechanisms cannot be excluded.

Whereas in treatment-naive KEP tumours the macrophage/neutrophil ratio is approximately 3/1, in anti-CSF-1R-treated tumours, either in the presence or absence of cisplatin, this ratio is reversed (Fig. 1d,e). However, the absolute number of intratumoural neutrophils was not increased upon CSF-1R inhibition (Supplementary Fig. 3e). Anti-CSF-1R treatment induced an increase in the number of monocytes and a modest, but not significant, and very variable increase in the number of intratumoural eosinophils and mast cells (Supplementary Fig. 3f–h). Together, these data show that cisplatin + anti-CSF-1R synergy is accompanied by changes in the myeloid immune landscape of tumours. Most notably, anti-CSF-1R treatment resulted in a surviving population of CD11b<sup>+</sup>F4/80<sup>+</sup> cells with an altered phenotype.

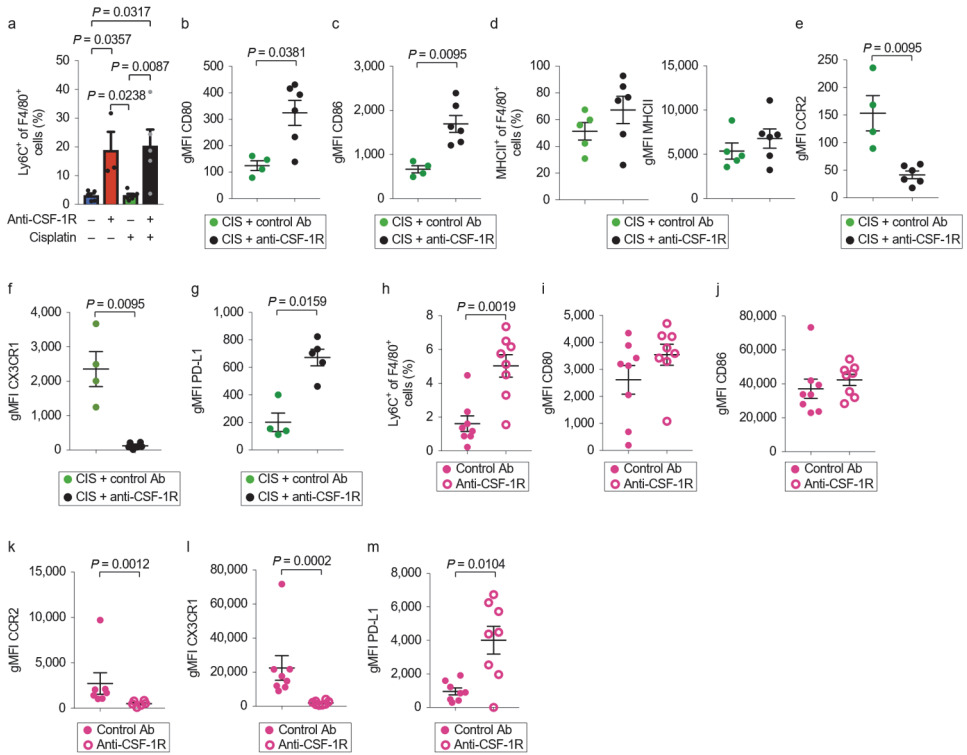


**Fig. 2 | Characterization of F4/80+ cells by flow cytometry in spontaneous KEP tumours and in orthotopically transplanted KP tumours after anti-CSF-1R treatment.** **a**, Percentage of CD11b+F4/80+ immune cells expressing Ly6C in end-stage KEP tumours (untreated: n = 5 animals; anti-CSF-1R: n = 3 animals; cisplatin: n = 6 animals; cisplatin + anti-CSF-1R: n = 5 animals). **b,c**, Geometric mean fluorescence intensity (gMFI) of CD80 (**b**) and CD86 (**c**) expression on F4/80+Siglec F<sup>-</sup> cells in KEP tumours (cisplatin + control Ab: n = 4 animals; cisplatin + anti-CSF-1R: n = 6 animals). **d**, Percentage of MHCII-expressing F4/80+Siglec F<sup>-</sup> cells (left) and gMFI (right) of MHCII on F4/80+Siglec F<sup>-</sup> in the KEP tumours (cisplatin + control Ab: n = 5 animals; cisplatin + anti-CSF-1R: n = 6 animals). gMFI was calculated by subtracting the gMFI of the MHCII-negative population from the gMFI of the MHCII-positive population. **e-g**, gMFI of CCR2 (**e**), CX3CR1 (**f**) and PD-L1 (**g**) expression on F4/80+Siglec F<sup>-</sup> cells in KEP tumours (CCR2 and CX3CR1: cisplatin + control Ab: n = 4 animals; cisplatin + anti-CSF-1R: n = 6 animals; PD-L1: cisplatin + control Ab: n = 4 animals; cisplatin + anti-CSF-1R: n = 5 animals). **h-m**, KP tumour pieces were orthotopically transplanted in the mammary fat pad of FVB/N mice. The percentage of CD11b+F4/80+Siglec F<sup>-</sup> immune cells expressing Ly6C in time-point-sacrificed KP tumours (**h**). gMFI of CD80 (**i**), CD86 (**j**), CCR2 (**k**), CX3CR1 (**l**) and PD-L1 (**m**) expression on F4/80+Siglec F<sup>-</sup> cells in time-point-sacrificed KP tumours (n = 8 animals per group, except CCR2: control Ab: n = 7 animals, anti-CSF-1R: n = 6 animals). The gMFI values presented in **b, c, e-g** and **i-m** were determined by subtracting the gMFIs of the fluorescence minus one staining from the gMFI of the full staining. Data presented in **a-m** are mean ± s.e.m., and statistical analysis was performed using the two-tailed Mann-Whitney test.

## **Macrophage blockade enhances cisplatin response by unleashing intratumoural type I IFN signalling**

To better characterize the phenotype of the anti-CSF-1R-surviving intratumoural CD11b<sup>+</sup>F4/80<sup>+</sup> cells, next-generation RNA sequencing (RNA-seq) analysis was performed on CD11b<sup>+</sup>F4/80<sup>+</sup> cells sorted from cisplatin + control antibody-treated or cisplatin + anti-CSF-1R-treated tumours. Hierarchical clustering of the top 400 variable genes revealed that CD11b<sup>+</sup>F4/80<sup>+</sup> cells from cisplatin + anti-CSF-1R-treated tumours displayed a different transcriptome profile, mainly characterized by a strong enrichment of genes involved in type I IFN signalling and type I IFN production, whereas cell-cycle-associated genes were reduced (Fig. 3a,b). Interestingly, CSF-1R expression levels were lower in the remaining CD11b<sup>+</sup>F4/80<sup>+</sup> cells from cisplatin + anti-CSF-1R-treated tumours (fold change: -2,04;  $P = 3.63 \times 10^{-5}$ ), perhaps explaining why these cells resisted anti-CSF-1R therapy. In parallel, we also performed RNA-seq on flow-sorted Ly6G<sup>+</sup>Ly6C<sup>low</sup> neutrophils isolated from tumours of cisplatin + control antibody-treated and cisplatin + anti-CSF-1R-treated KEP mice. Hierarchical clustering of the top 400 variable genes within this data set revealed that anti-CSF-1R treatment also had a significant effect on the transcriptome profile of tumour-associated neutrophils (Supplementary Fig. 4a). To ensure that these transcriptome alterations in neutrophils are not a direct effect of anti-CSF-1R on neutrophils, but rather an indirect consequence of macrophage targeting, we performed gene set enrichment analysis (GSEA) of target genes of early growth receptor 2 (EGR2), a transcription factor downstream of CSF-1R signalling<sup>29</sup>. No differences were observed in the expression of EGR2 target genes between neutrophils isolated from anti-CSF-1R-treated and control antibody-treated tumours (Supplementary Fig. 4b), suggesting that neutrophils are not directly influenced by anti-CSF-1R. Interestingly, BiNGO analysis of the top 100 upregulated and downregulated genes and Ingenuity pathway analysis of the differentially expressed genes revealed an enrichment in genes involved in type I IFN signalling in neutrophils isolated from cisplatin + anti-CSF-1R-treated tumours versus cisplatin + control antibody-treated tumours (Supplementary Fig. 4c,d and Supplementary Table 3). These data indicate that the therapeutic benefit of cisplatin + anti-CSF-1R is accompanied by induction of type I IFN-stimulated genes (ISGs) in both intratumoural CD11b<sup>+</sup>F4/80<sup>+</sup> cells and neutrophils.

We hypothesized that the enrichment of ISGs in these intratumoural immune populations was a consequence of increased levels of type I IFNs in KEP tumours upon CSF-1R blockade. Indeed, by using primers hybridizing to all *lfna* genes, mRNA expression of *lfna*, but not *lfnb*, was increased in tumours of cisplatin + anti-CSF-1R-treated KEP mice compared to cisplatin + control antibody-treated mice (Fig. 3c). In line with this, the mRNA levels of various intracellular pattern recognition receptors, such as *Tlr3*, *Rig1* and *Ifih1*, whose signals induce type I IFN production, were upregulated in cisplatin + anti-CSF-1R-treated tumours compared to cisplatin + control antibody treatment (Fig. 3d). Notably, the increase in type I IFN expression upon anti-CSF-1R was independent of chemotherapy treatment, as a similar intratumoural increase in *lfna* expression was observed upon anti-CSF-1R alone (Fig. 3e) or with docetaxel + anti-CSF-1R (Supplementary Fig. 5a). We also confirmed the increased expression of *lfna*—and of two ISGs, *Isg15* and *Oas1a*—upon anti-CSF-1R treatment in the independent KP-based tumour transplantation model and in inoculated MC38 colorectal adenocarcinoma tumours<sup>21</sup> (Fig. 3f,g and Supplementary Fig. 5b,c). Together, these data demonstrate that anti-CSF-1R induces type I IFN in the TME.

# Therapeutic targeting of macrophages enhances chemotherapy efficacy by unleashing type I interferon response

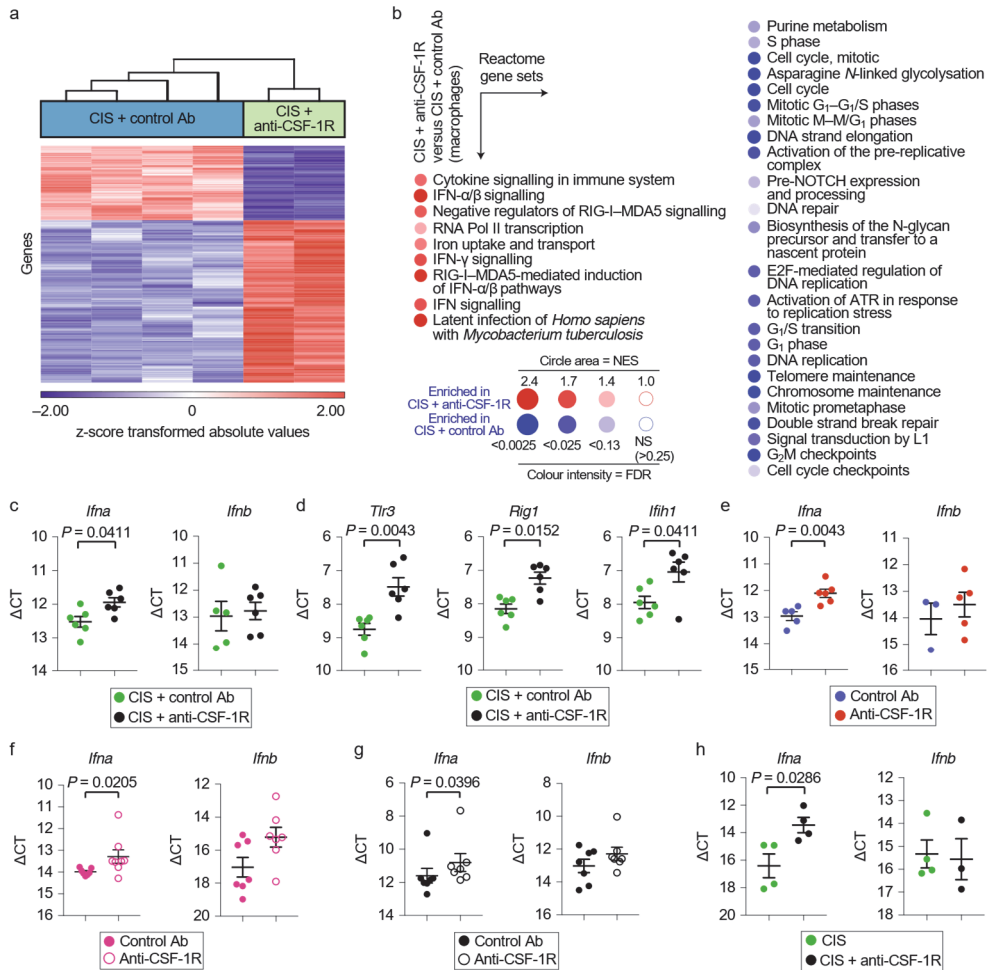


**Fig. 3 | CSF-1R inhibition alters TAM phenotype and induces type I IFN signalling in the TME.** **a**, Hierarchical clustering of the top 400 variable genes between CD11b<sup>+</sup>F4/80<sup>+</sup> cells isolated from KEP tumours treated with cisplatin + control Ab ( $n = 4$  animals) and cisplatin + anti-CSF-1R ( $n = 2$  biologically independent samples, a pool of five mice each). Fold change  $\geq 1.5$ ;  $P$  value with FDR correction  $\leq 0.05$ . Statistical analysis was performed using two-way ANOVA. **b**, BubbleGUM visualization of GSEA using reactome gene sets comparing CD11b<sup>+</sup>F4/80<sup>+</sup> cells from cisplatin + anti-CSF-1R-treated tumours versus macrophages from cisplatin + control Ab-treated tumours. Same mice as in **a**. Normalized enrichment score (NES)  $\geq 1$ , FDR value:  $\leq 0.25$ . The enrichment score was calculated using a weighted Kolmogorov–Smirnov-like statistic. MDA5, melanoma differentiation-associated protein 5 (encoded by *Ifih1*); Pol, polymerase; RIG-I, retinoic acid inducible gene I; ATR, ATM and Rad3-related; NS, not significant. **c**, Transcripts of *Ifna* ( $n = 6$  animals per group) and *Ifnb* ( $n = 5$  animals in cisplatin + control Ab;  $n = 6$  animals in cisplatin + anti-CSF-1R). **d**, *Tlr3*, *Rig1* and *Ifih1* in KEP mammary tumours isolated 1 d after the second cisplatin injection were determined by quantitative PCR and normalized to  $\beta$ -actin ( $n = 6$  animals per group). **e–g**, Transcripts of *Ifna* and *Ifnb* in KEP mammary tumours (*Ifna*:  $n = 5$  animals in control Ab,  $n = 6$  animals in anti-

CSF-1R; *Ifnb*:  $n = 3$  animals in control Ab,  $n = 5$  animals in anti-CSF-1R) (e), orthotopically transplanted KP mammary tumour (*Iffa*:  $n = 7$  animals in control Ab,  $n = 8$  animals in anti-CSF-1R; *Ifnb*:  $n = 7$  animals per group) (f) and subcutaneously inoculated MC38 tumours ( $n = 7$  animals per group) (g) treated with control Ab and anti-CSF-1R were determined by quantitative PCR and normalized to  $\beta$ -actin. Mice were analysed at a tumour size of 100 mm<sup>2</sup> (KP) or after 12 d from the start of the treatment (MC38). h, Transcripts of *Iffa* ( $n = 4$  animals per group) and *Ifnb* ( $n = 4$  animals in cisplatin,  $n = 3$  animals in cisplatin + anti-CSF-1R) in CD11b<sup>+</sup>F4/80<sup>+</sup> cells isolated from end-stage KEP tumours were determined by quantitative PCR and normalized to  $\beta$ -actin. Graphs in c–h show the mean  $\pm$  s.e.m. in  $\Delta$ CT values, and statistical analysis was performed using the two-tailed Mann–Whitney test.

To pursue the cellular source of type I IFN, we flow-sorted different cell populations from cisplatin and cisplatin + anti-CSF-1R-treated KEP tumours (Supplementary Fig. 5d) and compared *Iffa* and *Ifnb* transcript levels. Plasmacytoid dendritic cells are known for their ability to produce type I IFN; however, as very few plasmacytoid dendritic cells—less than 0.1% of the total intratumoural immune population—are present in KEP tumours (Supplementary Fig. 5e,f), we could not recover RNA of sufficient quality. Likewise, we did not obtain RNA of sufficient quality from sorted CD31<sup>+</sup> endothelial cells. Only the CD11b<sup>+</sup>F4/80<sup>+</sup> immune cell population displayed elevated *Iffa* expression levels upon CSF-1R blockade (Fig. 3h and Supplementary Fig. 5g,h). In line with these in vivo findings, in vitro treatment of bone marrow-derived macrophages (BMDMs) with anti-CSF-1R modestly induces *Iffa* levels after 24 h of culture (Supplementary Fig. 5i). These analyses suggest that the surviving population of intratumoural CD11b<sup>+</sup>F4/80<sup>+</sup> cells is an important source of IFN- $\alpha$  in cisplatin + anti-CSF-1R-treated KEP tumours.

To dissect the functional significance of type I IFN signalling in the therapeutic benefit of cisplatin + anti-CSF-1R therapy, we blocked the IFN- $\alpha/\beta$  receptor subunit 1 (IFNAR1) in KEP mice. Whereas blockade of type I IFN signalling did not influence the anticancer efficacy of cisplatin, anti-IFNAR1 treatment completely abrogated the synergistic effect of cisplatin + anti-CSF-1R treatment (Fig. 4a). These findings reveal that therapeutic targeting of macrophages with anti-CSF-1R in tumour-bearing KEP mice unleashes intratumoural type I IFN signalling, which enhances the therapeutic efficacy of cisplatin.

## **Emactuzumab treatment induces intratumoural type I ISGs in patients with cancer**

To validate our preclinical findings that CSF-1R blockade unleashes intratumoural type I IFN signalling in patients, we compared ISG expression levels in pre-treatment and on-treatment tumour biopsies from patients with advanced solid tumours treated with emactuzumab (RG7155), a humanized anti-human CSF-1R monoclonal antibody (NCT01494688)<sup>21,30</sup>. Gene expression profiling was performed on tumour biopsies taken before the start of treatment and after 4 weeks of emactuzumab therapy. We assessed the expression level of a set of 28 ISGs that was selected based on the RNA-seq results from our KEP mouse model (Fig. 3a, Supplementary Fig. 4a,c,d and Supplementary Table 3). The intratumoural expression of all 28 selected ISGs was increased in emactuzumab on-treatment biopsies versus pre-treatment biopsies, of which 11 ISGs were significantly upregulated (Fig. 4b,c). Thus, in line with our preclinical studies, these clinical findings indicate that CSF-1R blockade is a powerful strategy to augment intratumoural type I IFN signalling.

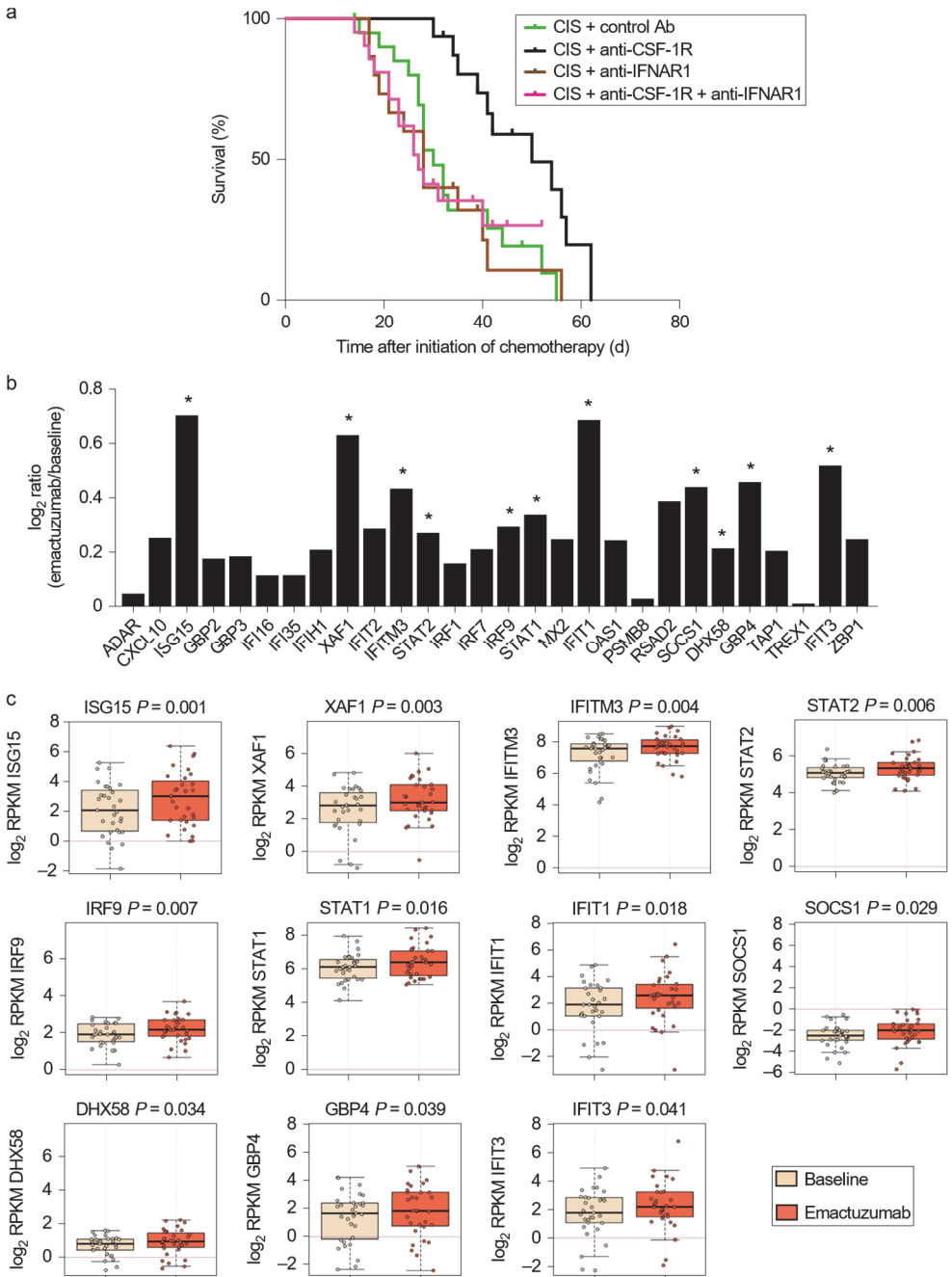


**Fig. 4 | CSF-1R blockade increases the expression of intratumoural type I IFN signalling in patients with cancer treated with emactuzumab and is essential for the therapeutic synergy of cisplatin + anti-CSF-1R in the KEP mouse model. a**, Kaplan–Meier tumour-specific survival curves of KEP mice treated with cisplatin + control Ab, cisplatin + anti-CSF-1R (same groups as in Fig. 1f), cisplatin + anti-IFNAR1 (n = 15 animals) or cisplatin + anti-CSF-1R + anti-IFNAR1 (n = 21 animals). Cisplatin + anti-CSF-1R versus

## Therapeutic targeting of macrophages enhances chemotherapy efficacy by unleashing type I interferon response

cisplatin + anti-CSF-1R + anti-IFNAR1:  $P = 0.0064$  (two-tailed log-rank test). **b**, log<sub>2</sub> ratio of intratumoural expression levels of 28 type I ISGs in emactuzumab (anti-CSF-1R)-treated patients ( $n = 31$  patients) normalized against the pre-treatment expression levels. **c**, Box plots of the expression level of the 11 statistically significant upregulated type I ISGs in tumours of emactuzumab-treated patients (data from **b**, indicated by asterisks). Expression levels in the pre-treatment (baseline) tumour biopsies are compared to on-treatment (emactuzumab) biopsies. The top-most line is the maximum, the top of the box is the third quartile, the centre line is the median, the bottom of the box is the first quartile and the bottom-most line is the minimum. RPKM, reads per kilobase of exon per million mapped reads. The P values were determined by a two-tailed Student's t-test.

## **Combined CSF-1R inhibition and neutrophil depletion engages antitumour immunity that further improves the therapeutic benefit of cisplatin**

Type I IFNs are emerging as key regulators of cancer growth and therapy response<sup>31,32</sup>. Type I IFNs can affect cancer biology via different mechanisms, including the induction of anti-proliferative and pro-apoptotic effects on IFNAR<sup>+</sup> cancer cells<sup>33,34</sup>. Indeed, exposure of a cell line derived from a spontaneous KEP mammary tumour to recombinant IFN- $\alpha$ 1 results in a dose-dependent decrease in colony-forming ability, also in combination with cisplatin, suggesting that type I IFNs have a direct inhibitory effect on KEP cancer cells (Fig. 5). Because type I IFNs are also key orchestrators of antitumour immunity<sup>33,34,35</sup>, we hypothesized that the anti-CSF-1R-induced type I IFN-enriched TME may foster antitumour CD8<sup>+</sup> T cell activity. However, we observed fewer numbers of tumour-infiltrating CD4<sup>+</sup> or CD8<sup>+</sup> T cells in cisplatin + anti-CSF-1R-treated tumours than in cisplatin + control antibody-treated tumours (Supplementary Fig. 6a–c), and the CD8/regulatory T cell ratio was not affected (Fig. 6a). More natural killer (NK) cells were infiltrating the cisplatin + anti-CSF-1R-treated KEP tumours; however, the number of granzyme B<sup>+</sup> cells was not affected compared to cisplatin + control antibody treatment (Fig. 6b,c and Supplementary Fig. 6d). We previously reported that cisplatin efficacy is independent of the adaptive immune system<sup>3</sup>, and, in line with the lack of more intratumoural granzyme B<sup>+</sup> cells and T cells, here, we also show that antibody-mediated depletion of CD8<sup>+</sup> T cells does not reduce the therapeutic efficacy of cisplatin + anti-CSF-1R therapy (Fig. 6d). In addition, genetic ablation of the entire adaptive immune system by crossing KEP mice with *Rag1*<sup>-/-</sup> mice did not affect therapeutic synergy (Fig. 6g). These data indicate that the anti-CSF-1R-mediated conversion of the TME into a type I IFN-enriched milieu in cisplatin-treated mice is not sufficient to successfully engage an endogenous antitumour T cell response.

Therapeutic targeting of macrophages enhances chemotherapy efficacy by unleashing type I interferon response

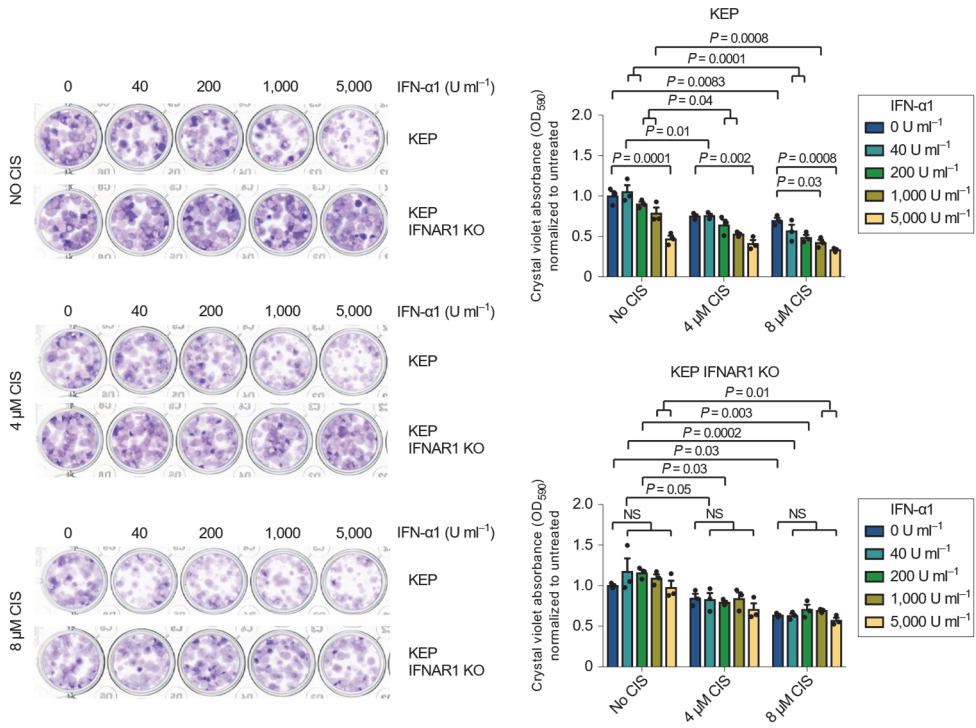


**Fig. 5 | Direct inhibitory effect of IFN- $\alpha$ 1 on a KEP-derived cancer cell line.** Representative images of a colony-forming assay with KEP-derived cancer cells and IFNAR1 KO KEP cancer cells treated with increasing concentrations of IFN- $\alpha$ 1 and cisplatin. After 7 d, crystal violet was dissolved and absorbance was measured at 590 nm. Data are representative of three independent experiments. Data are mean  $\pm$  s.e.m. The *P* value was determined by two-way ANOVA with Tukey's multiple comparison test.

We next hypothesized that it may be necessary to breach an additional layer of immunosuppression before antitumour immunity can be unleashed. The most abundant immune cell population in cisplatin + anti-CSF-1R-treated KEP tumours is neutrophils (Fig. 1e) and we have previously reported that KEP tumour-educated neutrophils are very immunosuppressive<sup>36</sup>. To address whether neutrophils impede antitumour immunity in cisplatin + anti-CSF-1R-treated mice, we treated tumour-bearing KEP mice with the neutrophil-specific anti-Ly6G antibody (clone 1A8). Immunohistochemistry for S100A9 confirmed a reduction in the number of neutrophils in the lungs and to a lesser extent in the tumour (Supplementary Fig. 6e,f). Cisplatin + anti-CSF-1R + anti-Ly6G treatment significantly improved tumour control and prolonged the survival of KEP mice compared to cisplatin + anti-CSF-1R therapy (Fig. 6e). Whereas cisplatin + anti-CSF-1R temporarily stabilizes tumour outgrowth, we observed tumour shrinkage in six out of ten mice treated with cisplatin + anti-CSF-1R + anti-Ly6G, and the mammary tumours of two of these mice regressed completely during treatment (Supplementary Fig. 6g,h). Anti-Ly6G treatment alone failed to influence primary tumour growth in KEP mice as previously shown<sup>36</sup>, neither did the combination of anti-CSF-1R + anti-Ly6G (Supplementary Fig. 6i) nor did anti-Ly6G alter the efficacy of cisplatin (Fig. 6e). Further characterization of cisplatin + anti-CSF-1R + anti-Ly6G-treated KEP tumours showed a significant reduction in the number of BrdU<sup>+</sup>-proliferating cells and  $\gamma$ -H2AX<sup>+</sup> DNA-damaged cells (Supplementary Fig. 6j,k). No statistically significant differences were observed in the number of apoptotic cells, CD31<sup>+</sup> vessels and cisplatin adducts (Supplementary Fig. 6l-n). Interestingly, the CD8/regulatory T cell ratio, the absolute number of NK cells and the absolute and relative number of granzyme B<sup>+</sup> immune cells were increased in cisplatin + anti-CSF-1R + anti-Ly6G-treated tumours compared to cisplatin + control antibody therapy (Fig. 6a-c and Supplementary Fig. 6d). Importantly, the additional therapeutic benefit obtained by anti-Ly6G treatment was partially lost after antibody-mediated depletion of CD8<sup>+</sup> T cells or NK cells (Fig. 6e,f) and was completely abrogated when the same treatment was performed in KEP;*Rag1*<sup>-/-</sup> mice (Fig. 6g). Collectively, these data indicate that the combined anti-CSF-1R-mediated conversion of the tumour milieu into a type I IFN-enriched environment and the relieve of neutrophil-dependent immunosuppression fosters engagement of antitumour immunity in the anticancer effect of cisplatin in this poorly immunogenic mouse tumour model.

## Therapeutic targeting of macrophages enhances chemotherapy efficacy by unleashing type I interferon response

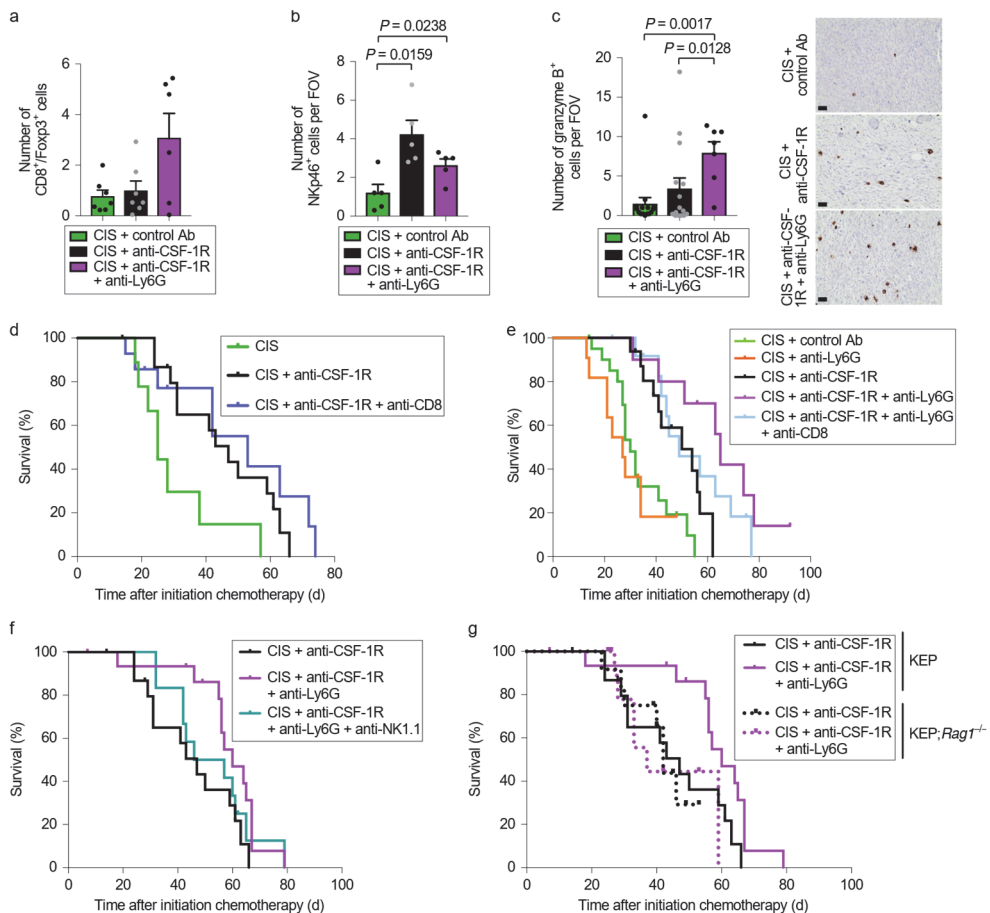


**Fig. 6 | Neutrophil inhibition engages antitumour immunity and further improves cisplatin + anti-CSF-1R efficacy.** **a**, CD8<sup>+</sup> T cell/Foxp3<sup>+</sup> T cell ratio based on immunohistochemistry staining in the tumour of time-point-sacrificed KEP mice (cisplatin + control Ab and cisplatin + anti-CSF-1R:  $n = 7$  animals; cisplatin + anti-CSF-1R + anti-Ly6G:  $n = 6$  animals). **b,c**, Quantification of NKp46<sup>+</sup> cells (**b**) and granzyme B<sup>+</sup> cells (**c**) in viable areas of mammary tumours of time-point-sacrificed KEP mice treated with cisplatin + control Ab (NKp46:  $n = 5$  animals; granzyme B:  $n = 15$  animals), cisplatin + anti-CSF-1R (NKp46:  $n = 5$  animals; granzyme B:  $n = 15$  animals) and cisplatin + anti-CSF-1R + anti-Ly6G (NKp46:  $n = 5$  animals; granzyme B:  $n = 7$  animals). The values represent the average number of positive cells per FOV quantified by counting five high-power microscopic fields per tumour. Representative granzyme B immunohistochemistry stainings are shown (**c**). Scale bars, 50  $\mu$ m. **d**, Kaplan–Meier tumour-specific survival curves of KEP mice treated with cisplatin + control Ab ( $n = 6$  animals), cisplatin + anti-CSF-1R ( $n = 16$  animals) and cisplatin + anti-CSF-1R + anti-CD8 ( $n = 14$  animals). Cisplatin + anti-CSF-1R + anti-CD8-treated mice versus cisplatin + anti-CSF-1R-treated mice:  $P = 0.3728$  (two-tailed log-rank test). **e**, Kaplan–Meier tumour-specific survival curves of KEP mice treated with cisplatin + control Ab, cisplatin + anti-CSF-1R (same groups as in Fig. 1f), cisplatin + anti-Ly6G ( $n = 11$  animals), cisplatin + anti-CSF-1R + anti-Ly6G ( $n = 10$  animals) or cisplatin + anti-CSF-1R + anti-

Ly6G + anti-CD8 ( $n = 13$  animals). Cisplatin + anti-CSF-1R-treated mice versus cisplatin + anti-CSF-1R + anti-Ly6G-treated mice:  $P = 0.0085$ ; cisplatin + anti-CSF-1R-treated mice versus cisplatin + anti-CSF-1R + anti-Ly6G + anti-CD8-treated mice:  $P = 0.1104$  (two-tailed log-rank test). **f**, Kaplan–Meier tumour-specific survival curves of KEP mice treated with cisplatin + anti-CSF-1R ( $n = 16$  animals, same curve as in **d**), cisplatin + anti-CSF-1R + anti-Ly6G ( $n = 17$  animals of which 4 mice were treated with cisplatin + anti-CSF-1R + anti-Ly6G + IgG2a; no differences were observed between cisplatin + anti-CSF-1R + anti-Ly6G and cisplatin + anti-CSF-1R + anti-Ly6G + IgG2a), or cisplatin + anti-CSF-1R + anti-Ly6G + anti-NK1.1 ( $n = 12$  animals). Cisplatin + anti-CSF-1R-treated mice versus cisplatin + anti-CSF-1R + anti-Ly6G-treated mice:  $P = 0.0226$ ; cisplatin + anti-CSF-1R-treated mice versus cisplatin + anti-CSF-1R + anti-Ly6G + anti-NK1.1-treated mice:  $P = 0.4073$  (two-tailed log-rank test). **g**, Kaplan–Meier tumour-specific survival curves comparing cisplatin + anti-CSF-1R and cisplatin + anti-CSF-1R + anti-Ly6G treatment in KEP (same as in **f**) and KEP;*Rag1*<sup>-/-</sup> mice. Cisplatin + anti-CSF-1R in KEP;*Rag1*<sup>-/-</sup> ( $n = 12$  animals) and cisplatin + anti-CSF-1R + anti-Ly6G in KEP;*Rag1*<sup>-/-</sup> ( $n = 11$  animals). Cisplatin + anti-CSF-1R + anti-Ly6G-treated KEP;*Rag1*<sup>-/-</sup> mice versus cisplatin + anti-CSF-1R-treated KEP;*Rag1*<sup>-/-</sup> mice:  $P = 0.9597$  (two-tailed log-rank test). Data presented in **a–c** are mean  $\pm$  s.e.m., and statistical analysis was performed using the two-tailed Mann–Whitney test.

## Discussion

There is a growing realization that immune-mediated mechanisms influence the responsiveness of tumours to chemotherapy<sup>1</sup>. Notably, macrophages actively interfere with the therapeutic efficacy of chemotherapy via several mechanisms in mouse tumour models, including suppression of antitumour immunity through IL-10 secretion<sup>5</sup>, secretion of chemoprotective proteases such as cathepsins<sup>12</sup> or secretion of lysophospholipids<sup>15</sup> that interfere with the DNA damage response. These macrophage-mediated chemotherapy resistance mechanisms are dependent on the production of soluble mediators from TAMs. Our study reveals a conceptually different mechanism of how therapeutic targeting of macrophages improves chemotherapy efficacy. Through in vivo mechanistic studies in the KEP transgenic mouse model for breast cancer, we demonstrate that macrophage inhibition with anti-CSF-1R induces intratumoural type I IFN signalling, which acts synergistically with cisplatin to inhibit tumour outgrowth and extend survival.

There is a growing interest in the effect of type I IFNs on cancer behaviour and response to immune checkpoint inhibitors, radiotherapy and chemotherapy<sup>32,37,38,39</sup>. Besides being associated with an improved prognosis<sup>40,41,42</sup>, an intratumoural IFN signature in patients with breast cancer has been correlated with improved chemotherapy response<sup>37</sup>, and preclinical studies reported that type I IFN enhanced chemotherapy

Therapeutic targeting of macrophages enhances chemotherapy efficacy by unleashing type I interferon response

efficacy<sup>37,43</sup>. However, IFN-related gene signatures have also been correlated with chemotherapy resistance<sup>44</sup>, consistent with a pleomorphic and still poorly understood role of type I IFN signalling in the tumour context. Importantly, impaired type I IFN signalling is a prominent feature of immune dysfunction in patients with cancer<sup>45</sup>. Our study reveals that anti-CSF-1R represents a powerful approach to induce intratumoural IFN signalling and to sensitize tumours to cisplatin. Notably, we find that anti-CSF-1R treatment in patients with cancer also results in increased intratumoural expression of ISGs, confirming our findings that anti-CSF-1R unleashes type I IFN response in tumours.

Our study shows that anti-CSF-1R depletes the majority of F4/80<sup>+</sup> TAMs; however, a small intratumoural CD11b<sup>+</sup>F4/80<sup>+</sup> population with a distinct phenotype survives. Interestingly, these surviving cells express lower levels of *Csf1r* and significantly higher *Ifna* mRNA levels than the CD11b<sup>+</sup>F4/80<sup>+</sup> cells in untreated tumours, probably accounting for the increased *Ifna* levels in the tumours. A shift in macrophage phenotype was also observed in pancreatic cancer and glioblastoma models upon interference with the CSF-1–CSF-1R pathway<sup>46,47,48,49</sup>. Similar to our model, targeting CSF-1 in the pancreatic cancer models on the one hand depleted TAMs and on the other hand reprogrammed the remaining macrophages to an antitumour phenotype. Interestingly, type I IFN was also found to be increased in these macrophages<sup>49</sup>; however, its effect was not functionally pursued in this study. These data, combined with our observation that IFN- $\alpha$  is also upregulated in anti-CSF-1R-treated MC38 colon adenocarcinoma tumours, indicate that anti-CSF-1R-mediated induction of type I IFNs is not limited to breast cancer, but extends to other cancer types.

Type I IFNs can directly affect cancer cells by inducing apoptosis or blocking proliferation, or indirectly by stimulating antitumour immune responses or inhibiting angiogenesis<sup>33</sup>. In line with the observed in vivo reduction of proliferating tumour cells upon anti-CSF-1R therapy, our in vitro studies indicate that IFN- $\alpha$ 1 can directly suppress KEP cancer cells. We did not observe an effect of CSF-1R inhibition on the number of intratumoural blood vessels or their pericyte coverage, excluding an angiogenesis effect. Despite a key role for type I IFNs in dictating antitumour immunity<sup>31,32</sup>, the increase in the number of intratumoural type I IFNs was not sufficient to induce effective antitumour T cell responses. In line with the immunosuppressive phenotype of tumour-educated neutrophils in KEP mice<sup>36</sup> and in other models<sup>50</sup>, the additional ablation of neutrophils

stimulated antitumour immunity. It may be surprising that we observed a therapeutic benefit of depletion of neutrophils with an IFN gene signature in cisplatin + anti-CSF-1R-treated KEP mice, whereas some studies have suggested that type I IFNs can induce antitumour properties in neutrophils<sup>51</sup>. However, in line with our data, a type I IFN transcriptional signature in neutrophils in malaria-infected hosts and in patients with active tuberculosis correlated with tissue damage and disease pathogenesis<sup>52,53</sup>, suggesting that, in these settings, type I IFN signalling in neutrophils may contribute to their harmful actions. In addition, although type I IFNs are often considered to exert antitumour functions, several studies on chronic viral infections show negative-feedback mechanisms when persistently present in the environment by, for example, generating an immunosuppressive milieu<sup>34,54,55</sup>. Perhaps in our study a similar mechanism is involved, explaining why the cytotoxic activity of platinum-based chemotherapy is enhanced by type I IFNs, but at the same time, this therapeutic synergy is limited by an immunosuppressive programme. Although T cell activation was implicated in controlling tumour growth upon combined macrophage and neutrophil depletion in a mouse model for pancreatic cancer<sup>20</sup>, the full mechanism in the context of chemotherapy was not completely resolved. Our *in vivo* data demonstrate that, although the release of type I IFN is necessary for cisplatin + anti-CSF-1R therapeutic synergy, it takes further depletion of neutrophils to engage an antitumour immune response during cisplatin treatment.

Interestingly, the platinum-based drugs cisplatin and oxaliplatin synergized with anti-CSF-1R treatment, whereas docetaxel did not, despite the induction of IFN- $\alpha$  in the docetaxel setting. It will be important to mechanistically understand how the type of chemotherapy dictates its ability to act in synergy with type I IFN signalling. These insights will facilitate the development of optimal combination therapies of CSF-1R-targeting drugs or other type I IFN-inducing agents, including STING (stimulator of IFN genes) agonists<sup>56</sup>, with chemotherapeutic agents. To maximize the therapeutic benefit of cytotoxic therapy in poorly immunogenic tumour types, it will be critical to simultaneously target neutrophil-dependent immunosuppression.

## Methods

### Mice

The generation and characterization of KEP mice have been previously described<sup>24</sup> and are commercially available via Taconic Biosciences. KEP mice were back-crossed onto the FVB/N background, and genotyping was performed by PCR analysis on tail-tip DNA as described<sup>24,36</sup>. KEP mice were crossed with *Rag1*<sup>-/-</sup> mice (FVB/N, a gift from L. Coussens, Oregon Health & Science University, Portland) to generate KEP;*Rag1*<sup>-/-</sup> mice<sup>3</sup>. Female KEP and KEP;*Rag1*<sup>-/-</sup> mice were monitored twice weekly for the spontaneous onset of mammary tumour formation by palpation starting at 4 months of age. Donor tumours from KEP and KP<sup>24</sup> mice were collected in ice-cold PBS, cut into small pieces and resuspended in DMEM F12 containing 30% FCS and 10% dimethyl sulfoxide and stored at -150 °C. The perpendicular tumour diameters of mammary tumours were measured twice a week using a caliper. Age-matched wild-type littermates were used as controls. Female FVB/N mice (10–12 weeks of age) were obtained from Charles River. mTmG mice<sup>57</sup> (back-crossed to the FVB/N background) express tdTomato ubiquitously and were used for the isolation of bone marrow monocytes. Mice were kept in individually ventilated cages at the animal laboratory facility of the Netherlands Cancer Institute (NKI; Amsterdam, the Netherlands). Food and water were provided ad libitum. Animal experiments were approved by the Animal Ethics Committee of the NKI and performed in accordance with institutional, national and European guidelines for animal care and use. The study is compliant with all relevant ethical regulations regarding animal research.

### In vivo intervention studies

KEP mice bearing spontaneous mammary tumours were randomized over the treatment groups before initiation of the treatment. Mice were injected intraperitoneally with the chimeric (hamster/mouse) anti-CSF-1R antibody (clone 2G2, Roche Innovation Center Munich; single loading dose of 60 mg per kg followed by 30 mg per kg once a week); control antibody (IgG1, MOPC21, Roche Innovation Center Munich; single loading dose of 60 mg per kg followed by 30 mg per kg once a week); anti-Ly6G antibody (1A8, BioXCell; single loading dose of 400 µg followed by 100

$\mu\text{g}$  three times a week); anti-IFNAR1 (MAR1-5A3, BioXCell; 100  $\mu\text{g}$  three times a week); anti-CD8 (2.43, BioXCell; single loading dose of 400  $\mu\text{g}$  followed by 100  $\mu\text{g}$  three times a week); anti-NK1.1 (PK136, BioXCell; single loading dose of 400  $\mu\text{g}$  followed by 100  $\mu\text{g}$  three times a week); and IgG2a (C1.18.4, BioXCell; single loading dose of 400  $\mu\text{g}$  followed by 100  $\mu\text{g}$  three times a week). The maximum tolerated dose (MTD) dose of cisplatin (5 mg per kg; Accord Healthcare Limited) was administered intravenously every other week for a total of four cycles. The MTD dose of docetaxel (15 mg per kg; Accord Healthcare Limited) was administered intravenously every week for a total of four cycles. The MTD dose of oxaliplatin (6 mg per kg diluted in NaCl; Fresenius Kabi) was administered intravenously every 10 days for three cycles.

Anti-CSF-1R, control antibodies, anti-Ly6G, anti-CD8 and anti-NK1.1 treatment started when mammary tumours reached a size of 25 mm<sup>2</sup>; and anti-IFNAR1, cisplatin, docetaxel and oxaliplatin treatment started when mammary tumours reached a size of 50 mm<sup>2</sup>. For survival curve experiments and end-stage analyses, antibody treatment continued until the tumour or the cumulative tumour burden reached a size of 225 mm<sup>2</sup>. For survival curve experiments, an event is defined as an animal with a cumulative tumour size of 225 mm<sup>2</sup>. The main cause of death of censored mice was ulcerated tumours or cisplatin-induced renal toxicity for cisplatin-treated mice.

For time-point analyses, mice were killed 1 d after the second chemotherapy injection (therapy- responsive phase) or at a tumour size of 100 mm<sup>2</sup> in chemotherapy-naive mice. To assess tumour cell proliferation, BrdU (50 mg per kg) was injected intraperitoneally into mice 90 min before being sacrificed.

KP tumour pieces were orthotopically transplanted into the mammary fat pad of 10–12-week-old FVB/N female mice. Before initiation of the treatment, mice were randomized over the experimental groups and treated either with control antibody or anti-CSF-1R as described above. Treatment started at a tumour size of 25 mm<sup>2</sup> and continued until the tumour reached a size of 100 mm<sup>2</sup> when the mice were sacrificed.

MC38 tumours were provided by Roche Innovation Center Munich. MC38 cells were subcutaneously injected into C57Bl6/N mice and, when the tumour volume reached 100 mm<sup>3</sup>, treated with either control antibody or

Therapeutic targeting of macrophages enhances chemotherapy efficacy by unleashing type I interferon response

anti-CSF-1R as described above. Mice were sacrificed 5 d after the second treatment<sup>21</sup>.

## **Intervention studies in the KEP-based spontaneous metastasis model**

The orthotopic KEP-based spontaneous metastasis model was described previously in detail<sup>27</sup>. Briefly, KEP tumour pieces (1 × 1 mm) were orthotopically transplanted into 10–12-week-old FVB/N female mice. Mammary tumours were surgically removed once they reached a tumour size of 225 mm<sup>2</sup>, after which mice were monitored and sacrificed when they reached the humane end point due to clinically overt metastatic disease. Tumour-bearing recipient mice were treated either with control antibody or with anti-CSF-1R once the mammary tumours reached 5 mm<sup>2</sup> (continuous setting) or 3 d after mastectomy (adjuvant setting). Antibody treatment continued until recipient mice developed clinical signs of distress caused by metastatic disease (for example, respiratory distress).

## **Histology, immunohistochemistry, immunofluorescence and RNA in situ hybridization**

All histochemical and immunohistochemical analyses, except NKp46 immunohistochemistry, were performed by the Animal Pathology facility at the NKI. NKp46 immunohistochemistry was performed at the Histology core facility within the Cancer Research UK Beatson Institute (Glasgow, UK). For histochemical analysis, formalin-fixed tissues were processed, sectioned and stained as described<sup>27</sup>. Briefly, tissues were fixed for 24 h in 10% neutral-buffered formalin, embedded in paraffin, sectioned at 4 µm and stained with haematoxylin and eosin (H&E) for histopathological evaluation. H&E slides were digitally processed using the Aperio ScanScope (Aperio). For the quantitative assessment of areas in the tumour that had lost viability, slides were analysed with ImageJ by quantifying the percentage of non-viable areas (defined as areas that lost cellularity) over the total tumour area. Histochemistry for mast cells was performed with Toluidine blue.

For immunohistochemical analysis, paraffin sections were cut and deparaffinized. Antibodies and antigen retrieval methods are described in Supplementary Table 1. Cisplatin adduct staining was performed on frozen tissues embedded in OCT. Quantification of positive cells was performed

manually by counting five high-power (40×) fields of view (FOVs) per tumour by two independent operators in a blinded manner. Samples were visualized with a BX43 upright microscope (Olympus) and images were acquired in bright field using cellSens Entry software (Olympus).

The percentages of metastasis-bearing spontaneous KEP mice were calculated based on the microscopic presence or absence of metastatic nodules in lungs and lymph nodes. In the metastasis model, the number of metastatic nodules in the lungs was based on cytokeratin 8 expression. Mice that developed overt metastatic disease were included in the analysis, and mice that were sacrificed because of local recurrence of the primary tumour were excluded.

Immunohistochemistry analysis for CD68 expression (1:2,000, clone KP1, Dako) was performed by the NKI-AvL Core Facility Molecular Pathology and Biobanking on formalin-fixed paraffin-embedded material of ILC breast cancer patients from the RATHER cohort<sup>58,59</sup> enrolled at the NKI. Anonymized archival tissue was used according to national guidelines regarding the use of archival material and with approval of the NKI-AVL translational research board.

Immunofluorescence analysis was performed on formalin-fixed paraffin-embedded material. The list of primary and secondary antibodies is provided in Supplementary Table 1. Sections were counterstained with DAPI (4,6-diamidino-2-phenylindole) and visualized with a Leica SP5 confocal microscope. Images were taken with LAS AF software (Leica) and values were obtained by counting  $\alpha$ -SMA<sup>+</sup>CD31<sup>+</sup> cells and total CD31<sup>+</sup> cells in six fields per tumour by two independent researchers.

In situ detection of *Csf1* mRNA was performed using the RNAscope 2.0 FFPE Assay (Advanced Cell Diagnostics) and performed according to the manufacturer's recommendations<sup>60</sup>.

## **Flow cytometry**

KEP tumours were collected in ice-cold PBS and processed as described<sup>61</sup>. Briefly, samples were mechanically chopped using the McIlwain tissue chopper (Mickle Laboratory Engineering) and enzymatically digested with 3 mg ml<sup>-1</sup> collagenase type A (Roche) and 25  $\mu$ g ml<sup>-1</sup> DNase I (Sigma) in serum-free medium for 1 h at 37°C in a shaking water bath. After washing,

cells were stained with fluorochrome-conjugated antibodies (Supplementary Table 1). For intracellular staining of granzyme B, single-cell suspensions were stimulated in IMDM containing 8% FCS, 100 IU ml<sup>-1</sup> penicillin, 100 µg ml<sup>-1</sup> streptomycin, 0.5% β-mercaptoethanol, 50 ng ml<sup>-1</sup> PMA, 1 µM ionomycin and Golgi-Plug (1:1,000; BD Biosciences) for 3 h at 37 °C. Following surface antigen staining, samples were fixed and permeabilized (BD Biosciences) and stained for intracellular proteins. Data acquisition was performed on BD LSRII or BD LSRFortessa flow cytometer using DIVA software (BD Biosciences) and data analysis was performed using FlowJo software version 9.9.6.

### Isolation of intratumoural cell populations

Primary mammary tumours were harvested from KEP mice 1 d after two cycles of chemotherapy (±100 mm<sup>2</sup>) or at end-stage (±225 mm<sup>2</sup>), and single-cell suspensions were generated as described above. Enrichment of CD11b<sup>+</sup> cells was performed using magnetic columns (Miltenyi Biotec), as described previously<sup>61</sup>. Briefly, single-cell suspensions were stained with anti-CD11b-APC (1:200; clone M1/70, eBioscience) for 20 min and incubated with magnetic anti-APC MicroBeads according to the manufacturer's instructions (Miltenyi Biotec). CD11b<sup>+</sup> cells were isolated with LS columns (Miltenyi Biotec) according to the manufacturer's instructions. For the isolation of macrophages and neutrophils from tumours at the therapy-responsive phase, the enriched CD11b<sup>+</sup> fraction was stained with antibodies against Ly6G-FITC (1:200; clone 1A8, BD Biosciences), F4/80-PE (1:200; clone BM8, eBioscience) and Ly6C-ef450 (1:400; clone hk1.4, eBioscience). LIVE/DEAD fixable aqua dead cell stain (Thermo Fisher Scientific) was added 1:100 in PBS to exclude dead cells. CD11b<sup>+</sup>F4/80<sup>+</sup> macrophages and F4/80<sup>-</sup>Ly6G<sup>+</sup>Ly6C<sup>low</sup> neutrophils were isolated with the BD FACSAria II sorter with DIVA software (BD Biosciences).

For the isolation of cell populations from end-stage tumours, we separated intratumoural CD11b<sup>+</sup> and CD11b<sup>-</sup> cells by magnetic cell sorting as described above. The CD11b<sup>-</sup> and CD11b<sup>+</sup> fractions were stained as described in Supplementary Table 1. CD11b<sup>+</sup>F4/80<sup>+</sup> macrophages, CD11b<sup>+</sup>F4/80<sup>-</sup>Ly6G<sup>-</sup>Ly6C<sup>+</sup> monocytes, CD11b<sup>+</sup>F4/80<sup>-</sup>Ly6G<sup>+</sup>Ly6C<sup>low</sup> neutrophils, CD11b<sup>-</sup>CD45<sup>+</sup>CD11c<sup>-</sup> lymphocytes and CD11b<sup>-</sup>CD45<sup>-</sup>CD31<sup>-</sup> tumour cells were isolated with BD FACSAria Fusion sorter with DIVA software (BD Biosciences).

## **Adoptive transfer of monocytes**

Front legs, hind legs and hips were collected from female mTmG mice and the bone marrow was flushed out. Bone marrow cells were incubated with Fc Block (1:50; CD16/CD32, BD Biosciences), stained with anti-Ly6G-APC (1:200; clone 1A8, BioLegend) and, consequently, negative selection for neutrophils was performed using magnetic columns (Miltenyi Biotec) as described previously<sup>61</sup>. The Ly6G<sup>-</sup> fraction was then stained with fluorochrome-conjugated antibodies (Supplementary Table 1). After gating out Lineage<sup>+</sup> cells (CD3, CD8, CD4, NKp46 and Ter119) and Siglec F<sup>+</sup>, Sca1<sup>+</sup> and cKIT<sup>+</sup> cells, tdTomato<sup>+</sup>CD11b<sup>int</sup>Ly6G<sup>-</sup>Ly6C<sup>+</sup> monocytes were isolated with BD FACSAria Fusion sorter with DIVA software (BD Biosciences). Between 1.5 and 2 × 10<sup>6</sup> tdTomato<sup>+</sup> monocytes were adoptively transferred into the tail vein of a tumour-bearing KEP mouse treated with control antibody or anti-CSF-1R. Antibody treatments started at a tumour size of 25 mm<sup>2</sup>, and 1 d after the second antibody injection (1 week apart), monocytes were transferred. KEP mice were sacrificed 4 d later and tumours were isolated for flow cytometry analysis. Antibodies are listed in Supplementary Table 1.

## **CRISPR–Cas9-mediated gene disruption and colony-forming assay**

IFNAR1 was knocked out (KO) from a cell line derived from a spontaneous KEP mammary tumour by transient transfection with a lentiCRISPRv2 (ref. <sup>62</sup>) containing IFNAR1-specific single guide RNA targeting exon 1 (sgRNA1: 5'-GCTCGCTGTCGTGGGCGCGG-3'). Twenty-four hours after transfection, cells were exposed to puromycin for 48 h. Cells were stained with IFNAR1-PE (1:200; clone MAR1-5A3, eBioscience) and IFNAR1-negative cells were sorted with BD FACSAria Fusion sorter with DIVA software (BD Biosciences).

KEP and IFNAR1 KO KEP cells (250 cells per well) were seeded in triplicate in a 24-well plate, and the next day, cells were treated with an increasing concentration of recombinant IFN- $\alpha$ 1 (BioLegend) for 7 d. On day 5, 4  $\mu$ M or 8  $\mu$ M cisplatin were added. At day 7, cells were washed, fixed in ice-cold methanol and incubated with 0.05% crystal violet. For quantification, crystal violet was dissolved in 10% acetic acid for 20 min and the absorbance was measured at 590 nm.

## **BMDMs**

To generate BMDMs, bone marrow cells were harvested from the hind legs of wild-type mice and cultured for 7 days in RPMI medium containing 8% FCS, 100 IU ml<sup>-1</sup> penicillin, 100 mg ml<sup>-1</sup> streptomycin and 20 ng ml<sup>-1</sup> recombinant M-CSF (PeproTech). After differentiation, BMDMs were harvested and seeded in a 24-well plate (400,000 BMDMs per well) and cultured overnight. The next morning, BMDMs were exposed to conditioned medium from a KEP cancer cell line in the presence of 8 µg ml<sup>-1</sup> of either control antibody or anti-CSF-1R for 24 h. Conditioned medium was obtained by culturing KEP cancer cells (80–90% confluency) for 24 h in RPMI containing 8% FCS, 100 IU ml<sup>-1</sup> penicillin and 100 mg ml<sup>-1</sup> streptomycin. The RNA of BMDMs was isolated with the Isolate II RNA Mini Kit (Bioline), and quantitative RT–PCR for *Ifna* was performed as described below.

## **RNA isolation and quantitative RT–PCR**

RNA from sorted cells and tumours of KEP mice was isolated using TRIzol (Invitrogen). Samples were treated with DNase I (Invitrogen) followed by RNA cleanup with the Qiagen RNeasy Mini Kit according to the manufacturer's recommendation. Isolated RNA was quantified with Nanodrop (Thermo Scientific). Transformation of RNA into cDNA was performed with the Cloned AMV First-Strand cDNA Synthesis Kit (Invitrogen) using oligo(dT) primers. cDNA (20 ng per well) was analysed by SYBR green real-time PCR with 500 nM primers (Supplementary Table 2) using a LightCycler 480 thermocycler (Roche). Samples were run in duplicate and were only further considered if the difference between the CT values of the duplo was less than one cycle. β-Actin was used as a reference gene.

## **Luminex cytokine array**

Tumours and mammary glands were prepared with Bio-Rad cell lysis buffer, and the protein concentration of lysates was determined using the Pierce BCA Protein Assay Kit (Thermo Fischer Scientific) according to the manufacturer's recommendations. CSF-1 concentration in protein lysates was determined using the Bio-Plex Pro Cytokine 23-Plex Kits (Bio-Rad) and measured according to the manufacturer's instruction. Data acquisition and analysis were performed on a Bio-Plex 200 reader, using Bio-Plex Manager 6.0 software (Bio-Rad).

## RNA-seq and data analysis

### RNA isolation, library construction and deep sequencing

CD11b<sup>+</sup>F4/80<sup>+</sup> and CD11b<sup>+</sup>F4/80<sup>-</sup>Ly6G<sup>+</sup>Ly6C<sup>low</sup> immune cell populations were isolated as described above from KEP tumours treated with either control antibody, anti-CSF-1R, cisplatin + control antibody or cisplatin + anti-CSF-1R at the therapy-responsive phase (tumour size  $\pm$  100 mm<sup>2</sup>). Some of the biological replicates consisted of pools of cells from two to six different mice. Total RNA was extracted using the RNeasy Mini and Microkits (Qiagen). According to the Ovation RNA-seq system V2 and Encore Rapid library systems protocols (NuGen), 10 ng RNA was converted into cDNA libraries, subsequently sequenced on a HiSeq 1500 system and demultiplexed using CASAVA v1.8 (Illumina).

### Preprocessing of sequenced data

Using default parameters, all reads were aligned against the murine mm10 reference genome by TopHat2 v2.0.11 (ref. <sup>63</sup>). The data were imported into Partek Genomics Suite v6.6 (PGS), and the gene and transcript information was deducted before conducting normalization utilizing statistical software R (v3.3.1) and the DESeq2 package (<https://doi.org/10.1101/002832>). Normalized read counts were floored to a value of at least one thereafter and the data set was trimmed by defining a gene as expressed if the maximum value over all group means was higher than ten.

### Identification of differentially expressed genes

Using PGS, a two-way analysis of variance (ANOVA) was performed to compute the top variable genes (treatment versus control) within the data set, as well as differentially expressed genes present in cisplatin + anti-CSF-1R neutrophils (versus cisplatin + control antibody neutrophils). Genes were defined to be differentially expressed when having a fold change of  $\geq 1.5$  and an unadjusted  $P \leq 0.05$ . Based on the ANOVA model, hierarchical clustering was performed on the top 400 variable genes within the data set (neutrophils and macrophages, cisplatin + anti-CSF-1R versus cisplatin + control antibody) using default settings in PGS.

## **Gene Ontology enrichment analysis, Gene Ontology network visualization, Ingenuity pathway analysis and GSEA**

To link transcriptome information to previous knowledge, we applied Gene Ontology enrichment analysis on the 100 most upregulated and 100 most downregulated genes (fold change  $\geq 1.5$ , unadjusted  $P \leq 0.05$ ) extracted from neutrophils exposed to cisplatin + anti-CSF-1R treatment (versus cisplatin + control antibody-exposed neutrophils). Subsequently, the data were visualized using BiNGO<sup>64</sup>, EnrichmentMap<sup>65</sup> and Word Clouding<sup>66</sup> plug-ins in Cytoscape. In addition, all differentially expressed genes found in neutrophils were analysed with Ingenuity pathway analysis (Qiagen).

GSEA was performed utilizing the BubbleGUM GSEA tool<sup>67</sup> to find enriched pathways in macrophages from cisplatin + anti-CSF-1R-treated tumours (versus cisplatin + control antibody macrophages). Pathways interrogated were derived from the reactome gene sets, and all pathways demonstrating a significant enrichment (false discovery rate (FDR)  $\leq 0.25$ ) in one condition were shown. Specifically addressing enrichment of EGR2 target genes in neutrophils from anti-CSF-1R-treated tumours versus neutrophils from control antibody-treated tumours, GSEA was employed on transcription factor target gene sets using the GSEA tool previously published<sup>68</sup>. The reactome and transcription factor target gene sets were obtained via the online available Molecular Signatures Database (MSigDB) of the Broad Institute (<http://software.broadinstitute.org/gsea/msigdb/index.jsp>).

No custom codes were used in the manuscript.

## **Evaluation of expression of ISGs in patient biopsies**

The selection of type I ISGs was based on the RNA-seq results from our KEP mouse model upon cisplatin + anti-CSF-1R. The genes belong to the biological processes listed in Supplementary Table 3. We assessed the effect of anti-CSF-1R on these selected genes in human tumours by analysing RNA-seq data of paired baseline and on-treatment tumour biopsies of patients enrolled in a clinical phase I trial with emactuzumab (RG7155), a humanized anti-human CSF-1R monoclonal antibody. Biopsies were taken from a multicentre, open-label study (ClinicalTrials.gov identifier NCT01494688). Patients received emactuzumab every 2 weeks as intravenous infusion. Tumour biopsies of 31 patients with a broad range of

different solid malignancies treated with either emactuzumab alone or in combination with paclitaxel (with an overrepresentation of breast cancer ( $n = 13$ ) and ovarian cancer ( $n = 7$ ) samples) were collected. The study was conducted in accordance with the Declaration of Helsinki, current International Conference on Harmonisation of Technical Requirements for Registration of Pharmaceuticals for Human Use guidelines and all applicable regulatory and ethical requirements. The study is compliant with all relevant ethical regulations regarding research involving human participants. All patients provided written informed consent before study-related procedures were performed. RNA extraction, RNA-seq and data analysis were performed as previously described<sup>69</sup>.

### **Statistics and reproducibility**

Information on study design, sample size, number of biological replicates, number of independent experiments and statistical analysis is reported in the main text and figure legends. The survival curves of cisplatin + control antibody (or cisplatin only)-treated, cisplatin + anti-CSF-1R-treated and cisplatin + anti-CSF-1R + anti-Ly6G-treated mice were repeated and confirmed in a separate animal facility (Figs. 1f and 6d–f); other in vivo interventions were performed once. In vitro experiments were repeated independently with similar results. Statistical analyses were performed using GraphPad Prism 7 and 8 (GraphPad Software Inc.). The two-tailed Mann–Whitney test was used for immunohistochemistry and flow cytometry analysis. Two-way ANOVA with Tukey’s multiple comparison test was used for the quantification of crystal violet absorbance. Two-tailed log-rank tests were used for Kaplan–Meier survival curves. Fisher’s exact test (two-sided) was used for metastasis analysis.  $P < 0.05$  was considered statistically significant.

### **Reporting Summary**

Further information on research design is available in the Nature Research Reporting Summary linked to this article.

## Data availability

The RNA-seq data derived from mouse samples that support the findings of this study have been deposited in the Gene Expression Omnibus (GEO) repository under accession number GSE101881. Source data for Figs. 1a,d–i, 2, 3c–h, 4, 5 and 6 and Supplementary Figs. 1a,b,e,f,h,i, 2, 3e–h, 5a–c,f–i and 6a–f,i–n have been provided as Supplementary Table 4. All other data supporting the findings of this study are available from the corresponding author on reasonable request.

## Additional information

**Publisher's note:** Springer Nature remains neutral with regard to jurisdictional claims in published maps and institutional affiliations.

## Acknowledgements

This work was supported by the European Union (FP7 MCA-ITN 317445 TIMCC), the Dutch Cancer Society (NKI10623), the European Research Council (ERC consolidator award INFLAMET 615300), Worldwide Cancer Research (AICR 11-0677), the Netherlands Organization for Scientific Research NWO VIDI (917.96.307) and Oncode. K. Kos is supported by an OOA/NWO Diamond grant. K.E.d.V. is an EMBO Young Investigator. J.L.S. is a member of the Excellence Cluster ImmunoSensation and is in part supported by the DFG (SFB704, Excellence Cluster ImmunoSensation). We thank M. D. Wellenstein, H. Garner, S. Bissinger, J. Borst and T. Schumacher for useful discussions. We thank M. Hauptmann for advice on statistical analyses on the mouse survival curves. We thank the clinical investigators J.-Y. Blay, C. Gomez-Roca, J.-P. Delord, M. Toulmond, C. le Tourneau and A. Italiano for running clinical trials with emactuzumab, and M. Cannarile, B. Quackenbush and A. Jegg for translational medicine support at Roche. We thank the histology core facility within the Cancer Research UK Beatson Institute for performing NKp46 immunohistochemistry on mouse tumour tissue. We thank K. Wartha, S. Klarenbeek and I. Peters Rit for technical assistance and the researchers involved in the RATHER project for generously providing tissue sections of human ILCs. We thank the flow cytometry facility, the animal facility, the animal pathology facility and the Core Facility Molecular Pathology and Biobanking at the NKI.

## **Contributions**

C.S., M.C., C.H.R., J.J. and K.E.d.V. conceived the ideas and designed the experiments. C.S., M.C., C.- S.H., S.B.C., K. Kersten, A.v.W., K.V., K. Kos and K.E.d.V. performed the experiments and analysed the data. C.H.R. provided the anti-CSF-1R antibody and control antibody. S.T., T.U. and J.L.S. prepared the samples and conducted the RNA-seq and bioinformatics analyses on murine cells. J.-Y.S. performed the metastasis scoring. C.-H.O., D.R. and P.A.C. were involved in the collection of patient samples and bioinformatic analysis of the human data. C.S. and K.E.d.V. wrote the paper.

## **Competing interests**

C.H.R., C.-H.O. and D.R. are employees of F. Hoffman La Roche. C.H.R. is an inventor of granted and pending patent applications relating to emactuzumab and a stockholder in F. Hoffman La Roche. F. Hoffman La Roche provided financial research support for the experiments with anti-CSF-1R. P.A.C. received funding from Roche for the described clinical trial and other Roche-sponsored studies.

## References

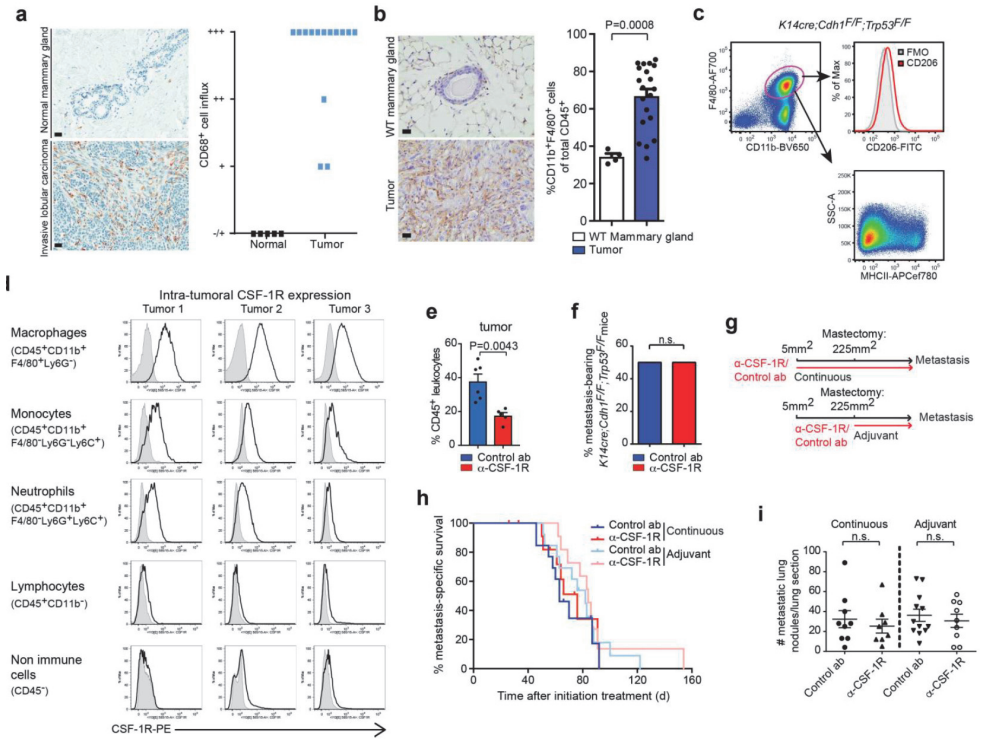
1. Coffelt, S. B. & de Visser, K. E. Immune-mediated mechanisms influencing the efficacy of anticancer therapies. *Trends Immunol.* **36**, 198–216 (2015).
2. Galluzzi, L., Buque, A., Kepp, O., Zitvogel, L. & Kroemer, G. Immunogenic cell death in cancer and infectious disease. *Nat. Rev. Immunol.* **17**, 97–111 (2017).
3. Ciampricotti, M., Hau, C. S., Doornebal, C. W., Jonkers, J. & de Visser, K. E. Chemotherapy response of spontaneous mammary tumors is independent of the adaptive immune system. *Nat. Med.* **18**, 344–346 (2012).
4. DeNardo, D. G. et al. Leukocyte complexity predicts breast cancer survival and functionally regulates response to chemotherapy. *Cancer Discov.* **1**, 54–67 (2011).
5. Ruffell, B. et al. Macrophage IL-10 blocks CD8<sup>+</sup> T cell-dependent responses to chemotherapy by suppressing IL-12 expression in intratumoral dendritic cells. *Cancer Cell* **26**, 623–637 (2014).
6. Campbell, M. J. et al. The prognostic implications of macrophages expressing proliferating cell nuclear antigen in breast cancer depend on immune context. *PLoS One* **8**, e79114 (2013).
7. Chua, W., Charles, K. A., Baracos, V. E. & Clarke, S. J. Neutrophil/lymphocyte ratio predicts chemotherapy outcomes in patients with advanced colorectal cancer. *Br. J. Cancer* **104**, 1288–1295 (2011).
8. Kishi, Y. et al. Blood neutrophil-to-lymphocyte ratio predicts survival in patients with colorectal liver metastases treated with systemic chemotherapy. *Ann. Surg. Oncol.* **16**, 614–622 (2009).
9. Miao, Y., Yan, Q., Li, S., Li, B. & Feng, Y. Neutrophil to lymphocyte ratio and platelet to lymphocyte ratio are predictive of chemotherapeutic response and prognosis in epithelial ovarian cancer patients treated with platinum-based chemotherapy. *Cancer Biomark.* **17**, 33–40 (2016).
10. Pistelli, M. et al. Pre-treatment neutrophil to lymphocyte ratio may be a useful tool in predicting survival in early triple negative breast cancer patients. *BMC Cancer* **15**, 195 (2015).
11. Paulus, P., Stanley, E. R., Schafer, R., Abraham, D. & Aharinejad, S. Colony-stimulating factor-1 antibody reverses chemoresistance in human MCF-7 breast cancer xenografts. *Cancer Res.* **66**, 4349–4356 (2006).
12. Shree, T. et al. Macrophages and cathepsin proteases blunt chemotherapeutic response in breast cancer. *Genes Dev.* **25**, 2465–2479 (2011).
13. Mitchem, J. B. et al. Targeting tumor-infiltrating macrophages decreases tumor-initiating cells, relieves immunosuppression, and improves chemotherapeutic responses. *Cancer Res.* **73**, 1128–1141 (2013).
14. Di Mitri, D. et al. Tumour-infiltrating Gr-1<sup>+</sup> myeloid cells antagonize senescence in cancer. *Nature* **515**, 134–137 (2014).

15. Houthuijzen, J. M. et al. Lysophospholipids secreted by splenic macrophages induce chemotherapy resistance via interference with the DNA damage response. *Nat. Commun.* **5**, 5275 (2014).
16. Acharyya, S. et al. A CXCL1 paracrine network links cancer chemoresistance and metastasis. *Cell* **150**, 165–178 (2012).
17. Olson, O. C., Kim, H., Quail, D. F., Foley, E. A. & Joyce, J. A. Tumor-associated macrophages suppress the cytotoxic activity of antimetabolic agents. *Cell Rep.* **19**, 101–113 (2017).
18. Weizman, N. et al. Macrophages mediate gemcitabine resistance of pancreatic adenocarcinoma by upregulating cytidine deaminase. *Oncogene* **33**, 3812–3819 (2014).
19. Nakasone, E. S. et al. Imaging tumor–stroma interactions during chemotherapy reveals contributions of the microenvironment to resistance. *Cancer Cell* **21**, 488–503 (2012).
20. Nywening, T. M. et al. Targeting both tumour-associated CXCR2<sup>+</sup> neutrophils and CCR2<sup>+</sup> macrophages disrupts myeloid recruitment and improves chemotherapeutic responses in pancreatic ductal adenocarcinoma. *Gut* **67**, 1112–1123 (2018).
21. Ries, C. H. et al. Targeting tumor-associated macrophages with anti-CSF-1R antibody reveals a strategy for cancer therapy. *Cancer Cell* **25**, 846–859 (2014).
22. Quail, D. F. & Joyce, J. A. Molecular pathways: deciphering mechanisms of resistance to macrophage-targeted therapies. *Clin. Cancer Res.* **23**, 876–884 (2017).
23. Crusz, S. M. & Balkwill, F. R. Inflammation and cancer: advances and new agents. *Nat. Rev. Clin. Oncol.* **12**, 584–596 (2015).
24. Derksen, P. W. et al. Somatic inactivation of E-cadherin and p53 in mice leads to metastatic lobular mammary carcinoma through induction of anoikis resistance and angiogenesis. *Cancer Cell* **10**, 437–449 (2006).
25. Hume, D. A. & MacDonald, K. P. Therapeutic applications of macrophage colony-stimulating factor-1 (CSF-1) and antagonists of CSF-1 receptor (CSF-1R) signaling. *Blood* **119**, 1810–1820 (2012).
26. Franklin, R. A. et al. The cellular and molecular origin of tumor-associated macrophages. *Science* **344**, 921–925 (2014).
27. Doornebal, C. W. et al. A preclinical mouse model of invasive lobular breast cancer metastasis. *Cancer Res.* **73**, 353–363 (2013).
28. Noy, R. & Pollard, J. W. Tumor-associated macrophages: from mechanisms to therapy. *Immunity* **41**, 49–61 (2014).

29. Bradley, E. W., Ruan, M. M. & Oursler, M. J. Novel pro-survival functions of the Kruppel-like transcription factor Egr2 in promotion of macrophage colony-stimulating factor-mediated osteoclast survival downstream of the MEK/ERK pathway. *J. Biol. Chem.* **283**, 8055–8064 (2008).
30. Gomez-Roca, C. A. et al. Phase I study of RG7155, a novel anti-CSF1R antibody, in patients with advanced/metastatic solid tumors. *J. Clin. Oncol.* **33**, 3005 (2015).
31. Zitvogel, L., Galluzzi, L., Kepp, O., Smyth, M. J. & Kroemer, G. Type I interferons in anticancer immunity. *Nat. Rev. Immunol.* **15**, 405–414 (2015).
32. Vacchelli, E. et al. Autocrine signaling of type 1 interferons in successful anticancer chemotherapy. *Oncoimmunology* **4**, e988042 (2015).
33. Parker, B. S., Rautela, J. & Hertzog, P. J. Antitumour actions of interferons: implications for cancer therapy. *Nat. Rev. Cancer* **16**, 131–144 (2016).
34. Snell, L. M., McGaha, T. L. & Brooks, D. G. Type I interferon in chronic virus infection and cancer. *Trends Immunol.* **38**, 542–557 (2017).
35. Fuentes, M. B. et al. Host type I IFN signals are required for antitumor CD8<sup>+</sup> T cell responses through CD8 $\alpha$ <sup>+</sup> dendritic cells. *J. Exp. Med.* **208**, 2005–2016 (2011).
36. Coffelt, S. B. et al. IL-17-producing  $\gamma\delta$  T cells and neutrophils conspire to promote breast cancer metastasis. *Nature* **522**, 345–348 (2015).
37. Sistigu, A. et al. Cancer cell-autonomous contribution of type I interferon signaling to the efficacy of chemotherapy. *Nat. Med.* **20**, 1301–1309 (2014).
38. Burnette, B. C. et al. The efficacy of radiotherapy relies upon induction of type I interferon-dependent innate and adaptive immunity. *Cancer Res.* **71**, 2488–2496 (2011).
39. Deng, L. et al. STING-dependent cytosolic DNA sensing promotes radiation-induced type I interferon-dependent antitumor immunity in immunogenic tumors. *Immunity* **41**, 843–852 (2014).
40. Bidwell, B. N. et al. Silencing of Irf7 pathways in breast cancer cells promotes bone metastasis through immune escape. *Nat. Med.* **18**, 1224–1231 (2012).
41. Callari, M. et al. Subtype-dependent prognostic relevance of an interferon-induced pathway metagene in node-negative breast cancer. *Mol. Oncol.* **8**, 1278–1289 (2014).
42. Snijders, A. M. et al. An interferon signature identified by RNA-sequencing of mammary tissues varies across the estrous cycle and is predictive of metastasis-free survival. *Oncotarget* **5**, 4011–4025 (2014).
43. Schiavoni, G. et al. Cyclophosphamide synergizes with type I interferons through systemic dendritic cell reactivation and induction of immunogenic tumor apoptosis. *Cancer Res.* **71**, 768–778 (2011).
44. Weichselbaum, R. R. et al. An interferon-related gene signature for DNA damage resistance is a predictive marker for chemotherapy and radiation for breast cancer. *Proc. Natl Acad. Sci. USA* **105**, 18490–18495 (2008).

45. Critchley-Thorne, R. J. et al. Impaired interferon signaling is a common immune defect in human cancer. *Proc. Natl Acad. Sci. USA* **106**, 9010–9015 (2009).
46. Pyonteck, S. M. et al. CSF-1R inhibition alters macrophage polarization and blocks glioma progression. *Nat. Med.* **19**, 1264–1272 (2013).
47. Quail, D. F. et al. The tumor microenvironment underlies acquired resistance to CSF-1R inhibition in gliomas. *Science* **352**, aad3018 (2016).
48. Yan, D. et al. Inhibition of colony stimulating factor-1 receptor abrogates microenvironment-mediated therapeutic resistance in gliomas. *Oncogene* **36**, 6049–6058 (2017).
49. Zhu, Y. et al. CSF1/CSF1R blockade reprograms tumor-infiltrating macrophages and improves response to T-cell checkpoint immunotherapy in pancreatic cancer models. *Cancer Res.* **74**, 5057–5069 (2014).
50. Coffelt, S. B., Wellenstein, M. D. & de Visser, K. E. Neutrophils in cancer: neutral no more. *Nat. Rev. Cancer* **16**, 431–446 (2016).
51. Pylaeva, E., Lang, S. & Jablonska, J. The essential role of type I interferons in differentiation and activation of tumor-associated neutrophils. *Front. Immunol.* **7**, 629 (2016).
52. Berry, M. P. et al. An interferon-inducible neutrophil-driven blood transcriptional signature in human tuberculosis. *Nature* **466**, 973–977 (2010).
53. Rocha, B. C. et al. Type I interferon transcriptional signature in neutrophils and low-density granulocytes are associated with tissue damage in malaria. *Cell Rep.* **13**, 2829–2841 (2015).
54. Teijaro, J. R. et al. Persistent LCMV infection is controlled by blockade of type I interferon signaling. *Science* **340**, 207–211 (2013).
55. Cunningham, C. R. et al. Type I and type II interferon coordinately regulate suppressive dendritic cell fate and function during viral persistence. *PLoS Pathog.* **12**, e1005356 (2016).
56. Corrales, L. et al. Direct activation of STING in the tumor microenvironment leads to potent and systemic tumor regression and immunity. *Cell Rep.* **11**, 1018–1030 (2015).
57. Muzumdar, M. D., Tasic, B., Miyamichi, K., Li, L. & Luo, L. A global double-fluorescent Cre reporter mouse. *Genesis* **45**, 593–605 (2007).
58. Michaut, M. et al. Integration of genomic, transcriptomic and proteomic data identifies two biologically distinct subtypes of invasive lobular breast cancer. *Sci. Rep.* **6**, 18517 (2016).
59. Schouten, P. C. et al. Robust BRCA1-like classification of copy number profiles of samples repeated across different datasets and platforms. *Mol. Oncol.* **9**, 1274–1286 (2015).
60. Wang, F. et al. RNAscope: a novel in situ RNA analysis platform for formalin-fixed, paraffin-embedded tissues. *J. Mol. Diagn.* **14**, 22–29 (2012).
61. Salvagno, C. & de Visser, K. E. Purification of immune cell populations from freshly isolated murine tumors and organs by consecutive magnetic cell sorting and multi-parameter flow cytometry-based sorting. *Methods Mol. Biol.* **1458**, 125–135 (2016).

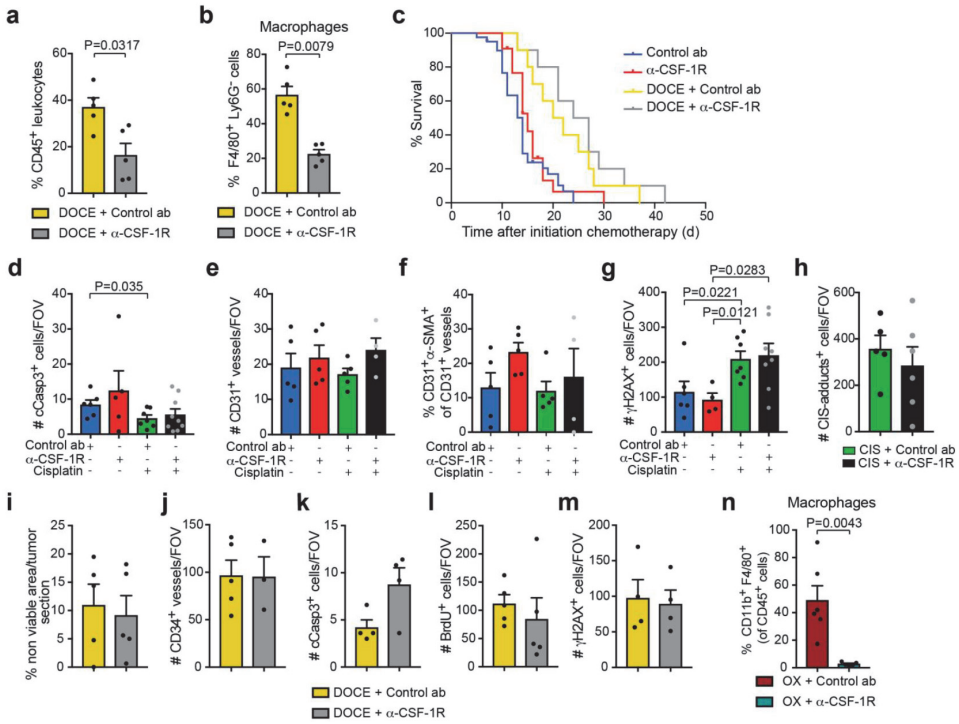
62. Sanjana, N. E., Shalem, O. & Zhang, F. Improved vectors and genome-wide libraries for CRISPR screening. *Nat. Methods* **11**, 783–784 (2014).
63. Kim, D. et al. TopHat2: accurate alignment of transcriptomes in the presence of insertions, deletions and gene fusions. *Genome Biol.* **14**, R36 (2013).
64. Maere, S., Heymans, K. & Kuiper, M. BiNGO: a Cytoscape plugin to assess overrepresentation of gene ontology categories in biological networks. *Bioinformatics* **21**, 3448–3449 (2005).
65. Merico, D., Isserlin, R., Stueker, O., Emili, A. & Bader, G. D. Enrichment map: a network-based method for gene-set enrichment visualization and interpretation. *PLoS One* **5**, e13984 (2010).
66. Oesper, L., Merico, D., Isserlin, R. & Bader, G. D. WordCloud: a Cytoscape plugin to create a visual semantic summary of networks. *Source Code Biol. Med.* **6**, 7 (2011).
67. Spinelli, L., Carpentier, S., Montanana Sanchis, F., Dalod, M. & Vu Manh, T. P. BubbleGUM: automatic extraction of phenotype molecular signatures and comprehensive visualization of multiple gene set enrichment analyses. *BMC Genomics* **16**, 814 (2015).
68. Subramanian, A. et al. Gene set enrichment analysis: a knowledge-based approach for interpreting genome-wide expression profiles. *Proc. Natl Acad. Sci. USA* **102**, 15545–15550 (2005).
69. Pradel, L. P. et al. Macrophage susceptibility to emactuzumab (RG7155) treatment. *Mol. Cancer Ther.* **15**, 3077–3086 (2016).



**Supplementary Fig. 1 | CSF-1R blockade does not influence spontaneous metastasis formation. (a)** Presence of CD68<sup>+</sup> macrophages in untreated human invasive lobular carcinomas and in adjacent normal breast tissue. Influx of CD68<sup>+</sup> macrophages was scored based on immunohistochemistry (normal breast tissue, n=5 patients; invasive lobular carcinomas, n=14 patients). Representative images are shown. Scale bar=25µm. **(b)** Representative IHC staining of F4/80<sup>+</sup> macrophages in a mammary tumor of a KEP mouse and in a normal mammary gland of an age-matched WT mouse. Scale bar=20µm. Percentage of CD11b<sup>+</sup>F4/80<sup>+</sup> macrophages gated on CD45<sup>+</sup> cells in KEP mammary tumors (n=20 animals) and in normal mammary glands of age-matched WT mice (n=4 animals). **(c)** Representative flow cytometry histogram and plot showing CD206 and MHCII expression, respectively, on F4/80<sup>+</sup> macrophages in a KEP mammary tumor. Data are representative of 5 independent KEP mammary tumors. **(d)** Flow cytometry histograms showing CSF-1R expression levels (white) and Fluorescence minus one (FMO) control (grey) in 3 independent KEP mammary tumors. **(e)** Proportion of CD45<sup>+</sup> immune cells of total live cells in tumors of time point-sacrificed KEP mice treated with control ab (n=6 animals) or anti-CSF-1R (n=5 animals) as determined by flow cytometry. **(f)** Organs collected from KEP mice bearing end-stage mammary tumors treated with control ab (n=20 animals) or anti-CSF-1R (n=22 animals) were microscopically analyzed for the presence of metastases. Percentage of tumor-bearing KEP mice with metastases is displayed. p=0.1 by Fisher's exact test (Two-sided). **(g)** Schematic overview of continuous and adjuvant antibody treatment in the KEP-based spontaneous metastasis model as described in Methods. **(h)** Kaplan-Meier metastasis-specific survival curves of recipient mice orthotopically transplanted with tumor fragments from KEP mice and treated either continuously (control ab n=13 animals, anti-CSF-1R

## Therapeutic targeting of macrophages enhances chemotherapy efficacy by unleashing type I interferon response

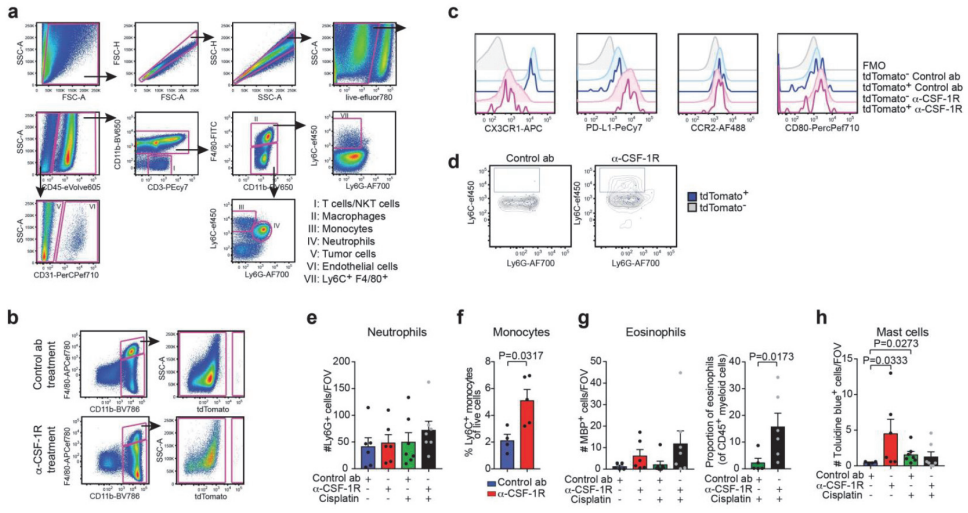
n=14 animals) or in an adjuvant setting (control ab n=13 animals, anti-CSF-1R n=11 animals). An event is defined as an animal that was sacrificed because of clinical signs of metastatic disease. **(i)** Quantification of the number of spontaneous pulmonary metastases in mice treated either continuously (control ab n=9 animals; anti-CSF-1R n=8 animals) or in an adjuvant setting (Control ab n=12 animals; anti-CSF-1R n=9 animals). Data presented in **b**, **e** and **i** are mean  $\pm$  SEM and statistical analysis was performed using two-tailed Mann–Whitney test.



**Supplementary Fig. 2 | CSF-1R blockade synergizes with platinum-based chemotherapy drugs, and not with docetaxel. (a- b)** Proportion of CD45<sup>+</sup> immune cells gated on live cells (a) and F4/80<sup>+</sup>Ly6G<sup>-</sup> macrophages gated on CD11b<sup>+</sup> cells (b) determined by flow cytometry in tumors of time point-sacrificed KEP mice treated as indicated (n=5 animals/group). (c) Kaplan Meier tumor-specific survival curves of KEP mice treated with control ab, anti-CSF-1R (same groups as Fig. 1f), docetaxel/control ab (n=10 animals) or docetaxel/anti-CSF-1R (n=10 animals). Docetaxel/control ab versus Control ab, p=0.0021; Docetaxel/control ab versus docetaxel/anti-CSF-1R, p=0.329 (two-tailed log-rank test). (d) Quantification of cleaved caspase 3<sup>+</sup> cells in viable areas of mammary tumors of time point-sacrificed KEP mice treated with control ab (n=6 animals), anti-CSF-1R (n=5 animals), cisplatin/control ab (n=7 animals) and cisplatin/anti-CSF-1R (n=9 animals) as determined by IHC. (e) Quantification of CD31<sup>+</sup> vessels in viable areas of mammary tumors of time point-sacrificed KEP mice treated with control ab (n=5 animals), anti-CSF-1R (n=5 animals), cisplatin/control ab (n=5 animals) and cisplatin/anti-CSF-1R (n=4 animals) as determined by immunofluorescence. Values represent average number of positive cells per FOV quantified by counting six fields per tumor. (f) Percentage of vessels covered by alpha-SMA<sup>+</sup> pericytes in viable areas of mammary tumors as determined by immunofluorescence. Same mice as e. Percentage was determined by counting alpha-SMA<sup>+</sup>CD31<sup>+</sup> cells and total CD31<sup>+</sup> cells in six high-power microscopic fields per tumor. (g-h) Quantification of  $\gamma$ H2AX<sup>+</sup> cells (g) and cisplatin adducts<sup>+</sup> cells (h) in viable areas of mammary tumors of time point-sacrificed KEP mice treated as indicated ( $\gamma$ H2AX: control ab n=6 animals, anti-CSF-1R n=4 animals, cisplatin/control ab n=7 animals, cisplatin/anti-CSF-1R n=8 animals; CIS-adducts: cisplatin/control ab n=5 animals, cisplatin/anti-CSF-1R n=6 animals). (i) Percentage of

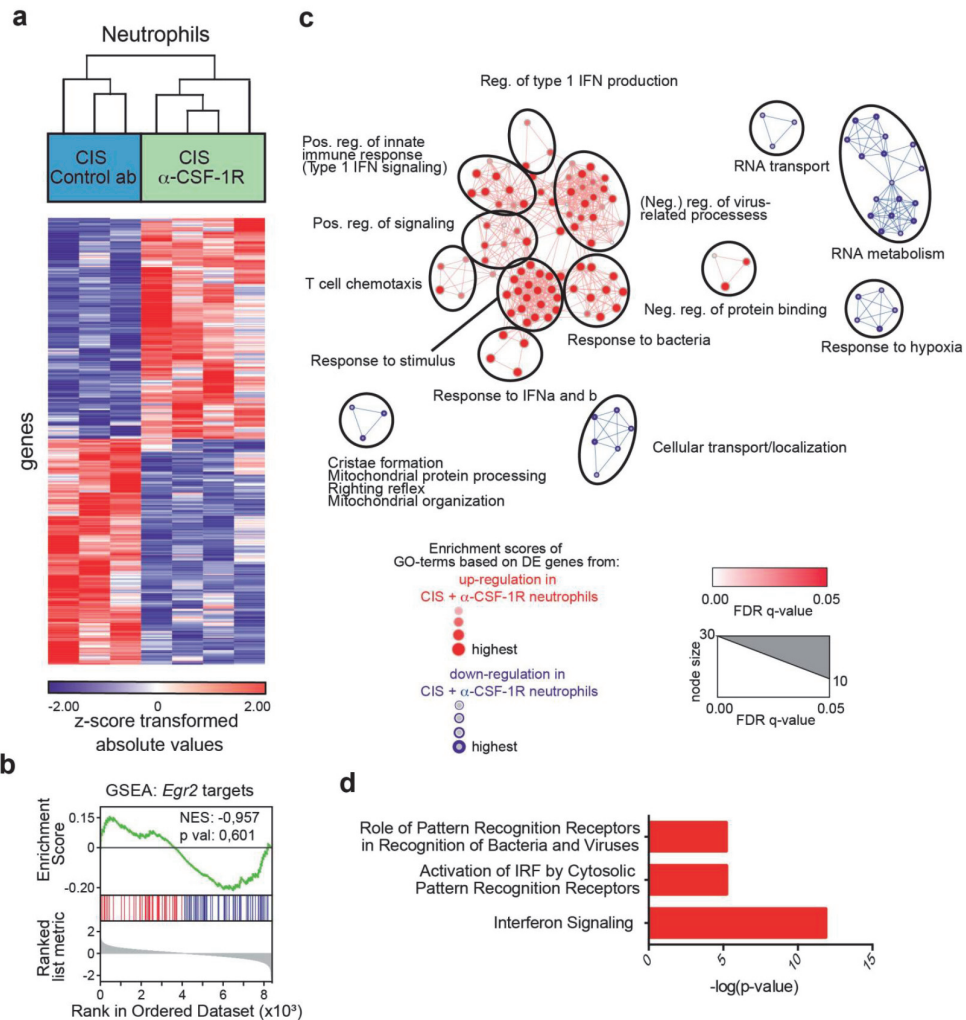
## Therapeutic targeting of macrophages enhances chemotherapy efficacy by unleashing type I interferon response

non-viable area per tumor section of time point-sacrificed KEP mice quantified by digital area analysis of H&E stained sections (n=5 animals/group). **(j-m)** Quantification of CD34<sup>+</sup> cells **(j)**, cleaved caspase 3<sup>+</sup> cells **(k)**, BrdU<sup>+</sup> cells **(l)**,  $\gamma$ H2AX<sup>+</sup> cells **(m)** in viable areas of mammary tumors of time point-sacrificed KEP mice treated as indicated (CD34: docetaxel/control ab n=5 animals, docetaxel/anti-CSF-1R n=3 animals; cCasp3: n=4 animals/group; BrdU: n=5 animals/group;  $\gamma$ H2AX: n=4 animals/group). **(n)** Proportion of CD11b<sup>+</sup>F4/80<sup>+</sup> macrophages gated on CD45<sup>+</sup> cells as determined by flow cytometry in tumors of end-stage KEP mice treated as indicated (oxaliplatin/Control ab treatment n=6 animals; oxaliplatin/anti-CSF-1R treatment n=5 animals). Data presented in **d, g-h, j-m** show average number of positive cells per field of view (FOV) quantified by counting five high-power microscopic fields per tumor. Data presented in **a-b** and **d-n** are mean values  $\pm$  SEM and statistical analysis was performed using two-tailed Mann–Whitney test. DOCE, docetaxel, CIS, cisplatin, OX, oxaliplatin.



**Supplementary Fig. 3 | Impact of CSF-1R inhibition on the intratumoral presence of diverse myeloid immune cell types.** (a) Representative dot plots of a KEP mammary tumor illustrating the gating strategy for the identification of cell populations. Antibody panel used: “tumor panel I” (see supplementary Table 1). Arrows indicate directionality of sub-gates. (b-d) tdTomato<sup>+</sup> (Lineage-SiglecF-cKIT-CD11b<sup>int</sup>Ly6G-Ly6C<sup>+</sup>) monocytes were isolated from the bone marrow of mTmG mice and adoptively transferred into tumor-bearing KEP mice that had previously received either control ab or anti-CSF-1R. 4 days after the monocyte transfer, the presence and phenotype of tdTomato<sup>+</sup> cells in tumors were analyzed. (b) Gating strategy showing intratumoral tdTomato<sup>+</sup> cells that express F4/80 in control ab- or anti-CSF-1R-treated recipient KEP mice. (c) Representative flow cytometry histograms showing CX3CR1, PD-L1, CCR2 and CD80 expression in tdTomato<sup>+</sup> and tdTomato<sup>-</sup> macrophages in KEP tumors. (d) Overlay of representative dot plots showing Ly6C expression in tdTomato<sup>+</sup> and tdTomato<sup>-</sup> macrophages in control ab- and anti-CSF-1R-treated KEP mice. Data presented in b-d are representative of 2 (control ab treatment) and 3 (anti-CSF-1R treatment) independent experiments. (e) Quantification of Ly6G<sup>+</sup> neutrophils in viable areas of mammary tumors of time point-sacrificed KEP mice treated with control ab (n=6 animals), anti-CSF-1R (n=6 animals), cisplatin/control ab (n=7 animals) or cisplatin/anti-CSF-1R (n=7 animals). (f) Proportion of Ly6C<sup>+</sup>Ly6G<sup>-</sup> monocytes determined by flow cytometry in KEP mammary tumors treated with control ab (n=4 animals) or anti-CSF-1R (n=5 animals). (g) Quantification of Major Basic Protein (MBP)<sup>+</sup> cells in viable areas of mammary tumors of time point-sacrificed KEP mice as determined by IHC (control ab n=5 animals, anti-CSF-1R n=6 animals, cisplatin/control ab n=7 animals, cisplatin/anti-CSF-1R n=7 animals) and proportion of Siglec F<sup>+</sup> eosinophils gated on intratumoral CD45<sup>+</sup> cells of time point-sacrificed KEP mice as determined by flow cytometry (cisplatin/control ab n=5 animals, cisplatin/anti-CSF-1R n=6 animals). (h) Quantification of Toluidine Blue<sup>+</sup> mast cells in viable areas of mammary tumors of time point-sacrificed KEP mice (control ab n=4 animals, anti-CSF-1R n=6 animals, cisplatin/control ab n=7 animals, cisplatin/anti-CSF-1R n=7 animals) as determined by histochemistry. Values in e, g and h represent average number of positive cells per field of view (FOV) quantified by counting five high-power microscopic fields per tumor. Data presented in e-h are mean values ± SEM. Statistical analysis was performed using two-tailed Mann–Whitney test.

# Therapeutic targeting of macrophages enhances chemotherapy efficacy by unleashing type I interferon response

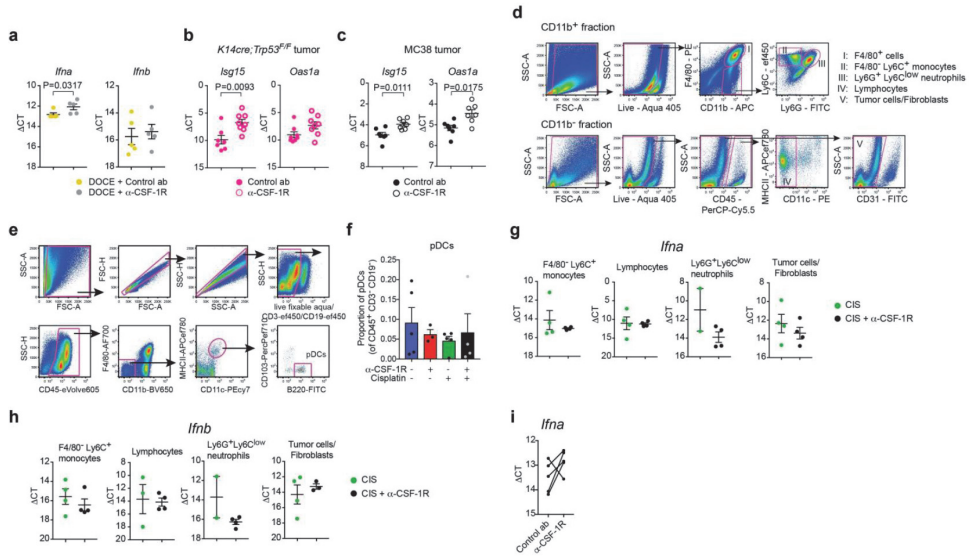


**Supplementary Fig. 4 | Intratumoral neutrophils show elevated expression levels of type I IFN-stimulated genes upon CSF-1R blockade.** (a) Hierarchical clustering of the top 400 variable genes between neutrophils isolated from tumors of KEP mice treated with cisplatin/control ab (n=3 biologically independent samples) and cisplatin/anti-CSF-1R (n=4 biologically independent samples). Mice were sacrificed one day after second cisplatin injection. FC:  $\geq 1.5$ ; unadjusted p-value:  $\leq 0.05$ . Statistical analysis was performed using two-way ANOVA. (b) Gene set enrichment analysis (GSEA) of *Egr2* target genes obtained from RNA-Seq data in tumor-infiltrating neutrophils of anti-CSF-1R-treated KEP mice compared to control ab-treated KEP mice (n=4 animals/group). Enrichment scores were calculated using a weighted Kolmogorov–Smirnov-like statistic. (c) Network visualization of GOEA of the top 100 up-regulated and top 100 down-regulated genes (cisplatin/anti-CSF-1R vs. cisplatin/control ab neutrophils; FC: 1.5, unadjusted p-value:  $\leq 0.05$ ) using BiNGO and EnrichmentMap. Red and blue nodes represent the positively and negatively enriched GO-terms, respectively. Node size represents corresponding enrichment p-values (FDR corrected p-value:  $\leq 0.05$ ). The

## Chapter 4

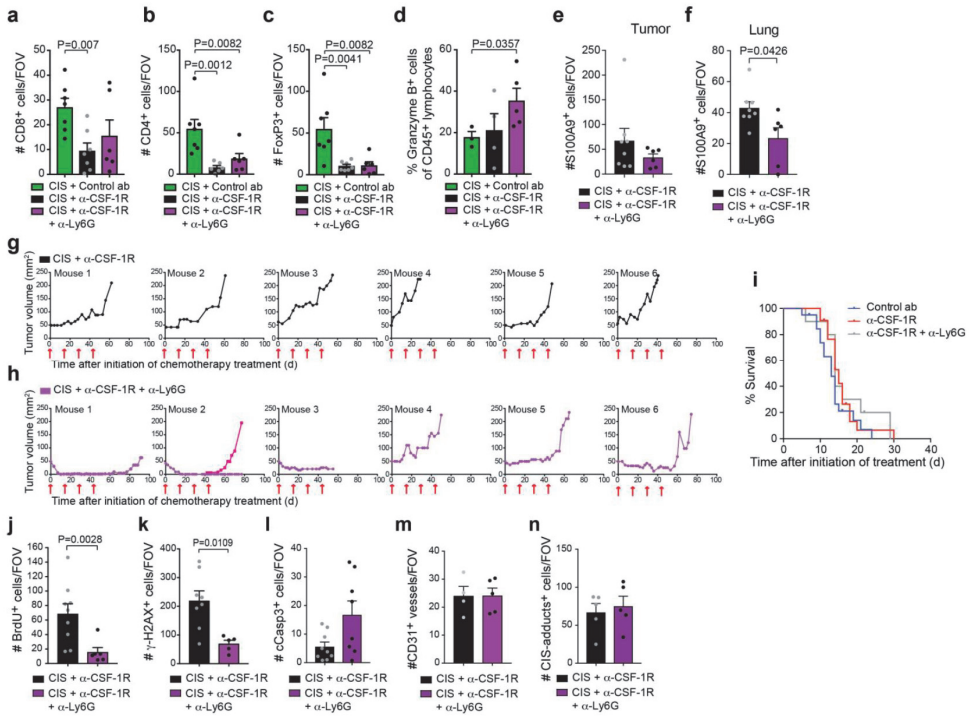
genes used as input for the BiNGO analysis are derived from the 2- way ANOVA model. The enrichment score was calculated with a hypergeometric statistical test, multiple testing correction was performed with the Benjamin & Hochberg FDR correction. **(d)** Top three canonical pathways identified using ingenuity pathway analysis (IPA) enriched in neutrophils isolated from cisplatin/anti-CSF-1R-treated tumors (n=4 biologically independent samples) compared to neutrophils from cisplatin/control ab-treated tumors (n=3 biologically independent samples). Statistical analysis was performed with standard IPA software statistics.

# Therapeutic targeting of macrophages enhances chemotherapy efficacy by unleashing type I interferon response



## Supplementary Fig. 5 | CSF-1R blockade increases intratumoral *Ifna* expression.

(a) Transcripts of *Ifna* and *Ifnb* in KEP mammary tumors were determined by qPCR and normalized to  $\beta$ -actin (n=5 animals/group). Mice were analyzed one day after the second docetaxel injection. Graphs show the mean  $\pm$  SEM in  $\Delta$ Ct values. (b-c) Transcripts of *Isg15* and *Oas1a* in orthotopically transplanted *K14cre; Trp53<sup>fl/fl</sup>* (KP) tumors (*Isg15*: control ab n=7 animals, anti-CSF-1R n=8 animals; *Oas1a*: n=8 animals/group) (b) and subcutaneous MC38 tumors (n=8 animals/group) (c) treated as indicated were determined by qPCR and normalized to  $\beta$ -actin. Mice were analysed at a tumor size of 100mm<sup>2</sup> (KP) or after 12 days from the start of the treatment (MC38). Graphs show the mean  $\pm$  SEM in  $\Delta$ Ct values. (d) Representative dot plots of a KEP tumor illustrating the gating strategy for cell sorting by flow cytometry. After cell separation based on CD11b expression by magnetic columns, the CD11b<sup>+</sup> and CD11b<sup>-</sup> fractions were stained as described in Methods followed by flow cytometry-based sorting of intratumoral cell populations. (e) Representative dot plots of a KEP tumor illustrating the gating strategy for the identification of pDCs. Antibody panel “tumor panel II” was used. Arrows indicate directionality of sub-gates. (f) Proportion of plasmacytoid dendritic cells (pDCs) in mammary tumors of end-stage KEP mice as determined by flow cytometry (control ab n=5 animals, anti-CSF-1R n=3 animals, cisplatin/control ab n=5 animals, cisplatin/anti-CSF-1R n=4 animals). (g-h) Transcripts of *Ifna* and *Ifnb* in CD11b<sup>+</sup>F4/80<sup>+</sup>Ly6G<sup>+</sup>Ly6C<sup>+</sup> monocytes (*Ifna* and *Ifnb*: n=4 animals/group), CD45<sup>+</sup>CD11b<sup>+</sup>CD11c<sup>-</sup> lymphocytes (*Ifna*: n=4 animals/group; *Ifnb*: cisplatin/control ab n=3 animals, cisplatin/anti-CSF-1R n=4 animals), CD11b<sup>+</sup>F4/80<sup>+</sup>Ly6G<sup>+</sup>Ly6C<sup>low</sup> neutrophils (*Ifna* and *Ifnb*: cisplatin/control ab n=2 animals, cisplatin/anti-CSF-1R n=4 animals) and CD45<sup>+</sup>CD11b<sup>+</sup>CD31<sup>-</sup> tumor cells/fibroblasts (*Ifna*: n=4 animals/group; *Ifnb*: cisplatin/control ab n=4 animals, cisplatin/anti-CSF-1R n=3 animals) isolated from end-stage KEP tumors were determined by qPCR and normalized to  $\beta$ -actin. (i) Transcript of *Ifna* in cultured bone marrow-derived macrophages treated for 24h with either control antibody or anti-CSF-1R in the presence of KEP cancer cell line-derived conditioned medium. Data are representative of 4 independent experiments. Data presented in a-c and f-h are mean values  $\pm$  SEM and statistical analysis was performed using two-tailed Mann–Whitney test. CIS, cisplatin; DOCE, docetaxel.



**Supplementary Fig. 6 | Neutrophil inhibition enhances intratumoral granzyme B expression and improves the synergistic anti-cancer effect of cisplatin/anti-CSF-1R in *K14cre; Cdh1<sup>F/F</sup>; Trp53<sup>F/F</sup>* mice.** (a-c) Quantification of CD8<sup>+</sup> T cells (a), CD4<sup>+</sup> T cells (b) and FoxP3<sup>+</sup> regulatory T cells (c) in viable areas of mammary tumors of time point-sacrificed KEP mice (CD8: cisplatin/control ab n=7 animals, cisplatin/anti-CSF-1R n=7 animals, cisplatin/anti-CSF-1R/anti-Ly6G n=7 animals; CD4: cisplatin/control ab n=7 animals, cisplatin/anti-CSF-1R n=6 animals, cisplatin/anti-CSF-1R/anti-Ly6G n=6 animals; FoxP3: cisplatin/control ab n=7 animals, cisplatin/anti-CSF-1R n=7 animals, cisplatin/anti-CSF-1R/anti-Ly6G n=6 animals). (d) Proportion of granzyme B<sup>+</sup> CD45<sup>+</sup> lymphocytes (lymphocyte gate was based on SSC and FSC) determined by flow cytometry in the tumor of time point-sacrificed KEP mice treated as indicated (cisplatin/control ab n=3 animals, cisplatin/anti-CSF-1R n=4 animals, cisplatin/anti-CSF-1R/anti-Ly6G n=5 animals). (e-f) Quantification of S100A9<sup>+</sup> cells in viable areas of mammary tumors (e) and lung (f) of end-stage KEP mice treated with cisplatin/anti-CSF-1R (n=8 animals) or cisplatin/anti-CSF-1R/anti-Ly6G (n=6 animals). (g-h) Representative tumor growth graphs of six individual KEP mice treated with cisplatin/anti-CSF-1R (g) and cisplatin/anti-CSF-1R/anti-Ly6G (h). Data are representative of 16 cisplatin/anti-CSF-1R-treated mice and 10 cisplatin/anti-CSF-1R/anti-Ly6G-treated mice. Red arrows indicate cisplatin injections. In pink, growth curve of a secondary tumor that developed in another mammary gland during the treatment. (i) Kaplan-Meier tumor-specific survival curves of KEP mice treated with control ab, anti-CSF-1R (same groups as Fig. 1f) or anti-CSF-1R/anti-Ly6G (n=10 animals). (j-n) Quantification of BrdU<sup>+</sup> (j) γH2AX<sup>+</sup> cells (k), cleaved caspase 3<sup>+</sup> cells (l), CD31<sup>+</sup> vessels (m) and cisplatin adducts<sup>+</sup> cells (n) in viable areas of mammary tumors of time point-sacrificed KEP mice treated with cisplatin/anti-CSF-1R (same as Fig. 1h and Supplementary Fig. 2) and cisplatin/anti-

## Therapeutic targeting of macrophages enhances chemotherapy efficacy by unleashing type I interferon response

CSF-1R/anti-Ly6G (BrdU n=6 animals;  $\gamma$ H2AX n=5 animals; cCasp3 n=8 animals; CD31 n=5 animals; CIS adducts n=5 animals). Values presented in **a-c**, **e-f**, **j-l** and **n** represent average number of positive cells per field of view (FOV) as determined by IHC quantified by counting five high-power microscopic fields per tumor. Values presented in **m** represent average number of positive cells per FOV as determined by immunofluorescence by counting six field per tumor. Data presented in **a-f** and **j-n** are mean values  $\pm$  SEM. Statistical analysis was performed using two-tailed Mann–Whitney test. CIS, cisplatin.

**Supplementary Table 1: List of antibodies used***Immunohistochemistry*

Antibody	Antigen retrieval	Clone	Vendor	Dilution	Catalog number
BrdU	TRIS/EDTA pH 9.0	Bu20a	DakoCytomation	1:100	M 0744
CD3	TRIS/EDTA pH 9.0	SP7	Thermo Scientific	1:600	RM-9107
CD4	TRIS/EDTA pH 9.0	4SM95	eBioscience	1:1000	14-9766-80
CD8	TRIS/EDTA pH 9.0	4SM15	eBioscience	1:2000	14-0808
FoxP3	Citrate buffer	FJK-16s	eBioscience	1:400	14-5773
F4/80	Proteinase K 20µg/ml	Cl:A3-1	AbD Serotec	1:400	MCA497
Granzyme B	Citrate buffer	-	Novus Biologicals	1:200	NB100-684
Ly6G	Proteinase K 20µg/ml	1A8	BD Biosciences	1:150	551459
Cleaved Caspase 3	TRIS/EDTA pH 9.0	-	Cell Signaling	1:400	#9661
CD34	TRIS/EDTA pH 9.0	MEC 14.7	Abcam	1:500	ab8158
γH2AX (Ser139)	Citrate buffer	-	Cell Signaling	1:50	#2577
S100A9	TRIS/EDTA pH 9.0	HPA004193	Atlas Antibodies	1:1000	HPA 004193
NKp46	PT module buffer 1 (Thermo, TA- 250-PM1X)	-	R&D systems	1:100	AF2225
MBP	Pepsin solution	-	Lee Laboratory, Mayo Clinic	1:500	-
cytokeratin 8	Citrate buffer	Troma 1	Developmental Studies Hybridoma Bank, University of Iowa	1:600	Troma I
Cisplatin adducts	-	-	NKI-A59	1:100	-

*Immunofluorescence*

Antibody	Antigen retrieval	Clone	Vendor	Dilution	Catalog number
actin α-Smooth muscle-Cy3	Citrate Buffer	1A4	Sigma-Aldrich	1:200	C6198
CD31	Citrate Buffer	-	Abcam	1:200	ab28364
Donkey anti- rabbit AF647	-	-	Invitrogen, ThermoFisher Scientific,	1:500	A-31573

## Flow cytometry

### CSF-1R expression panel:

Antibody	Fluorophore	Clone	Vendor	Dilution	Catalog number
CD45	eVolve605	30-F11	eBioscience	1:100	83-0451-42
CD11b	BV650	M1/70	Biolegend	1:400	101239
F4/80	APCef780	BM8	eBioscience	1:200	47-4801-82
Ly6C	ef450	hk1.4	eBioscience	1:400	48-5932-82
Ly6G	AF700	1A8	Biolegend	1:200	127622
CD115 (CSF-1R)	PE	AFS98	eBioscience	1:200	12-1152-82
7AAD			eBioscience	1:20	00-6993-50

### Intratumoral macrophage panel:

Antibody	Fluorophore	Clone	Vendor	Dilution	Catalog number
CD16/CD32	-	2.4G2	BD Biosciences	1:50	553141
CD45	BUV395	30-F11	BD Biosciences	1:200	564279
CD11b	BV650	M1/70	Biolegend	1:400	101239
F4/80	AF700	BM8	Biolegend	1:200	123130
MHCII	APCef780	M5/114.15.2	eBioscience	1:200	47-5321-82
CD206	AF488	MR5D3	AbD serotec	1:100	MCA2235
7AAD			eBioscience	1:20	00-6993-50

### Tumor panel I:

Antibody	Fluorophore	Clone	Vendor	Dilution	Catalog number
CD45	eVolve605	30-F11	eBioscience	1:100	83-0451-42
CD11b	BV650	M1/70	Biolegend	1:400	101239
Ly6C	ef450	hk1.4	eBioscience	1:400	48-5932-82
Ly6G	AF700	1A8	Biolegend	1:200	127622
F4/80	FITC	BM8	eBioscience	1:200	11-4801-82
CD3	PE-cy7	145-2c11	eBioscience	1:200	17-0031-82
CD31	PercPef710	390	eBioscience	1:200	46-0311-82
Fixable Viability Dye eFluor® 780			eBioscience	1:1000	65-0865-14

### Tumor panel II:

Antibody	Fluorophore	Clone	Vendor	Dilution	Catalog number
CD45	eVolve605	30-F11	eBioscience	1:100	83-0451-42
CD11b	BV650	M1/70	Biolegend	1:400	101239
F4/80	AF700	BM8	Biolegend	1:200	123130
CD103	PercPef710	2E7	eBioscience	1:200	46-1031-82
B220	FITC	RA3-6B2	eBioscience	1:200	11-0452-82
MHCII	APCef780	M5/114.15.2	eBioscience	1:200	47-5321-82
CD11c	PE-cy7	HL3	BD Biosciences	1:200	558079
CD3 (dump)	ef450	145-2c11	eBioscience	1:200	48-0031-82
CD19 (dump)	ef450	ebio1D3	eBioscience	1:200	48-0193-82
LIVE/DEAD® Fixable Aqua Dead Cell Stain, for 405 nm excitation			ThermoFisher Scientific	1:100	L34957

*tumor panel III (oxaliplatin-treated mice):*

Antibody	Fluorophore	Clone	Vendor	Dilution	Catalog number
CD16/CD32	-	2.4G2	BD Biosciences	1:50	553141
CD45	APCef780	30-F11	eBioscience	1:200	47-0451-82
CD11b	BV786	M1/70	BD Biosciences	1:400	740861
Ly6C	BV605	hk1.4	Biolegend	1:400	128035
Ly6G	AF700	1A8	Biolegend	1:200	127622
F4/80	Ef450	BM8	eBioscience	1:200	48-4801-82
7AAD				1:20	00-6993-50

*Lymphocyte panel:*

Antibody	Fluorophore	Clone	Vendor	Dilution	Catalog number
CD45	eVolve605	30-F11	eBioscience	1:100	83-0451-42
CD3	PE-cy7	145-2c11	eBioscience	1:200	17-0031-82
CD8	PerCPef710	53-6.7	eBioscience	1:200	46-0081-82
CD4	PE-cy5	H129.19	BD Biosciences	1:200	553654
Granzyme B	PE	GB-11	Pellicluster Sanquin	1:100	M2289
F4/80 (dump)	APCef780	BM8	eBioscience	1:200	47-4801-82
CD11b (dump)	APCef780	M1/70	eBioscience	1:200	47-0112-82
CD19 (dump)	APCef780	ebio1D3	eBioscience	1:200	47-0193-82
Fixable Viability Dye eFluor® 780			eBioscience	1:1000	65-0865-14

*Macrophage characterization panel 1:*

Antibody	Fluorophore	Clone	Vendor	Dilution	Catalog number
CD16/CD32	-	2.4G2	BD Biosciences	1:50	553141
CD45	BUV395	30-F11	BD Biosciences	1:200	564279
CD11b	BV650	M1/70	Biolegend	1:400	101239
F4/80	FITC	BM8	eBioscience	1:200	11-4801-82
Ly6C	PE/Dazzle	hk1.4	Biolegend	1:400	128044
MHCII	APCef780	M5/114.15.2	eBioscience	1:200	47-5321-82
CD11c	PE-cy7	HL3	BD Biosciences	1:200	558079
CD80	PerCPef710	16-10A1	eBioscience	1:200	46-0801-82
CD86	PE	GL1	eBioscience	1:400	12-0862-82
Siglec F	BV605	E50-2440	BD Biosciences	1:200	740388
Ly6G	AF700	1A8	Biolegend	1:200	127622
CD3 (dump)	ef450	145-2c11	eBioscience	1:200	48-0031-82
CD19 (dump)	ef450	ebio1D3	eBioscience	1:200	48-0193-82
CD49b (dump)	ef450	DX5	eBioscience	1:200	48-5971-82
DAPI			Sigma-Aldrich	1:20	D9542

*Macrophage characterization panel 2:*

Antibody	Fluorophore	Clone	Vendor	Dilution	Catalog number
CD16/CD32	-	2.4G2	BD Biosciences	1:50	553141
CD45	BUV395	30-F11	BD Biosciences	1:200	564279
CD11b	BV650	M1/70	Biolegend	1:400	101239
F4/80	AF700	BM8	Biolegend	1:200	123130
Ly6C	PE/Dazzle	hk1.4	Biolegend	1:400	128044
MHCII	APCef780	M5/114.15.2	eBioscience	1:200	47-5321-82

Therapeutic targeting of macrophages enhances chemotherapy efficacy by  
unleashing type I interferon response

Antibody	Fluorophore	Clone	Vendor	Dilution	Catalog number
CD274	PerCPeF710	MIH5	eBioscience	1:200	46-5982-82
Siglec F	BV605	E50-2440	BD Biosciences	1:200	740388
Ly6G (dump)	ef450	1A8	eBioscience	1:400	48-9668-82
CD3 (dump)	ef450	145-2c11	eBioscience	1:200	48-0031-82
CD19 (dump)	ef450	ebio1D3	eBioscience	1:200	48-0193-82
CD49b (dump)	ef450	DX5	eBioscience	1:200	48-5971-82
DAPI			Sigma-Aldrich	1:20	D9542

*Macrophage characterization panel 3:*

Antibody	Fluorophore	Clone	Vendor	Dilution	Catalog number
CD16/CD32	-	2.4G2	BD Biosciences	1:50	553141
CD45	BUV395	30-F11	BD Biosciences	1:200	564279
CD11b	BV650	M1/70	Biolegend	1:400	101239
F4/80	FITC	BM8	eBioscience	1:200	11-4801-82
Ly6C	PE/Dazzle	hk1.4	Biolegend	1:400	128044
MHCII	APCef780	M5/114.15.2	eBioscience	1:200	47-5321-82
CCR2	PE	475301	R&D systems	1:100	FAB5538P-025
CX3CR1	APC	SA011F11	Biolegend	1:400	149008
Siglec F	BV605	E50-2440	BD Biosciences	1:200	740388
Ly6G (dump)	ef450	1A8	eBioscience	1:400	48-9668-82
CD3 (dump)	ef450	145-2c11	eBioscience	1:200	48-0031-82
CD19 (dump)	ef450	ebio1D3	eBioscience	1:200	48-0193-82
CD49b (dump)	ef450	DX5	eBioscience	1:200	48-5971-82
DAPI			Sigma-Aldrich	1:20	D9542

*Macrophage characterization in K14cre; Trp53F/F tumor panel 1:*

Antibody	Fluorophore	Clone	Vendor	Dilution	Catalog number
CD16/CD32	-	2.4G2	BD Biosciences	1:50	553141
CD45	BUV395	30-F11	BD Biosciences	1:200	564279
CD11b	BV786	M1/70	BD Biosciences	1:400	740861
F4/80	APCef780	BM8	eBioscience	1:200	47-4801-82
Ly6C	ef450	hk1.4	eBioscience	1:400	48-5932-82
Ly6G	FITC	1A8	BD Biosciences	1:200	551460
Siglec F	BV605	E50-2440	BD Biosciences	1:200	740388
CD86	PE	GL1	eBioscience	1:400	12-0862-82
CX3CR1	APC	SA011F11	Biolegend	1:400	149008
CD80	PercPef710	16-10A1	eBioscience	1:200	46-0801-82
CD274	PEcy7	MIH5	eBioscience	1:200	25-5982-82
7AAD				1:20	00-6993-50

*Macrophage characterization in K14cre; Trp53F/F tumor panel 2:*

Antibody	Fluorophore	Clone	Vendor	Dilution	Catalog number
CD16/CD32	-	2.4G2	BD Biosciences	1:50	553141
CD45	BUV395	30-F11	BD Biosciences	1:200	564279
CD11b	BV786	M1/70	BD Biosciences	1:400	740861
F4/80	APCef780	BM8	eBioscience	1:200	47-4801-82
Ly6C	ef450	hk1.4	eBioscience	1:400	48-5932-82
Ly6G	AF700	1A8	Biolegend	1:200	127622

Antibody	Fluorophore	Clone	Vendor	Dilution	Catalog number
Siglec F	BV605	E50-2440	BD Biosciences	1:200	740388
CCR2	PE	475301	R&D systems	1:200	FAB5538P-025
7AAD				1:20	00-6993-50

*tdTomato+ monocyte panel:*

Antibody	Fluorophore	Clone	Vendor	Dilution	Catalog number
CD16/CD32	-	2.4G2	BD Biosciences	1:50	553141
CD45	BUV395	30-F11	BD Biosciences	1:200	564279
CD11b	BV786	M1/70	BD Biosciences	1:400	740861
F4/80	APCef780	BM8	eBioscience	1:200	47-4801-82
Ly6C	ef450	hk1.4	eBioscience	1:400	48-5932-82
Ly6G	AF700	1A8	Biolegend	1:200	127622
Siglec F	BV605	E50-2440	BD Biosciences	1:200	740388
CCR2	AF488	475301	R&D systems	1:200	FAB55381RG-100UG
CX3CR1	APC	SA011F11	Biolegend	1:400	149008
CD80	PercPef710	16-10A1	eBioscience	1:200	46-0801-82
CD274	PEcy7	MIH5	eBioscience	1:200	25-5982-82
7AAD				1:20	00-6993-50

*Isolation of mTmG monocytes from bone marrow:*

Antibody	Fluorophore	Clone	Vendor	Dilution	Catalog number
CD11b	BV786	M1/70	BD Biosciences	1:400	740861
Ly6C	Ef450	hk1.4	eBioscience	1:400	48-5932-82
Siglec F	BV605	E50-2440	BD Biosciences	1:200	740388
cKIT	BV605	2B8	BD Biosciences	1:200	563146
Sca1	BV605	D7	Biolegend	1:200	108133
CD3	FITC	145-2C11	eBioscience	1:200	11-0031-63
CD8	FITC	53-6.7	eBioscience	1:400	11-0081-82
CD4	FITC	GK1.5	eBioscience	1:400	11-0041-82
NKp46	FITC	29A1.4	eBioscience	1:200	11-3351-82
Ter119	FITC	TER-119	Biolegend	1:200	116205
F4/80	APCef780	BM8	eBioscience	1:200	47-4801-82
7AAD			eBioscience	1:20	00-6993-50

*Isolation of cells populations from intratumoral CD11b+ fraction:*

Antibody	Fluorophore	Clone	Vendor	Dilution	Catalog number
Ly6G	FITC	1A8	BD Biosciences	1:200	551460
F4/80	PE	BM8	eBioscience	1:200	12-4801-82
Ly6C	Ef450	hk1.4	eBioscience	1:400	48-5932-82

*Isolation of cells populations from intratumoral CD11b- fraction:*

Antibody	Fluorophore	Clone	Vendor	Dilution	Catalog number
CD45	PercPcy5.5	30-F-11	eBioscience	1:200	45-0451-82
B220	PE-Cy7	RA3-6B2	eBioscience	1:200	25-0452-82
CD31	FITC	390	eBioscience	1:200	11-0311-82
CD11c	PE	N418	eBioscience	1:200	12-0114-82
MHCII	APCef780	M5/114.15.2	eBioscience	1:200	47-5321-82
CD19	Ef450	eBio1D3	eBioscience	1:200	48-0193-82

Therapeutic targeting of macrophages enhances chemotherapy efficacy by unleashing type I interferon response

Antibody	Fluorophore	Clone	Vendor	Dilution	Catalog number
LIVE/DEAD® Fixable Aqua Dead Cell Stain, for 405 nm excitation			ThermoFisher Scientific	1:100	L34957

**Supplementary Table 2: List of primer sequences used for RT-PCR.**

Gene	Primer Forward (5'-3')	Primer Reverse (5'-3')
IFN $\alpha$ (all genes)	TCTGATGCAGCAGGTGGG	AGGGCTCTCCAGACTTCTGCTCTG
IFN $\beta$	GCACTGGGTGGAATGAGACT	AGTGGAGAGCAGTTGAGGACA
TLR3	GTGAGATAACAACGTAGCTGACTG	TCCTGCATCCAAGATAGCAAGT
RIG-1	CCACCTACATCCTCAGCTACATGA	TGGGCCCTTGTGTCTCTCT
IFIH1	GTGATGACGAGGCCAGCAGTTG	ATTCATCCGTTTCGTCCAGTTTCA
ISG15	GGTGTCCGTGACTAACTCCAT	TGGAAAGGGTAAGACCGTCTCT
OAS1A	GCCTGATCCCAGAATCTATGC	GAGCAACTCTAGGGCGTACTG
$\beta$ -actin	CCTCATGAAGATCCTGACCGA	TTTGATGTCACGCACGATTC

4

**Supplementary Table 3: List of type I IFN-related pathways and genes**

*List of type I IFN-related pathways and corresponding genes selected from BiNGO and Ingenuity Pathway Analysis (IPA) that are differentially expressed in neutrophils from cisplatin/anti-CSF-1R-treated tumors (n=4 biological independent samples) compared to neutrophils from cisplatin/control ab-treated tumors (n=3 biological independent samples). Statistical analysis was performed using two-way ANOVA*

Biological processes by BiNGO Analysis	Genes	Fold change	p-value
POSITIVE REGULATION OF RESPONSE TO CYTOKINE STIMULUS	ZBP1	3.91	0.0027
	IRF7	3.17	0.0014
	NLRC5	2.84	0.0065
REGULATION OF RESPONSE TO CYTOKINE STIMULUS	ZBP1	3.91	0.0027
	IRF7	3.17	0.0014
	NLRC5	2.84	0.0065
REGULATION OF CYTOKINE-MEDIATED SIGNALING PATHWAY	ZBP1	3.91	0.0027
	IRF7	3.17	0.0014
	NLRC5	2.84	0.0065

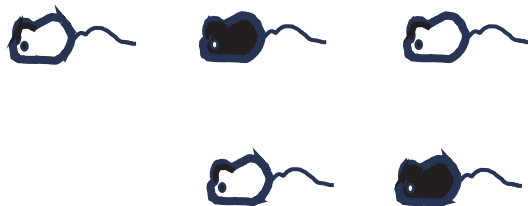
Biological processes by BiNGO Analysis	Genes	Fold change	p-value
REGULATION OF INNATE IMMUNE RESPONSE	ZBP1	3.91	0.0027
	IRF7	3.17	0.0014
	NLRC5	2.84	0.0065
	TAP1	2.8	0.0052
	DHX58	3.32	0.0006
REGULATION OF TYPE I INTERFERON-MEDIATED SIGNALING PATHWAY	ZBP1	3.91	0.0027
	IRF7	3.17	0.0014
	NLRC5	2.84	0.0065
POSITIVE REGULATION OF TYPE I INTERFERON-MEDIATED SIGNALING PATHWAY	ZBP1	3.91	0.0027
	IRF7	3.17	0.0014
	NLRC5	2.84	0.0065
POSITIVE REGULATION OF CYTOKINE-MEDIATED SIGNALING PATHWAY	ZBP1	3.91	0.0027
	IRF7	3.17	0.0014
	NLRC5	2.84	0.0065
NEGATIVE REGULATION OF TYPE I INTERFERON PRODUCTION	GBP4	11	0.002
	DHX58	3.32	0.0006
REGULATION OF TYPE I INTERFERON PRODUCTION	IRF7	3.17	0.0014
	GBP4	11	0.002
	DHX58	3.32	0.0006
REGULATION OF INTERFERON-ALPHA PRODUCTION	IRF7	3.17	0.0014
	GBP4	11	0.002
CELLULAR RESPONSE TO INTERFERON-BETA	IFI205	4.68	0.0073
	GBP2B	3.79	8.40E-05
	TREX1	2.86	6.10E-05
	GBP2	2.78	0.0043
	IFI202B	2.94	0.011
	IFIT1	2.89	0.0002
	IFIT3	3.58	0.0001
RESPONSE TO INTERFERON-BETA	IFI205	4.68	0.0073
	GBP2B	3.79	8.40E-05
	TREX1	2.86	6.10E-05
	GBP2	2.78	0.0043
	XAF1	3.89	0.0029
	IFI202B	2.94	0.011
	IFIT1	2.89	0.0002
	IFIT3	3.58	0.0001
RESPONSE TO INTERFERON-ALPHA	IFIT1	2.89	0.0002
	IFIT3	3.58	0.0001
	IFIT2	3.42	0.0003
CELLULAR RESPONSE TO INTERFERON-ALPHA	IFIT1	2.89	0.0002
	IFIT3	3.58	0.0001
	IFIT2	3.42	0.0003

Therapeutic targeting of macrophages enhances chemotherapy efficacy by unleashing type I interferon response

Biological processes by BiNGO Analysis	Genes	Fold change	p-value
<b>DEFENSE RESPONSE TO VIRUS</b>	ZBP1	3.91	0.0027
	GBP2B	3.79	8.40E-05
	RSAD2	3.14	0.0063
	MX2	3.02	0.001
	IFIT1	2.89	0.0002
	IFIT3	3.58	0.0001
	IFIT2	3.42	0.0003
	CXCL10	2.75	0.0005
	DHX58	3.32	0.0006

Biological processes by IPA	Genes	Fold change	p-value
<b>INTERFERON SIGNALING</b>	IFI35	2.02	0.0066
	IFIT1	2.89	0.0002
	IFIT3	3.58	0.0001
	IFITM3	2.42	0.002
	IRF1	2.25	0.0006
	IRF9	2.12	0.0015
	MX2	3.02	0.001
	OAS1a	2.37	0.0023
	OAS1g	4.21	0.0008
	PSMB8	1.97	0.0465
	SOCS1	2.59	0.0176
	STAT1	2.24	0.0029
	STAT2	2.46	0.0002
	TAP1	2.8	0.0052
<b>ACTIVATION OF IRF BY CYTOSOLIC PATTERN RECOGNITION RECEPTORS</b>	ADAR	1.67	0.0463
	DHX58	3.32	0.0006
	IFIH1	2.38	0.0009
	IFIT2	3.42	0.0003
	IRF7	3.17	0.0014
	IRF9	2.12	0.0015
	ISG15	2.46	0.0022
	STAT1	2.24	0.0029
	STAT2	2.46	0.0002
ZBP1	3.91	0.0027	

## Chapter 5



# General discussion

Breast cancer is a very heterogeneous disease; distinct subtypes of breast cancer are dependent on different oncogenic pathways and are likely to be differentially regulated by the immune system. Chemotherapy denotes one of the main treatments that breast cancer patients receive, but response rates vary amongst patients. A better understanding of the adaptive and innate immune system in breast cancer initiation, progression, metastasis formation and chemotherapy response is essential for the development of new therapeutic approaches to improve survival rates. For instance, immunomodulatory agents targeting myeloid cells are currently being assessed in clinical trials. To maximize the success of these compounds, it is essential to understand the effects and mechanisms of these drugs. The overall goal of the research described in this thesis is to better understand the interaction between the immune system and breast cancer. I have studied the roles of the adaptive immune system during breast cancer tumorigenesis and chemotherapy response. In addition, I have studied the consequences and underlying mechanisms of targeting macrophages via CSF-1R blockade during breast cancer development and chemotherapy treatment. We focused on the following main research questions by using genetically engineered mouse models (GEMMs) for metastatic breast cancer:

1. Does the adaptive immune system play a role during HER2-positive breast cancer formation, progression and metastasis?
2. Is the adaptive immune system important for chemotherapy response of breast cancer?
3. What is the impact, optimal combination partner and mechanism of anti-CSF-1R antibody targeting during breast cancer development and chemotherapy treatment?

## **Impact of the adaptive immune system on HER2-positive breast cancer**

A body of accumulating clinical data indicates that different molecular subtypes of tumors are characterized by distinct immune landscapes<sup>1-3</sup>. Depending on the tumor type, stage and treatment, different types of adaptive immune cells can play opposite functions, ranging from tumor-promoting, tumor preventing to no role<sup>4-8</sup>. In breast cancer, preclinical studies with a variety of mouse models have demonstrated that certain

tumor-associated adaptive immune cell subsets are important for metastasis formation<sup>8-11</sup>. For example, metastasis formation in the transgenic MMTV-PyMT mouse model for spontaneous breast adenocarcinomas was shown to be dependent on interleukin 4 (IL-4)-expressing CD4<sup>+</sup> T cells that stimulated EGF production from tumor-associated macrophages (TAMs)<sup>9</sup>. In **Chapter 2** the causal link between the adaptive immune system in HER2-positive breast cancer formation and metastatic spread was investigated. Using a mouse model for spontaneous HER2-driven mammary tumorigenesis *i.e.*, *MMTV-NeuT* mice, our findings reveal that genetic elimination of the complete adaptive immune system did not affect premalignant progression, tumor latency, tumor growth, tumor multiplicity, and *de novo* pulmonary metastasis formation. These findings indicate that HER2+ breast tumors and metastasis formation in this preclinical model are not suppressed by immunosurveillance mechanisms, nor promoted by the adaptive immune system.

The data in **Chapter 2** reveal that absence of the complete adaptive immune system does not impact mammary tumorigenesis in *MMTV-NeuT* mice. An important question that our work leaves open is whether individual (sub)populations of adaptive immune cells play a role during cancer formation and metastasis in *MMTV-NeuT* mice. By using *Rag*<sup>-/-</sup> deficient mice, in which T and B cells are depleted from birth on, we cannot exclude the existence of opposing roles of individual components of the adaptive immune system in our model *e.g.*, Tregs, CD8<sup>+</sup> T or  $\gamma\delta$  T cells. For instance, HER2-positive breast tumors are frequently infiltrated by Tregs<sup>12,13</sup>. Increased numbers of FOXP3<sup>+</sup> Tregs in tumors generally correlate with worse patient outcomes<sup>14,15</sup> and Treg accumulation within sentinel lymph nodes is a predictor of disease progression and metastatic spread in breast cancer<sup>16</sup>. Furthermore, a distinct group of T cell receptor-expressing innate lymphoid cells, termed ILTC1, were found to have a critical role in cancer immunosurveillance in MMTV-PyMT mice<sup>17</sup>. The generation of these lymphocytes is dependent on the cytokine IL-15<sup>17</sup>. Interestingly, IL-15 deficiency in *MMTV-NeuT* mice has resulted in accelerated tumor growth compared to wild-type (WT) *MMTV-NeuT* mice<sup>18</sup>. Since all T cells require RAG to develop, the *MMTV-NeuT* mice used in **Chapter 2** also lacked the ILTC1 cell population. Future experiments targeting one specific subset of T cells such as Tregs or ILTC1 cells before and during tumor development will help answer whether distinct adaptive immune cells are important in HER2-positive breast cancer.

It is surprising that we did not find a clear role for the adaptive immune system while based on the immunosurveillance hypothesis<sup>19</sup>, we would have expected impact. In fact, preclinical and clinical data in HER2-positive breast cancer have suggested that the endogenous adaptive immune cell repertoire is not completely lacking tumor-specific immune cells and could potentially be involved in immunosurveillance mechanisms. For example, two studies found CD4<sup>+</sup> T cell responses directed against HER2 (neu or ErbB2) in the MMTV-*NeuT* mouse model during the pre-malignant phase<sup>20,21</sup> and HER2-specific CD4<sup>+</sup> and CD8<sup>+</sup> T cell responses have been described in patients with HER2<sup>+</sup> breast cancer<sup>22,23</sup>. In addition, antibody-mediated depletion of T cells in MMTV-*NeuT* mice resulted in a momentary and minimal increase in tumor multiplicity<sup>24</sup>. Although T cells and Neu-specific T cells are present in MMTV-*NeuT* mice and HER2<sup>+</sup> breast cancer patients, it is very likely that immunosuppression is at play. With the advancing stages of HER2-positive cancer, the infiltrating cell composition is prone to changes like what has been seen in many cancers; the effector cells become fewer and less activated, while the TME becomes dominated by cells with regulatory and immunosuppressive activities<sup>25,26</sup>. The immune-editing process in its most complete manifestation is composed of three sequential phases of tumor “elimination,” “equilibrium,” and “escape” and is illustrated by studies showing that carcinogen-induced sarcomas and spontaneous epithelial carcinomas were more immunogenic when induced in mice lacking lymphocytes as compared to immunocompetent mice<sup>19</sup>. Indeed, ex vivo expanded HER-2/neu-specific T cells failed to reject transplanted Her2<sup>+</sup> tumor cells<sup>27</sup>, but neu-specific antibody responses were restored in these transplanted Her2<sup>+</sup> tumors with the depletion of MDSC's<sup>27</sup>. Besides MDSCs, regulatory T cells and regulatory dendritic cells have been found to suppress anti-tumor T cell immune responses in MMTV-*NeuT* mice<sup>27-29</sup>. Thus likely, tumor antigen-specific CD8<sup>+</sup> T cell responses are induced but their activities are restrained from inducing effective cancer immunosurveillance by their immunosuppressive environment.

The treatment with HER2-targeting therapeutic antibodies has significantly improved the survival of patients with HER2-positive breast cancer<sup>30</sup>. Similar results have been found in MMTV-*NeuT* mice<sup>31-33</sup>. Importantly, preclinical studies in transplantation models for Her2-positive breast cancer showed that PD-1 and CTLA-4 inhibition improves HER2-targeted therapies through activation of CD8<sup>+</sup> T cells<sup>32,34</sup>. These data have provided a basis for

the clinical use of immune checkpoint inhibitors for the treatment of HER2<sup>+</sup> breast cancer patients and their combination with HER2-targeted treatments<sup>30</sup>.

In conclusion, we found that absence of the complete adaptive immune does not impact mammary tumorigenesis in MMTV-*NeuT* mice. Further research is needed to determine what the exact immunosuppressive networks are to engage anti-tumor immunity. Moreover, increasing immunity towards HER2<sup>+</sup> tumors with immunotherapy may overcome the unresponsiveness of the adaptive immune system and result in effective tumor inhibition.

In contrast to our findings in **Chapter 2**, Tan and colleagues found that metastatic spread of orthotopically transplanted mammary tumors derived from the MMTV-*NeuT* transgenic mouse model was reduced in *Rag1*<sup>-/-</sup> and *CD4*<sup>-/-</sup> recipient mice as compared to WT recipients<sup>10</sup>. How can a promoting effect versus no effect of the adaptive immune system on metastasis formation be obtained from two independent studies that focus on the same subtype of breast cancer *i.e.*, Her2<sup>+</sup> -positive mammary tumors? There are three fundamental differences between these two studies:

1. Tan *et al.* used transgenic mice expressing the WT Her2 receptor, whereas in **Chapter 2** transgenic mice expressing an activated form of Her2 are used.
2. Tan *et al.* used mice on the FVB/N background, whereas in **Chapter 2** studies are performed on the Balb/c background.
3. Tan *et al.* performed their studies in mice that were orthotopically transplanted with freshly isolated tumor cells or cell lines from MMTV-*NeuT* transgenic mice, whereas in **Chapter 2** spontaneous mammary tumorigenesis was studied in transgenic MMTV-*NeuT* mice.

Due to somatic mutations within the *Her2* transgene, mammary tumors from MMTV-*NeuT* transgenic mice expressing WT *Her2* display activation of intrinsic Her2 receptor tyrosine kinase activity<sup>35,36</sup>. Therefore, both MMTV-*NeuT* mammary tumor models express activated Her2, and it is thus unlikely that the different results can be attributed to the activation status of the *Her2* transgene.

It is possible that the genetic variation between mouse inbred strains can provide the basis for fundamentally different mechanisms underlying metastasis formation. In the PyMT mouse model for breast carcinoma, PyMT *Rag1*<sup>-/-</sup> mice had significantly reduced tumor latency compared with PyMT WT mice in the C57BL/6 background, a result that was not seen when using PyMT mice on the FVB/NJ background<sup>37</sup>. Certainly, evaluation of metastasis formation in MMTV-*NeuT* transgenic mice on the FVB/N background intercrossed with *Rag1*<sup>-/-</sup> mice can help to resolve the impact of the genetic background versus the impact of *de novo* tumorigenesis on the influence of the adaptive immune system on metastatic HER2<sup>+</sup> breast cancer. However, it is also conceivable that the different outcome between both studies can be explained by the use of transplanted HER2-positive mammary tumors in the Tan *et al.* study, versus spontaneous HER2-positive mammary tumors in **Chapter 2**. Transplantation models, based on engraftment of cultured cells or freshly isolated single-cell suspension models, as used in the Tan *et al.* study, derived from end-stage tumors have shown to not fully recapitulate *de novo* tumor formation with co-evolving tumor-host interactions and an immunosuppressive microenvironment<sup>38</sup>. Other disadvantages are derangement of the normal tumor architecture, compared to spontaneous tumors, and cancer cell lines are generally poor predictors of clinical response<sup>39</sup>. In addition, mammary epithelial cells in the MMTV-*NeuT* mouse model disseminate already during the premalignant phase and this early dissemination is not recapitulated in tumor transplantation models as the premalignant phase is bypassed<sup>38,40,41</sup>. Other evidence of discordant results between the MMTV-*NeuT* allograft model versus the MMTV-*NeuT* spontaneous tumor model comes from Gonzalez-Suarez and colleagues who by using spontaneous MMTV-*NeuT* mice on the FVB/N background showed that RANKL is expressed in mammary epithelial cells before tumor onset, but not in epithelial or stromal cells of *de novo* adenocarcinomas<sup>42</sup>. RANKL inhibition in MMTV-*NeuT* mice resulted in decreased spontaneous mammary tumorigenesis<sup>42</sup>. Consistently, RANKL expression by breast cancer cells was also seen in a recent study on human estrogen receptor-positive/HER2- breast cancer cells and patients<sup>43</sup>. In contrast, in the Tan *et al.* study, RANKL expression was predominantly detected in Tregs infiltrating transplanted Her2<sup>+</sup> tumors and RANKL inhibition only affected primary tumor outgrowth marginally<sup>10</sup>.

In conclusion, given these discordant findings with transplanted Her2<sup>+</sup> tumors versus HER2<sup>+</sup> patient data and two *de novo* models of Her2<sup>+</sup> tumors

on different backgrounds it is most likely that the observed promoting effect in the Tan *et al.* study versus no effect of the adaptive immune system on metastasis formation in our study (**Chapter 2**) is caused by using transplanted Her2<sup>+</sup> mammary tumors versus spontaneous Her2<sup>+</sup> mammary tumors.

While the findings in **Chapter 2** represent a negative finding, it is a surprising result considering that other breast cancer subtypes are dependent on the adaptive immune system for metastasis formation <sup>9-11</sup>. One possible explanation is that the genetic driver of mammary tumorigenesis in MMTV-*NeuT* mice, the activation of the HER2 oncogene, influences the composition and the activation status of the immune landscape differently compared to other driver mutations that are active in the other breast cancer subtypes. In fact, the idea that genetic events, activation of oncogenes, or loss of tumor suppressor genes (TSGs) in cancer cells, shape the immune landscape is emerging <sup>1,44</sup>. This concept was further investigated in a recent study from our group where 16 mouse models for breast cancer with different tissue-specific mutations were used, revealing that loss of p53 shapes the local immune composition of primary breast tumors to drive pro-metastatic systemic inflammation <sup>8</sup>. Thus, genetic aberrations in tumors influence the immune composition, activation states and therefore different immune responses, including therapy response <sup>45,46</sup>. MMTV-*NeuT* tumors are characterized by the overexpression of an activated form of the epidermal growth factor receptor (EGFR) family member HER2 <sup>47</sup>, which does not require ligand binding for receptor activation. Instead, in the MMTV-PyMT mice it was shown that CD4<sup>+</sup> T cells instructed TAMs to produce EGF to stimulate EGFR-dependent metastasis formation <sup>9</sup>. Furthermore, our group demonstrated that mammary tumors from the genetically engineered *K14cre; Cdh1<sup>F/F</sup>; Trp53<sup>F/F</sup>* (KEP) mouse model for invasive lobular carcinoma (ILC), driven by loss of p53, activate systemic pro-metastatic inflammation in a Wnt-dependent manner <sup>8</sup>. Thus, in other breast cancer subtypes where there is no cell-autonomous EGFR family member activation, tumors may rely on immune cells to drive metastasis.

In conclusion, the metastatic capacity of NeuT-overexpressing tumors might be a cancer cell-autonomous trait. Our findings indicate that it is essential to investigate the impact of the adaptive immune system in other breast cancer subtypes as they can have a different role. Furthermore, to optimally harness an effective anti-tumor immune response and improve therapy outcomes in

HER2-positive patients we need to obtain a deeper understanding of the immunosuppressive pathways.

## Impact of the adaptive immune system on chemotherapy response

Chemotherapy is frequently used to treat cancer patients. Although most tumors initially respond to chemotherapeutic drugs, tumors develop mechanisms of resistance to the treatment. Cancer cell-intrinsic factors like resistance to apoptosis or overexpression of drug transporter proteins have been identified as causes of therapy resistance <sup>48</sup>. However, also cancer cell-extrinsic processes underlying poor chemotherapy response have been recognized <sup>48-51</sup>. Experimental studies in highly immunogenic tumor models, e.g., cancer cell line inoculation models and chemically-induced sarcomas such as the 3-methylcholanthrene (MCA) fibrosarcoma model, have indicated that T cells can contribute to the anti-cancer efficacy of certain chemotherapeutics <sup>52-56</sup>. Cytotoxic drugs, such as doxorubicin, oxaliplatin, cyclophosphamide, epothilone B, mitoxantrone, and melphalan have been reported to lose their therapeutic efficacy on tumor cell line outgrowths in mice with a defective adaptive immune cell function, including *Rag*<sup>-/-</sup> mice <sup>52-54,57</sup>. The success of these chemotherapy treatments is dependent on the stimulation of immunogenic tumor cell death (ICD), as initially proposed by Dr. Zitvogel and Dr. Kroemer <sup>58</sup>, which is a type of regulated cell death that stimulates CD8<sup>+</sup> T-dependent tumor killing responses via damage-associated molecular patterns (DAMPs) emission such as calreticulin, nuclear protein high mobility group box 1 (HMGB1) and adenosine triphosphate (ATP) <sup>52-54,59</sup>.

Considering that engraftment of cultured cells derived from end-stage tumors do not fully recapitulate *de novo* tumor formation with co-evolving tumor-host interactions and an immunosuppressive microenvironment <sup>38</sup>, and that the *de novo* MCA-induced tumours are highly immunogenic, we hypothesized that in established spontaneous tumors that are relatively poorly immunogenic, like breast cancer, chemotherapy might not be powerful enough to activate adaptive immunity. In **Chapter 3** we have tested this hypothesis and describe that the adaptive immune system does not contribute to the therapeutic efficacy of three different chemotherapy drugs in two independent clinically relevant *de novo* mammary tumor models *i.e.*, MMTV-*NeuT* mice for HER2-positive breast cancer and *K14cre; Cdh1<sup>F/F</sup>*;

*Trp53<sup>F/F</sup>* (KEP) mice for invasive lobular carcinoma (ILC). Cisplatin, oxaliplatin or doxorubicin were equally effective in inhibiting the growth of *de novo* mammary tumors in T cell– and B cell–deficient MMTV-*NeuT*;*Rag2*<sup>-/-</sup> mice as in MMTV-*NeuT*;*Rag2*<sup>+/-</sup> mice. Similarly, the therapeutic benefit of cisplatin and oxaliplatin was the same in *KEP*;*Rag1*<sup>+/-</sup> and *KEP*;*Rag1*<sup>-/-</sup> mice. In addition, we performed CD8<sup>+</sup> T cell depletion alone or in combination with oxaliplatin in tumor-bearing *KEP*;*Rag1*<sup>+/-</sup> mice and did not see a change in the therapeutic efficacy of oxaliplatin. Thus, the adaptive immune system does not dictate the therapeutic efficacy of chemotherapy in these two *de novo* mouse models. Our data in **Chapter 3** stand in contrast with previous experimental studies in highly immunogenic tumor models where the adaptive immune system dictates the therapeutic efficacy of certain chemotherapeutics<sup>52-54,59</sup>. Several differences between these studies and our study may explain the difference in findings. For example, different cancer (sub)types, different backgrounds, different chemotherapy regimens and the use of different mouse models *i.e.*, cancer cell line inoculation models versus *de novo* mouse models. Several important distinctions between these two types of mouse tumor models have been described. For example, spontaneous tumors were found to have different chemotherapy response profiles compared to inoculated tumor cells isolated from these spontaneous tumors<sup>60</sup>. Furthermore, immunotherapy efficacy exhibited enhanced sensitivity in mice with subcutaneously implanted tumors compared to mice bearing orthotopic tumors from a genetically similar pool of tumor cells, indicating that the host normal tissue has an enormous impact on the tumor microenvironment and therefore on endogenous T cell responses<sup>61</sup>. Hence, it is most conceivable that the differences between our findings from **Chapter 3** and previously described experiments by Zitvogel and Kroemer are caused by the fact that we employed spontaneous mammary tumor models in **Chapter 3** instead of tumor cell line transplantation models or the immunogenic MCA fibrosarcoma model<sup>62</sup>. To test this concept experimentally, we generated a tumor cell line from a KEP tumor and conducted an analogous experiment as previously described in several papers<sup>52-54,57</sup>. Consistent with previous findings in cancer cell line inoculation models and in contrast to our findings in the transgenic KEP model (**Chapter 3**), we observed that tumor outgrowths from a KEP tumor cell line inoculated in *Rag1*<sup>+/-</sup> mice responded to oxaliplatin treatment while tumor outgrowths from the same KEP tumor cell line inoculated in *Rag1*<sup>-/-</sup> mice did not respond to oxaliplatin treatment (Fig.1; unpublished). Though this experiment should be reproduced with more cell lines, different chemotherapeutics and with MMTV-*ErbB2* tumor cell lines, we here report

that oxaliplatin loses its therapeutic efficacy on KEP tumor cell line outgrowths in mice with a defective adaptive immune cell function. Thus, **Chapter 3** and these unpublished data illustrate the distinction in impact of the adaptive immune system on chemotherapy response between *de novo* tumor models and tumor transplantation models.

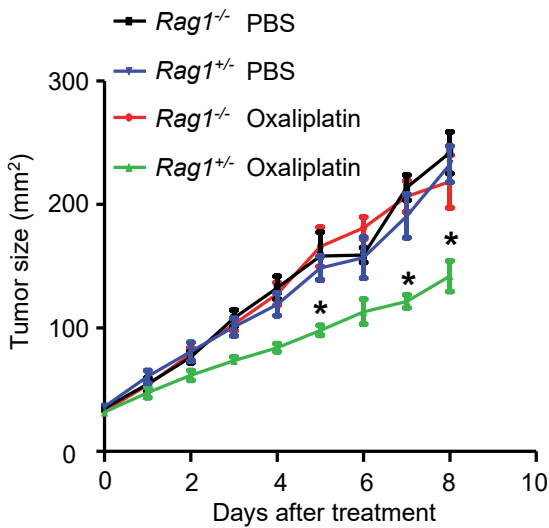


**Figure 1. Impact of the adaptive immune system on the efficacy of oxaliplatin in a KEP mammary cell line transplantation model.** Mice (*Rag1*<sup>+/-</sup> or *Rag1*<sup>-/-</sup>) were injected s.c in the flank with 3 million KEP tumor cells. When the tumors reached 30 mm<sup>2</sup> in size, mice were treated with PBS or oxaliplatin (6mg/kg, i.v) at day 0. Tumor growth in oxaliplatin-treated *Rag1*<sup>+/-</sup> mice compared to untreated *Rag1*<sup>+/-</sup> mice was significantly different at 3 time-points, \*p<0.05 by Mann-Whitney test. Each treatment group included 8 mice and was repeated two times with identical results.

How can we explain that there is no role for the adaptive immune system in chemotherapy response of spontaneous mouse tumor models? From earlier studies by others we know that subcutaneous inoculation of cancer cell suspensions results in massive tumor cell necrosis and early release of tumor antigens which could trigger acute adaptive immune responses, whereas spontaneously arising tumors that take months to develop often are known to trigger a more chronic inflammatory response that prevents acute T cell priming (immunosuppression) <sup>63-65</sup>. This could explain why the adaptive immune system contributed to the chemotherapy response of injected tumors, but not of established spontaneous tumors. Similarly, both T and B cells in the MCA-induced sarcoma model have been demonstrated as a critical factor in suppressing tumor initiation <sup>66</sup>, suggesting that in immunogenic tumor models expressing strong antigens, chemotherapy-induced ICD is effective in activating CD8<sup>+</sup> T cells to contribute to the chemotherapy response <sup>62</sup>. We hypothesize that in established spontaneous tumors, chemotherapy is not able to activate adaptive immunity that is powerful enough to overcome the immunosuppressive networks in the microenvironment of *de novo* tumors. This hypothesis has been proven correct by others <sup>67-69</sup> and in **Chapter 4** in which we show that targeting

macrophages and neutrophils in combination with chemotherapy improved survival of KEP mice in a CD8<sup>+</sup> T cell-dependent mechanism. Our study in **Chapter 4** demonstrates that to boost an adaptive immune response in the KEP model during platinum-containing chemotherapy it is pivotal to create a type I interferons (IFNs)-enriched TME. Whether ICD is induced in KEP tumor models upon targeting of macrophages and neutrophils during platinum-containing chemotherapy remains unknown. Adaptive immunity has been engaged by synergistic effects of chemotherapy and immunotherapy in clinical settings and in *de novo* cancer mouse models<sup>70-74</sup> including MMTV-*NeuT* mice<sup>75</sup> and our KEP mouse model (unpublished). It is possible that ICD is important for these synergistic effects. Lastly, although we did not detect major changes in intra-tumoral CD4/CD8<sup>+</sup> T cell ratio or proportion of FoxP3<sup>+</sup> cells after chemotherapy treatment of MMTV-*NeuT*; *Rag2*<sup>+/-</sup> and KEP; *Rag1*<sup>+/-</sup> mice, we cannot exclude that other distinct adaptive immune populations such as Tregs or  $\gamma\delta$  T cells have opposing roles during chemotherapy.

The ICD concept has been established in hundreds of publications based on transplantation models<sup>76</sup>, yet GEMMs have shown to represent human tumors better than transplantation models<sup>77</sup>, We (**Chapter 3**) and others<sup>67-69</sup> have not seen evidence for a contributing role of the adaptive immune system upon chemotherapy treatment in *de novo* mouse tumor models. Thus, our study continues to urge for a careful analysis of the involvement of the adaptive immune system in chemotherapy response in a larger set of *de novo* tumor models that represent different solid human cancer types and extend these findings to the clinical situation.

## Targeting macrophages as anti-cancer therapy

The TME of solid tumors contains many cell types of which macrophages are frequently the largest population. For many cancer types, including breast cancer, macrophage presence in tumors is a negative prognostic factor<sup>78-81</sup>. Indeed, our group recently showed that a gene signature derived from tumor-associated macrophages (TAMs) from KEP mammary tumors could be used to predict poor survival in two separate cohorts of ILC patients<sup>82</sup>. Preclinical studies have established that macrophages contribute to the various cancer hallmarks including cancer proliferation, suppression of anti-tumor immune responses, angiogenesis and migration<sup>83,84</sup>. Therapeutic approaches targeting TAMs focus on inhibiting pro-tumor macrophage

function via depletion, blockade of their recruitment or repolarization of macrophages towards an anti-tumor phenotype<sup>84</sup>. Blocking the CSF-1/CSF-1R signaling pathway, essential for macrophage survival, has proven to be an attractive strategy to eliminate or reprogram macrophages and suppress tumor growth in preclinical studies<sup>85</sup>. This has resulted in the development and clinical testing of CSF-1R signaling pathway inhibitors, including antibodies against the receptor (anti-CSF-1R), the ligand (anti-CSF-1), and inhibitors of the tyrosine kinase domain of CSF-1R<sup>34,85-89</sup>. However, monotherapy treatment with CSF-1R inhibitors does not exert anti-tumor effects in several models<sup>90</sup>, including in the KEP mouse model (**Chapter 4**). Differences in anti-tumor effects of CSF-1/CSF-1R pathway targeting are likely caused by different cancer (sub)types and cancer mouse models with their different TME, use of a different type of inhibitor, doses and timing of the initiation of treatment.

CSF-1R blockade was tolerated well during phase I and II clinical trials but has shown only marginal therapeutic benefit<sup>85</sup>. Therefore, current clinical and experimental efforts are focused on finding the right combination partners for TAM targeting<sup>85</sup>. These combination partners may vary from immune checkpoint blockade, adoptive T cell transfer, radiotherapy to chemotherapy. In **Chapter 4** we set out to obtain a better understanding of the mechanisms of action of anti-CSF-1R *in vivo* and to identify the optimal combination partner among existing anti-cancer therapies to enhance their efficacy. CSF-1R pathway targeting has shown to enhance the cytotoxic efficacy of chemotherapy in various experimental tumor models<sup>68,69,91-94</sup>, including in the KEP model, as described in **Chapter 4** of this thesis. However, our study reveals a distinct mechanism of how therapeutic targeting of macrophages enhances chemotherapy efficacy. In **Chapter 4** we demonstrated that anti-CSF-1R induces type I IFN signaling in KEP mammary tumors, which acts synergistically with cisplatin to prevent tumor outgrowth and to prolong survival. Furthermore, we showed that anti-CSF-1R synergized with platinum-containing drugs, *i.e.* cisplatin and oxaliplatin, but not with the taxane docetaxel, though IFN $\alpha$  was induced.

The exact mechanism that induces the type I IFN expression in cisplatin/anti-CSF-1R-treated mice is mostly unknown. While our data showed that CSF-1R blockade depletes 80% of intratumoral macrophages, we noted a small population of remaining TAMs expressing high levels of IFN $\alpha$ . These TAMs are most likely causative of the increased IFN $\alpha$  levels in the tumors. Of note, as CSF-1R expression was significantly lower in the

remaining TAMs, it could explain their resistance to the anti-CSF-1R therapy. Moreover, our study shows that circulating monocytes can infiltrate into the tumor of anti-CSF-1R-treated mice, suggesting that these IFN $\alpha$  expressing TAMs are either newly recruited monocytes or remaining TAMs. It is unclear from our study whether the remaining macrophages upon anti-CSF1R treatment are repolarized, though noteworthy, three studies using either CSF-1R neutralizing antibodies or CSF-1R small molecule inhibitors discovered that TAMs were repolarized towards a tumor-inhibiting state in a preclinical pancreatic cancer, glioblastoma and lung cancer mouse model<sup>95-97</sup>. Induction of type I IFN expression by targeting macrophage function has not only been seen by us in **Chapter 4** but also by others; for instance type I IFNs were also increased in macrophages of the pancreatic cancer model after CSF-1R neutralizing antibodies<sup>95</sup>. Furthermore, we also noticed IFN $\alpha$  upregulation in anti-CSF-1R treated MC38 colon adenocarcinoma tumors, indicating that anti-CSF-1R unleashes type I IFN signaling in other cancers besides breast cancer. Lastly, a study targeting macrophages via their MerTK receptor resulted in the accumulation of apoptotic cells within transplanted MC38 colon carcinoma tumors and was associated with circulating cell-free tumor-derived DNA which triggered a type I interferon response by macrophages<sup>98</sup>. It is therefore likely that in our KEP model the dying cancer cells and/or dying macrophages released cytosolic DNA, which is scavenged by the remaining macrophages and activates the cGAS-STING pathway which triggers IFN $\alpha$  expression by these macrophages.

There is a vital interest in the development of clinically more effective combination therapies that combine IFN-I based therapies with for instance immune checkpoint inhibitors or chemotherapy<sup>99-102</sup>. The type I IFN family includes 13 different IFN $\alpha$  proteins (14 in mice), one IFN $\beta$  protein and others less well defined family members such as IFN $\epsilon$  and IFN $\omega$ <sup>103</sup>. Type I IFN molecules bind to their receptor that is composed of IFNAR1 and IFNAR2 subunits in a heterodimer or an IFNAR1 homodimer<sup>103</sup>. IFNs activate the kinases Janus kinase 1 (JAK1) and tyrosine kinase 2 (TYK2) which phosphorylate STAT1 and STAT2 to promote the expression of type I IFN-stimulated genes (ISGs). These innate immune signals enhance tumor antigen presentation and thereby augment the antigen-specific CD8<sup>+</sup> T cells response<sup>104,105</sup>. Indeed, type I IFN gene signatures have shown to correlate with increased bone metastasis-free survival or with metastasis-free survival in general in breast cancer patients<sup>106-108</sup>. Furthermore, type I IFN signaling is essential for the function and survival of cytotoxic T cells<sup>109</sup> and NK

cells<sup>110</sup>. Notably, impaired type I IFN signaling is a feature of immune dysfunction in patients with cancer and is linked with poor prognosis<sup>109,111,112</sup>. We detected an increase in ISGs in advanced solid tumor biopsies of cancer patients treated with emactuzumab, a humanized anti-human CSF-1R monoclonal antibody, compared to their reference levels, which is in line with our findings in the KEP mouse model (**Chapter 4**). Thus, the data shown in **Chapter 4** highlight that CSF-1R blockade may be used as a strategy to induce an intra-tumoral type I IFNs response.

An important question that our work leaves open is what the molecular mechanisms are of how type I IFN employs its anti-cancer efficacy in cisplatin/anti-CSF-1R-treated mice. Surprisingly, CD8<sup>+</sup> T cells were not unleashed upon cisplatin/anti-CSF-1R-treatment and CD8<sup>+</sup> T cell depletion did not influence the survival in cisplatin/anti-CSF-1R-treated mice. Though additional studies investigating other cytotoxic cells are required, these data indicate that another mechanism is responsible for the anti-cancer efficacy. Type I IFNs can have a direct effect on tumor progression by blocking proliferation or inducing apoptosis in cancer cells<sup>113</sup>. Concomitant, our *in vitro* work in **Chapter 4** of this thesis demonstrated that high concentrations of IFN $\alpha$ , subtype IFN $\alpha$ 1, has a direct inhibitory effect on KEP cancer cells. Of note, it will be interesting to evaluate other IFN $\alpha$  molecules and IFN $\beta$  as their influence against viral infections<sup>114</sup> and their anti-proliferative effects on cancer cells<sup>115</sup> have shown to differ and could be cumulative. However, no increase of apoptotic cells was found in tumors of cisplatin/anti-CSF-1R-treated mice (**Chapter 4**), suggesting that a different mechanism such as necroptosis, an inflammatory programmed form of necrosis, or senescence might at play. In this regard, studies have shown that both cisplatin<sup>116,117</sup> and type I IFNs<sup>118,119</sup> can induce senescence in cancer cells, suggesting that senescence in cisplatin/anti-CSF-1R-treated tumors could perhaps explain the reduced proliferation and lack of apoptosis. Since the majority of breast cancer deaths are caused by metastatic disease<sup>120</sup>, it will be of great value to study whether type I IFNs influences metastasis formation upon anti-CSF-1R with platinum based chemotherapy<sup>13</sup>. Monotherapy of CSF-1R blockade did not affect the metastasis-specific survival in the KEP-based model of spontaneous breast metastasis (**Chapter 4**).

Studies in preclinical cancer models and patients have described that chemotherapeutic drugs, such as anthracyclines and cyclophosphamide, induce type I IFN production, which is required for their therapeutic efficacy as blockade of type I IFN signaling results in loss of the anti-cancer efficacy

<sup>99,121</sup>. However, in our study in **Chapter 4** cisplatin response was not affected by blockade of type I IFN signaling. Only the combination of cisplatin/anti-CSF-1R induced a type I IFNs response that led to enhanced survival. Interestingly, the increase in type I IFN during anti-CSF-1R therapy did not enhance the efficacy of the taxane docetaxel. What could have caused the synergy of CSF-1R blockade with cisplatin and oxaliplatin but not with docetaxel? The two conventional chemotherapeutics have a different mode of action: while platinum-based anticancer drugs cause crosslinks in the DNA and prompt apoptosis, taxanes affect cell division through stabilization of microtubules. In line with this notion, a comprehensive study into the mutagenic impact of common chemotherapeutics found that cisplatin induces the highest amounts of single nucleotide variant (SNV)'s, indels and deletions compared to several other standard cytotoxics, including the taxane paclitaxel <sup>122</sup>. It is now well-known that distinct cytotoxic drugs differentially affect immune cells and the influence of the immune system on chemo-responsiveness has shown to depend on the type of chemotherapeutic drug and dosing <sup>49,123,124</sup>. Especially cisplatin has shown to induce antitumor immunomodulation in multiple preclinical and clinical studies <sup>125-128</sup>. Hence, it is conceivable that platinum-based anticancer drugs create a milieu in KEP tumors that is preventing type 1 IFN signaling. In line with this notion, cisplatin response was not affected by blockade of type I IFN signaling (**Chapter 4**). To this end, it will be interesting to investigate whether alterations effecting genes or pathways of the IFN signaling cascade are present in KEP tumors after cisplatin and docetaxel treatments. Furthermore, two clinical trials recently combined paclitaxel with CSF-1R blockade; emactuzumab in patients with advanced/metastatic solid tumors <sup>129</sup> and pexidartinib (PLX3397) in patients with refractory solid tumors <sup>130</sup>. Only the combination of paclitaxel with pexidartinib noted an objective response rate of 16% <sup>130</sup>, while no anti-tumor activity alone or in combination with paclitaxel was found with emactuzumab <sup>129</sup>. Based on our data, cisplatin may have been a more optimal combination chemotherapeutic drug. However, synergistic effects with CSF-1R blockade may also depend on the tumor (sub)type, stage, prior treatments and CSF-1R blockade drug. Future studies should expand tumor models, numbers and types of chemotherapeutic agents used in the clinic to examine synergistic effects with anti-CSF-1R and choose the optimal cytotoxic drug to maximize the effects of CSF-1R targeting agents.

## Targeting neutrophil-dependent immunosuppression further improves cisplatin/anti-CSF-1R efficacy

In contrast to cancer cells which develop mechanisms of resistance to therapies, immune cells are not under the same mutational pressure and thus unlikely to develop therapy resistance. However, bidirectional feedback between cancer cells and their microenvironment can induce resistance of the tumor microenvironment to immuno-modulation of CSF-1R targeting. In several models, resistance to CSF-1R targeting or macrophage inhibition was seen by the recruitment of tumor-promoting neutrophils<sup>131-135</sup>. These newly recruited neutrophils embodied similar pro-tumor mechanisms as the depleted TAMs, such as regulating processes like immunosuppression and angiogenesis<sup>134,135</sup>. However, different than those studies, neutrophils did not take over the function of macrophages upon CSF-1R blockade and cisplatin in KEP tumors, but unlike macrophages, neutrophils exhibited immunomodulatory functions (**Chapter 4**). In the poorly immunogenic KEP model, we targeted the immunosuppressive neutrophils in cisplatin/anti-CSF-1R-treated mice to obtain an effective CD8<sup>+</sup> T cell response that contributed to tumor control and extended survival (**Chapter 4**). Moreover, antibody-mediated depletion of NK cells resulted in a partial loss of the benefit of neutrophil depletion, suggesting that not only CD8<sup>+</sup> T cells but also NK cells are necessary to engage anti-tumor immunity upon neutrophil depletion in cisplatin/anti-CSF-1R-treated mice. Engagement of anti-tumor immunity upon macrophage and neutrophil targeting was also seen in a mouse model for pancreatic cancer<sup>133</sup>, but whether type I IFN signaling was induced is unknown. However, since we did not observe an increase in neutrophil recruitment by absolute neutrophil numbers unlike other studies have noted, it is likely that a different mechanism influenced neutrophil function in the KEP mouse model upon macrophage targeting.

The exact TME signals that instructed neutrophils to acquire pro-tumor functions upon CSF-1R blockade are unknown, although it is plausible that prolonged type I IFN signaling could have led to immunosuppressive circuits. While several studies have suggested that type I IFNs induce anti-tumor properties in neutrophils<sup>136-138</sup>, other studies in chronic infections such as malaria-infected hosts and patients with active tuberculosis found that a type I IFN transcriptional signature in neutrophils is correlated with tissue damage and disease pathogenesis<sup>139,140</sup>. Moreover, negative-feedback mechanisms were reported in studies on chronic viral infections when type I IFN signaling persisted and lead for example to the generation of an

immunosuppressive environment<sup>93,141,142</sup>. In fact, higher levels of PD-L1 were found on type I IFN-producing macrophages upon anti-CSF-1R treatment in KEP mice (**Chapter 4**), suggesting that perhaps an autocrine mechanism was present to resolve the inflammatory responses. Whether sustained type I IFN signaling can rewire neutrophils in cisplatin/anti-CSF-1R-treated mice should be addressed in future studies. Furthermore, RNA-sequencing analysis on neutrophils isolated from cisplatin/anti-CSF-1R-treated mouse tumors displayed elevated expression levels of type I IFN-stimulated genes compared to neutrophils in tumors of cisplatin/control antibody-treated mice (**Chapter 4**). It is unclear whether the type I IFN signaling of neutrophils promotes their immunosuppressive abilities.

How neutrophils exert their immunosuppressive functions needs to be further elucidated. Interestingly, a correlation was recently found between type I IFN signaling and ROS production of neutrophils in a melanoma model<sup>138</sup>. Immunosuppressive- pro-metastatic neutrophils in the KEP mouse model have previously shown to express high levels of inducible nitric oxide synthase (iNOS)<sup>11,143</sup>. By influencing conformational changes in TCR recognition, iNOS prevents specific peptide recognition by T cells<sup>144</sup>. To elucidate whether neutrophils employ iNOS to prevent an anti-tumor immune response in cisplatin/anti-CSF-1R-treated mice additional studies are required.

Since neutrophils have shown to influence various tumor-promoting processes, neutrophils have become interesting putative targets for therapeutic intervention<sup>145</sup>. Moreover, a high neutrophil-to-lymphocyte ratio in the circulation of multiple cancers is linked to poor prognosis in patients<sup>146</sup>. Currently, the chemokine receptors CXCR1 and CXCR2 that are important for neutrophil recruitment are under clinical evaluation<sup>147,148</sup>. Our study shows that the therapeutic efficacy of targeting macrophages and neutrophils in cisplatin-treated KEP mice is mediated by the induction of type I IFNs and by unleashing anti-tumor responses. To this end, it will be important to evaluate the development of protumor functions by neutrophils in patients that receive combinational therapy of chemotherapy with anti-CSF-1R or type I IFN-stimulating drugs and the subsequent testing of neutrophil-targeting therapy efficacy.

## Concluding remarks and future perspectives

The work presented in this thesis focuses on obtaining a better understanding of the adaptive immune system in breast cancer initiation, progression, metastasis and chemotherapy response. In addition, this thesis focuses on maximizing the success of immunomodulatory agents targeting myeloid cells using genetically engineered mouse models. This thesis demonstrates that unlike other breast cancer mouse models<sup>9-11</sup>, the adaptive immune system is not involved in primary tumor and metastasis formation in a *de novo* tumor mouse model of HER2-positive breast cancer (**Chapter 2**). To harness successful anti-tumor immunity and increase therapy outcomes in HER2-positive patients, future research should be aimed at understanding the immunosuppressive networks in HER2-positive breast cancer. Furthermore, while the endogenous adaptive immune system has shown to play an important role during chemotherapy response of immunogenic cancer models<sup>76</sup>, our research shows that the adaptive immune system is not important during chemotherapy response in two *de novo* breast tumor mouse models. Remarkably, by performing studies with CSF-1R blockade to target macrophages, we demonstrate that the use of agents that trigger type I IFN responses enhances the anti-cancer efficacy of chemotherapy. This thesis further elucidates that engagement of anti-tumor immunity can be reached with the addition of neutrophil depletion during chemotherapy and CSF-1R blockade. Thus, these data suggest that a combination strategy triggering the removal of the immunosuppressive TME networks and subsequent type I IFN response is the mechanism of action to acquire a proficient adaptive immune response in the less immunogenic ILC mouse model upon chemotherapy treatment. This thesis reveals that investigating the function of the adaptive immune system during tumor development and chemotherapy in a larger set of solid breast cancer subtypes is essential for the development of immunomodulatory approaches. Lastly, the data in this thesis describe that the synergy of combined chemotherapy and CSF-1R blockade is chemotherapy dependent as we found that only platinum drugs, but not docetaxel, synergized with CSF-1R blockade and increased survival further. These data indicate that therapeutic approaches using type I IFN-inducing agents such as CSF-1R-targeting drugs or STING agonists are important for successful anti-cancer therapy, however future research should obtain more insights into the synergistic effects of combinatorial therapies with myeloid targeting and evaluate immunomodulatory drug-induced resistance. Considering the realization that cancer subtype, the genetic background of the tumors, disease stage and treatment history affect anti-cancer immunity, the vision for immunomodulatory therapies must change to a more personalized treatment.

## References

- 1 Wellenstein, M. D. & de Visser, K. E. Cancer-Cell-Intrinsic Mechanisms Shaping the Tumor Immune Landscape. *Immunity* **48**, 399-416, doi:10.1016/j.immuni.2018.03.004 (2018).
- 2 Busch, S. E. *et al.* Lung Cancer Subtypes Generate Unique Immune Responses. *The Journal of Immunology* **197**, 4493-4503, doi:10.4049/jimmunol.1600576 (2016).
- 3 Tekpli, X. *et al.* An independent poor-prognosis subtype of breast cancer defined by a distinct tumor immune microenvironment. *Nature Communications* **10**, 5499, doi:10.1038/s41467-019-13329-5 (2019).
- 4 Casanovas, O., Hicklin, D. J., Bergers, G. & Hanahan, D. Drug resistance by evasion of antiangiogenic targeting of VEGF signaling in late-stage pancreatic islet tumors. *Cancer Cell* **8**, 299-309 (2005).
- 5 de Visser, K. E., Korets, L. V. & Coussens, L. M. De novo carcinogenesis promoted by chronic inflammation is B lymphocyte dependent. *Cancer Cell* **7**, 411-423 (2005).
- 6 Andreu, P. *et al.* FcR $\gamma$  activation regulates inflammation-associated squamous carcinogenesis. *Cancer Cell* **17**, 121-134, doi:10.1016/j.ccr.2009.12.019 (2010).
- 7 Haybaeck, J. *et al.* A lymphotoxin-driven pathway to hepatocellular carcinoma. *Cancer Cell* **16**, 295-308, doi:S1535-6108(09)00294-3 [pii] 10.1016/j.ccr.2009.08.021 (2009).
- 8 Wellenstein, M. D. *et al.* Loss of p53 triggers WNT-dependent systemic inflammation to drive breast cancer metastasis. *Nature*, doi:10.1038/s41586-019-1450-6 (2019).
- 9 DeNardo, D. G. *et al.* CD4(+) T cells regulate pulmonary metastasis of mammary carcinomas by enhancing protumor properties of macrophages. *Cancer Cell* **16**, 91-102, doi:S1535-6108(09)00216-5 [pii] 10.1016/j.ccr.2009.06.018 (2009).
- 10 Tan, W. *et al.* Tumour-infiltrating regulatory T cells stimulate mammary cancer metastasis through RANKL-RANK signalling. *Nature* **470**, 548-553, doi:10.1038/nature09707 (2011).
- 11 Coffelt, S. B. *et al.* IL-17-producing gammadelta T cells and neutrophils conspire to promote breast cancer metastasis. *Nature* **522**, 345-348, doi:10.1038/nature14282 (2015).
- 12 Glajcar, A., Szpor, J., Hodorowicz-Zaniewska, D., Tyrak, K. E. & Okoń, K. The composition of T cell infiltrates varies in primary invasive breast cancer of different molecular subtypes as well as according to tumor size and nodal status. *Virchows Arch* **475**, 13-23, doi:10.1007/s00428-019-02568-y (2019).
- 13 Garner, H. & de Visser, K. E. Immune crosstalk in cancer progression and metastatic spread: a complex conversation. *Nat Rev Immunol* **20**, 483-497, doi:10.1038/s41577-019-0271-z (2020).

- 14 Sasada, T., Kimura, M., Yoshida, Y., Kanai, M. & Takabayashi, A. CD4+CD25+ regulatory T cells in patients with gastrointestinal malignancies: possible involvement of regulatory T cells in disease progression. *Cancer* **98**, 1089-1099, doi:10.1002/cncr.11618 (2003).
- 15 Nishikawa, H. & Sakaguchi, S. Regulatory T cells in tumor immunity. *Int J Cancer* **127**, 759-767, doi:10.1002/ijc.25429 (2010).
- 16 Nakamura, R. *et al.* Accumulation of regulatory T cells in sentinel lymph nodes is a prognostic predictor in patients with node-negative breast cancer. *Eur J Cancer* **45**, 2123-2131, doi:10.1016/j.ejca.2009.03.024 (2009).
- 17 Dadi, S. *et al.* Cancer Immunosurveillance by Tissue-Resident Innate Lymphoid Cells and Innate-like T Cells. *Cell* **164**, 365-377, doi:10.1016/j.cell.2016.01.002 (2016).
- 18 Croci, S. *et al.* Interleukin-15 is required for immunosurveillance and immunoprevention of HER2/neu-driven mammary carcinogenesis. *Breast Cancer Res* **17**, 70, doi:10.1186/s13058-015-0588-x (2015).
- 19 Shankaran, V. *et al.* IFN $\gamma$  and lymphocytes prevent primary tumour development and shape tumour immunogenicity. *Nature* **410**, 1107-1111 (2001).
- 20 Takeuchi, N. *et al.* Anti-HER-2/neu immune responses are induced before the development of clinical tumors but declined following tumorigenesis in HER-2/neu transgenic mice. *Cancer Res* **64**, 7588-7595, doi:10.1158/0008-5472.CAN-04-1081 (2004).
- 21 Kmiecik, M. *et al.* Danger signals and nonself entity of tumor antigen are both required for eliciting effective immune responses against HER-2/neu positive mammary carcinoma: implications for vaccine design. *Cancer Immunol Immunother* **57**, 1391-1398, doi:10.1007/s00262-008-0475-8 (2008).
- 22 Disis, M. L. *et al.* Immunity to the HER-2/neu oncogenic protein. *Ciba Found Symp* **187**, 198-207; discussion 207-111, doi:10.1002/9780470514672.ch13 (1994).
- 23 Peoples, R., Milatovich, A. & Francke, U. Hemizyosity at the insulin-like growth factor I receptor (IGF1R) locus and growth failure in the ring chromosome 15 syndrome. *Cytogenet Cell Genet* **70**, 228-234, doi:10.1159/000134040 (1995).
- 24 Park, J. M., Terabe, M., Donaldson, D. D., Forni, G. & Berzofsky, J. A. Natural immunosurveillance against spontaneous, autochthonous breast cancers revealed and enhanced by blockade of IL-13-mediated negative regulation. *Cancer Immunol Immunother* **57**, 907-912, doi:10.1007/s00262-007-0414-0 (2008).
- 25 Hanahan, D. & Coussens, L. M. Accessories to the crime: functions of cells recruited to the tumor microenvironment. *Cancer cell* **21**, 309-322, doi:10.1016/j.ccr.2012.02.022 (2012).
- 26 Joyce, J. A. & Fearon, D. T. T cell exclusion, immune privilege, and the tumor microenvironment. *Science* **348**, 74-80, doi:10.1126/science.aaa6204 (2015).

- 27 Morales, J. K. *et al.* Adoptive transfer of HER2/neu-specific T cells expanded with alternating gamma chain cytokines mediate tumor regression when combined with the depletion of myeloid-derived suppressor cells. *Cancer Immunol Immunother* **58**, 941-953, doi:10.1007/s00262-008-0609-z (2009).
- 28 Ambrosino, E. *et al.* Immunosurveillance of ErbB2 carcinogenesis in transgenic mice is concealed by a dominant regulatory T-cell self-tolerance. *Cancer Res* **66**, 7734-7740, doi:10.1158/0008-5472.CAN-06-1432 (2006).
- 29 Norian, L. A. *et al.* Tumor-infiltrating regulatory dendritic cells inhibit CD8+ T cell function via L-arginine metabolism. *Cancer Res* **69**, 3086-3094, doi:10.1158/0008-5472.CAN-08-2826 (2009).
- 30 Costa, R. L. B. & Czerniecki, B. J. Clinical development of immunotherapies for HER2(+) breast cancer: a review of HER2-directed monoclonal antibodies and beyond. *NPJ Breast Cancer* **6**, 10, doi:10.1038/s41523-020-0153-3 (2020).
- 31 Park, S. *et al.* The therapeutic effect of anti-HER2/neu antibody depends on both innate and adaptive immunity. *Cancer Cell* **18**, 160-170, doi:10.1016/j.ccr.2010.06.014 (2010).
- 32 Stagg, J. *et al.* Anti-ErbB-2 mAb therapy requires type I and II interferons and synergizes with anti-PD-1 or anti-CD137 mAb therapy. *Proc Natl Acad Sci U S A* **108**, 7142-7147, doi:10.1073/pnas.1016569108 (2011).
- 33 Conti, L. *et al.* Immunotargeting of the xCT Cystine/Glutamate Antiporter Potentiates the Efficacy of HER2-Targeted Immunotherapies in Breast Cancer. *Cancer Immunol Res* **8**, 1039-1053, doi:10.1158/2326-6066.CIR-20-0082 (2020).
- 34 Cassier, P. A. *et al.* CSF1R inhibition with emactuzumab in locally advanced diffuse-type tenosynovial giant cell tumours of the soft tissue: a dose-escalation and dose-expansion phase 1 study. *The Lancet. Oncology* **16**, 949-956, doi:10.1016/S1470-2045(15)00132-1 (2015).
- 35 Guy, C. T. *et al.* Expression of the neu protooncogene in the mammary epithelium of transgenic mice induces metastatic disease. *Proc Natl Acad Sci U S A* **89**, 10578-10582, doi:10.1073/pnas.89.22.10578 (1992).
- 36 Siegel, P. M., Dankort, D. L., Hardy, W. R. & Muller, W. J. Novel activating mutations in the neu proto-oncogene involved in induction of mammary tumors. *Mol Cell Biol* **14**, 7068-7077, doi:10.1128/mcb.14.11.7068 (1994).
- 37 Gross, E. T. *et al.* Immunosurveillance and immunoediting in MMTV-PyMT-induced mammary oncogenesis. *Oncoimmunology* **6**, e1268310, doi:10.1080/2162402X.2016.1268310 (2017).
- 38 Ruiter, J. R. d., Wessels, L. F. A. & Jonkers, J. Mouse models in the era of large human tumour sequencing studies. *Open Biology* **8**, 180080, doi:doi:10.1098/rsob.180080 (2018).
- 39 de Ruiter, J. R., Wessels, L. F. A. & Jonkers, J. Mouse models in the era of large human tumour sequencing studies. *Open Biol* **8**, doi:10.1098/rsob.180080 (2018).
- 40 Zoi, I., Karamouzis, M. V., Adamopoulos, C. & Papavassiliou, A. G. RANKL Signaling and ErbB Receptors in Breast Carcinogenesis. *Trends Mol Med* **22**, 839-850, doi:10.1016/j.molmed.2016.07.009 (2016).

- 41 Harper, K. L. *et al.* Mechanism of early dissemination and metastasis in Her2+ mammary cancer. *Nature* **540**, 588-592, doi:10.1038/nature20609 (2016).
- 42 Gonzalez-Suarez, E. *et al.* RANK ligand mediates progestin-induced mammary epithelial proliferation and carcinogenesis. *Nature* **468**, 103-107, doi:10.1038/nature09495 (2010).
- 43 Gomes, I. *et al.* Expression of receptor activator of NFkB (RANK) drives stemness and resistance to therapy in ER+HER2- breast cancer. *Oncotarget* **11**, 1714-1728, doi:10.18632/oncotarget.27576 (2020).
- 44 Chen, D. S. & Mellman, I. Oncology meets immunology: the cancer-immunity cycle. *Immunity* **39**, 1-10, doi:10.1016/j.immuni.2013.07.012 (2013).
- 45 Li, B., Cui, Y., Nambiar, D. K., Sunwoo, J. B. & Li, R. The Immune Subtypes and Landscape of Squamous Cell Carcinoma. *Clinical Cancer Research* **25**, 3528-3537, doi:10.1158/1078-0432.Ccr-18-4085 (2019).
- 46 Xu, F. *et al.* Analysis of Lung Adenocarcinoma Subtypes Based on Immune Signatures Identifies Clinical Implications for Cancer Therapy. *Molecular Therapy - Oncolytics* **17**, 241-249, doi:10.1016/j.omto.2020.03.021 (2020).
- 47 Yarden, Y. & Sliwkowski, M. X. Untangling the ErbB signalling network. *Nat Rev Mol Cell Biol* **2**, 127-137, doi:10.1038/35052073 (2001).
- 48 Vasan, N., Baselga, J. & Hyman, D. M. A view on drug resistance in cancer. *Nature* **575**, 299-309, doi:10.1038/s41586-019-1730-1 (2019).
- 49 Shiao, S. L., Ganesan, A. P., Rugo, H. S. & Coussens, L. M. Immune microenvironments in solid tumors: new targets for therapy. *Genes & development* **25**, 2559-2572, doi:25/24/2559 [pii] 10.1101/gad.169029.111 (2011).
- 50 de Visser, K. E. & Jonkers, J. Towards understanding the role of cancer-associated inflammation in chemoresistance. *Curr Pharm Des* **15**, 1844-1853, doi:10.2174/138161209788453239 (2009).
- 51 Coffelt, S. B. & de Visser, K. E. Immune-mediated mechanisms influencing the efficacy of anticancer therapies. *Trends Immunol* **36**, 198-216, doi:10.1016/j.it.2015.02.006 (2015).
- 52 Apetoh, L. *et al.* Toll-like receptor 4-dependent contribution of the immune system to anticancer chemotherapy and radiotherapy. *Nature medicine* **13**, 1050-1059, doi:10.1038/nm1622 (2007).
- 53 Obeid, M. *et al.* Calreticulin exposure dictates the immunogenicity of cancer cell death. *Nature medicine* **13**, 54-61, doi:nm1523 [pii] 10.1038/nm1523 (2007).
- 54 Ghiringhelli, F. *et al.* Activation of the NLRP3 inflammasome in dendritic cells induces IL-1beta-dependent adaptive immunity against tumors. *Nature medicine* **15**, 1170-1178, doi:nm.2028 [pii] 10.1038/nm.2028 (2009).
- 55 Vacchelli, E., Prada, N., Kepp, O. & Galluzzi, L. Current trends of anticancer immunochemotherapy. *Oncoimmunology* **2**, e25396, doi:10.4161/onci.25396 (2013).
- 56 Ma, Y. *et al.* Anticancer chemotherapy-induced intratumoral recruitment and differentiation of antigen-presenting cells. *Immunity* **38**, 729-741, doi:10.1016/j.immuni.2013.03.003 (2013).

- 57 Bezu, L. *et al.* Combinatorial strategies for the induction of immunogenic cell death. *Front Immunol* **6**, 187, doi:10.3389/fimmu.2015.00187 (2015).
- 58 Casares, N. *et al.* Caspase-dependent immunogenicity of doxorubicin-induced tumor cell death. *Journal of Experimental Medicine* **202**, 1691-1701, doi:10.1084/jem.20050915 (2005).
- 59 Galluzzi, L. *et al.* Consensus guidelines for the definition, detection and interpretation of immunogenic cell death. *Journal for ImmunoTherapy of Cancer* **8**, e000337, doi:10.1136/jitc-2019-000337 (2020).
- 60 Olive, K. P. *et al.* Inhibition of Hedgehog signaling enhances delivery of chemotherapy in a mouse model of pancreatic cancer. *Science* **324**, 1457-1461, doi:1171362 [pii] 10.1126/science.1171362 (2009).
- 61 Devaud, C. *et al.* Tissues in different anatomical sites can sculpt and vary the tumor microenvironment to affect responses to therapy. *Molecular therapy : the journal of the American Society of Gene Therapy* **22**, 18-27, doi:10.1038/mt.2013.219 (2014).
- 62 Mattarollo, S. R. *et al.* Pivotal role of innate and adaptive immunity in anthracycline chemotherapy of established tumors. *Cancer Res* **71**, 4809-4820, doi:0008-5472.CAN-11-0753 [pii] 10.1158/0008-5472.CAN-11-0753 (2011).
- 63 Schreiber, K., Rowley, D. A., Riethmuller, G. & Schreiber, H. Cancer immunotherapy and preclinical studies: why we are not wasting our time with animal experiments. *Hematology/oncology clinics of North America* **20**, 567-584, doi:10.1016/j.hoc.2006.03.001 (2006).
- 64 Yu, P., Rowley, D. A., Fu, Y. X. & Schreiber, H. The role of stroma in immune recognition and destruction of well-established solid tumors. *Curr Opin Immunol* **18**, 226-231 (2006).
- 65 Willimsky, G. *et al.* Immunogenicity of premalignant lesions is the primary cause of general cytotoxic T lymphocyte unresponsiveness. *J Exp Med* **205**, 1687-1700, doi:jem.20072016 [pii] 10.1084/jem.20072016 (2008).
- 66 Shankaran, V. *et al.* IFN $\gamma$  and lymphocytes prevent primary tumour development and shape tumour immunogenicity. *Nature* **410**, 1107-1111 (2001).
- 67 Denardo, D. G. *et al.* Leukocyte complexity predicts breast cancer survival and functionally regulates response to chemotherapy. *Cancer Discovery* **1**, 54-55 (2011).
- 68 Mitchem, J. B. *et al.* Targeting tumor-infiltrating macrophages decreases tumor-initiating cells, relieves immunosuppression, and improves chemotherapeutic responses. *Cancer Res* **73**, 1128-1141, doi:10.1158/0008-5472.Can-12-2731 (2013).
- 69 Ruffell, B. *et al.* Macrophage IL-10 blocks CD8 $^{+}$  T cell-dependent responses to chemotherapy by suppressing IL-12 expression in intratumoral dendritic cells. *Cancer Cell* **26**, 623-637, doi:10.1016/j.ccell.2014.09.006 (2014).
- 70 Nistico, P. *et al.* Chemotherapy enhances vaccine-induced antitumor immunity in melanoma patients. *Int J Cancer* **124**, 130-139, doi:10.1002/ijc.23886 (2009).

- 71 Ramakrishnan, R. *et al.* Chemotherapy enhances tumor cell susceptibility to CTL-mediated killing during cancer immunotherapy in mice. *J Clin Invest* **120**, 1111-1124, doi:40269 [pii] 10.1172/JCI40269 (2010).
- 72 Robert, C. *et al.* Ipilimumab plus dacarbazine for previously untreated metastatic melanoma. *N Engl J Med* **364**, 2517-2526, doi:10.1056/NEJMoa1104621 (2011).
- 73 Schmid, P. *et al.* Atezolizumab and Nab-Paclitaxel in Advanced Triple-Negative Breast Cancer. *N Engl J Med* **379**, 2108-2121, doi:10.1056/NEJMoa1809615 (2018).
- 74 (<https://ClinicalTrials.gov/show/NCT03515798>).
- 75 Workenhe, S. T. *et al.* De novo necroptosis creates an inflammatory environment mediating tumor susceptibility to immune checkpoint inhibitors. *Commun Biol* **3**, 645, doi:10.1038/s42003-020-01362-w (2020).
- 76 Galluzzi, L. *et al.* Consensus guidelines for the definition, detection and interpretation of immunogenic cell death. *J Immunother Cancer* **8**, doi:10.1136/jitc-2019-000337 (2020).
- 77 Guerin, M. V., Finisguerra, V., Van den Eynde, B. J., Bercovici, N. & Trautmann, A. Preclinical murine tumor models: a structural and functional perspective. *eLife* **9**, e50740, doi:10.7554/eLife.50740 (2020).
- 78 Zhang, Q. W. *et al.* Prognostic significance of tumor-associated macrophages in solid tumor: a meta-analysis of the literature. *PLoS One* **7**, e50946, doi:10.1371/journal.pone.0050946 (2012).
- 79 Zhao, X. *et al.* Prognostic significance of tumor-associated macrophages in breast cancer: a meta-analysis of the literature. *Oncotarget* **8**, 30576-30586, doi:10.18632/oncotarget.15736 (2017).
- 80 Yuan, X. *et al.* Prognostic significance of tumor-associated macrophages in ovarian cancer: A meta-analysis. *Gynecol Oncol* **147**, 181-187, doi:10.1016/j.ygyno.2017.07.007 (2017).
- 81 Yagi, T. *et al.* Tumour-associated macrophages are associated with poor prognosis and programmed death ligand 1 expression in oesophageal cancer. *Eur J Cancer* **111**, 38-49, doi:10.1016/j.ejca.2019.01.018 (2019).
- 82 Tuit, S. *et al.* Transcriptional Signature Derived from Murine Tumor-Associated Macrophages Correlates with Poor Outcome in Breast Cancer Patients. *Cell Rep* **29**, 1221-1235 e1225, doi:10.1016/j.celrep.2019.09.067 (2019).
- 83 Mantovani, A., Marchesi, F., Malesci, A., Laghi, L. & Allavena, P. Tumour-associated macrophages as treatment targets in oncology. *Nat Rev Clin Oncol* **14**, 399-416, doi:10.1038/nrclinonc.2016.217 (2017).
- 84 Zhou, J. *et al.* Tumor-Associated Macrophages: Recent Insights and Therapies. *Frontiers in Oncology* **10**, doi:10.3389/fonc.2020.00188 (2020).
- 85 Kowal, J., Kornete, M. & Joyce, J. A. Re-education of macrophages as a therapeutic strategy in cancer. *Immunotherapy* **11**, 677-689, doi:10.2217/imt-2018-0156 (2019).
- 86 Ries, C. H. *et al.* Targeting tumor-associated macrophages with anti-CSF-1R antibody reveals a strategy for cancer therapy. *Cancer Cell* **25**, 846-859, doi:10.1016/j.ccr.2014.05.016 (2014).

- 87 Ries, C. H., Hoves, S., Cannarile, M. A. & Ruttinger, D. CSF-1/CSF-1R targeting agents in clinical development for cancer therapy. *Curr Opin Pharmacol* **23**, 45-51, doi:10.1016/j.coph.2015.05.008 (2015).
- 88 von Tresckow, B. *et al.* An Open-Label, Multicenter, Phase I/II Study of JNJ-40346527, a CSF-1R Inhibitor, in Patients with Relapsed or Refractory Hodgkin Lymphoma. *Clin Cancer Res* **21**, 1843-1850, doi:10.1158/1078-0432.CCR-14-1845 (2015).
- 89 Cannarile, M. A. *et al.* Colony-stimulating factor 1 receptor (CSF1R) inhibitors in cancer therapy. *J Immunother Cancer* **5**, 53, doi:10.1186/s40425-017-0257-y (2017).
- 90 DeNardo, D. G. *et al.* Leukocyte complexity predicts breast cancer survival and functionally regulates response to chemotherapy. *Cancer Discov* **1**, 54-67, doi:10.1158/2159-8274.Cd-10-0028 (2011).
- 91 Paulus, P., Stanley, E. R., Schäfer, R., Abraham, D. & Aharinejad, S. Colony-stimulating factor-1 antibody reverses chemoresistance in human MCF-7 breast cancer xenografts. *Cancer Res* **66**, 4349-4356, doi:10.1158/0008-5472.Can-05-3523 (2006).
- 92 Olson, O. C., Kim, H., Quail, D. F., Foley, E. A. & Joyce, J. A. Tumor-Associated Macrophages Suppress the Cytotoxic Activity of Antimitotic Agents. *Cell Rep* **19**, 101-113, doi:10.1016/j.celrep.2017.03.038 (2017).
- 93 Weizman, N. *et al.* Macrophages mediate gemcitabine resistance of pancreatic adenocarcinoma by upregulating cytidine deaminase. *Oncogene* **33**, 3812-3819, doi:10.1038/onc.2013.357 (2014).
- 94 Alhudaithi, S. S. *et al.* Local Targeting of Lung-Tumor-Associated Macrophages with Pulmonary Delivery of a CSF-1R Inhibitor for the Treatment of Breast Cancer Lung Metastases. *Mol Pharm*, doi:10.1021/acs.molpharmaceut.0c00983 (2020).
- 95 Zhu, Y. *et al.* CSF1/CSF1R blockade reprograms tumor-infiltrating macrophages and improves response to T-cell checkpoint immunotherapy in pancreatic cancer models. *Cancer Res* **74**, 5057-5069, doi:10.1158/0008-5472.Can-13-3723 (2014).
- 96 Pyonteck, S. M. *et al.* CSF-1R inhibition alters macrophage polarization and blocks glioma progression. *Nature medicine* **19**, 1264-1272, doi:10.1038/nm.3337 (2013).
- 97 Zhang, H., Almuqbil, R. M., Alhudaithi, S. S., Sunbul, F. S. & da Rocha, S. R. P. Pulmonary administration of a CSF-1R inhibitor alters the balance of tumor-associated macrophages and supports first-line chemotherapy in a lung cancer model. *Int J Pharm* **598**, 120350, doi:10.1016/j.ijpharm.2021.120350 (2021).
- 98 Zhou, Y. *et al.* Blockade of the Phagocytic Receptor MerTK on Tumor-Associated Macrophages Enhances P2X7R-Dependent STING Activation by Tumor-Derived cGAMP. *Immunity* **52**, 357-373.e359, doi:10.1016/j.immuni.2020.01.014 (2020).
- 99 Sistigu, A. *et al.* Cancer cell-autonomous contribution of type I interferon signaling to the efficacy of chemotherapy. *Nat Med* **20**, 1301-1309, doi:10.1038/nm.3708 (2014).

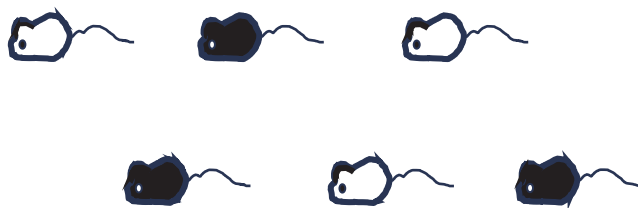
- 100 Vacchelli, E. *et al.* Autocrine signaling of type 1 interferons in successful anticancer chemotherapy. *Oncoimmunology* **4**, e988042, doi:10.4161/2162402X.2014.988042 (2015).
- 101 Arico, E., Castiello, L., Capone, I., Gabriele, L. & Belardelli, F. Type I Interferons and Cancer: An Evolving Story Demanding Novel Clinical Applications. *Cancers (Basel)* **11**, doi:10.3390/cancers11121943 (2019).
- 102 Benci, J. L. *et al.* Tumor Interferon Signaling Regulates a Multigenic Resistance Program to Immune Checkpoint Blockade. *Cell* **167**, 1540-1554 e1512, doi:10.1016/j.cell.2016.11.022 (2016).
- 103 McNab, F., Mayer-Barber, K., Sher, A., Wack, A. & O'Garra, A. Type I interferons in infectious disease. *Nat Rev Immunol* **15**, 87-103, doi:10.1038/nri3787 (2015).
- 104 Deng, L. *et al.* STING-Dependent Cytosolic DNA Sensing Promotes Radiation-Induced Type I Interferon-Dependent Antitumor Immunity in Immunogenic Tumors. *Immunity* **41**, 843-852, doi:10.1016/j.immuni.2014.10.019 (2014).
- 105 Corrales, L. *et al.* Direct Activation of STING in the Tumor Microenvironment Leads to Potent and Systemic Tumor Regression and Immunity. *Cell Rep* **11**, 1018-1030, doi:10.1016/j.celrep.2015.04.031 (2015).
- 106 Bidwell, B. N. *et al.* Silencing of Irf7 pathways in breast cancer cells promotes bone metastasis through immune escape. *Nature medicine* **18**, 1224-1231, doi:10.1038/nm.2830 (2012).
- 107 Snijders, A. M. *et al.* An interferon signature identified by RNA-sequencing of mammary tissues varies across the estrous cycle and is predictive of metastasis-free survival. *Oncotarget* **5**, 4011-4025, doi:10.18632/oncotarget.2148 (2014).
- 108 Callari, M. *et al.* Subtype-dependent prognostic relevance of an interferon-induced pathway metagene in node-negative breast cancer. *Mol Oncol* **8**, 1278-1289, doi:10.1016/j.molonc.2014.04.010 (2014).
- 109 Katlinski, K. V. *et al.* Inactivation of Interferon Receptor Promotes the Establishment of Immune Privileged Tumor Microenvironment. *Cancer Cell* **31**, 194-207, doi:10.1016/j.ccell.2017.01.004 (2017).
- 110 Swann, J. B. *et al.* Type I IFN contributes to NK cell homeostasis, activation, and antitumor function. *J Immunol* **178**, 7540-7549, doi:10.4049/jimmunol.178.12.7540 (2007).
- 111 Critchley-Thorne, R. J. *et al.* Impaired interferon signaling is a common immune defect in human cancer. *Proc Natl Acad Sci U S A* **106**, 9010-9015, doi:10.1073/pnas.0901329106 (2009).
- 112 Castiello, L. *et al.* Disruption of IFN-I Signaling Promotes HER2/Neu Tumor Progression and Breast Cancer Stem Cells. *Cancer Immunol Res* **6**, 658-670, doi:10.1158/2326-6066.CIR-17-0675 (2018).
- 113 Parker, B. S., Rautela, J. & Hertzog, P. J. Antitumour actions of interferons: implications for cancer therapy. *Nat Rev Cancer* **16**, 131-144, doi:10.1038/nrc.2016.14 (2016).

- 114 Koyama, T. *et al.* Divergent activities of interferon-alpha subtypes against intracellular hepatitis C virus replication. *Hepatology Res* **34**, 41-49, doi:10.1016/j.hepres.2005.10.005 (2006).
- 115 Tanimoto, T. *et al.* The combination of IFN-alpha2 and IFN-alpha8 exhibits synergistic antiproliferative activity on renal cell carcinoma (RCC) cell lines through increased binding affinity for IFNAR-2. *J Interferon Cytokine Res* **27**, 517-523, doi:10.1089/jir.2007.0155 (2007).
- 116 Wang, X. *et al.* Evidence of cisplatin-induced senescent-like growth arrest in nasopharyngeal carcinoma cells. *Cancer Res* **58**, 5019-5022 (1998).
- 117 Chatterjee, N. *et al.* REV1 inhibitor JH-RE-06 enhances tumor cell response to chemotherapy by triggering senescence hallmarks. *Proc Natl Acad Sci U S A* **117**, 28918-28921, doi:10.1073/pnas.2016064117 (2020).
- 118 Yang, H., Wang, H., Ren, J., Chen, Q. & Chen, Z. J. cGAS is essential for cellular senescence. *Proc Natl Acad Sci U S A* **114**, E4612-e4620, doi:10.1073/pnas.1705499114 (2017).
- 119 Dou, Z. *et al.* Cytoplasmic chromatin triggers inflammation in senescence and cancer. *Nature* **550**, 402-406, doi:10.1038/nature24050 (2017).
- 120 Seyfried, T. N. & Huysentruyt, L. C. On the origin of cancer metastasis. *Crit Rev Oncog* **18**, 43-73, doi:10.1615/critrevoncog.v18.i1-2.40 (2013).
- 121 Moschella, F. *et al.* Cyclophosphamide induces a type I interferon-associated sterile inflammatory response signature in cancer patients' blood cells: implications for cancer chemoimmunotherapy. *Clin Cancer Res* **19**, 4249-4261, doi:10.1158/1078-0432.Ccr-12-3666 (2013).
- 122 Szikriszt, B. *et al.* A comprehensive survey of the mutagenic impact of common cancer cytotoxics. *Genome Biol* **17**, 99, doi:10.1186/s13059-016-0963-7 (2016).
- 123 Shree, T. *et al.* Macrophages and cathepsin proteases blunt chemotherapeutic response in breast cancer. *Genes & development* **25**, 2465-2479, doi:25/23/2465 [pii] 10.1101/gad.180331.111 (2011).
- 124 Kersten, K., Salvagno, C. & de Visser, K. E. Exploiting the Immunomodulatory Properties of Chemotherapeutic Drugs to Improve the Success of Cancer Immunotherapy. *Front Immunol* **6**, 516, doi:10.3389/fimmu.2015.00516 (2015).
- 125 de Biasi, A. R., Villena-Vargas, J. & Adusumilli, P. S. Cisplatin-induced antitumor immunomodulation: a review of preclinical and clinical evidence. *Clin Cancer Res* **20**, 5384-5391, doi:10.1158/1078-0432.CCR-14-1298 (2014).
- 126 Rebe, C., Demontoux, L., Pilot, T. & Ghiringhelli, F. Platinum Derivatives Effects on Anticancer Immune Response. *Biomolecules* **10**, doi:10.3390/biom10010013 (2019).
- 127 Wang, W. *et al.* Identification of an Immune-Related Signature for Predicting Prognosis in Patients With Pancreatic Ductal Adenocarcinoma. *Front Oncol* **10**, 618215, doi:10.3389/fonc.2020.618215 (2020).
- 128 Liu, W. *et al.* Cisplatin remodels the tumor immune microenvironment via the transcription factor EB in ovarian cancer. *Cell Death Discov* **7**, 136, doi:10.1038/s41420-021-00519-8 (2021).

- 129 Gomez-Roca, C. A. *et al.* Phase I study of emactuzumab single agent or in combination with paclitaxel in patients with advanced/metastatic solid tumors reveals depletion of immunosuppressive M2-like macrophages. *Ann Oncol* **30**, 1381-1392, doi:10.1093/annonc/mdz163 (2019).
- 130 Wesolowski, R. *et al.* Phase Ib study of the combination of pexidartinib (PLX3397), a CSF-1R inhibitor, and paclitaxel in patients with advanced solid tumors. *Ther Adv Med Oncol* **11**, 1758835919854238, doi:10.1177/1758835919854238 (2019).
- 131 Swierczak, A. *et al.* The promotion of breast cancer metastasis caused by inhibition of CSF-1R/CSF-1 signaling is blocked by targeting the G-CSF receptor. *Cancer Immunol Res* **2**, 765-776, doi:10.1158/2326-6066.Cir-13-0190 (2014).
- 132 Kumar, V. *et al.* Cancer-Associated Fibroblasts Neutralize the Anti-tumor Effect of CSF1 Receptor Blockade by Inducing PMN-MDSC Infiltration of Tumors. *Cancer Cell* **32**, 654-668.e655, doi:10.1016/j.ccell.2017.10.005 (2017).
- 133 Nywening, T. M. *et al.* Targeting both tumour-associated CXCR2(+) neutrophils and CCR2(+) macrophages disrupts myeloid recruitment and improves chemotherapeutic responses in pancreatic ductal adenocarcinoma. *Gut* **67**, 1112-1123, doi:10.1136/gutjnl-2017-313738 (2018).
- 134 Rivera, L. B. *et al.* Intratumoral myeloid cells regulate responsiveness and resistance to antiangiogenic therapy. *Cell Rep* **11**, 577-591, doi:10.1016/j.celrep.2015.03.055 (2015).
- 135 Pahler, J. C. *et al.* Plasticity in tumor-promoting inflammation: impairment of macrophage recruitment evokes a compensatory neutrophil response. *Neoplasia* **10**, 329-340, doi:10.1593/neo.07871 (2008).
- 136 Pylaeva, E., Lang, S. & Jablonska, J. The Essential Role of Type I Interferons in Differentiation and Activation of Tumor-Associated Neutrophils. *Front Immunol* **7**, 629, doi:10.3389/fimmu.2016.00629 (2016).
- 137 Andzinski, L. *et al.* Type I IFNs induce anti-tumor polarization of tumor associated neutrophils in mice and human. *Int J Cancer* **138**, 1982-1993, doi:10.1002/ijc.29945 (2016).
- 138 Kalafati, L. *et al.* Innate Immune Training of Granulopoiesis Promotes Anti-tumor Activity. *Cell* **183**, 771-785.e712, doi:10.1016/j.cell.2020.09.058 (2020).
- 139 Berry, M. P. *et al.* An interferon-inducible neutrophil-driven blood transcriptional signature in human tuberculosis. *Nature* **466**, 973-977, doi:10.1038/nature09247 (2010).
- 140 Rocha, B. C. *et al.* Type I Interferon Transcriptional Signature in Neutrophils and Low-Density Granulocytes Are Associated with Tissue Damage in Malaria. *Cell Rep* **13**, 2829-2841, doi:10.1016/j.celrep.2015.11.055 (2015).
- 141 Sivick, K. E. *et al.* Magnitude of Therapeutic STING Activation Determines CD8(+) T Cell-Mediated Anti-tumor Immunity. *Cell Rep* **29**, 785-789, doi:10.1016/j.celrep.2019.09.089 (2019).
- 142 Spaapen, R. M. *et al.* Therapeutic activity of high-dose intratumoral IFN- $\beta$  requires direct effect on the tumor vasculature. *J Immunol* **193**, 4254-4260, doi:10.4049/jimmunol.1401109 (2014).

- 143 Kersten, K. *et al.* Mammary tumor-derived CCL2 enhances pro-metastatic systemic inflammation through upregulation of IL1beta in tumor-associated macrophages. *Oncoimmunology* **6**, e1334744, doi:10.1080/2162402X.2017.1334744 (2017).
- 144 Nagaraj, S. *et al.* Altered recognition of antigen is a mechanism of CD8+ T cell tolerance in cancer. *Nature medicine* **13**, 828-835, doi:10.1038/nm1609 (2007).
- 145 Jaillon, S. *et al.* Neutrophil diversity and plasticity in tumour progression and therapy. *Nat Rev Cancer* **20**, 485-503, doi:10.1038/s41568-020-0281-y (2020).
- 146 Shaul, M. E. & Fridlender, Z. G. Tumour-associated neutrophils in patients with cancer. *Nat Rev Clin Oncol* **16**, 601-620, doi:10.1038/s41571-019-0222-4 (2019).
- 147 Schott, A. F. *et al.* Phase Ib Pilot Study to Evaluate Reparixin in Combination with Weekly Paclitaxel in Patients with HER-2-Negative Metastatic Breast Cancer. *Clin Cancer Res* **23**, 5358-5365, doi:10.1158/1078-0432.Ccr-16-2748 (2017).
- 148 (<https://ClinicalTrials.gov/show/NCT03177187>).

## Chapter 6



## **Addenda**

**English Summary**

**Dutch Summary**

**Acknowledgements**

**Curriculum Vitae**

**Publications**

## English Summary

The heterogeneous nature of cancer, inter- and intra-tumor heterogeneity, is not only a consequence of aberrant mutations but also of the composition and activation states of the inflammatory tumor microenvironment (TME). The TME does not only consists of cancer cells but it also contains fibroblasts, endothelial cells, and immune cells. These cells secrete inflammatory mediators, such as elements of the extracellular matrix, metabolites, cytokines, and chemokines, that play a vital role in the cancer cells' ability to grow and metastasize. The immune system has shown to be an important player in tumorigenesis, being able to attack and kill cancer cells but also to promote tumorigenesis. To date, it remains largely unclear why certain tumors elicit anti-tumor immune responses whereas other tumors elicit pro-tumor immune responses or are not regulated by the immune system at all. For the development of therapeutic strategies that target the tumor-associated stroma, it is important to understand how cancer-promoting and cancer-inhibiting immune responses are regulated.

Chemotherapy is the mainstay treatment for most cancer types. Chemotherapeutic drugs do not only kill tumor cells but also influence the number and the phenotype of immune cells. Understanding how different chemotherapeutic agents impact the immune system could facilitate the rational design of combination therapies and thereby increase chemo-responsiveness and/or prevent chemo-resistance.

Macrophages are frequently the most abundant immune cell type present in cancer and represent key orchestrators of various tumor-promoting processes. Therefore, macrophages have become interesting putative targets for therapeutic intervention. Immunomodulatory agents that target macrophage function via CSF-1/CSF-1R signaling have recently been developed and are currently being tested in clinical trials. To maximize the clinical success of therapies targeting macrophage function, we need to understand what the exact mechanisms are by which these agents lead to therapeutic benefit and identify the optimal partner among existing conventional anti-cancer therapies to maximize their efficacy.

The scope of the work in this thesis (outlined in **Chapter 1**) is to advance the development of anti-cancer therapies by understanding the impact of the immune system on breast tumorigenesis and chemotherapy response. This involves the assessment of the adaptive immune response in tumorigenesis

of HER2+ breast cancer, the assessment of the involvement of the adaptive immune system in chemotherapy response, and the evaluation to optimize macrophage-targeted based therapies in breast cancer genetically engineered mouse models (GEMMs). In **Chapter 1**, I also review the current understanding of the paradoxical roles of adaptive immune cells and macrophages in tumorigenesis and chemotherapy response. Furthermore, I discuss how to further understand the inherent complexity of the immune system in cancer for the identification of novel prognostic and predictive biomarkers, and for the design of novel immunomodulatory treatment strategies to fight cancer.

### **Adaptive immune response in HER2+ breast tumorigenesis**

Different cancer types and subtypes have been described to be regulated differently by the adaptive immune system. In **Chapter 2**, we assess the impact of the adaptive immune system on HER2+ breast cancer during (pre-) malignant progression and pulmonary metastasis formation in MMTV-*NeuT* transgenic mice. By genetically eliminating the adaptive immune system from the transgenic MMTV-*NeuT* mouse model via intercrossing with *Rag2*<sup>-/-</sup> mice, lacking B and T lymphocytes, we reveal that, unlike other breast cancer subtypes, spontaneous HER2-driven mammary tumorigenesis and metastasis formation are neither suppressed nor promoted by the adaptive immune system.

6

### **Chemotherapy and adaptive immune responses in GEMMs**

Tumor cell line transplantation models have shown that the adaptive immune system dictates the therapeutic efficacy of certain chemotherapeutics. Studies have elucidated major limitations of tumors produced by inoculation of cancer cells as they do not resemble de novo tumors with co-evolving tumor-host interactions and an immunosuppressive microenvironment. In **Chapter 3** of this thesis we generated T and B cell-deficient spontaneous mammary tumors of MMTV-*NeuT* and *K14cre; Cdh1*<sup>F/F</sup>; *Trp53*<sup>F/F</sup> mice by intercrossing both mouse tumor models with *Rag2*<sup>-/-</sup> mice. We evaluated the capacity of the adaptive immune system response to various conventional chemotherapeutic drugs. We describe that in both mammary tumor models, lack of T and B cells did not affect chemotherapy response. In **Chapter 3**, we then highlight that the role of the endogenous adaptive immune system

in chemotherapy response might not be as crucial as proposed previously when using tumor cell line transplantation models.

### **Targeting macrophages as anti-cancer therapy**

Macrophages have been shown to counteract the anti-cancer effects of chemotherapeutic drugs. In **Chapter 4** of this thesis we show that targeting macrophages, by using CSF-1R inhibition in the non-immunogenic spontaneous *K14cre; Cdh1<sup>FF</sup>; Trp53<sup>FF</sup>* model for breast cancer, enhanced chemotherapy efficacy in a drug-dependent manner. We observed that anti-CSF-1R synergizes with platinum-containing drugs but not with docetaxel. In addition, we identified that CSF-1R inhibition stimulated intratumoral type I interferon signaling which is essential for the synergistic anti-cancer effect of cisplatin and the anti-CSF-1R combination. Finally, we show that also targeting immunosuppressive neutrophils in this setting was essential to unleash an effective anti-tumor immunity. In conclusion, in **Chapter 4** our findings underscore the potential of targeting macrophages and neutrophils to improve the therapeutic outcomes of chemotherapy in breast cancer, leveraging the activation of intratumoral type I interferon signaling and unleashing a robust anti-tumor immune response.

### **Concluding remarks and future perspectives**

**Chapter 5** contains the general discussion where I contextualize the findings of this thesis with the current literature and propose clinical implications based on our findings. This thesis is focused on the use of genetically modified mice and immunotherapeutic treatments to obtain an immunological relevant understanding of breast tumorigenesis and chemotherapy response for the development of anti-cancer therapies. As such the work presented may improve clinical applications of immunomodulatory therapies targeting macrophages.

## Dutch Summary

De heterogene aard van kanker, heterogeniteit tussen tumoren en heterogeniteit binnen de tumor, is niet alleen een gevolg van afwijkende mutaties, maar ook van de samenstelling en mate van activatie van het micro-milieu van tumoren (TME). Het TME bestaat niet alleen uit kankercellen maar het bevat ook fibroblasten, endotheelcellen en immuuncellen. Deze cellen scheiden ontstekingsmediatoren af, zoals elementen van de extracellulaire matrix, metaboliëten, cytokinen en chemokinen, die een vitale rol spelen bij het vermogen van de kankercellen om te groeien en uit te zaaien. Het is gebleken dat het immuunsysteem een belangrijke rol speelt bij het ontstaan en de progressie van kanker, omdat het kankercellen kan aanvallen en doden, maar ook kan bevorderen. Tot op heden blijft het grotendeels onduidelijk waarom bepaalde tumoren anti-tumor immuunreacties uitlokken terwijl andere tumoren pro-tumor immuunreacties uitlokken of helemaal niet gereguleerd worden door het immuunsysteem. Voor de ontwikkeling van therapeutische strategieën die zich richten tegen het tumor-geassocieerde stroma, is het belangrijk om te begrijpen hoe kanker-bevorderende en kanker-remmende immuunreacties worden gereguleerd.

Chemotherapie is de meest gebruikelijke behandeling voor de meeste soorten kankertypes. De chemotherapeutica doden niet alleen tumorcellen, maar beïnvloeden ook het aantal en het fenotype van immuuncellen. Hoe verschillende chemotherapeutische medicijnen het immuunsysteem beïnvloeden is nog onduidelijk. Begrip hierover kan het ontwikkelen van combinatietherapieën vergemakkelijken, en zo de effectiviteit van chemotherapie verhogen en/of chemoresistentie voorkomen.

Macrofagen zijn het meest voorkomende type immuuncellen in kanker. Daarbij staan macrofagen bekend om verschillende tumor bevorderende processen te beïnvloeden waardoor zij potentiële doelwitten zijn voor therapeutische interventie. Immunomodulerende middelen die macrofagen uitputten door het interfereren met de CSF-1/CSF-1R-signalering route zijn recent ontwikkeld en worden momenteel getest in klinische studies. Om het klinische succes van op macrofaag gerichte medicijnen te maximaliseren, moeten we begrijpen wat de concrete mechanismen zijn waarmee deze middelen tot therapeutisch voordeel leiden. Het is ook erg belangrijk om de optimale partner te vinden onder de bestaande conventionele anti-kanker therapieën.

Het doel van het werk in dit proefschrift is het bevorderen van de ontwikkeling van anti-kanker therapieën door de functie van het immuunsysteem te begrijpen bij het ontstaan en het metastaseren van borsttumoren en de respons op chemotherapie (beschreven in **Hoofdstuk 1**). Deze thesis omvat het onderzoek naar de functie van het adaptieve immuunsysteem bij het ontstaan en de progressie van HER2+ borstkanker. Ook wordt de rol van het adaptieve immuunsysteem bij de respons op chemotherapie onderzocht. Daarnaast is het onderzoek gericht naar hoe de effectiviteit van anti-CSF-1R door combinaties met chemotherapieën gemaximaliseerd kan worden. Het werk in dit proefschrift is uitgevoerd met behulp van genetische gemodificeerde muismodellen (GEMMs) van borstkanker.

In **Hoofdstuk 1** geef ik ook een overzicht van de huidige kennis over de paradoxale rol van adaptieve immuuncellen en macrofagen tijdens de ontwikkeling en progressie van tumoren en de respons op chemotherapie. Verder bespreek ik hoe het begrijpen van de inherente complexiteit van het immuunsysteem in kanker kan leiden tot de ontwikkeling van nieuwe prognostische en voorspellende biomarkers, en nieuwe immunomodulerende behandelingsstrategieën om kanker te bestrijden.

## **De rol van het adaptieve immuunsysteem bij het ontstaan en de progressie van HER2+ borstkanker**

Van verschillende kankertypes en subtypes is beschreven dat ze anders worden gereguleerd door het adaptieve immuunsysteem. In **Hoofdstuk 2** onderzoeken we of de adaptieve immuuncellen in HER2-borstkanker belangrijk zijn tijdens (pre-) maligne progressie en metastasering naar de longen in MMTV-*NeuT* transgene muizen. We hebben genetische eliminatie van het adaptieve immuunsysteem in het transgene MMTV-*NeuT* muismodel verkregen via kruising met *Rag2*<sup>-/-</sup> muizen die B- en T-lymfocyten missen. In tegenstelling tot andere borstkankersubtypes hebben we aangetoond dat het ontstaan en de progressie van spontane HER2-gedreven borstkanker en metastasering noch onderdrukt, noch bevorderd worden door het adaptieve immuunsysteem.

## **Chemotherapie en adaptieve immuunreacties in GEMM's**

Studies in tumorcellijntransplantatiemodellen hebben aangetoond dat de therapeutische effectiviteit van bepaalde cytostatica door het adaptieve

immuunsysteem wordt gediceerd. Echter hebben verscheidene studies belangrijke nadelen gevonden van tumoren die geproduceerd worden door inoculatie van kankercellen omdat ze niet lijken op *de novo* tumoren met co-evoluerende tumor-gastheerinteracties en een immunosuppressieve micro-omgeving. In **Hoofdstuk 3** van dit proefschrift hebben we T en B-cel-deficiënte spontane borsttumoren gegenereerd van MMTV-*NeuT* en *K14cre*; *Cdh1<sup>F/F</sup>*; *Trp53<sup>F/F</sup>* muizen door beide muis-tumormodellen te kruisen met *Rag<sup>-/-</sup>* muizen. We onderzochten de functie van het adaptieve immuunsysteem op de effectiviteit van verschillende conventionele chemotherapeutische geneesmiddelen. We beschrijven dat in beide borsttumormodellen het ontbreken van T- en B-cellen geen invloed had op de effectiviteit van chemotherapie. In **Hoofdstuk 3** benadrukken we vervolgens dat de rol van het endogene adaptieve immuunsysteem wellicht niet zo cruciaal is voor de effectiviteit van chemotherapie in tegenspraak tot wat eerder werd voorgesteld met het gebruik van tumorcellijn transplantatie modellen.

### Macrofagen uitputten als anti-kanker therapie

Eerdere studies hebben aangetoond dat macrofagen het anti-tumor effect van verschillende chemotherapeutische geneesmiddelen tegenwerken. In **Hoofdstuk 4** van dit proefschrift laten we zien dat het uitputten van macrofagen, met het gebruik van antilichamen tegen CSF-1R in het niet-immunogene spontane *K14cre*; *Cdh1<sup>F/F</sup>*; *Trp53<sup>F/F</sup>* model voor borstkanker, de effectiviteit van chemotherapie versterkt, afhankelijk van het type chemotherapie. We stelden vast dat het medicijn anti-CSF-1R synergetisch werkt met platinabevattende geneesmiddelen, maar niet met docetaxel. Bovendien stelden we vast dat CSF-1R inhibitie intratumorale type I interferon signalering stimuleert, wat essentieel is voor het synergetische anti-kanker effect van cisplatine en de anti-CSF-1R combinatie. Tenslotte tonen we aan dat in deze setting het ook uitputten van neutrofielen essentieel is om een effectieve anti-tumor immuniteit tot stand te brengen. In **Hoofdstuk 4** benadrukken we het veelbelovende potentieel van het richten op macrofagen en neutrofielen om de therapeutische uitkomsten van borstkankerchemotherapie aanzienlijk te verbeteren door de activering van intratumorale type I interferon signalering en het ontketenen van een krachtige immuunrespons tegen tumoren.

## **Afsluitende opmerkingen en toekomstperspectieven**

**Hoofdstuk 5** bevat de algemene discussie waarin de bevindingen van dit proefschrift in verband worden gebracht met de huidige literatuur en daarnaast, op basis van onze bevindingen, voorstellen worden gedaan voor anti-kanker behandelingen in de kliniek. Dit proefschrift maakt gebruik van genetisch gemodificeerde muizen en immunotherapeutische behandelingen om inzicht te verkrijgen in de rol van het immuunsysteem tijdens het ontstaan en de progressie van borsttumoren en de effectiviteit op chemotherapie voor de ontwikkeling van anti-kanker therapieën. Als zodanig, kan dit proefschrift voor verbeterende klinische toepassingen zorgen voor immunomodulerende therapieën die gericht zijn op macrofagen.

## Acknowledgements

Met een gevoel van blijdschap en triomf heb ik mijn langverwachte thesis eindelijk voltooid. Hoewel de weg naar dit moment lang en soms hobbelig is geweest, was het ook een pad vol waardevolle leerervaringen.

Allereerst wil ik mijn oprechte dank uitspreken aan mijn begeleider, Karin. Je geduld, aanmoediging en steun waren van onschatbare waarde gedurende dit proces. Het was een eer om je eerste PhD-student te zijn en samen hebben we mooie wetenschappelijke artikelen geproduceerd. Jouw begeleiding heeft een onschatbare impact gehad op mijn ontwikkeling als wetenschapper en ik ben je daar zeer dankbaar voor.

Ik wil ook graag mijn dank uitspreken aan Jos, die altijd een co-begeleider is geweest. De meetings en reisjes met jouw lab hebben mij enorm veel geleerd en ik ben erg dankbaar voor onze samenwerking.

Ook wil ik mijn oprechte dank betuigen aan mijn geliefde familie en vrienden: mijn moeder, dankje mamsie voor je oneindig geloof in mij. Je bent een bron van inspiratie en motivatie en ik waardeer je liefde en steun enorm. Ik ben ook erg trots op jou!

Nicole, thank you for being there for me every step of the way, for all the support and patience you've shown, even during those many dinners when I made you wait. Your understanding and encouragement have meant the world to me.

Omie, Oom Eric, Evelien, Marian, Sam, Rie, Serenella e Maurizio, Anne, Richard en Alex. Mijn paranimfen Dominique en Valentijn. Jullie steun en liefde hebben me door de uitdagende tijden gedragen en me gemotiveerd om vol te houden. Grazie!

Aan de eerste leden van de Karin de Visser-groep: Tisee, Chris, Seth, Kelly, Camilla en Kim, bedankt voor de tijd in het lab. Ik heb ontzettend prettig met jullie samengewerkt, veel geleerd, gediscussieerd, veel gelachen en soms gehuild. Camilla, thanks for finishing our paper and see you back in NY.

Janneke, Feline, Bo, Pia, Rachel en Ricardo dank jullie wel voor de vriendschap.

Jos Jonkers' lab: Marieke, Linda, Martine, Ewa, Ellen, Ingrid, Hanneke, Peter, Rinske, Joost, Tanya en Ute, bedankt voor de samenwerking en vriendschap.

My New York friends who have never given up on pushing and believing in me, thank you Viola, Alvaro and Angeliki.

Dank aan iedereen die een rol heeft gespeeld in deze reis. Jullie bijdragen hebben het verschil gemaakt en ik waardeer het enorm.

## Curriculum Vitae

Metamia Ciampricotti was born on April 24, 1984 in Son en Breugel, The Netherlands. She followed her high school gymnasium at SSG De Rede in Terneuzen, where she received her diploma in June 2002. In September 2002 she started her bachelor's in biology at Utrecht University in Utrecht. In 2006 she commenced with the prestige Master program Cancer, Genomics & Developmental Biology. Her first research internship took place at the department of Biomedical Genetics, Metabolic and Endocrine Diseases at University Medical Center (UMC) Utrecht under supervision of prof. dr. Bart van de Sluis. For her second internship that lasted nine months she worked in the laboratory of prof. dr. Jeroen Bakkers at the Hubrecht Institute (Netherlands Institute for Developmental Biology). Here she studied genetics of cardiac development in zebrafish.

After obtaining her Master of Science degree at Utrecht University, Metamia started working as a PhD student in the laboratory of prof. dr. Karin E. de Visser at the Netherlands Cancer Institute in Amsterdam in February 2009. For 5 years she investigated the inflammatory tumor microenvironment and its impact on breast cancer development and therapy. With her research Metamia won travel scholarships for Keystone, Cold Spring Harbor Laboratory and EACR symposia and presentation awards from MedImmune and the Dutch Cancer Society. Metamia continued her scientific work in the group of Chief of Thoracic Oncology dr. Charles M. Rudin at Memorial Sloan Kettering in New York, USA, in November 2014. Here she has developed a gene fusion small cell lung cancer mouse model via CRISPR-Cas9 engineering and is characterizing intrinsic and extrinsic pathways of primary small cell lung cancer subtypes using IHC and single nuclei RNA sequencing with prof. dr. Aviv Regev at the Broad Institute.

## Publications

Jaspers JE, Khan JF, Godfrey WD, Lopez AV, **Ciampricotti M**, Rudin CM, Brentjens RJ. L-18-secreting CAR T cells targeting DLL3 are highly effective in small cell lung cancer models.

*J Clin Invest.* 2023 May 1;133(9):e166028.

Chow A, Uddin FZ, Liu M, Dobrin A, Nabet BY, Mangarin L, Lavin Y, Rizvi H, Tischfield SE, Quintanal-Villalonga A, Chan JM, Shah N, Allaj V, Manoj P, Mattar M, Meneses M, Landau R, Ward M, Kulick A, Kwong C, Wierzbicki M, Yavner J, Egger J, Chavan SS, Farillas A, Holland A, Sridhar H, **Ciampricotti M**, Hirschhorn D, Guan X, Richards AL, Heller G, Mansilla-Soto J, Sadelain M, Klebanoff CA, Hellmann MD, Sen T, de Stanchina E, Wolchok JD, Merghoub T, Rudin CM.

The ectonucleotidase CD39 identifies tumor-reactive CD8<sup>+</sup> T cells predictive of immune checkpoint blockade efficacy in human lung cancer.

*Immunity.* 2023 Jan 10;56(1):93-106.e6.

Quintanal-Villalonga A, Taniguchi H, Hao Y, Chow A, Zhan YA, Chavan SS, Uddin F, Allaj V, Manoj P, Shah NS, Chan JM, Offin M, **Ciampricotti M**, Ray-Kirton J, Egger J, Bhanot U, Linkov I, Asher M, Roehrl MH, Qiu J, de Stanchina E, Hollmann TJ, Koche RP, Sen T, Poirier JT, Rudin CM.

Inhibition of XPO1 sensitizes small cell lung cancer to first- and second-line chemotherapy.

*Cancer Res.* 2022 Feb 1;82(3):472-483.

**Ciampricotti M**, Karakousi T, Richards AL, Quintanal-Villalonga A, Karatza A, Caesar R, Costa EA, Allaj V, Manoj P, Spainhower KB, Kombak FE, Sanchez-Rivera FJ, Jaspers JE, Zavitsanou AM, Maddalo D, Ventura A, Rideout WM 3rd, Akama-Garren EH, Jacks T, Donoghue MTA, Sen T, Oliver TG, Poirier JT, Papagiannakopoulos T, Rudin CM.

*Rlf-Mycl* Gene Fusion Drives Tumorigenesis and Metastasis in a Mouse Model of Small Cell Lung Cancer.

*Cancer Discov.* 2021 Dec 1;11(12):3214-3229.

Quintanal-Villalonga A, Taniguchi H, Zhan YA, Hasan MM, Chavan SS, Meng F, Uddin F, Manoj P, Donoghue MTA, Won HH, Chan JM, **Ciampricotti M**, Chow A, Offin M, Chang JC, Ray-Kirton J, Tischfield SE, Egger JV, Bhanot UK, Linkov I, Asher M, Sinha S, Silber J, Iacobuzio-Donahue CA, Roehrl MH, Hollmann TJ, Yu HA, Qiu J, de Stanchina E, Baine MK, Rekhman N, Poirier JT, Loomis B, Koche RP, Rudin CM, Sen T.

Multi-omic analysis of lung tumors defines pathways activated in neuroendocrine transformation.

*Cancer Discov.* 2021 Dec 1;11(12):3028-3047.

Quintanal-Villalonga A, Taniguchi H, Zhan YA, Hasan MM, Chavan SS, Meng F, Uddin F, Allaj V, Manoj P, Shah NS, Chan JM, **Ciampricotti M**, Chow A, Offin M, Ray-Kirton J, Egger JD, Bhanot UK, Linkov I, Asher M, Roehrl MH, Ventura K, Qiu J, de Stanchina E, Chang JC, Rekhman N, Houck-Loomis B, Koche RP, Yu HA, Sen T, Rudin CM.

Comprehensive molecular characterization of lung tumors implicates AKT and MYC signaling in adenocarcinoma to squamous cell transdifferentiation.

*J Hematol Oncol.* 2021 Oct 16;14(1):170.

Caesar R, Hulton C, Costa E, Durani V, Little M, Chen X, Tischfield SE, Asher M, Kombak FE, Chavan SS, Shah NS, **Ciampricotti M**, de Stanchina E, Poirier JT, Rudin CM, Sen T.

MAPK pathway activation selectively inhibits ASCL1-driven small cell lung cancer.

*iScience.* 2021 Oct 5;24(11):103224.

## Chapter 6

Salvagno C, **Ciampricotti M**, Tuit S, Hau CS, van Weverwijk A, Coffelt SB, Kersten K, Vrijland K, Kos K, Ulas T, Song JY, Ooi CH, Rüttinger D, Cassier PA, Jonkers J, Schultze JL, Ries CH, de Visser KE.

Therapeutic targeting of macrophages enhances chemotherapy efficacy by unleashing type I interferon response.

*Nat Cell Biol.* 2019 Apr;21(4):511-521.

Kersten K, Coffelt SB, Hoogstraat M, Versteegen NJM, Vrijland K, **Ciampricotti M**, Doornebal CW, Hau CS, Wellenstein MD, Salvagno C, Doshi P, Lips EH, Wessels LFA, de Visser KE.

Mammary tumor-derived CCL2 enhances pro-metastatic systemic inflammation through upregulation of IL1 $\beta$  in tumor-associated macrophages.

*Oncoimmunology.* 2017 Jun 19;6(8):e1334744.

Doornebal CW, Vrijland K, Hau CS, Coffelt SB, **Ciampricotti M**, Jonkers J, de Visser KE, Hollmann MW.

Morphine does not facilitate breast cancer progression in two preclinical mouse models for human invasive lobular and HER2<sup>+</sup> breast cancer.

*Pain.* 2015 Aug;156(8):1424-1432.

Coffelt SB, Kersten K, Doornebal CW, Weiden J, Vrijland K, Hau CS, Versteegen NJM, **Ciampricotti M**, Hawinkels LJAC, Jonkers J, de Visser KE.

IL-17-producing  $\gamma\delta$  T cells and neutrophils conspire to promote breast cancer metastasis.

*Nature.* 2015 Jun 18;522(7556):345-348.

Doornebal CW, Klarenbeek S, Braumuller TM, Klijn CN, **Ciampricotti M**, Hau CS, Hollmann MW, Jonkers J, de Visser KE.

A preclinical mouse model of invasive lobular breast cancer metastasis.

*Cancer Res.* 2013 Jan 1;73(1):353-63.

de Visser KE, **Ciampricotti M**, Michalak EM, Tan DW, Speksnijder EN, Hau CS, Clevers H, Barker N, Jonkers J.

Developmental stage-specific contribution of LGR5(+) cells to basal and luminal epithelial lineages in the postnatal mammary gland.

*J Pathol.* 2012 Nov;228(3):300-9.

**Ciampricotti M**, Hau CS, Doornebal CW, Jonkers J, de Visser KE.

Chemotherapy response of spontaneous mammary tumors is independent of the adaptive immune system.

*Nat Med.* 2012 Mar 6;18(3):344-6.

de Pater E, **Ciampricotti M**, Priller F, Veerkamp J, Strate I, Smith K, Lagendijk AK, Schilling TF, Herzog W, Abdelilah-Seyfried S, Hammerschmidt M, Bakkens J.

Bmp signaling exerts opposite effects on cardiac differentiation.

*Circ Res.* 2012 Feb 17;110(4):578-87.

**Ciampricotti M**, Vrijland K, Hau CS, Pemovska T, Doornebal CW, Speksnijder EN, Wartha K, Jonkers J, de Visser KE.

Development of metastatic HER2(+) breast cancer is independent of the adaptive immune system.

*J Pathol.* 2011 May;224(1):56-66.

Evers B, Speksnijder EN, Schut E, **Ciampricotti M**, Smalley MJ, Derksen PW, Jonkers J, de Visser KE.

A tissue reconstitution model to study cancer cell-intrinsic and -extrinsic factors in mammary tumorigenesis.

*J Pathol.* 2010 Jan;220(1):34-44.